

---

**MANIPULATION OF SOIL NITROGEN TO INCREASE  
EFFICIENCY OF MINTUBER SEED PRODUCTION IN  
TASMANIA**

**JAMES KIRKHAM**

**SUBMITTED IN FULFILMENT OF THE REQUIREMENT FOR  
THE DEGREE OF DOCTOR OF PHILOSOPHY**

**University of Tasmania (June 2010)**

---

---

## SUPERVISORS

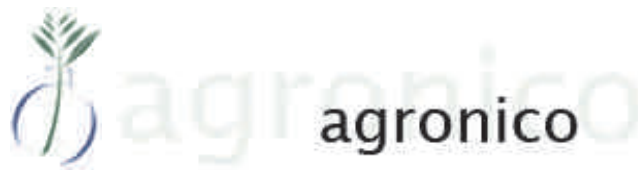
Supervisors:

Dr Richard Doyle

Dr Philip Brown

Dr James Hills (Industry Supervisor)

This project has been facilitated by Horticultural Australia (Project PT06011) in partnership with Agronico Technology Pty Ltd and the University of Tasmania's Post Graduate Research Scholarship scheme. It has been funded by voluntary contributions from Agronico Technology. The Australian Government provides matched funding for all HAL's research and development activities.



---

## DECLARATION OF ORIGINALITY

This thesis contains no material which has been accepted for a degree or diploma by the University or any other institution, except by way of background information and duly acknowledged in the thesis, and to the best of the candidate's knowledge and belief no material previously published or written by another person except where due acknowledgement is made in the text of the thesis, nor does the thesis contain any material that infringes copyright.

x\_\_\_\_\_

James Kirkham

\_\_\_/\_\_\_/\_\_\_

Date

## AUTHORITY OF ACCESS

This thesis may be made available for loan and limited copying in accordance with the *Copyright Act 1968*.

x\_\_\_\_\_

James Kirkham

\_\_\_/\_\_\_/\_\_\_

Date

---

## ABSTRACT

The management and manipulation of soil nitrogen (N) was investigated as a means of influencing plant growth to increase tuber numbers produced from early generation seed potato crops. The project focussed on crops grown from minitubers, small potatoes produced under controlled environment conditions from tissue culture plantlets. The use of minitubers as planting material for first field generation seed potato crops reduces the risk of disease but is commercially challenging as the plants tend to produce low tuber numbers, limiting the seed multiplication rate. The first field generation is a high value crop grown on a small land area and there is therefore potential for intensive management of factors such as nutrient supply to increase the number of tubers and the subsequent rate of multiplication in the field.

Nitrogen has been shown to influence tuber number and tuber growth in both hydroponics and field experiments, and was therefore the nutrient investigated in this study. Initial glasshouse and laboratory experiments demonstrated that manipulation of N availability could alter tuber development in potato plants. In contrast to evidence in the literature from hydroponics experiments, a high constant N supply did not delay or inhibit the onset of tuberization. High N supply increased tuber set and growth, demonstrating the importance of sufficient N supply during early plant growth up to tuberization. Rapidly reducing N supply to plants at the onset of tuberization increased tuber growth rate by 60% compared to control plants two weeks after treatment application. It was concluded that the treatment may reduce the rate of tuber resorption during the tuber bulking phase, and therefore increase tuber number at harvest.

Under field conditions, application of a leaching treatment based on calculations from laboratory and glasshouse trials did not result in any significant change in tuber number. Three potato cultivars were used in the trial and 150 plants per treatment were assessed. Although N was applied to the crop as  $\text{NO}_3^-$  to increase the likelihood of leaching during treatment application, soil analysis indicated that  $\text{NO}_3^-$  concentrations were only reduced in the upper 20 cm of soil. Roots were distributed throughout the top 40 cm of the soil and therefore plants still had access to significant  $\text{NO}_3^-$  concentrations after treatment application. The use of a drip irrigation system,

---

the volume of water applied and the presence of anion adsorption contributed to limited movement of  $\text{NO}_3^-$  through the soil profile. The field results demonstrated a need for better understanding of N movement in the Red Ferrosol soil so a more effective strategy for rapidly reducing N concentrations in the root zone could be developed.

Accurate and detailed measurements of water and  $\text{NO}_3^-$  movement in the Red Ferrosol soil were obtained from laboratory experiments. The presence of anion adsorption was observed and therefore an adsorption isotherm for  $\text{NO}_3^-$  was developed. Using the data collected from the laboratory experiments, parameters for the Hydrus 2D/3D soil model were validated for the soil and this model was used to estimate the distribution of water and  $\text{NO}_3^-$  under different irrigation scenarios in the field. Simulations indicated an overhead irrigation system was a more effective method for rapidly reducing soil  $\text{NO}_3^-$  concentrations in the root zone than a dripper system due to the predominantly vertical displacement of  $\text{NO}_3^-$  however water applications of over 300 mm of water were required. Further simulations in an alternative sandy soil indicated that the leaching volume required was less than half that of the Red Ferrosol due to the soils lower water holding capacity and absence of anion adsorption. It was therefore concluded that serious consideration of soil type should be made during the design of future experiments investigating strategic  $\text{NO}_3^-$  control in potato crops.

This study provides preliminary evidence that careful management of N in potato crops has the potential to increase tuber growth rate and tuber number. However treatments that involve manipulation of N availability are difficult to apply in field environments where plant roots are widely distributed. Models such as Hydrus 2D/3D are useful tools for investigating water and nutrient movement under various flow scenarios however reliability of model predictions depends on the level of validation against measured data.

---

## ACKNOWLEDGEMENTS

Firstly I would like to thank my supervisors Dr Richard Doyle and Dr Phil brown for their support and time committed throughout my PhD, particularly with my move interstate for the final 18 months of my study. Your encouragement and positivity were just as vital as the intellectual advice you provided me over the period of my candidature.

I am also deeply indebted to Dr Chris Smith and Dr David Smiles from CSIRO land and water for the significant supervision they provided my for the work reported in Chapters 4 and 5 of this thesis. Thankyou for the time you both committed to helping me develop as scientist. I am also grateful for the laboratory, analytical and modelling resources that I was provided during my time spent in Canberra.

To my wonderful Fiancé Caroline, thankyou for your support from day one. For your patience and encouragement over this time I will forever be in debt.

Thanks also to:

Ross Corkrey for his statistical advice and assistance provided throughout my study.

Agronico Technology for providing funding for the project and to Horticulture Australia for provided matched project funds.

The University of Tasmania and the Tasmanian Institute of Agricultural Research for giving me the opportunity to undertake this project and the Australian Postgraduate Award I was provided during my studies.

Agronico Employees Stewart Mackay and Robin Tate for their assistance in the field and production of the excellent quality potato seed supplied for the project.

Adrian Hunt who provided outstanding assistance with the field experiment.

To past and present University of Tasmania staff Andrew Meesham, Bill Peterson, Rose Bullough, Rochelle Emery, Jane Bailey and Angela Richardson for their administration and technical assistance.

To CSIRO staff Seija Tuomi, Gordon McLachlan, Ruth Palmer and Mark Glover for their laboratory and administration assistance during my time in Canberra.

---

To my friends in Tasmania and those I have made in Canberra for all the potato jokes and general encouragement over the last few years.

Finally, thankyou to my parents for your unfailing love and support. You have given me the opportunity to reach this point in my life and career.

---

## TABLE OF CONTENTS

DECLARATION OF ORIGINALITY .....	iii
AUTHORITY OF ACCESS.....	iii
ABSTRACT .....	iv
ACKNOWLEDGEMENTS .....	vi
TABLE OF CONTENTS .....	viii
LIST OF TABLES.....	xii
LIST OF FIGURES .....	xvi
LIST OF PLATES .....	xxi
<b>CHAPTER 1 INTRODUCTION.....</b>	<b>1</b>
<b>CHAPTER 2 EFFECTS OF NITROGEN AND SOIL TYPE ON TUBER INITIATION AND TUBER DEVELOPMENT.....</b>	<b>7</b>
INTRODUCTION .....	7
LITERATURE REVIEW .....	7
Effects of Nitrogen on Tuberization.....	7
Carbohydrate Regulation of Tuber Initiation and Growth.....	9
A New Method for Increasing Tuber Number and Yields? .....	12
EXPERIMENTAL OVERVIEW.....	13
MATERIALS AND METHODS.....	14
Tuber Initiation and Tuber Growth: The Influence of High N Supply.....	14
Vertical Column Leaching Studies .....	16
The Influence of Soil Type on Plant Emergence and Tuberization.....	19
Effects of Reducing N availability at Tuberization on Tuber Set and Growth.....	21
RESULTS.....	24
Tuber Initiation and Tuber Growth: The Influence of High N Supply.....	24
Vertical Column Leaching Studies .....	30
The Influence of Soil Type on Plant Emergence and Tuberization.....	35
Effects of Reducing N Availability at Tuberization on Tuber Set and Growth.....	36
DISCUSSION.....	39
CONCLUSION.....	42

---



---

<b>CHAPTER 3 APPLICATION OF THE “N LEACH” TREATMENT TO A RED FERROSOL IN THE FIELD .....</b>	<b>43</b>
INTRODUCTION .....	43
LITERATURE REVIEW .....	43
Effects of Nitrogen on Tuber Number in the Field .....	43
Root Development and Distribution in Potatoes .....	44
Water and Solute Dynamics under Dripper Systems and their Impact on Plant Growth.....	45
Environmental and Agronomic Impacts of Leaching .....	46
EXPERIMENTAL OVERVIEW .....	47
MATERIALS AND METHODS .....	48
RESULTS .....	61
DISCUSSION .....	72
CONCLUSION .....	77
<b>CHAPTER 4 NITRATE ADSORPTION AND ITS CONSEQUENCES IN A RED FERROSOL     78</b>	
INTRODUCTION .....	78
LITERATURE REVIEW .....	78
Adsorption of Anions by Soils .....	78
Adsorption Isotherms .....	80
Methods for Measuring the Adsorption Isotherm .....	83
Column Studies to Measure Water and Solute Transport .....	87
THEORY OF WATER AND SOLUTE FLOW .....	88
Water Flow .....	89
Solute Flow .....	90
Initial and Boundary Condition s for Absorption Experiments .....	91
Boltzmann Substitution .....	92
The Piston Front and Solute Front .....	93
Location and Shape of the Solute Front .....	94
EXPERIMENTAL OVERVIEW .....	96
PART A – HORIZONTAL COLUMN AND BATCH EXPERIMENTS .....	97
Materials and Methods .....	97
Statistical Analysis .....	103

---

Results.....	105
Preliminary Discussion and Conclusions .....	113
<b>PART B – HORIZONTAL COLUMN EXPERIMENTS INVESTIGATING TFE</b>	
<b>DISPLACEMENT .....</b>	<b>114</b>
Materials and Methods .....	114
Results.....	118
Comparisons of Adsorption in the Red Ferrosol with Other Studies .....	129
<b>GENERAL DISCUSSION .....</b>	<b>131</b>
Isotherm Measurement.....	131
Fitting the Adsorption Isotherm.....	133
Significance of Nitrate Retardation.....	135
Experiment Assumptions.....	136
<b>CONCLUSION.....</b>	<b>137</b>
<b>CHAPTER 5   MODELLING WATER AND NITRATE MOVEMENT.....</b>	<b>138</b>
INTRODUCTION .....	138
LITERATURE REVIEW .....	138
Modelling Water and Solute Transport .....	138
EXPERIMENTAL OVERVIEW.....	140
MATERIALS AND METHODS .....	141
Measuring Soil Hydraulic Properties .....	141
Estimating Hydraulic Parameters for Hydrus .....	142
Simulating Horizontal Absorption of Water and Nitrate.....	143
Simulating Point Source Infiltration of Water and Nitrate .....	144
Simulating Line Source Infiltration of Water and Nitrate .....	148
Statistical Analysis.....	151
RESULTS.....	152
Model Validation: Horizontal Absorption.....	152
Model Validation: 3D Wedge Infiltration .....	156
Simulating Nitrate Distribution in the Field .....	161
DISCUSSION.....	171
Model Validation .....	171
Field Simulations .....	173

---

CONCLUSION.....	178
<b>CHAPTER 6 DISCUSSION .....</b>	<b>179</b>
CONCLUSIONS AND RECOMENDATIONS .....	187
REFERENCES .....	189
APPENDICES .....	207

---

## LIST OF TABLES

Table 2-1: Concentration of the nutrient solutions applied in the experiment .....	15
Table 2-2: Timetable of treatment applications.....	19
Table 2-3: Treatments applied to the soils. FC=Field Capacity. ....	19
Table 2-4: Concentration of the nutrient solutions applied in the trial. N was applied in the form of $\text{NO}_3^-$ .....	20
Table 2-5: Treatments applied in the glasshouse trial.....	22
Table 2-6: Nutrient solutions applied to the plants. ....	23
Table 2-7: Tuber numbers at the first four plant assessments for individual plants. NA indicates the plant did not emerge and was not measured. ....	25
Table 2-8: Distribution of total $\text{NO}_3^-$ in each sampling section of the column and leachate.....	33
Table 2-9: Mass balance calculations of total $\text{NO}_3^-$ added to the soil columns. Values in parentheses indicate the standard deviation of measurements. Due to the size of the values the amounts are presented in $\text{mmol}_c (\mu\text{mol}_c \times 10^3)$ .....	34
Table 2-10: Soil $\text{NO}_3^-$ concentration and at the completion of the treatment application and average tuber mass measured 14 days after treatment application. Values in parentheses indicate the standard deviation of measurements. ....	36
Table 2-11: Tuber and stem number and stem mass. Values with different symbols are significant to the ( $P < 0.05$ ) levels as calculated from the LSD. Values in parentheses indicate the standard error of the mean.....	37
Table 3-1: Basic soil properties for the Red Ferrosol field soil described according to the Australian soil classification (Isbell 1996a).....	48
Table 3-2: pH and EC of the 0–10 cm soil layer (methods 4A1, 4B1 and 3A1; Rayment and Higginson 1992).....	49

---

Table 3-3: Concentrations of macro nutrients in the 0–10 cm topsoil at the experiment site prior to fertiliser application (methods L1b, L2b, L3b, L4b, 9C1 Rayment and Higginson 1992). .....	49
Table 3-4: Exchangeable cations and the total cation exchange capacity (CEC) in the 0-10 cm layer of the field soil (15D3 method for Ca, Mg, Na and K (Rayment and Higginson 1992) and Barium Chloride-Triethanolamine method for exchangeable hydrogen (Peech <i>et al.</i> 1962)).....	49
Table 3-5: Soil organic carbon percentages down the soil profile .....	50
Table 3-6: Clay mineralogy of the Ref Ferrosol soil profile. ....	51
Table 3-7: Particle size analysis measured down the profile after treatment for organic matter or both organic matter and Fe and Al oxides.....	52
Table 3-8: Field experiment layout.....	53
Table 3-9: Fertiliser banded at planting .....	55
Table 3-10: Fertiliser applied post planting .....	55
Table 3-11: Nitrate, water application and rainfall during the trial. Irrigation applications for the leaching treatments are shown in Table 3-12. ....	56
Table 3-13: Time of treatment application and sampling for each variety (DAE = days after emergence). Emergence was calculated as the time when 90% of plants in each variety had emerged .....	57
Table 3-14: Details of plant emergence in the field compared to a glasshouse experiment. ....	61
Table 3-15: Tuber and stem measurements 14 days post treatment application. No statistical significance was measured between treatments within potato varieties. Values in parentheses indicate the standard deviation of the mean.....	68
Table 3-16: Tuber and stem measurements at plant maturity. No statistical significance was measured between treatments within potato varieties. Values in parentheses indicate the standard deviation of the mean. ....	69

Table 4-1: Symbols used in equations. ....	88
Table 4-2: Soil chemical and physical properties for the surface soil (0-15 cm depth). .....	98
Table 4-3: Details for individual column experiments. $\rho$ is the bulk density ( $\text{g cm}^{-3}$ ), $\theta_i$ is the initial column water content, $\theta_0$ is the water content at $x=0$ , $t>0$ . Values in parentheses represent the standard deviation of the mean. ....	99
Table 4-4: Root mean square error (RMSE) and $R^2$ values for the different isotherm equations fitted to the batch data using direct or linear fitting models. The Langmuir and Freundlich isotherms were fitted either directly using SAS (version 9.1, 2003) or by derivation using the linear form of the isotherm equations (4-2 and 4-4). ....	110
Table 4-5: Details for individual column experiments in Part B. Symbols are described in. ....	114
Table 4-6: Root mean square error (RMSE) and $R^2$ values for the different isotherm fitting methods fitted to the TFE isotherm. The Langmuir and Freundlich isotherms were fitted either directly using SAS (version 9.1, 2003) or by derivation with the linear form of the isotherm equations (4-2 and 4-4). ....	124
Table 4-7: Mean inflowing solution concentration and soil solution $\text{NO}_3^-$ concentrations near the inlet of the column ( $X < 0.01 \text{ cm s}^{-1/2}$ ) for the batch and TFE isotherms. ....	125
Table 4-8: Summarised soil properties for three example isotherms shown in Figure 4-12. ....	130
Table 5-1: Inverse optimizations conducted in Hydrus 1D. Each optimisation scenario was conducted with and without soil moisture retention values included in the inverse data set. Ticks indicate optimised parameters while X indicates the parameters were set for each scenario. In all procedures $\alpha$ , $n$ , and $l$ were set to values from the 12 default soils in the Hydrus soil catalogue. ....	143
Table 5-2: Bulk density of the Red Ferrosol soil profile measure in the field. ....	150
Table 5-3: Parameter estimation results for the best inverse parameters. Values in parentheses indicate the 95 % confidence intervals of the fitted parameters. ....	152
Table 5-4: Root mean square error (RMSE) of the fit of the predicted water and $\text{NO}_3^-$ profiles in comparison to the measured data in the horizontal column experiments	

---

presented in Figure 5-7 using the *Fit All* and *Fit All (ret)* parameter sets. The “measured” RMSE values in the table indicate the variation in the measured data calculated from the columns from Part B of Chapter 4 where two  $\text{NO}_3^-$  and water measurements were made at identical points in the columns..... 156

Table 5-5: Root mean square error (RMSE) of the fit of the two parameter sets used to predict water and  $\text{NO}_3^-$  distribution in the wedge experiments. The “measured” RMSE values in the table indicate the variation in the measured data calculated from the wedge experiments from Irrigation Scenario B columns where two  $\text{NO}_3^-$  and water measurements were made at identical points in the wedges..... 158

---

## LIST OF FIGURES

Figure 2-1: Fitted curves for actual measurements of tuber number per stem at each sample time. Vertical lines indicate times at which 10 and 80% of the total tuber number were formed. ....	27
Figure 2-2: Tuber number per stem. Error bars represent the standard error of the mean. ....	28
Figure 2-3: Total tuber mass per stem Error bars represent the standard error of the mean. ....	28
Figure 2-4: Average individual stem mass. Error bars represent the standard error of the mean. ....	29
Figure 2-5: Soil $\text{NO}_3^-$ concentrations (Chart A) and water content (Chart B) in the washed fine sand after the $\text{NO}_3^-$ pulse and water applications Table 2-3. Horizontal error bars represent the standard error of the mean. FC = field capacity. ....	31
Figure 2-6: Soil $\text{NO}_3^-$ concentrations (Chart A) and water content (Chart B) in the Red Ferrosol after the $\text{NO}_3^-$ pulse and water applications Table 2-3. Horizontal error bars represent the standard error of the mean. FC = field capacity. ....	32
Figure 2-7: Tuber size distribution in the Washed Sand (Chart A) and Red Ferrosol soil (Chart B). Error bars represent the standard error of the mean. ....	38
Figure 3-1: Soil bulk density. Error bars represent the standard error of the mean....	51
Figure 3-2: Soil $\text{NO}_3^-$ ( $\mu\text{mol}_\text{c} \text{ cm}^{-3}$ oven dry soil) under the centre of the mound in the Bintje (Chart A) and Markies (Chart B) potato cultivars in the Constant N and N Leach treatments. Error bars represent the standard error of the mean. ....	63
Figure 3-3: Soil $\text{NO}_3^-$ ( $\mu\text{mol}_\text{c} \text{ cm}^{-3}$ oven dry soil) in the Russet Burbank variety under the centre of the mound (Chart A) and in the inter-row space (Chart B) in the constant N and N Leach treatments. Error bars represent the standard error of the mean. ....	64
Figure 3-4: Soil $\text{NH}_4^+$ ( $\mu\text{mol}_\text{c} \text{ cm}^{-3}$ oven dry soil) under the centre of the mound in the Bintje (Chart A) and Markies (Chart B) potato cultivars in the Constant N and N Leach treatments. Error bars represent the standard error of the mean. ....	65



---

Figure 3-5: Soil  $\text{NH}_4^+$  ( $\mu\text{mol}_\text{c} \text{ cm}^{-3}$  oven dry soil) in the Russet Burbank variety under the centre of the mound (Chart A) and in the inter-row space (Chart B) in the constant N and N Leach treatments. Error bars represent the standard error of the mean. .... 66

Figure 3-6: Percentage of tubers in selected size ranges in the variety Bintje at the first sample time. Error bars represent the standard error of the mean. .... 70

Figure 3-7: Percentage of tubers in selected size ranges in the variety Bintje at the second sample time. Error bars represent the standard error of the mean. .... 71

Figure 4-1: Water profile indicating the sorptivity ( $a+b$ ) and the piston front  $X^*$  where  $c=b$ . .... 93

Figure 4-2: Diagram showing how the position of the solute front,  $X_s$  ( $\text{cm s}^{-1/2}$ ), is estimated where areas  $a$  and  $b$  are equal. .... 95

Figure 4-3: Volumetric water content profiles  $\theta_v$  ( $\text{cm}^3 \text{ cm}^{-3}$ ) for the horizontal columns. Chart A shows the profiles plotted against horizontal distance,  $x$  (cm) and Chart B shows the profiles plotted against the Boltzmann variable,  $X$  ( $\text{cm s}^{-1/2}$ ). The solid vertical line in Chart B indicates the location of the piston front calculated with equation 4-23 ( $X=0.22 \text{ cm s}^{-1/2}$ ). .... 106

Figure 4-4: Total  $\text{NO}_3^-$  profiles in the horizontal columns ( $\mu\text{mol}_\text{c} \text{ NO}_3^- \text{ cm}^{-3}$  oven dry soil). Chart A shows the profiles plotted against horizontal distance,  $x$  (cm) and Chart B shows the profiles plotted against the Boltzmann variable,  $X$  ( $\text{cm s}^{-1/2}$ ). The solid vertical line in Chart B indicates the location of the piston front ( $X=0.22 \text{ cm s}^{-1/2}$ ) and the dashed line indicates the location of the solute front ( $X=0.19 \text{ cm s}^{-1/2}$ ). .... 107

Figure 4-5: The Langmuir equation fitted to the batch adsorption isotherm data. The dotted line indicated the 95% confidence intervals of the curve fit. The diluted column indicates that the batch measurements follow the same trend at the lower solution concentrations measured in the horizontal column experiments. .... 110

Figure 4-6: Solution  $\text{NO}_3^-$  profiles calculated from batch adsorption isotherms plotted against the  $X$  coordinate ( $\text{cm sec}^{-1/2}$ ) for solution (Chart A) and adsorbed (Chart B)  $\text{NO}_3^-$ . The solid vertical line indicates the position of the piston front ( $0.22 \text{ cm sec}^{-1/2}$ ) and the dashed line indicates the location of the solute front ( $0.19 \text{ cm sec}^{-1/2}$  for  $C_w$  and  $0.21 \text{ cm sec}^{-1/2}$  for  $C_a$ ) for the  $\text{NO}_3^-$  profiles. .... 112

Figure 4-7: Diluted column volumetric water content ( $\text{cm}^3 \text{ cm}^{-3}$ ) and total  $\text{NO}_3^-$  ( $\mu\text{mol}_\text{c} \text{ NO}_3^- \text{ cm}^{-3}$  soil) profiles plotted against the Boltzmann variable ( $\text{cm sec}^{-1/2}$ ). The solid vertical line indicates the position of the piston front ( $0.21 \text{ cm sec}^{-1/2}$ ) and

---

---

the dashed line indicates the location of the solute front ( $0.18 \text{ cm sec}^{-1/2}$ ) for the total  $\text{NO}_3^-$  profile..... 119

Figure 4-8: TFE column volumetric water content ( $\text{cm}^3 \text{ cm}^{-3}$ ) and total  $\text{NO}_3^-$  ( $\mu\text{mol}_c \text{ NO}_3^- \text{ cm}^{-3} \text{ soil}$ ) profiles plotted against the Boltzmann variable ( $\text{cm sec}^{-1/2}$ ). The solid vertical line indicates the position of the piston front ( $0.21 \text{ cm sec}^{-1/2}$ ) and the dashed line indicates the location of the solute front ( $0.18 \text{ cm sec}^{-1/2}$ ) for the total  $\text{NO}_3^-$  profile. .... 121

Figure 4-9: Isotherms from the TFE columns (Chart A) and the Batch experiments (Chart B) plotted against the diluted column data from part B. The solid line represent the Langmuir equation fitted to the TFE or batch data using SAS (version 9.1, 2003) and the dashed lines indicate the 95% confidence intervals of the fitted equation. The round symbols represent the diluted column data from Part B. These values were not included in the isotherm fit..... 123

Figure 4-10: Solution  $\text{NO}_3^-$  profiles calculated from the TFE and batch adsorption isotherms plotted against the  $X$  coordinate ( $\text{cm sec}^{-1/2}$ ) for columns from Part A (Figure A), and Part B (Figure B). The solid vertical line indicates the position of the piston front ( $0.21 \text{ cm sec}^{-1/2}$ ) and the dashed line indicates the location of the solute front ( $0.18 \text{ cm sec}^{-1/2}$ ) for the solution  $\text{NO}_3^-$  profile..... 126

Figure 4-11: Adsorbed  $\text{NO}_3^-$  profiles calculated from the TFE and batch adsorption isotherms plotted against the  $X$  coordinate ( $\text{cm sec}^{-1/2}$ ) for the column data from Part A (Figure A), and Part B (Figure B). The solid vertical line indicates the position of the piston front ( $0.21 \text{ cm sec}^{-1/2}$ ) and the dashed line indicates the location of the solute front ( $0.19 \text{ cm sec}^{-1/2}$ ) for the adsorbed  $\text{NO}_3^-$  profile. .... 128

Figure 4-12: Comparisons of adsorption isotherms. Chart A: The Red Ferrosol from this study and isotherms described by Black and Waring (1976c) and Duwig *et al.* (2003). Chart B: The Red Ferrosol from this study and the isotherm reported by Katou *et al.* (1996). .... 130

Figure 4-13: The linear plot of the Langmuir isotherm (equation 4-4) for the diluted column data from Part A and B (Figure A) and the TFE column data (Figure B)... 134

Figure 5-1: Diagram and photograph of the wedge. .... 144

Figure 5-2: Schematic showing the two irrigation scenarios applied t the wedge columns. .... 145

Figure 5-3: A typical sampling pattern for the wedge column. The dots indicate the centre of the sample (2 cm diameter)..... 146

---

Figure 5-4: Geometry of the 2D axi-symmetrical vertical flow domain in Hydrus 2D. Horizontal and vertical transects and their symbols correspond to the water and solute profile plots in Figure 5-8 and Figure 5-9. ....	148
Figure 5-5: Boundary and initial concentrations in the soil. Chart A shows the variable flux boundary (purple area) applied to simulate the dripper application and the atmospheric boundary (green area) for simulation of overhead irrigation. Chart B shows the initial soil solution concentration prior to any leaching. The initial soil solution $\text{NO}_3^-$ concentrations ( $\mu\text{mol}_\text{c} \text{ cm}^{-3}$ ) were based on the untreated control from the field experiment measured directly below the drip tape. ....	149
Figure 5-6: The moisture retention curves of the <i>Fit All</i> and <i>Fit All (ret)</i> parameters sets plotted against the measured soil moisture retention data. ....	153
Figure 5-7: Fit of <i>Fit All</i> (solid line) and <i>Fit All (ret)</i> (dotted line) parameters to the measured water profile data (square symbols) from columns in Part B of Chapter 4 not included in the inverse parametisation (Figure A) and soil solution $\text{NO}_3^-$ data from all horizontal columns from Chapter 4 (square symbols; Figure B). The soil hydraulic properties were fitted to the water contents of column from Part A in Chapter 4 and were therefore not included in the figures. The predicted lines are from a single infiltration time (70 minutes). ....	155
Figure 5-8: Horizontal and vertical transects of water content ( $\text{cm}^3 \text{ cm}^{-3}$ ) in the wedge columns. The symbols indicate measured points, the solid line represents simulations using the <i>Fit All</i> inverse parameters and the dotted line represents simulations using the <i>Fit All (ret)</i> parameters. Figures A to D show transects from irrigation scenario A (2hr experiment; Figure 5-2) and figures E to G; transects from irrigation scenario B (24hr experiment; Figure 5-2). The location of these transects is shown in Figure 5-4. ....	159
Figure 5-9: Horizontal and vertical transects of soil solution $\text{NO}_3^-$ concentration ( $\mu\text{mol}_\text{c} \text{ cm}^{-3}$ ) in the wedge columns. The symbols indicate measured points, the solid line represents simulations using the <i>Fit All</i> parameters and the dotted line represents simulations with the <i>Fit All (ret)</i> parameters. The $\text{NO}_3^-$ reaction parameters were included in all the simulations. Figures A to D show transects from irrigation scenario A (2hr experiment; Figure 5-2) and figures E to G; transects from irrigation scenario B (24hr experiment; Figure 5-2). The location of these transects is shown in Figure 5-4. ....	160
Figure 5-10: Vertical $\text{NO}_3^-$ distribution both measured in the field trial and simulated in Hydrus. The leached data represents concentrations after the initial 26 mm application and two subsequent 7.5 mm applications over the following 7 days prior to assessment of $\text{NO}_3^-$ concentrations (Table 5-3). ....	161

---

Figure 5-11: Simulated water and  $\text{NO}_3^-$  distribution in the Red Ferrosol from the field experiment after 120 mm of irrigation. Figure A and B show the simulated water and  $\text{NO}_3^-$  distribution through the drip system and Figure C and D show the simulated water and  $\text{NO}_3^-$  distribution through an overhead irrigation system after the equivalent water applications. The shaded area of the profile indicates the root zone estimated from field observations..... 165

Figure 5-12: Simulated  $\text{NO}_3^-$  distribution in the Red Ferrosol from the field experiment after 325 mm of irrigation through contrasting irrigation systems. Figure A shows the simulated  $\text{NO}_3^-$  distribution through the drip system, Figure B shows distribution using and overhead irrigation system and Figure C shows the distribution when a second drip line is placed on the soil surface in the inter-row space. The shaded area of the profile indicates the root zone estimated from field observations. .... 167

Figure 5-13: Simulated  $\text{NO}_3^-$  distribution in a contrasting sandy soil under conditions of the field experiment after 135 mm of irrigation. Figure A shows the simulated  $\text{NO}_3^-$  distribution through the drip system. Figure B shows the distribution after irrigation through an overhead irrigation system. Figure C shows the  $\text{NO}_3^-$  distribution after water application through the drip system at a rate of  $400 \text{ cm}^3 \text{ hr}^{-1}$  in comparison to  $1200 \text{ cm}^3 \text{ hr}^{-1}$  in Figure A. Figure D shows the  $\text{NO}_3^-$  distribution after water was applied through the buried drip line and a second drip line sitting on the soil surface in the inter-row space. The shaded area of the profile indicates the root zone estimated from field observations..... 170

Appendix Figure 14: Volumetric water content (Figure A) and total  $\text{NO}_3^-$  content (Figure B) of the Acid Kurosol..... 208

Appendix Figure 15: Comparison of the Langmuir equation fit to the batch isotherm data using direct fitting in SAS (Figure A) and the linear fit method using equation 4-4 (Figure B). .... 211

Appendix Figure 16: Comparison of the Langmuir equation fit to the TFE isotherm data using direct fitting in SAS (Figure A) and the linear fit method using equation 4-4 (Figure B). .... 212

Appendix Figure 17: Comparison of the Freundlich equation fit to the batch isotherm data using direct fitting in SAS (Figure A) and the linear fit method using equation 4-2 (Figure B). .... 213

Appendix Figure 18: Comparison of the Freundlich equation fit to the batch isotherm data using direct fitting in SAS (Figure A) and the linear fit method using equation 4-2 (Figure B). .... 214

---

---

## LIST OF PLATES

Plate 2-1: Nutrient solution supply system to pots. Each of the four supply lines was connected to a single dripper for each pot.....	15
Plate 2-2: Red Ferrosol being collected from the field for laboratory and glasshouse trials.....	17
Plate 2-3: Vertical columns with flasks supplying water and conical flasks to capture leachate (PlateA) and Washed Sand column with outer PVC tuber removed showing plastic sheath which can be cut away during sampling (Plate B).....	18
Plate 3-1: Irrigation system in place prior to plant emergence.....	55
Plate 3-2: Presence tubers during one of the many tuberization assessments.....	58
Plate 3-3: Soil pit excavated for root observations and bulk density measurement. ..	59
Plate 3-4: Root density in the centre of the mound from augured samples at 0–20 cm depth (A), 20–40 cm depth (B) and 40–60 cm depth (C). .....	67
Plate 4-1: Soil column attached to the Mariotte bottle. ....	97
Plate 4-2: A soil column showing the position of the wetting front in the column. By releasing the clamp pressure and pushing down on the sections the column was rapidly divided. ....	100

# CHAPTER 1

## INTRODUCTION

Potatoes (*Solanum tuberosum*) are the largest vegetable production industry in Tasmania, Australia, accounting for 56% of the farm gate value and worth approximately 108 million dollars to the Tasmania economy (IRIS 2009). On a national scale, Tasmanian potato production accounts for approximately 25% of Australian production (IRIS 2009). The industry currently faces a major challenge due to competition in the processed potato sector from cheaper production countries, and is therefore examining options for increasing production efficiency. The availability of low cost, high quality seed tubers is an important component of processing potato crop production efficiency. This project was established in partnership with a major player in the Tasmanian seed production sector, Agronico Technology Pty Ltd, and was part of an ambitious plan to develop novel crop management techniques to increase seed crop productivity.

Seed potato production in Tasmania occurs predominantly in the northwest, the main processing potato production region, and utilises the basalt derived Red Ferrosol's favoured by vegetable crop producers throughout the state. Red Ferrosol's are the dominant cropping soil because of their moderate nutrient holding capacity, strong structure, rapid drainage and good water storage characteristics (Loveday and Farquhar 1958a). This soil type supports a significant proportion of Tasmania's potato production as well as the production of various other vegetable crops, dairy farming and forestry (Cotching and Wright 1994; IRIS 2009; Loveday and Farquhar 1958b). The development of novel methods to increase seed potato production efficiency may be more rapidly adopted if they are applicable to Red Ferrosol's, and this soil type was therefore the major focus of this study.

The production of quality potato seed is important since it is the basis for optimal crop production in the entire potato industry (Bus and Wustman 2007). In most cases potatoes are vegetatively propagated by planting a whole or cut potato tubers, known as potato seed (Struik and Wiersema 1999). This method of propagation is advantageous because each plant represents a plant clone and therefore plant traits are maintained between generations. Theoretically the potato crop can be continuously

---

regenerated from tubers retained from previous crops however continual propagation using this method leads to reductions in yield due to the build up of pathogens, particularly viruses. This is known as seed degeneration and can only be overcome by limiting the number of generations seed is multiplied in the field (Bus and Wustman 2007). The production of high yielding crops therefore relies on methods of producing and propagating seed tubers free from or low in disease.

The initial disease free clonal material use in seed production schemes is generally produced through tissue culture. Tissue cultured plants may then be grown under controlled environment conditions with exclusion of virus vectors to produce the initial supply of disease free tubers (Struik and Wiersema 1999). A common method used to produce disease free seed is production of minitubers in hydroponics. The term minitubers refers to tuber size since minitubers are smaller than conventional seed tubers (usually 0.5-2.5 cm; Struik 2007a). These tubers are grown from certified disease free tissue culture plantlets which can be rapidly multiplied and transferred into hydroponic systems for minituber production. A common hydroponic system used is the nutrient film technique (NFT; Lommen 2007). Production in hydroponics, particularly under an NFT system, facilitates sequential harvests of tubers from the plants which enables high yields from each hydroponic crop. The system also enables accurate control of nutrient and environmental conditions. By controlling these various factors plant growth can be manipulated to maximise tuber number and yield.

Manipulation of nutrient concentrations, hydroponic solution pH, light interception and daylength have all been used as techniques in hydroponic systems to control plant growth. Reducing  $\text{NO}_3^-$  availability to plants grown in hydroponics has been shown to stimulate tuberization and therefore provides a method of controlling the initiation of potato growth (Krauss 1980). By applying a pH shock plants in hydroponics 30 days after planting, Rolot and Seutin (1999) increased the number of tubers formed per plant. They were also able to increase tuber yield by increasing the supply of phosphorus 30 days after planting. Reductions in photoperiod by covering plants with black cloth was found to increase tuber yield during hydroponic production of seed tubers (Boersig and Wagner 1988). Artificial lighting is also used to extend daylength to delay tuberization to allow greater leaf area production following establishment when minitubers are grown in hydroponics under short days (Dr J

---



---

Hills, personal communication, 2007). Wurr *et al.* (1997) observed that maintaining temperature at 20 °C increased the number of stolons produced per plant in hydroponics and indicated that this could indirectly increase tuber number by increasing the number of sites for tuber growth. These examples indicate that the hydroponic system enables various factors that influence plant growth to be manipulated to maximise tuber number and yield per plant.

Minitubers produced under hydroponic conditions are planted in the field to produce the first field generation of potato seed. While the use of minitubers as propagules for the first field generation has become wide spread in the seed potato industry, one issue that has emerged with their use is the tendency for fewer tubers per plant to be produced compared to plants grown from traditional potato seed tubers (Struik 2007a). Because of the costs associated with production in hydroponics, a number of field generations are required to multiply the quantity of seed to produce sufficient amounts for commercial production. As long as the disease levels are low, and care is taken to minimise infection during production of each crop, a number of generations can be multiplied before disease levels have a significant impact on yield (Bus and Wustman 2007). Because the minituber crop represents the first of a number of multiplications, the low number of tubers produced can have a significant impact on the multiplication rate, increasing the number of field generations required to produce sufficient volumes of affordable seed and thereby increasing the risk of seed pathogen infection. Any techniques that can potentially increase the tuber number in these crops has the potential to reduce the number of subsequent multiplications required, improving efficiency and reducing the risks of pathogen accumulation in the seed.

The number of tubers formed on a potato plant is determined by the number of tuber formation sites (stolon tips) present on the plant, the percentage of these sites on which tubers initiate, and the percentage of initiated tubers that grow to maturity rather than being resorbed (Ewing and Struik 1992). Physiological age of the tuber is the primary factor determining tuber formation site number through its impact on stem number and plant vigour (Struik and Wiersema 1999). Physiological age can be influenced by treatment of the mother plant but is primarily influenced by chronological age and storage temperature (Struik 2007b). In an ideal scenario, minitubers are produced so that the most suitable physiological age is reached at the

---



---

time of planting. However, the grower does not always have control over the treatment of seed prior to purchase and therefore may require other techniques to maximise yield. Furthermore, the supplier may not be able to produce minitubers at the correct time to obtain the ideal physiological age for planting if demand is high, an occurrence that has increased in frequency with the possibility of year round production of hydroponic minitubers crops under controlled environment conditions. Investigation of other methods to increase tuber number to account for such issues and to complement this technique will help to maximise tuber numbers in crops grown from minitubers.

The first field generation grown from minitubers are small (area generally less than 1 ha), high value crops and as a result there is scope for intensive management to maximise productivity and yield. Some of the techniques applied in hydroponics to control plant development may potentially be adapted for use in a field scenario. The level of light interception and the temperature may be controlled to a limited extent in the field by adjusting planting date however the environmental conditions are far more variable in comparison to glasshouse production. Due to the soil buffering capacity, altering pH is also difficult and changes cannot be made rapidly (McBride 1994). There is however scope for manipulation of plant nutrient availability during growth. The manipulation of nutrients in a soil environment is however more difficult than in hydroponics. Rapid changes in nutrient supply are simple in hydroponics because changes in the concentration of the nutrient solution have a rapid effect on availability of the nutrient to the plant. In a field environment rapid changes, particularly reductions, in nutrient availability are more difficult due to the range of soil chemical and biological reactions that influence nutrient concentrations in the soil solution. Knowledge of these processes is thus required to successfully manipulate nutrient availability in a soil environment.

Manipulation of nutrients, specifically in the Red Ferrosol cropping soils of northwest Tasmania, may be a challenge because of the high organic carbon content of the soil. The organic carbon content contributes to the cation exchange capacity of the soil and supports greater microbiological activity that provides a source of nutrients due to its mineralisation (Isbell 1994; Jansson and Persson 1982). Furthermore, these soils may have a moderate anion exchange capacity (Isbell 1996b) as a result of their high kaolin clay content (40-80%) as well as high iron oxide contents (>5%). Each of

---

---

these factors will impact on soil nutrient concentration and mobility in the soil, and therefore an understanding of these processes in the Red Ferrosol soil will be required if effective strategies to precisely manage soil nutrients are to be developed.

There are a number of nutrients that have been shown to influence tuber initiation and growth that could potentially be used to increase tuber number. Calcium availability has been linked to tuberization and tuber number in potatoes. The presence of  $\text{Ca}^{2+}$  is required in growth media to enable tuberization in potato cuttings (Balamani *et al.* 1986). Calcium has also been found to influence tuber number and size in pot experiments (Ozgen and Palta (2004). Applications of calcium to soils already containing sufficient levels led to a reduction in tuber number however total tuber yield was not reduced. Simmons and Kelling (1987) also found improvement in tuber quality and yield as a result of  $\text{Ca}^{2+}$  application, however no data on tuber numbers was reported. Phosphorus has also been found to affect tuber number. Dubetz and Bole (1975) found higher phosphorus applications increased tuber number but not to the same extent as nitrogen applications in the same experiment. Allison *et al.* (2001) observe phosphorus was necessary to maximise leaf area, which in turn resulted in an increase in tuber production.

Despite other nutrients having been shown to influence tuber number in some studies, nitrogen (N) clearly stands out as the nutrient that has the largest impact on tuber initiation, growth and development in the potato plant (Ewing 1990; Krauss 1980; O'Brien *et al.* 1998). The majority of studies have been conducted in hydroponics with limited detailed study of the influence of N on tuber initiation and effects of varying levels of N on tuber growth rate. Field studies have predominantly focussed on N application rates rather than strategic nutrient control during growth (Belanger *et al.* 2001; Castro 1988; Choudhury *et al.* 1996). There is also evidence that N supply may influence the partitioning of assimilates in the potato plant, indicating potential for strategic N control to provide a technique for manipulating tuber development (Kursanov 1984; Oparka *et al.* 1987).

Based on the evidence from the literature, nitrogen was chosen as the nutrient to be examined in this study. Given the ambitious nature of the overall project objective, to develop a novel nitrogen management strategy to increase tuber number in first generation seed crops grown from minitubers, this study adopted a two pronged approach. Firstly, examination of tuber initiation and development following varying

---

---

nitrogen management treatments was undertaken to determine if the treatments may form the basis of an effective strategy to increase tuber number. Secondly, key soil processes were examined in order to model patterns of  $\text{NO}_3^-$  movement in Red Ferrosol soil under different soil conditions and irrigation application scenarios. The aim of this approach was to produce the background knowledge upon which further development of a novel crop management strategy based on nitrogen manipulation could be based.

The thesis is presented in seven chapters with Chapters 2 and 3 documenting glasshouse and field trials on the effects of  $\text{NO}_3^-$  and irrigation applications on tuber yield. Chapter 4 examines the movement of water and  $\text{NO}_3^-$  in Red Ferrosol surface soil and the adsorption of  $\text{NO}_3^-$  due to their anion exchange capacity. Chapter 5 examines the validation of the soil water model Hydrus and runs simulations of  $\text{NO}_3^-$  transport in the field. Chapters 6 provides a general discussion, review of the key findings, conclusion and recommendations for future research.

## CHAPTER 2

# EFFECTS OF NITROGEN AND SOIL TYPE ON TUBER INITIATION AND TUBER DEVELOPMENT

### INTRODUCTION

Laboratory and glasshouse experiments were undertaken to investigate aspects of nitrogen (N) availability on tuber formation, with the aim of developing a method of increasing tuber number through manipulating N availability to the plants. Treatments applied in these trials were selected based on useful lines of investigation identified in the literature. The influence of N on the timing of tuberization and the effect of reducing N availability at tuberization were investigated.

### LITERATURE REVIEW

#### Effects of Nitrogen on Tuberization

The effect of N supply on the timing of tuberization has been studied predominantly in hydroponic experiments with limited *in situ* laboratory, glasshouse and field experiments reported in the literature. These studies have used whole plants, cuttings, stolons and isolated buds to investigate the effect of N treatments on the tuberization process (Ewing and Struik 1992). O'Brien *et al.* stated that the earliest experiments on the effects of N were published by Werner in 1934. In these studies Werner found that limiting N supply to plants grown under long days and warm temperatures retarded shoot growth and led to acceleration of tuberization.

A large number of studies documenting tuberization responses to N supply in hydroponics were conducted in the 1970's by Adolf Krauss and his colleagues (Krauss 1978; 1980; 1985; Krauss and Marschner 1982). Whole plants were grown in nutrient solutions containing  $3.57 \mu\text{mol}_\text{c} \text{ N cm}^{-3}$  for approximately four weeks at 20°C and 12 hours day length. Whole plants or parts of the plants were then transferred to nutrient solutions containing no N. These plants immediately tuberized while those remaining in an N solution did not. If N was returned for an extended period to the induced plants, tuber growth was halted and stolon growth resumed.

---

Earlier studies also found  $\text{NH}_4^+$  to have the same effect (Krauss and Marschner 1976). In further experiments Sattelmacher and Marschner (1979) showed applications of N to plant leaves did not stop tuberization when it was withdrawn from the roots. Krauss (1985) suggested that the changes in N availability triggered tuberization via altering hormone levels in the plant. He also suggested the signal pathway was also likely to involve secondary messengers. The findings by Sattelmacher and Marschner (1979) indicated that the roots may be the source of the tuberization stimulus.

The effect of N on tuberization was variable in *in vitro* studies. Vecchio *et al.* (2004) found that the onset of tuberization on isolated buds was significantly accelerated when  $\text{NO}_3^-$  supply was interrupted in comparison to the constant N control. Koda and Okazawa (1983) found N depressed tuberization but only when sucrose concentrations in the growth medium were less than 4% while Ewing (1985) found that the presence of N in the growth medium improved tuberization. Ewing (1990) suggests that these differences are likely to be a result of the methods used. Although *in vitro* experiments may not be relevant to responses in whole plants, these and other studies (Jackson 1999; Xu *et al.* 1998) show sucrose supply was related to tuberization. From a whole plant perspective this may be related to carbohydrate supply. The effect of N may therefore be influenced by factors effecting carbohydrate production such as temperature, supply of other nutrients, light intensity and daylength.

The experiments conducted in hydroponic systems provided clear evidence that N can inhibit tuberization. However, when the studies conducted by Krauss and co-workers were repeated under higher light intensities, the influence of N on tuberization was found to be much smaller (Struik and Coster, year not stated, cited by Ewing and Struik (1992)). This finding supports the conclusion that the effects of N supply on tuberization may be modified by carbon assimilation and distribution patterns in the plant.

The significance of the findings from controlled environment studies for explaining field responses to N nutrition have been questioned in the literature. O'Brien *et al.* (1998) state that the early findings by Werner (1934) and later experiments in hydroponic media probably bear little relation to what may occur in crops under different husbandry and environmental conditions. Despite the interesting findings in

---

hydroponics, there appears to have been very little detailed work conducted in the field investigating effects of N supply on tuberization. The work conducted to date involved single large applications of fertiliser rather than the steady rate supplied in hydroponics. This limits the ability to compare field and glasshouse results. Radley (1963) conducted some of the earliest field work and reported that at high N application tuber initiation was delayed and tuber growth was slow relative to the two lower rates in the trial. O'Brien and Allen (1986) also reported that tuberization was delayed by high applications of N in the field. The same authors however found no such effect in later studies investigating the onset and duration of initiation when frequent sampling was employed to accurately measure the time of initiation (O'Brien *et al.* 1998). Both Ewing and Struik (1992) and O'Brien *et al.* (1998) highlight the necessity of large sample sizes, replication and frequent sampling in field trials due to site and plant variation. If sample size, number and frequency are low, the likelihood of measuring small differences between treatments is negligible.

It is clear that under some circumstances N can have a significant effect on tuberization in the plant. The influence of light intensity on plant responses in hydroponics and sucrose concentrations in *in vitro* studies indicates that growing conditions will influence the N effects. Studies from field experiments generally indicate that tuberization is not delayed significantly by N supply however there is some evidence to the contrary. Factors such as deficiencies in the sampling strategy or an overriding effect of other factors, particularly those impacting on carbon metabolism, may be masking effects of N supply particularly if the delay is only small.

### **Carbohydrate Regulation of Tuber Initiation and Growth**

Carbohydrates have been implicated in the regulation of tuber initiation and may play a direct role in the tuberization stimulus. Xu *et al.* (1998) found plant cuttings grown in nutrient media only tuberized when the sucrose concentration was above 2%, with the number of stolons tuberizing increasing with higher sucrose availability. Peterson and Barker (1979) also showed plant cuttings required sucrose to tuberize in *in vitro* experiments. If the results are extrapolated to whole plants, these findings indicate that increasing carbohydrate supply to tubers may provide a way of increasing the tuberization stimulus and increasing the number of tubers set on the plant.

---

Nitrogen availability can influence the distribution of carbohydrates in the potato plant. Sweetlove *et al.* (1998) showed that reactions occurring in the leaf cells prior to loading into the phloem was responsible for a least 80% of the control of carbon flux from the source to the sink in potatoes. In a following study Sweetlove and Hill (2000) found that restricting N supply to the plant further increased the control of assimilate distribution by the source to 90%. They hypothesised that this was due to limited N reducing the capacity of photosynthetic enzymes. Kursanov (1984) suggested that when N deficiency first occurs, there is no change in the rate of phloem loading and transport in the plant but rather a suppression of meristem growth. The reduction in assimilate production by the leaves due to N deficiency may therefore not be immediate and assimilate may therefore be metabolised by storage organs rather than vegetative areas of the plant. Oparka *et al.* (1987) reported that high N supply reduced the export of carbohydrates to the tubers and instead retained assimilate in the leaf and increased partitioning to the stem. Kursanov (1984) explains that when N is in high supply, shoots and roots are stimulated to grow and therefore begin to consume more carbohydrates themselves. Competition for assimilates therefore increases and supply to storage organs is reduced.

The effect of N supply on final tuber number may be related to the supply of carbohydrate to the tubers. O'Brien *et al.* (1998) found that as long as N supply was sufficient to maximise leaf area then maximum tuber set was achieved. If N was limiting during early vegetative growth, tuber number was restricted. The benefit of N supply on tuber number has also been reported by Sharma and Ezekiel (1993) and Painter and Augustin (1976) who both reported increases in tuber number as a result of higher N fertiliser applications. Roberts *et al.* (1982) reported similar results in pot trials where tuber numbers were lower in plants receiving N after tuberization compared those that had N from planting. They hypothesised that a sufficient supply of N is desired to stimulate tuberization during early growth. If the mechanism described by O'Brien *et al.* (1998) is correct, the lower tuber number observed in the study by Roberts *et al.* (1982) may not have been a direct effect of low N availability. The observed result may instead have resulted from the lower N supply restricting leaf area. This would have reduced assimilate production in the plant and thus limited tuber set. The positive effect of N on tuber number through increased photosynthetic capacity is further supported by Sweetlove and Hill (2000). They

---



---

suggest that the limiting factor in tuber growth is the supply of carbohydrates to the stolons, linked to plant photosynthetic capacity, rather than a regulatory system limiting tuber uptake of carbohydrates.

Although the general consensus in the literature is that N application to potatoes has a positive effect on tuber number, there is also evidence that increasing N supply can be detrimental to tuber number (Dubetz and Bole 1975; Roberts *et al.* 1982; Sommerfeldt and Knutson 1968). However it is likely that the negative effect of N reported by these authors was due to excess application. Belanger *et al.* (2002), O'Brien *et al.* (1998) and O'Brien and Allen (1986) all observed that increasing N applications was beneficial to tuber number up to a certain application rate after which tuber number and mass decreased. Low N will limit leaf area and subsequently the supply of assimilates to the tubers. High N will increase competition for carbohydrates because stems and leaves which are stimulated to grow under conditions of high N (Kursanov 1984).

Tuber resorption can have a significant impact on the number of tubers retained at harvest. Tubers may also be resorbed if demand for assimilate by other tubers or plant organs is strong. Cho and Ifanti (1983) found that resorption in the variety Russet Burbank was 23-40% and 30-40% in the 1979 and 1980 seasons respectively (estimations by Ewing and Struik (1992) from graphical data). Studies by Burstall *et al.* (1987) found that at approximately 21 weeks after planting the number of tubers >1 cm was related to the final number of tubers suggesting that anything under that size at the sampling time was later resorbed. The process of resorption is particularly undesirable in seed potato crops since a larger number of smaller tubers are desired. Maximising the supply of assimilates to tubers throughout the life of the plant is therefore critical in maximising tuber number.

The variation in the tuber response to N supply indicates that N supply must be carefully managed to ensure tuber set is maximised. The correct N supply will ensure maximum crop photosynthetic capacity. A balance is also required so competition from the stems and leaves for carbohydrates is not too high. Possible strategies for maximising tuber number are discussed below.



---

**A New Method for Increasing Tuber Number and Yields?**

Considering the findings of O'Brien *et al.* (1998), Oparka *et al.* (1986) and Kursanov (1984), it appears that if tuber number and yield are to be maximised supply of N needs to be controlled during two stages of growth: i) the time between plant emergence and tuberization and; ii) after tuberization has commenced. Prior to tuberization, N supply needs to be sufficient to ensure complete canopy ground coverage so the crop reaches its maximum photosynthetic ability. Once tuberization has commenced, N supply needs to be reduced to a level where it will not restrict supply of carbohydrates to the tubers by increasing competition from above ground plant organs. Simply applying sufficient N early in plant growth and allowing concentrations in the soil to decrease through plant uptake may help to achieve full tuber set and reduce any detrimental effects of high N during tuber growth. However the correct application of N in a treatment such as this may be difficult because factors such as soil type, temperature, irradiance and moisture supply will influence how quickly N rates decline. Concentrations may therefore drop too rapidly restricting leaf area expansion, or alternatively concentrations may remain at a level after tuberization that restricts carbohydrate translocation to the tubers. Both of these scenarios would have the potential to reduce the number of tubers set and tuber yield.

An alternative technique which may be possible under a situation of intensive management and monitoring would involve luxury N supply throughout the period of early crop growth. At the onset of tuber initiation N would be rapidly lowered to encourage partitioning of carbohydrates to the tubers. This strategy would involve leaching N from the root zone with an extended irrigation application. The practical and environmental aspects of this technique would have to be considered, however on a small scale in high value first generation seed crops a technique such as this which could increase the number of tubers set and increase tuber growth may be a viable option.

There has been a large volume of work published on N movement in soils, most of which consider the negative impacts that N leaching can have on both agricultural productivity and the environment (Keeney 1982; Stevenson 1985)<sup>1</sup>. Since soil type has a strong influence on N movement, information available in the literature cannot

---

<sup>1</sup> The environmental impacts of nitrogen leaching are discussed in chapter 3

---

give an accurate figure for how N will move in relation to water applications in soils chosen for this project.

Previous studies conducted by Zhou *et al.* (2006) and Black and Waring (1976c) investigated the movement of  $\text{NO}_3^-$  through soil columns. They observed movement of a pulse of  $\text{NO}_3^-$  through soils packed at a uniform density. A range of water volumes were applied following the solute application. The columns were then sectioned and water and  $\text{NO}_3^-$  concentrations were measured. This simple method provides a way of observing any impediment of N movement in soil water due to interactions with soil chemistry. It is appropriate methodology for predicting N movement in glasshouse pot trials since the soils used in both experiments is disturbed and repacked.

## EXPERIMENTAL OVERVIEW

The objective of the trials described in this chapter was to investigate the effects of soil N concentration on the onset of tuberization and subsequent tuber growth. The two factors tested were the effect of high N supply on the timing of tuber initiation and the effect of rapidly lowering N supply at the start of tuberization.

## MATERIALS AND METHODS

Three glasshouse experiments and a laboratory experiment were undertaken. The first glasshouse experiment investigated the effect of high N supply on the timing of tuber initiation. The second glasshouse experiment examined the influence of soil type on the time of potato emergence and tuberization. The laboratory experiment investigated the movement of  $\text{NO}_3^-$  through soils following irrigation application. The third glasshouse experiment tested the effect of leaching N from the plant root zone at the start of tuberization.

### **Tuber Initiation and Tuber Growth: The Influence of High N Supply**

The objectives for this glasshouse experiment were to observe the effect of a high N supply on the timing of tuber initiation and subsequent tuber growth and development.

#### ***Trial Design and Treatment Application***

The trial was a randomised block design with 5 replicates and two treatments; low soil N concentration and high soil N concentration. Plants were grown from minitubers planted at a depth of 15 cm in 10 L pots. Plants were grown in a sand/perlite media mixed in a 7:3 ratio. Both the high N and low N treatments received  $220 \text{ cm}^{-3}$  applications of nutrient solution every 5 hours (Table 2-1). The nutrient solution was applied at  $2000 \text{ cm}^3 \text{ hr}^{-1}$  through a dripper system with four output points distributed across the pot surface (Plate 2-1).

**Table 2-1:** Concentration of the nutrient solutions applied in the experiment

Nutrient	Trt 1-low N ( $\mu\text{mol}_\text{c} \text{ cm}^{-3}$ )	Trt 2-high N ( $\mu\text{mol}_\text{c} \text{ cm}^{-3}$ )
N <sup>1</sup>	0.71	10.71
P	1.94	1.94
K	7.61	7.61
Ca	5.28	5.28
Mg	2.06	2.06
Mn	0.02	0.02
Cu	0.0003	0.0003
B	0.0093	0.0093
Fe	0.07	0.07
Mo	0.0002	0.0002
Zn	0.0072	0.0072
S	5.02	5.02
Cl	9.86	0.99

<sup>1</sup>N was applied in the form of  $\text{NO}_3^-$



**Plate 2-1:** Nutrient solution supply system to pots. Each of the four supply lines was connected to a single dripper for each pot.

---

### *Assessments and Analysis*

Plants were sampled at ten time intervals: 10, 14, 18, 22, 26, 30, 34, 38, 42 and 70 days after emergence. Five plants were sampled from each treatment at each sampling date. Tuber and stem number and mass were measured for each sampled plant as well as stem length. Soil samples were taken at day 36 from the sampled pots and analysed for mineral  $\text{NO}_3^-$  and  $\text{NH}_4^+$ . This was converted to  $\text{NO}_3^-$  and  $\text{NH}_4^+$  per unit volume of soil,  $\Gamma$  ( $\mu\text{mol}_\text{c} \text{ N cm}^{-3}$  soil), using equation 2-1:

$$\Gamma = \frac{C_k V_s}{V_{od}}, \quad 2-1$$

where  $C_k$  is the concentration of the KCl extract ( $\mu\text{mol}_\text{c} \text{ N cm}^{-3}$ ),  $V_s$  is the total volume of solution in the soil sample during extraction ( $\text{cm}^3$ ) and  $V_{od}$  is the volume of oven dry soil in the sample ( $\text{cm}^3$ ) calculated from the mass of soil and the bulk density of the in situ soil.

The commencement and completion of tuberization were calculated as the time when 10 and 80% of the total population of tubers formed per stem were present respectively according to the method described by O'Brien *et al.* (1998).

The number of plants measured (replicates) at each sampling interval was restricted due to the high frequency recommended by O'Brien *et al.* (1998) to obtain a satisfactory estimation of the onset and period of tuberization. Because of the limited sample size the data set was expanded mathematically using the bootstrap method which involves randomly sampling the data a chosen number of times (Davison and Hinkley 1997). The data was sampled 1000 times for the bootstrapping calculation in this experiment. This technique provides a prediction of results obtained from a larger sample size and also allows confidence intervals for the data to be calculated.

Analysis of variance was used for analysis of tuber and stem number (Tukey-kramer multiple comparisons analysis).

### **Vertical Column Leaching Studies**

The column studies were conducted to measure the rate of  $\text{NO}_3^-$  movement through two soil types to be used in glasshouse trials. Results were then used to predict the amount of water required to leach N from pots in the glasshouse experiment. A Red

---

Ferrosol, Acid Kurosol and washed sand were used in the experiment. The Kurosol soil was not included in the glasshouse trial and therefore parameters and results are presented in Appendix 1.

### ***Soil Preparation and Parameterisation***

Topsoil samples (0-15 cm) of a Red Ferrosol were collected from a field site in Sulphur Creek, Tasmania (Plate 2-2). Soil was collected from a site that had been under pasture for the last 15 years. The washed fine sand was sourced from Males Sands Ltd in South Hobart, Tasmania. Collected soils were air dried at 20° C, sieved to less than 2.0 mm diameter and stored.



**Plate 2-2:** Red Ferrosol being collected from the field for laboratory and glasshouse trials

Prior to conducting the column studies, field capacity, particle density and porosity were calculated for the soils. Field capacity was measured by wetting and sealing a soil column the same as those described below and allowing redistribution for 48 hours. Subsamples were then taken from sections 5 cm below the soil surface and oven dried to calculate water content. Particle density was calculated using the pycnometer method described by (Loveday 1974). Porosity was calculated from the bulk density and the particle density (McKenzie *et al.* 2002).



---

### ***Soil Column Details and Treatment Application***

Soil columns were constructed from 90 mm diameter PVC pipe and were 40 cm in length. The columns were lined with clear plastic overhead sheets to enable the soil to be easily sampled in 5 cm layers (Plate 2-3). The base of the column was sealed with 0.25 mm mesh held in place by a perforated end cap. Columns were packed to a bulk density of  $0.93 \text{ g cm}^{-3}$  for the Red Ferrosol and  $1.45 \text{ g cm}^{-3}$  for the washed fine sand by gentle tapping and shaking of the columns.

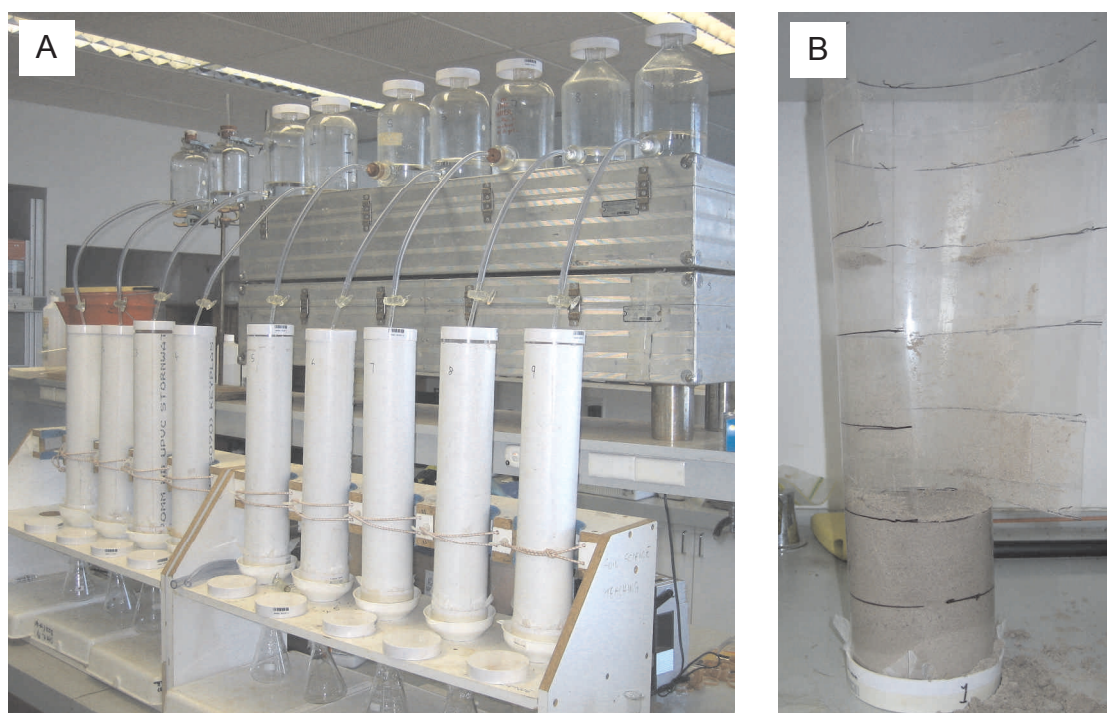


**Plate 2-3:** Vertical columns with flasks supplying water and conical flasks to capture leachate (Plate A) and Washed Sand column with outer PVC tuber removed showing plastic sheath which can be cut away during sampling (Plate B).

All treatments were applied at  $100 \text{ cm}^3 \text{ hr}^{-1}$  through burette taps connected to reservoirs. The experiment was carried out in a series of steps (Table 2-2) with treatment details presented in Table 2-3. Nitrate was applied in a  $50 \text{ cm}^3$  pulse of concentrate solution ( $485.7 \mu\text{mol}_\text{c} \text{ cm}^{-3} \text{ NO}_3\text{-N}$ ) to represent a field application rate of  $530 \text{ kg N ha}^{-1}$ , approximately double a typical basal application of fertilizer in potatoes (Sparrow and Chapman 2003).

**Table 2-2:** Timetable of treatment applications

Day	Activity
1	Soil wet to Field capacity (Table 2-3)
3	50 ml NO <sub>3</sub> <sup>-</sup> pulse applied
5	Leaching solutions applied
8	Columns sampled

**Table 2-3:** Treatments applied to the soils. FC=Field Capacity.

Treatment	Soil	Soil field capacity (cm <sup>3</sup> cm <sup>-3</sup> )	Initial water application (cm <sup>3</sup> )	Leaching volume (cm <sup>3</sup> )	Pore volume applied
No Irrigation	Washed Sand	3.2	150	0	0
	Red Ferrosol	28.0	643	0	0
75% FC	Washed Sand	3.2	150	118	0.11
	Red Ferrosol	28.0	643	482	0.33
150% FC	Washed Sand	3.2	150	236	0.21
	Red Ferrosol	28.0	643	1016	0.69

### ***Sampling and Measurement***

Columns were sampled three days after the leaching applications. The outer PVC column was removed and the inner plastic was cut away to expose the soil (Plate 2-3B). Soil was sampled in 5 cm increments, mixed thoroughly and sub sampled for water content and mineral N determination. Water content was determined by oven drying for 48 hours at 105 °C. Samples for N analysis were shaken for one hour with a 2M KCl solution in a 1:5 soil to solution ratio to extract NO<sub>3</sub><sup>-</sup>. Samples were then centrifuged and decanted. The supernatant was analysed for mineral NO<sub>3</sub><sup>-</sup> by steam distillation (Rayment and Higginson 1992). This was converted to total NO<sub>3</sub><sup>-</sup> per unit volume of soil,  $T$  (μmolc NO<sub>3</sub><sup>-</sup> cm<sup>-3</sup> soil) using equation 2-1.

### **The Influence of Soil Type on Plant Emergence and Tuberization**

The objective of this experiment was to measure effects of soil type on the timing of plant emergence and tuber initiation of potatoes grown under long days.



---

### *Experimental Design and Treatment Application*

The experiment was a randomised block design with five replicates. Soil type represented the treatments in this experiment. Growing conditions were the same as those used in the High versus Low N experiment. The nutrient solution applied to the plants is shown in Table 2-4. To replicate day lengths plants would experience in the field lights were installed above the plants to extend day length to 15 hours each day.

**Table 2-4:** Concentration of the nutrient solutions applied in the trial. N was applied in the form of  $\text{NO}_3^-$ .

Nutrient	Solution concentration ( $\mu\text{mol}_\text{c} \text{ cm}^{-3}$ )
$\text{N}^\text{I}$	10.71
P	1.94
K	7.61
Ca	5.28
Mg	2.06
Mn	0.02
Cu	0.0003
B	0.0093
Fe	0.07
Mo	0.0002
Zn	0.0072
S	5.02
Cl	0.99

---

### *Assessments and Data Analysis*

Plants were sampled at six time intervals: 14, 18, 22, 26, 30 and 36 days after emergence. At each sampling time plants were inspected for the presence of tubers and, if present, the number and mass per stem were measured. Green stem number and mass were also recorded. Soil samples were taken at day 26 and analysed for major nutrients.

---

Analysis of variance was used for analysis of plant emergence (Tukey-kramer multiple comparisons analysis). The onset of tuberization was measured using logistical regression.

### **Effects of Reducing N availability at Tuberization on Tuber Set and Growth**

The objective of this experiment was to test the effect of reducing soil N at tuberization on tuber number and development. The influence of two contrasting growing media on the plant response was also investigated. Since only a single irrigation system was used for the two growing media types, leaching volumes were calculated from the Red Ferrosol data since it required the largest water applications to move  $\text{NO}_3^-$  through the profile. It was recognised that the soil columns did not completely replicate the conditions in the glasshouse due to differences in bulk density in the Red Ferrosol and addition of perlite to the washed sand. Even though the Ferrosol was collected from a site under pasture that was well aggregated, care was taken not to degrade the structure which included gentle packing into pots. The lower bulk density of the glasshouse pots was taken into consideration when leaching volumes were calculated. Since the washed sand used in the laboratory studies was fine ( $<0.2$  mm) it was mixed with perlite to increase aeration for the glasshouse studies. Since the perlite is an unreactive media the only impact its addition had was to increase pore space therefore reducing the bulk density.

### *Soil Type and Trial Design*

Two soil types were used in the trial, a sand/perlite media mixed in a 7:3 ratio and a Red Ferrosol classified as acidic, mesotrophic, medium, non-gravelly, clay loamy/clayey, and very deep (Isbell 1996a). The Red Ferrosol was collected from a site that had been under pasture for the last 15 years in Northwest Tasmania, Australia.

The trial was a completely randomised 2 x 2 factorial design replicated 20 times. Individual plants were grown from minitubers planted at a depth of 15 cm in 10 L pots. Individual plants were grown in 10 L pots and received 220 cm<sup>3</sup> of nutrient solution every 5 hours (Table 2). Each pot received the nutrient solution at a rate of 2000 cm<sup>3</sup> h<sup>-1</sup>, and dripper layout enabled output to be applied at four points on the pot

---

surface. Artificial lighting was applied to provide a day length of 15 h, the equivalent of day length plants are exposed to during the growing season in Tasmania.

### *Treatment Application*

The constant N treatment received the nutrient solution (Table 2-5) throughout the period of the trial. The N Leach treatment received the same N supply during plant growth up until the commencement of tuberization. At tuberization, plants receiving the N Leach treatment were flushed with 3.4 L of water over 2.5 hours. A nutrient solution containing no N was then supplied for four days after which N was returned in three concentration steps of 2.5, 5.0 and 10.7  $\mu\text{mol}_\text{c} \text{ cm}^{-3}$  over four days (Table 2-6). The volume and timing of the leaching application was calculated based on results from laboratory leaching columns.

**Table 2-5:** Treatments applied in the glasshouse trial.

Treatment	Soil	Nitrogen
1	Sand/Perlite (70/30)	Constant N
2	Sand/Perlite (70/30)	N Leach
3	Red Ferrosol	Constant N
4	Red Ferrosol	N Leach

**Table 2-6:** Nutrient solutions applied to the plants.

Nutrient	Standard Soln ( $\mu\text{mol}_\text{c} \text{ cm}^{-3}$ )	No $\text{NO}_3^-$ ( $\mu\text{mol}_\text{c} \text{ cm}^{-3}$ )	2.5 $\text{NO}_3^-$ ( $\mu\text{mol}_\text{c} \text{ cm}^{-3}$ )	5.0 $\text{NO}_3^-$ ( $\mu\text{mol}_\text{c} \text{ cm}^{-3}$ )
N	10.71	0.0	2.50	5.00
P	1.94	1.94	1.94	1.94
K	7.61	7.61	7.61	7.61
Ca	5.28	5.28	5.28	5.28
Mg	2.06	2.06	2.06	2.06
Mn	0.02	0.02	0.02	0.02
Cu	0.0003	0.0003	0.0003	0.0003
B	0.0093	0.0093	0.0093	0.0093
Fe	0.07	0.07	0.07	0.07
Mo	0.0002	0.0002	0.0002	0.0002
Zn	0.0072	0.0072	0.0072	0.0072
S	5.02	5.02	5.02	5.02
Cl	1.00	10.48	8.27	6.08

### *Assessments and Analysis*

Plants were destructively sampled 14 days after the onset of tuberization. Tuber mass, tuber diameter and stem mass were measured. Soil samples were taken at the completion of the N Leach treatment and analysed for mineral N. Soil samples were collected and extracted with 2M KCL and analysed colourimetrically. This was converted to total  $\text{NO}_3^-$  and  $\text{NH}_4^+$  per unit volume of soil,  $T$  ( $\mu\text{mol}_\text{c} \text{ NO}_3^- \text{ cm}^{-3} \text{ soil}$ ) using equation 2-1.

Analysis was carried out using analysis of variance for tuber and stem mass and numbers (Fischer LSD). Chi squared analysis was used to compare the tuber size distribution between treatments.

---

## RESULTS

### **Tuber Initiation and Tuber Growth: The Influence of High N Supply**

#### *Soil Nitrogen*

The soil  $\text{NO}_3^-$  content measured 26 days after plant emergence (DAE) was 11.60 and 0.73  $\mu\text{mol}_\text{c} \text{ cm}^{-3}$  of soil in the high and low N treatments respectively and statistical analysis confirmed these concentrations were significant ( $P < 0.001$ ). Ammonium levels were 1.42  $\mu\text{mol}_\text{c} \text{ cm}^{-3}$  of soil solution in the high N treatment and 0.97  $\mu\text{mol}_\text{c} \text{ cm}^{-3}$  of soil in the low N treatment and were not statistically significant. These results confirm a difference in the availability of N to plants in the high and low N treatments.

#### *Tuberization Timing and Length*

Tubers were present on all five plants sampled 18 DAE in the low N treatment while in the high N treatment tuberization in all plants was not observed until the following assessment, 22 DAE (Table 2-7). Analysis of tuber initiation times indicated that the N treatment did not have a significant effect ( $P < 0.05$ ), however the sample size was low and the P value (0.09) was suggestive of a trend towards earlier tuberization in the low N treatment.

**Table 2-7:** Tuber numbers at the first four plant assessments for individual plants. NA indicates the plant did not emerge and was not measured.

Time (DAE)	High N		Low N	
	Plant (Rep)	Tuber Number	Plant (Rep)	Tuber Number
10	1	0	1	0
	2	0	2	0
	3	0	3	0
	4	0	4	0
	5	0	5	0
14	1	0	1	1
	2	0	2	0
	3	0	3	0
	4	0	4	0
	5	0	5	0
18	1	0	1	4
	2	2	2	5
	3	NA	3	3
	4	0	4	2
	5	0	5	1
22	1	19	1	5
	2	12	2	7
	3	7	3	6
	4	10	4	7
	5	9	5	6

---

The onset of tuberization was determined using the definition given by O'Brien *et al.* (1998). It was calculated at the completion of the trial when average tuber number per plant could be determined. The commencement of tuberization, when 10% of total tubers were present, was equivalent to the presence of a single tuber in both the low and high N treatments. The completion of tuberization, when 80% of total tubers were present, was equivalent to the presence of four tubers in the low N treatment and ten tubers in the high N treatment. The values for tuberization were calculated separately between the treatments because there was a significant difference in tuber number (Figure 2-2).

The use of the bootstrap model provides a way of determining whether the length of the tuberization window was influenced by the N treatment when sample size was restricted. Predictions showed that the period of tuberization between the treatments was not significant ( $P < 0.05$ ). The length of the tuberization window was slightly shorter in the low N treatment (1.47 days) compared to the high N treatment (1.81 days) and was therefore much too short to have any influence of subsequent tuber development (Figure 2-1). O'Brien *et al.* (1998) observed in field studies that the period of tuberisation was as low as 4 days. The shorter period calculated in the glasshouse experiment may be a result of the warm conditions and generally favourable growing conditions however a larger sample size would be recommended to increase the confidence in this measurement. The slightly longer period in the high N treatment maybe because over twice as many tubers had to be formed on plants in this treatment before tuberization was complete using the definition of O'Brien *et al.* (1998).

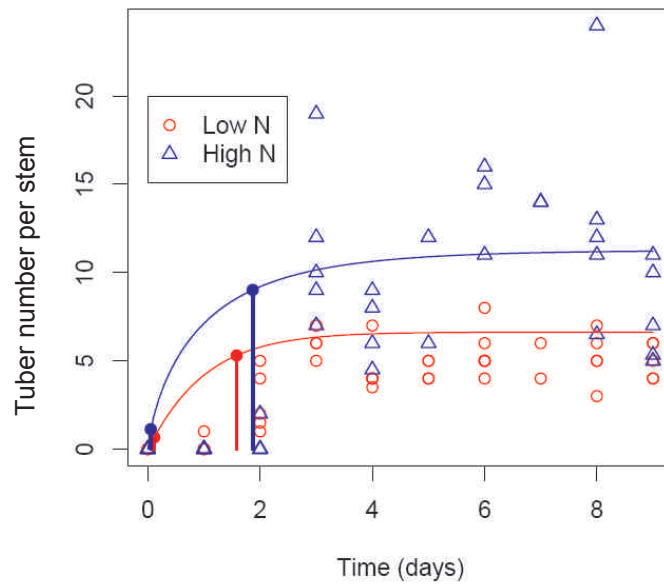


**Figure 2-1:** Fitted curves for actual measurements of tuber number per stem at each sample time. Vertical lines indicate times at which 10 and 80% of the total tuber number were formed.

### ***Tuber Number and Mass***

Tuber number per stem was significantly higher in the high N treatment at all assessments conducted from 22 days after emergence (Figure 2-2). Tuber numbers in the final 70 DAE assessment were lower than previous assessments, indicating tuber resorption presumably as a result of increasing competition for plant assimilate between tubers. The sudden, statistically significant ( $P < 0.05$ ), drop in tuber numbers in the high N treatment at 26 DAE may also indicate some desorption after the initial rapid increase in tuber numbers at the 22 DAE assessments. A similar but less dramatic, and not significant, trend also appears in the low N treatment. These results indicate that although supplying larger amounts of N increased the number of tubers set it may also increase the variability in tuber numbers produced and adsorbed.



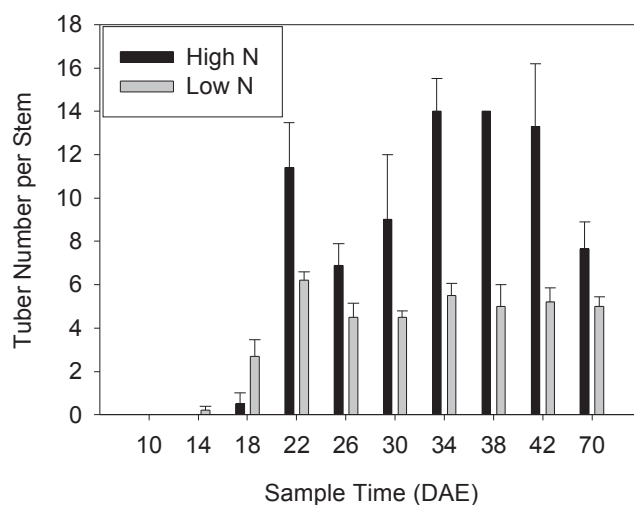


**Figure 2-2:** Tuber number per stem. Error bars represent the standard error of the mean.

The average total tuber mass was significantly higher ( $P < 0.0001$ ) in treatments receiving high constant N applications (Figure 2-3). The increased tuber mass is likely to be related to the higher above ground mass (Figure 2-4) and consequently the larger leaf area which may have enabled more carbohydrate production and an increase in supply to the tubers.

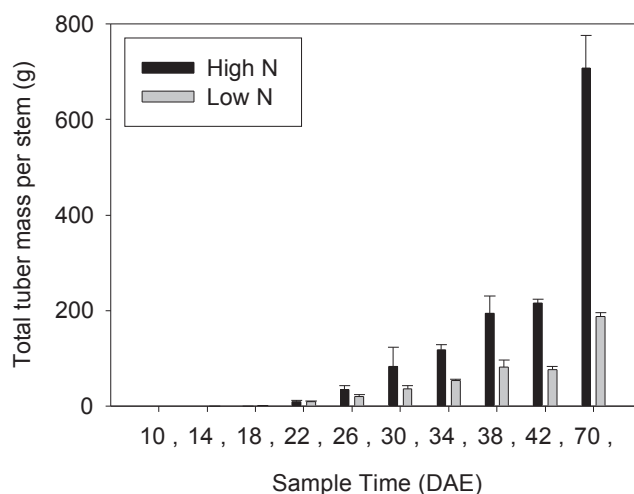


**Figure 2-3:** Total tuber mass per stem Error bars represent the standard error of the mean.

### *Stem and Leaf Data*

The combined green stem and leaf mass which was significantly higher ( $P < 0.0001$ ) in the high N treatment (Figure 2-4). Statistical analysis indicated that N supply did not influence stem number.

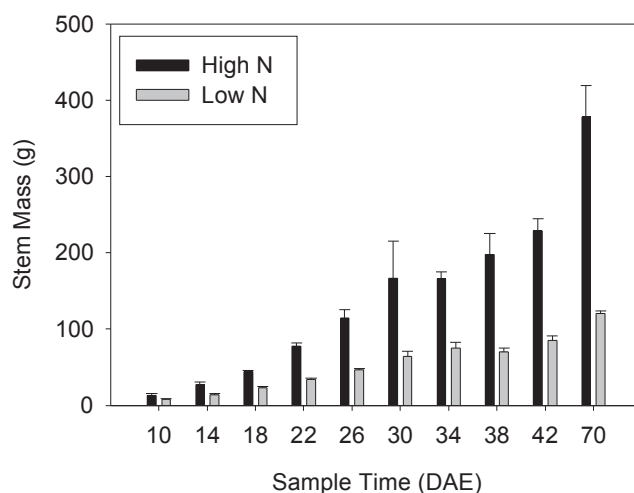


**Figure 2-4:** Average individual stem mass. Error bars represent the standard error of the mean.

### *Preliminary Discussion*

The significant effect of N supply on the growth and development of the tubers in these initial experiments indicated there was scope for some manipulation of tuber development by altering levels of this nutrient. This further confirms the previous findings in the literature by O'Brien *et al.* (1998), Oparka *et al.* (1986) and Kursanov (1984) who also found N supply had an impact on tuber development. A method for reducing N concentration in the soil at the onset of tuber initiation was therefore investigated with the aim of increasing tuber numbers. This was done by conducting preliminary leaching studies in the laboratory followed by further glasshouse experiments detailed below.

### Vertical Column Leaching Studies

Concentrations of  $\text{NO}_3^-$  and soil water content in the soil solution throughout the soil column are presented in Figure 2-5 for the washed sand and Figure 2-6 for the Red Ferrosol. Table 2-8 shows the proportion of total  $\text{NO}_3^-$  in each sampling section of the column demonstrating distribution of  $\text{NO}_3^-$  after each water application in the two soils. These figures and tables show the majority remaining near the surface when no further water was applied in comparison to the majority accumulating at the base on the column after application of the 150% FC treatment.

Nitrate infiltrated further through the column in the fine sand than the Red Ferrosol even when no water was applied following the solute pulse. Both soils received the same  $50 \text{ cm}^3 \text{ NO}_3^-$  pulse however the water holding capacity of the sand is lower than the Red Ferrosol (Figure 2-5B and Figure 2-6B). Therefore the added  $\text{NO}_3^-$  solution moved further through the column in the sand. These results indicate that more water is required to leach  $\text{NO}_3^-$  through the Red Ferrosol soil and therefore leaching treatments should be based around this soil to ensure sufficient leaching is achieved in the glasshouse experiments. This is further highlighted by the fact that even though less water was applied in terms of pore volumes were applied to the Washed Sand, similar patterns of leaching were observed in the two soils.

Figure 2-5a and Figure 2-6a also show a high build up of  $\text{NO}_3^-$  at the bottom of the columns in the 150% FC treatments for the two soils. This is a result of i) the increased leaching of  $\text{NO}_3^-$  due to the higher water volume applied and; ii) the higher water content at the bottom of these columns (Figure 2-5b and Figure 2-6b). The increased leaching volume obviously led to more  $\text{NO}_3^-$  accumulating toward the base of the column however the the concentration of  $\text{NO}_3^-$  is presented per unit volume of soil ( $\mu\text{mol cm}^{-3}$ ) which somewhat exaggerates this concentration. Because the soil moisture content is significantly higher at the base of the 150% FC in comparison to the pther treatments, even if the solution concentration is the same, the concentration of  $\text{NO}_3^-$  per unit mass of soil ( $\mu\text{mol cm}^{-3}$  oven dry soil) will be higher in comparison to the other treatments.

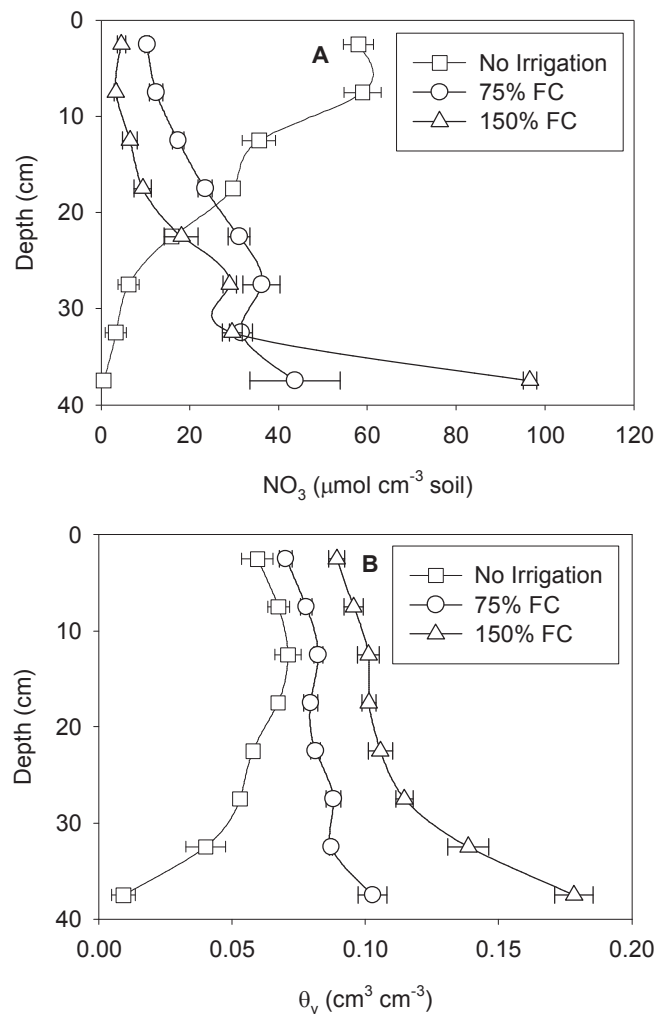


**Figure 2-5:** Soil  $\text{NO}_3^-$  concentrations (Chart A) and water content (Chart B) in the washed fine sand after the  $\text{NO}_3^-$  pulse and water applications Table 2-3. Horizontal error bars represent the standard error of the mean. FC = field capacity.

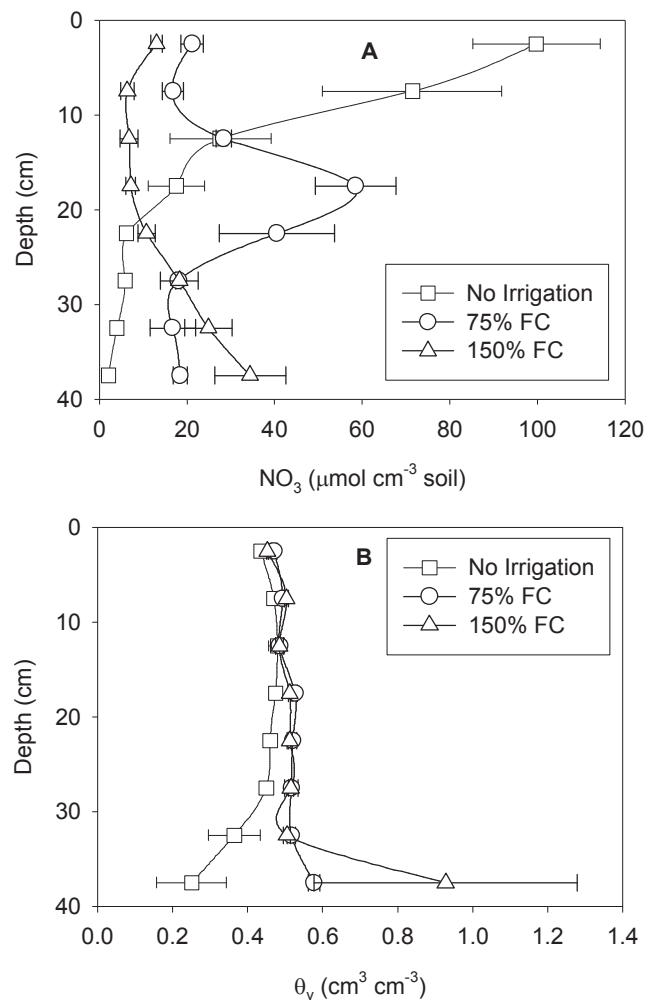


**Figure 2-6:** Soil  $\text{NO}_3^-$  concentrations (Chart A) and water content (Chart B) in the Red Ferrosol after the  $\text{NO}_3^-$  pulse and water applications Table 2-3. Horizontal error bars represent the standard error of the mean. FC = field capacity.

**Table 2-8:** Distribution of total  $\text{NO}_3^-$  in each sampling section of the column and leachate.

	Depth (cm)	Ferralsol % N	Washed Sand % N
No Irrigation	0-5	43.23	27.84
	5-10	30.05	28.27
	10-15	11.60	17.08
	15-20	7.35	14.25
	20-25	2.60	7.67
	25-30	2.48	3.01
	30-35	1.75	1.62
	35-40	0.94	0.26
	Leachate	0.00	0.00
75% FC	0-5	10.01	5.04
	5-10	7.77	6.06
	10-15	13.24	8.44
	15-20	26.14	11.38
	20-25	18.17	15.08
	25-30	8.13	17.51
	30-35	7.55	15.31
	35-40	7.74	21.19
	Leachate	1.26	0.00
150% FC	0-5	10.22	2.37
	5-10	6.00	1.73
	10-15	5.15	3.38
	15-20	5.30	4.87
	20-25	10.00	9.32
	25-30	13.45	14.82
	30-35	18.55	15.03
	35-40	28.48	48.49
	Leachate	2.83	0.00

Table 2-9 shows the mass balance calculations for the soil columns. The similar  $\text{NO}_3^-$  values for the two soils in the no irrigation treatment indicate that the same amount of  $\text{NO}_3^-$  was added but also indicates large variations in the measurements. The decrease in the recovery of  $\text{NO}_3^-$  between the three treatments, particularly in the Red Ferrosol, was not expected. One possible explanation is denitrification in the collected leachate and saturated zone of the soils. Leachate from the columns was collected however it remained in the collection flask at room temperature during the period of the experiment. Furthermore, since there was no suction applied to the bottom of the soil columns a saturated zone developed in this area as indicated in Figure 2-5B and Figure 2-6B. Broadbent and Clark (1965) state that under anaerobic conditions denitrifying bacteria can build up and  $\text{NO}_3^-$  can be converted to  $\text{NO}_2$  gas and lost to the atmosphere. This would explain the decreasing recovery of  $\text{NO}_3^-$  with the increasing amount of leachate applied since more leachate was collected and there was therefore greater potential for loss of  $\text{NO}_3^-$  through denitrification.

**Table 2-9:** Mass balance calculations of total  $\text{NO}_3^-$  added to the soil columns. Values in parentheses indicate the standard deviation of measurements. Due to the size of the values the amounts are presented in  $\text{mmol}_c$  ( $\mu\text{mol}_c \times 10^3$ ).

Treatment	Ferrosol	Washed Sand
	N applied ( $\text{mmol}_c$ )	N applied ( $\text{mmol}_c$ )
No irrigation	55.90 (23.83)	63.82 (10.06)
75% FC	49.12 (14.12)	62.41 (12.73)
150% FC	29.16 (10.12)	58.67 (7.67)

**The Influence of Soil Type on Plant Emergence and Tuberization**

This trial was undertaken to develop the pot trial methodology for studies investigating effects of varying N availability in soils on tuberization and tuber growth. The time between planting and emergence in the sand/perlite media was 15.9 compared to 14.7 days in the Red Ferrosol topsoil and this difference was not statistically significant ( $P < 0.05$ ). Tuberization was observed in potato plants approximately 30 days after plant emergence. No significant difference ( $P < 0.05$ ) in the onset of tuberization was observed between the two soils. Since there was no difference between treatments in early plant and tuber development, it was concluded that the application of treatments in the proceeding glasshouse experiment could occur at the same time in the different soil types.



## Effects of Reducing N Availability at Tuberization on Tuber Set and Growth

### *Soil Nitrogen*

A significant interaction effect ( $P < 0.05$ ) was measured between soil type and N content. Results are therefore presented separately for the two soils (Table 2-10). Soil N was extracted with a KCl extract and therefore concentrations are presented per unit volume of soil. Because of the higher water holding capacity of the Red Ferrosol N concentrations appear much higher than in the sand. This difference was smaller but still significantly different, when concentrations were calculated based on the soil water content (14.13 versus 7.95  $\mu\text{mol}_\text{c} \text{ cm}^{-3}$  solution in the control treatment of the Red Ferrosol and sand respectively). Significantly lower  $\text{NO}_3^-$  concentrations were measured in the N Leach treatment compared to the control when soil N was measured at the completion of treatment application in both soils indicating that the N Leach treatment was successful in reducing soil  $\text{NO}_3^-$  concentrations.

**Table 2-10:** Soil  $\text{NO}_3^-$  concentration and at the completion of the treatment application and average tuber mass measured 14 days after treatment application. Values in parentheses indicate the standard deviation of measurements.

Soil	N Treatment	$\text{NO}_3\text{-N}$ ( $\mu\text{mol}_\text{c} \text{ cm}^{-3}$ soil)	$\text{NH}_4\text{-N}$ ( $\mu\text{mol}_\text{c} \text{ cm}^{-3}$ soil)	Average Tuber Mass (g)
Ferrosol	Constant N	12.67 (2.26) <sup>a</sup>	0.51 (0.04) <sup>a</sup>	1.50 (0.23) <sup>a</sup>
Ferrosol	N Leach	4.19 (2.18) <sup>b</sup>	0.79 (0.19) <sup>a</sup>	3.20 (0.41) <sup>b</sup>
Sand	Constant N	1.58 (0.18) <sup>a</sup>	0.23 (0.18) <sup>a</sup>	2.13 (0.46) <sup>a</sup>
Sand	N Leach	0.30 (0.34) <sup>b</sup>	0.10 (0.06) <sup>a</sup>	2.34 (0.29) <sup>a</sup>

Values with different symbols are significant to the ( $P < 0.05$ ) levels as calculated from the LSD

### *Plant Measurements*

Analysis of the average individual tuber mass showed a close to significant interaction between the N treatment and soil type ( $P < 0.057$ ). Results are therefore presented separately for the two soils. The average tuber mass was significantly higher in the N Leach treatment ( $P < 0.05$ ) than the control in the Red Ferrosol but not the sand (Table 2-11). The same observation was made in the analysis of the total

tuber mass per stem however a trend of higher tuber mass due to the N Leach treatment was also observed in this soil although the difference was not significant.

No effect of the N Leach treatment was measured on tuber number or stem number and mass (Table 2-11). The fact that no increase in tuber number was achieved using this treatment indicates that sufficient N for tuber set was supplied to the plants in both treatments prior to application of the N Leach treatment.

These results indicate that the N Leach treatment was more effective in the Red Ferrosol treatment and although there was a similar trend in the sand soil no significant differences were measured.

**Table 2-11:** Tuber and stem number and stem mass. Values with different symbols are significant to the ( $P < 0.05$ ) levels as calculated from the LSD. Values in parentheses indicate the standard error of the mean.

Soil	N Treatment	Average Tuber Mass (g)	Total Tuber mass per stem (g)	Average Tuber Number per stem	Average green Stem Mass (g)
Ferrosol	Constant N	1.50 (0.23) <sup>a</sup>	12.22 (3.44) <sup>a</sup>	6.93 (0.89) <sup>a</sup>	245.9 (21.8) <sup>a</sup>
Ferrosol	N Leach	3.20 (0.41) <sup>b</sup>	24.04 (4.02) <sup>b</sup>	7.68 (1.08) <sup>a</sup>	190.3 (39.2) <sup>a</sup>
Sand	Constant N	2.13 (0.46) <sup>a</sup>	16.27 (4.10) <sup>a</sup>	6.81 (0.83) <sup>a</sup>	236.5 (28.9) <sup>a</sup>
Sand	N Leach	2.34 (0.29) <sup>a</sup>	23.74 (6.10) <sup>a</sup>	9.52 (1.96) <sup>a</sup>	123.0 (22.5) <sup>a</sup>

The effect of the N Leach treatment on tuber growth is evident in the tuber size distribution (Figure 2-7). The size distribution was calculated by sorting the individual tubers into mass categories. Results are presented separately for the two soil types because of the interaction measured between treatment and soil type in the individual tuber mass analysis. A significant effect of N ( $P < 0.05$ ) on the percentage of tubers in the six size ranges was measured in the Red Ferrosol soil (Figure 2-7B). No significant effect was measured in the sand/perlite soil media however a similar trend in size distribution can be observed between the N Leach and control treatments (Figure 2-7A). Figure 2-7B indicates that the growth of tubers may have been increased by the N Leach treatment since there are fewer tubers less than one gram and an increase in tubers in the three size categories above four grams.

Results from this trial indicate that tuber mass was increased by leaching N in the Red Ferrosol soil and although a similar trend was observed in the sand significant differences were not measured.

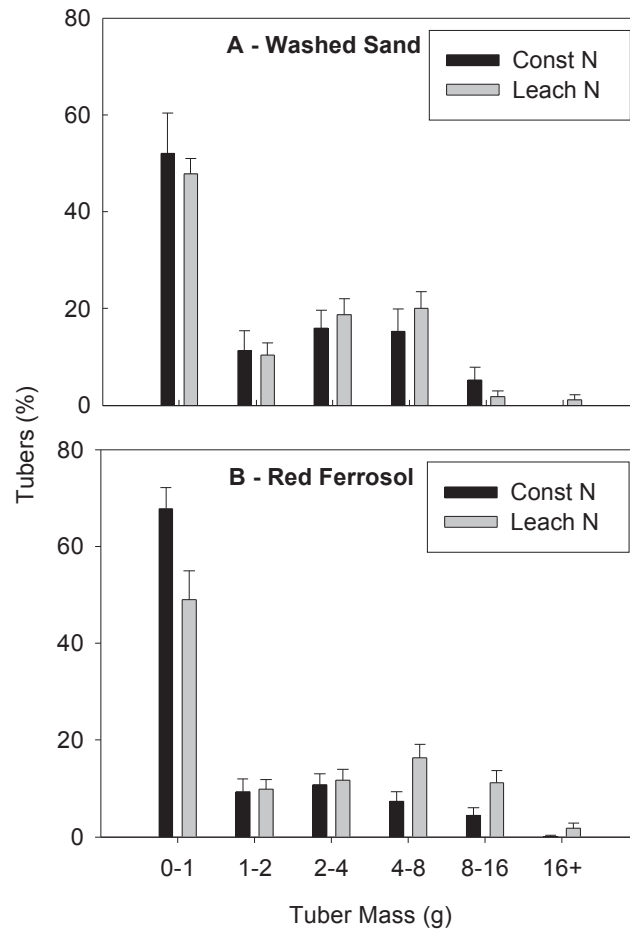


**Figure 2-7:** Tuber size distribution in the Washed Sand (Chart A) and Red Ferrosol soil (Chart B).

Error bars represent the standard error of the mean.

## DISCUSSION

Varying soil N availability during and shortly after tuberization was demonstrated to affect tuber growth. Rapidly reducing soil N levels at the onset of tuberization led to an increase in the average tuber mass in potato plants and also affected the tuber size distribution 14 days after the treatment was imposed in the Red Ferrosol soil. Although tuber mass was increased no influence on tuber number was measured. Studies by Oparka *et al.* (1987) showed high N can reduce the proportion of assimilates supplied to the below ground plant parts. Furthermore Kursanov (1984) suggested that when N was in high supply, shoot and root growth was stimulated resulting in reduced partitioning to tubers. No direct measurements of carbohydrate partitioning were made in the experiment however, based on the evidence in the literature, reducing N availability to the potato plants at tuberization may have reduced the demand for assimilates by the leaves and stem, making more available to the tubers.

The finding that tuber growth was only influenced in the Red Ferrosol was surprising because laboratory columns indicated that  $\text{NO}_3^-$  could be leached more readily than the sand treatment and soil analysis indicated significant reductions were achieved using the leaching treatment in both soils. The similar, but not significant, trend in the tuber data from the plants grown in the sand suggest that with further replication and potentially a longer period of  $\text{NO}_3^-$  restriction, the same treatment effect may be measured in this soil.

Although the same applications of nutrients were applied to the two soils analysis indicated that concentrations were higher in the Red Ferrosol in comparison to the sand. The higher concentrations in the Ferrosol may have been due to anion adsorption in this soil since this is known to occur in these soil types (Isbell 1994). However only a KCl extraction was used to determine N concentrations in the soil and therefore the presence of adsorption can only be speculated.

The Red Ferrosol had a higher water holding capacity than the sand however this is unlikely to have directly influenced the plant response to the N Leach treatment. Both soils received regular water application and it is unlikely that plants grown in either soil were subject to water stress at any stage during their growth. If water

---

---

content was to have any influence it is again likely to be related to nutrient availability since nutrients were applied in the irrigation. Therefore if a soil contains a greater volume of solution then the total mass of nutrients available for uptake in the pot is also greater.

Maintenance of constant soil N concentrations at different levels during plant growth resulted in significantly higher tuber numbers being obtained with the high N treatment. Unlike previous studies conducted in hydroponics, a high constant N supply did not inhibit or delay the onset of tuberization. The increase in tuber number and mass resulting from the high N treatment is in agreement with findings from previous authors (O'Brien *et al.* 1998; Oparka *et al.* 1987).

O'Brien *et al.* (1998) suggests that the key to maximising tuber set is to ensure sufficient N is available during early growth to achieve maximum leaf area and consequently sufficient carbohydrate production for tuber growth. This scenario was the case in both the N Leach and constant N treatments since both were supplied with high N applications up to the tuberization stage. Furthermore, even though Oparka *et al.* (1987) found a reduction in the proportion of assimilates partitioned to tubers in response to high N application, the overall supply of carbohydrates to the tubers was still increased. The significantly higher number of tubers produced in the constant high N treatment compared to the constant low N treatment (Figure 2-3) provides support to the findings of Oparka *et al.* (1987). It is therefore probable that in both the N Leach and constant N treatments sufficient carbohydrates were available for maximum tuber set to be achieved and therefore the effect of reducing N availability was only observed once tubers began to grow and the demand for assimilates was further increased.

Although the number of tubers initiated was not increased by the N Leach treatment, the increased tuber growth rate stimulated by the treatment may reduce the likelihood of tuber resorption. Analysis of tuber size distribution revealed that the percentage tubers less than 1.0 g were reduced in the N Leach treatment, compared to the constant N control. Furthermore the percentage of tubers in all size ranges above 4.0 g, which were considered less likely to be resorbed, were significantly increased. The resorption process involves assimilates stored in tubers being remobilised and transported elsewhere for use by growing parts of the plant. This situation can occur if demand for assimilate by competing tubers or other plant parts is strong and supply

---

---

of carbohydrates from the leaves cannot keep up with demand (Moody 1994). In the high versus low N experiment a lower tuber number was observed at 70 DAE in the high N treatment compared to numbers observed in earlier assessments (Figure 2-2). This shows that resorption may be occurring even in an environment where growing conditions are highly favourable. Burstall *et al.* (1987) reported that at approximately 21 weeks after planting the number of tubers >1 cm was related to the final number suggesting that anything under this size at the sampling time was later resorbed. Furthermore Cho and Ifanti (1983) found that in Russet Burbank tubers were resorbed in sequential seasons showing that tuber resorption can have a considerable impact on the number of tubers that are retained at harvest. If the N Leach treatment imposed in the glasshouse experiment increases the assimilate supply to the tubers then this may enable a greater proportion of tubers on the plant to grow to a size where sink strength is sufficient to resist resorption. This could therefore result in an increase in the number of tubers retained at harvest.

Predictions from bootstrapped data showed that high N application did not influence the time of tuber initiation when compared to low N application. The high N treatment was expected to lead to a delay in the onset of tuberization compared to the low N treatment, as shown by previous hydroponic studies (Krauss 1980; Krauss and Marschner 1982; Sattelmacher and Marschner 1979). The published hydroponics work showing the inhibitory effect of N on tuberization suggests that it can influence the tuberization stimulus. However the findings presented in this chapter and the evidence provided by Ewing and Struik (1992) and O'Brien *et al.* (1998) indicate that under most growing conditions N does not have a significant effect on the timing of tuberization.

## CONCLUSION

Reducing N levels at the tuberization stage resulted in increased average tuber mass and indicated that tubers grew at a faster rate over a short period in the glasshouse study in the Red Ferrosol. Although a significant difference in tuber mass was not observed in the sand, the trends in the data indicate that with greater replication increased plant sampling this same result is likely to be observed in this soil.

The finding of increased tuber growth rate warrants further investigation since the treatment period was short and samples were only taken early during tuber growth, 14 days after treatment application. If this treatment can be shown to have a longer term influence on the rate of tuber growth and can reduce the proportion of tubers resorbed during periods of high demand for plant assimilates then it may be of real benefit to industry. The finding that N supply had no significant effect on the time of tuberization indicates that factors other than N availability during early crop growth are affecting the rate and period of tuber set. The results of these glasshouse trials were sufficiently encouraging to warrant assessment of the N Leach treatment under field conditions to determine if tuber number and/or yield in seed potato crops grown from minitubers may be increased.

## CHAPTER 3

# APPLICATION OF THE “N LEACH” TREATMENT TO A RED FERROSOL IN THE FIELD

### INTRODUCTION

Evidence from the literature, and from the experiments presented in Chapter 2, suggested that altering nitrogen availability during potato tuberisation alters the pattern of tuber development. The N Leach treatment, involving adequate N supply followed by a rapid reduction in soil N levels at tuberisation, was tested under glasshouse conditions (Chapter 2) and promoted increased partitioning to developing tubers. Duplication of this response under field conditions may increase tuber yield and tuber number. This Chapter describes a large scale field trial designed to test the N Leach treatment under field conditions in a commercial seed potato production site.

### LITERATURE REVIEW

#### Effects of Nitrogen on Tuber Number in the Field

The development of strategies to increase tuber number has been a focus of seed potato production research. Increasing seed tuber number minimises the number of field production generations required to produce the required quantity of seed. In commercial ware crop production, management practices to manipulate other factors including total yield, shape and specific gravity are the main focus of research. While there are differences in the focus of seed and ware crop production, the management of nitrogen during early growth is often similar. While many studies have been undertaken on nitrogen management in potatoes under field conditions, most have focused on commercial production and only present the effect of N application on total yield (Painter and Augustin 1976; Roberts *et al.* 1982).

Field studies that have reported the effect of N on tuber number generally show that increased N applications result in higher tuber numbers per plant. O'Brien *et al.* (1998) states tuber set will be maximised as long as vegetative growth is not restricted during early plant growth. Nitrogen is an important factor in achieving the



---

optimal leaf area for sufficient production of carbohydrates by the plant for maximum tuber set. The benefit of nitrogen supply on tuber number has also been reported by other authors (Belanger *et al.* 2000; 2002; Dubetz and Bole 1975; Sharma and Ezekiel 1993). Although sufficient N application is required to maximise tuber number, there is evidence that excess N may have the opposite effect. In a study of commercial crops, yield was reduced when N application exceeded rates between 150–250 kg Ha<sup>-1</sup> (Belanger *et al.* (2000). Dubetz and Bole (1975) found that increasing N application from 224 kg ha<sup>-1</sup> to 448 kg ha<sup>-1</sup> increased the number of tubers, however a further increase had no effect on tuber number but decreased the total yield. O'Brien *et al.* (1998) and O'Brien and Allen (1986) have also reported the detrimental effect of excess N on both tuber number and mass.

All the field studies reported in the literature are based on either a single or a small number of N applications during crop growth. The general consensus is that if N supply is sufficient, tuber number will be maximised. However, there is no work describing effects of strategic N applications at important plant growth stages on tuber number, or of effects of treatments designed to rapidly reduce N availability. Findings from Chapter 2 suggest that if N availability can be lowered at the tuberization stage the tuber growth rate may be increased. This may lead to more tubers being retained at harvest.

### **Root Development and Distribution in Potatoes**

In a field environment, plant roots can spread further both vertically and horizontally than in the glasshouse experiments reported in Chapter 2. As a result, nitrogen may need to be moved a greater distance to reduce concentrations in the root zone. Several studies have documented the extent of the potato root system. The majority of potato roots (up to 85%) in field grown crops have been reported to be in the top 30 cm of the soil (Lesczynski and Tanner 1976; Smith 1968). In contrast, Stalham and Allen (2001) published a comprehensive study, including data from 11 separate field trials, and showed only 61% of the roots were in the 0–30 cm layer of the soil in irrigated potato crops. Root concentration increased between 10 and 20 cm, peaked between 20 and 30 cm and then decreased rapidly below this depth. The rapid decrease below 30 cm indicates that the vast majority of roots were concentrated in the upper 40 cm of the soil. Maximum rooting depths for potato plants were found to be up to 1.5

---

---

meters, however on average most varieties approached a maximum depth of 60 cm (Smith 1968; Stalham and Allen 2001).

Root development follows a general pattern of distribution in potato, but can be influenced by varietal, soil and agronomic factors. Stalham and Allen (2001) found differences in maximum rooting depths between varieties, however they did not report on varietal differences in root distribution throughout the profile. They also observed that growing plants without irrigation throughout the season resulted in deeper and sparser rooting in the plants. Lesczynski and Tanner (1976) observed that irrigation altered the maximum rooting density and the time at which this occurred during plant development. Measurement of root development in cotton indicated that the root growth followed the distribution of water in the soil, with more roots developing in soil ridges under drip irrigation compared to furrow irrigation (Hodgson *et al.* 1990). Similarly, higher root density was observed around the drip line than elsewhere throughout the soil under grapefruit trees again indicating a tendency for roots to accumulate in the area where water is available (Zhang *et al.* 1996). As root distribution may be affected by patterns of water movement within the soil, the effect of the N Leach treatment in field grown potatoes may be influenced by irrigation rate and the type of irrigation system used in the crop.

### **Water and Solute Dynamics under Dripper Systems and their Impact on Plant Growth**

Dripper irrigation systems allow precise control of irrigation rate and placement (Cote *et al.* 2003). Dripper systems are advantageous in situations where water and nutrient use efficiency are important. Waddell *et al.* (1999) found that drip irrigation in potatoes significantly reduced irrigation volumes required compared to sprinkler irrigation without effecting potato yield or quality. Subsurface drippers supply water to the very centre of the mound where roots are concentrated. In contrast, systems such as overhead sprinkler irrigation result in much of the applied water accumulating in the furrows because of run-off from the canopy and mound (Cooley *et al.* 2007). Root distribution may be reduced under drippers, resulting in a reduced area of the soil that must be leached using the N Leach treatment. However leaching N may be more difficult because solute will move laterally as well as vertically with the infiltrating soil water (Li *et al.* 2003).

---

Rainfall must also be taken into account since it may reduce the benefits of the dripper system. If there is little precipitation over the growing season, and small frequent irrigation applications are made through a dripper system, then the roots will not advance to the extent they would if the soil was wet deeper into the profile (Stalham and Allen 2001). However precipitation events have been shown to result in roots extending beyond the wetted zone created by the dripper because water content outside the dripper zone was increased (Kamara *et al.* (1991). Therefore restriction of root distribution under a dripper system is dependent on negligible rainfall over the growing season.

### **Environmental and Agronomic Impacts of Leaching**

The application of a N Leach treatment is dependent on leaching of nitrogen, principally  $\text{NO}_3^-$ , to a point below the majority of plant roots in the soil. Because  $\text{NO}_3^-$  is generally associated with the soil water, irrigation or a rainfall event may lead to  $\text{NO}_3^-$  movement beneath the root zone. Movement deeper into the soil profile can however be environmentally damaging.

Leaching of  $\text{NO}_3^-$  and  $\text{NH}_4^+$  reduces agricultural productivity, pollutes surface and groundwater and can adversely impact human health. Mmolawa and Or (2000) suggest that leaching is probably the dominant way in which N is lost in the soil-plant system, especially when high soil  $\text{NO}_3^-$  levels are present. Under an agricultural production system, particularly intensive cropping, the higher inputs of N fertiliser and use of irrigation increase the risk of  $\text{NO}_3^-$  leaching below the root zone (Stevenson 1985). From an agricultural perspective, leaching is disadvantageous because of both the economic loss and the environmental degradation. Leaching is usually more significant in situations where N is applied as fertiliser and there is therefore a direct economic cost if some of this supplemental N is lost through leaching and not available for plants to increase crop productivity (Stevenson 1985).

The loss of  $\text{NO}_3^-$  from the root zone under small scale field experiments and small scale seed production may not result in significant economic loss. First generation potato field crops are small and the potential economic gain from the N Leach treatment may outweigh the loss of a small amount of applied N. The potential for environmental impact, however, is an area of concern. Although leaching is a natural phenomenon significant losses of N below the root zone can have environmental

impacts. Some of the N lost below the root zone may be converted to  $\text{N}_2\text{O}$ , NO and finally  $\text{N}_2$  gas through denitrification if anaerobic conditions occur due to waterlogging in the soil, however the required reducing bacteria and organic carbon source for this process decrease with depth in the soil (Firestone 1982). The amount of denitrification at these depths may therefore be too low to remove an appreciable amount of  $\text{NO}_3^-$  from the soil. Since first generation seed crops are only grown at a particular location once due to issues with disease only one leaching event would occur at a particular site. This combined with the fact that the areas these crops are grown on are small means that the N lost to the roots zone is unlikely to make a significant contribution to N that is lost from agricultural production systems on a broader scale.

## EXPERIMENTAL OVERVIEW

The objective of the experiment described in this chapter was to document the pattern of nitrogen movement under drip irrigation in a field environment and assess the impact of a N Leach treatment on potato tuber development. A number of assumptions were made in developing the N Leach treatment for field conditions: i) the majority of roots would be concentrated in the upper 40 cm of the soil profile, based on root distribution studies in the literature; ii) the rate of  $\text{NO}_3^-$  leaching was assumed to be similar under field conditions to the laboratory column experiments conducted and glasshouse pot conditions used. This would allow irrigation rates for leaching of N below the 40 cm root zone to be calculated based on previous experiments; iii) the pattern of water distribution under drip irrigation was assumed to contain sufficient downwards movement to N Leach from the root zone. Each of these assumptions was tested in the various experiments in order to inform decision making on development of a N Leach treatment that could be applied under field conditions.

## MATERIALS AND METHODS

The field experiment was conducted at a site chosen to suit seed potato production. The soil was a free draining Red Ferrosol that had been previously under pasture for over 20 years. The site was located at 41° 29' 28.80" S and 14° 60' 34.70" E, at an elevation of 508 m above sea level. This high elevation and inland location helps to minimise the occurrence of insects known to carry potato pathogens. Minutubers were sown on the 27<sup>th</sup> of November 2007 and the final harvest was conducted on the 26<sup>th</sup> of March 2008.

### *Soil Conditions*

The soil used in the field experiment was a free draining, well structured Red, Mesotrophic, Humus, Ferrosol; medium, slightly gravelly, clay loamy, clayey, deep (Isbell 1996a). The full soil profile description is shown in Appendix 2.

**Table 3-1:** Basic soil properties for the Red Ferrosol field soil described according to the Australian soil classification (Isbell 1996a).

Depth (cm)	Horizon	Texture	Structure		
			Grade	Ped type	Size
0–25	A1	Clay Loam	Strong	PO	50–10 mm
25–50	B21	Light Clay	Strong	PO	10–20 mm
50–75	B22	Light Clay	Strong	PO	5–10 mm
75–105+	D	Silty Clay Loam	Strong	PO	10–20 mm

---

*Preliminary Nutrient Status*

Samples from the 0–10 cm soil layer were taken prior to the start of the field experiment and analysed for soil pH (1:5), water soluble nutrients and exchangeable cations by SWEP analytical laboratories, Victoria (Table 3-2, Table 3-3 and Table 3-4). The methods for these analyses are described by Rayment and Higginson (1992) unless otherwise stated. These results were used by the commercial seed production company Agronico Pty Ltd to develop fertiliser recommendations for the seed potato crop.

**Table 3-2:** pH and EC of the 0–10 cm soil layer (methods 4A1, 4B1 and 3A1; Rayment and Higginson 1992)

Measurement	Value
pH (1:5 soil:water)	5.8
pH (1:5 soil:0.01M CaCl <sub>2</sub> )	5.2
EC1:5 (μS/cm)	37

**Table 3-3:** Concentrations of macro nutrients in the 0–10 cm topsoil at the experiment site prior to fertiliser application (methods L1b, L2b, L3b, L4b, 9C1 Rayment and Higginson 1992).

Nutrient	Concentration (μmol <sub>c</sub> cm <sup>-3</sup> soil)
N	0.007
P	0.97
K	2.6
S	0.12

**Table 3-4:** Exchangeable cations and the total cation exchange capacity (CEC) in the 0-10 cm layer of the field soil (15D3 method for Ca, Mg, Na and K (Rayment and Higginson 1992) and Barium Chloride-Triethanolamine method for exchangeable hydrogen (Peech *et al.* 1962)).

Cation	Concentration (μmol <sub>c</sub> cm <sup>-3</sup> soil)
Ca	300
Mg	6.8
Na	1.6
K	2.6
H	228
CEC	269

---

---

### *Organic Carbon*

Soil organic carbon in the top 100 cm of the soil profile was analysed by CSBP laboratories using methods described by Walkley and Black (1934). Data is presented in Table 3-5. Organic carbon levels were high at this site because it had been under pasture for 20 years prior to the planting of the seed potato crop. A large amount of decomposing turf was also present in the topsoil throughout crop growth since the site was cultivated shortly before planting (Plate 3-1). Therefore total organic matter in the topsoil was significantly higher than indicated by the organic carbon measurements.

**Table 3-5:** Soil organic carbon percentages down the soil profile

Depth (cm)	Organic Carbon (%)
0-20	4.73
20-40	4.66
40-60	2.28
60-80	0.86
80-100	0.56

### *Bulk Density*

Bulk density was sampled in 7.5 x 10 cm cores taken in duplicate at 20 cm increments down the soil profile to a depth. These samples were taken in three pits around the trial perimeter (Plate 3-3). Cores were hammered into the profile horizontally and carefully trimmed top and bottom. Cores were then oven-dried at 105°C and weighed. Bulk density was calculated by dividing the mass of the oven dry soil by the volume of the soil core.

Average soil bulk densities from the three pits are shown in Figure 3-1. The data highlights the very low bulk densities of the surface cultivated soil containing significant quantities of decomposing turf.

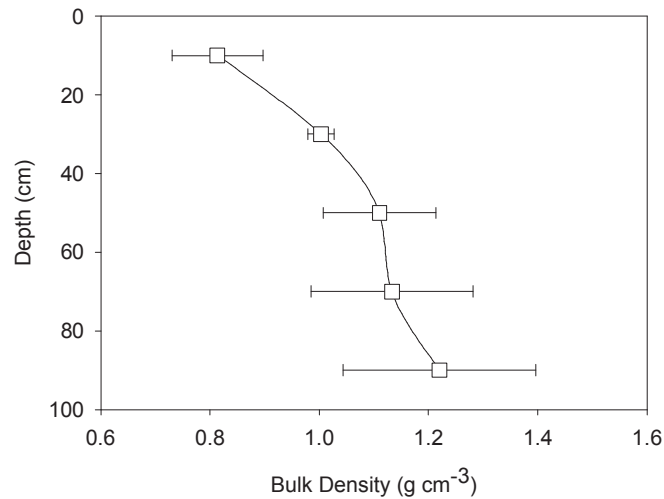


**Figure 3-1:** Soil bulk density. Error bars represent the standard error of the mean.

### *Clay Mineralogy*

Clay mineralogy was measured by Mineral Resources Tasmania using X-ray diffraction in bulked samples taken between 0–20, 20–40 and 40–60 cm down the soil profile (Table 3-6). The "amorphous" in the table represents Fe and Al Oxides (McKenzie *et al.* 2002).

**Table 3-6:** Clay mineralogy of the Ref Ferrosol soil profile.

Depth	25 -35%	15%-25%	10-15%	5-10%	2-5%	<2%
0-20 cm	Quartz	Amorphous	Kaolinite, Organic	Garnet, Gibbsite	Epidote	Smectite, Rutile, Amphibole
20-40 cm	Amorphous, Quartz		Garnet	Kaolinite, Gibbsite, Epidote	Organic	Smectite, Rutile, Amphibole
40-60 cm	Amorphous	Quartz, Garnet		Gibbsite, Kaolinite, Organic, Epidote	Amphibole	Smectite, Rutile



### *Particle Size Analysis*

Particle size analysis was measured using the pipette method according to method protocols 517.02 (pre-treatment for organic carbon) and 517.07 (pre-treatment for Fe and Al oxides) in Cresswell (2002) by Mineral Resources Tasmania (Figure 3-6).

**Table 3-7:** Particle size analysis measured down the profile after treatment for organic matter or both organic matter and Fe and Al oxides

Depth	Particle Size	organics removed	organics + oxides removed
0-20	Sand	80	45
	Silt	12	22
	Clay	8	33
20-40	Sand	77	47
	Silt	18	20
	Clay	5	33
40-80	Sand	73	45
	Silt	15	27
	Clay	12	28

### *Field Trial Design*

The trial was a 2 x 2 factorial design with five replicates (Table 3-8). Three potato cultivars, Bintje, Russet Burbank and Markies, were included in the trial and each cultivar was contained within an individual block to enable separate applications of water and  $\text{NO}_3^-$  particular varieties when necessary. Each plot consisted of a 5 m long section of four rows. At the end of each plot was a buffer of four plants. Two buffer rows of Russet Burbank were planted between the experimental blocks (cultivars).

**Table 3-8:** Field experiment layout

Russet Burbank					Bintje			Markies		
row 1	row 2	row 3-6	row 7	row 8	row 9-12	row 13	row 14	row 15-18	row 19	row 20
		Buffer 4 plants			Buffer 4 plants			Buffer 4 plants		
assess	Buffer	Trt 1 Rep 1 4 rows * 15 plants	Buffer	Buffer	Trt 2 Rep 1 4 rows * 15 plants	Buffer	Buffer	Trt 2 Rep 1 4 rows * 15 plants	Buffer	assess
		Buffer 4 plants			Buffer 4 plants			Buffer 4 plants		
root		Trt 2 Rep 1 4 rows * 15 plants	Buffer	Buffer	Trt 1 Rep 1 4 rows * 15 plants	Buffer	Buffer	Trt 1 Rep 1 4 rows * 15 plants		root
		Buffer 4 plants			Buffer 4 plants			Buffer 4 plants		
Bintje	Buffer	Trt 1 Rep 2 4 rows * 15 plants	Buffer	Buffer	Trt 1 Rep 2 4 rows * 15 plants	Buffer	Buffer	Trt 2 Rep 2 4 rows * 15 plants	Buffer	Bintje
		Buffer 4 plants			Buffer 4 plants			Buffer 4 plants		
		Trt 2 Rep 2 4 rows * 15 plants			Trt 2 Rep 2 4 rows * 15 plants		Buffer	Trt 1 Rep 2 4 rows * 15 plants		
		Buffer 4 plants			Buffer 4 plants			Buffer 4 plants		
	Buffer	Trt 1 Rep 3 4 rows * 15 plants	Buffer	Buffer	Trt 1 Rep 3 4 rows * 15 plants	Buffer	Buffer	Trt 2 Rep 3 4 rows * 15 plants	Buffer	
		Buffer 4 plants			Buffer 4 plants			Buffer 4 plants		
		Trt 2 Rep 3 4 rows * 15 plants			Trt 2 Rep 3 4 rows * 15 plants		Buffer	Trt 1 Rep 3 4 rows * 15 plants		
		Buffer 4 plants			Buffer 4 plants			Buffer 4 plants		
		Trt 2 Rep 4 4 rows * 15 plants			Trt 1 Rep 4 4 rows * 15 plants		Buffer	Trt 2 Rep 4 4 rows * 15 plants		
		Buffer 4 plants			Buffer 4 plants			Buffer 4 plants		
	Buffer	Trt 1 Rep 4 4 rows * 15 plants	Buffer	Buffer	Trt 2 Rep 4 4 rows * 15 plants	Buffer	Buffer	Trt 1 Rep 4 4 rows * 15 plants	Buffer	
		Buffer 4 plants			Buffer 4 plants			Buffer 4 plants		

### *Minituber Production and Varieties*

As with the previous glasshouse experiments, all minitubers were produced by Agronico Pty Ltd. Disease free tissue culture plants were propagated and transferred into a nutrient film hydroponics system. Plants were grown under carefully controlled nutrient, temperature and light conditions and tubers were hand harvested when they reached the desired size. Tubers were cured and stored for three months at 3°C to break dormancy prior to planting.

Three cultivars of minitubers were used in the experiment; Bintje, Russet Burbank and Markies. Bintje was chosen as the cultivar had been used in all previous experiments, had been the focus of a large amount of previous research and was capable of producing large numbers of tubers per stem. Russet Burbank was selected because it is the main processing cultivar produced in Tasmania and the main cultivar grown for seed by the project industry partner, Agronico. Markies was included in the experiment because of previous observations by Dr J Hills (Personnel communication, 2007) that the cultivar had highly variable tuber numbers in response to N application.

### *Irrigation Application*

Plants received irrigation and fertiliser through drip tape placed in the centre of the mound 5 cm beneath the surface, directly above the seed tuber. The drip tape (Netafim Streamline 16080) had an emitter spacing of 20 cm and each dripper had an approximate output of 1.2 litres per hour. Water was supplied to the drip tape from the nearby stream (250 m laterally and 20 m vertically) with a portable Onga Blazemaster B55H, 5.5 horse power petrol pump.

To facilitate treatment randomisation and replication, the irrigation design required a complicated layout with separate 0.625 cm poly pipe supply lines running the length every second row (Plate 3-1). Each supply line was connected to the appropriate plot section through a T-junction connected to a small length of 0.625 cm poly pipe attached to the drip tape. The individual supply lines were connected to the main supply line and a tap was fitted to each line so that applications could be separately applied to desired treatments and rows.

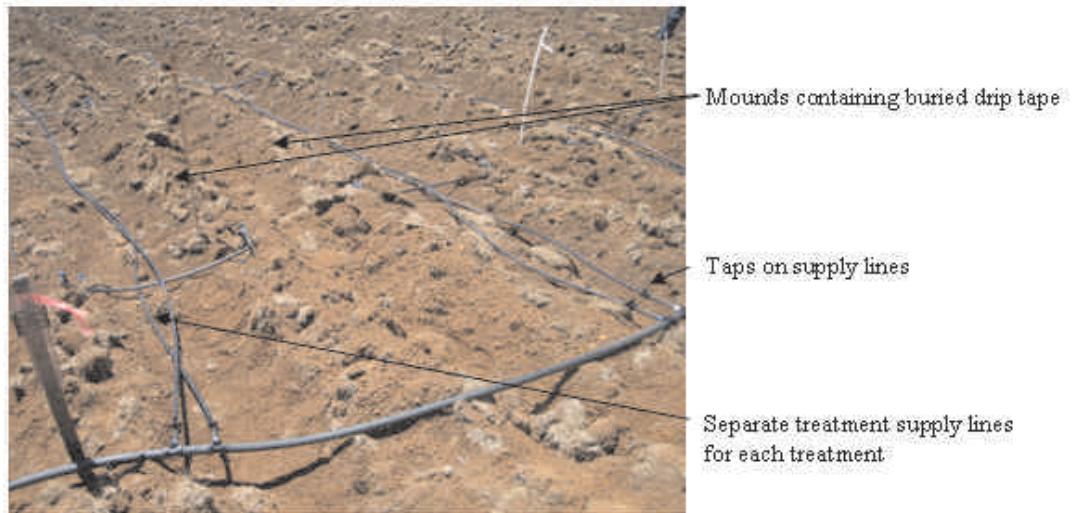


**Plate 3-1:** Irrigation system in place prior to plant emergence

### *Fertiliser Application*

Table 3-9 and Table 3-10 show fertiliser applications applied over the period of the trial. All fertiliser applications post-planting were supplied via the dripper system. No nitrogen was applied in the initial fertiliser banding to prevent any areas of high N concentration in the soil lying beyond the dripper wetting zone. Such an occurrence may have lead to difficulties with successful N leaching at the tuberization stage.

**Table 3-9:** Fertiliser banded at planting

Nutrient	Rate (kg ha <sup>-1</sup> )
Phosphorus	221
Potassium	272
Sulphur	51
Magnesium	25.5

**Table 3-10:** Fertiliser applied post planting

Nutrient	Application Date	Rate (kg ha <sup>-1</sup> )
Zinc	16/01/08	16
Boron	16/01/08	11
Molybdenum	16/01/08	0.15
Potassium	26/01/08	84.3

---

### *Nitrogen Applications*

A total of 177 kg N ha<sup>-1</sup> was applied during the experiment in the form of Ca(NO<sub>3</sub>)<sub>2</sub>. All applications were made through the dripper irrigation system directly into the soil. Small frequent applications were made throughout the initial growth of the trial up to tuberization to keep N at a consistent concentration in the soil (Table 3-11).

**Table 3-11:** Nitrate, water application and rainfall during the trial. Irrigation applications for the leaching treatments are shown in Table 3-12.

Date	Nitrogen Application (kg ha <sup>-1</sup> )	Irrigation (mm)	Rainfall (mm)
3/12/08	-	-	50
12/12/07	85	18.1	-
16/12/07	15.4	5.4	-
18/12/07	15.4	7.2	-
20/12/07	15.4	3.6	-
23/12/07	15.4	5.4	60
27/12/07	15.4	9.0	1
31/12/07	15.4	7.2	-
2/01/08	15.4	7.2	-
6/01/08	15.4	7.2	-
9/01/08	15.4	7.2	-
10/01/08	-	-	20
11/01/08	15.4	7.2	8
14/01/08	15.4	5.4	-
16/01/08	15.4	5.4	-
18/01/08	15.4	7.2	-
21/01/08	15.4	5.4	-
23/01/08	15.4	5.4	-
25/01/08	15.4	7.2	-
28/01/08	15.4	7.2	-

---

### *N Leach Treatment*

At the start of tuberization, irrigation was applied to the N Leach treatments for 3.5 hours, an application equivalent to 26 mm over the entire trial. The N Leach treatment was applied on separate dates for each cultivar because they developed at

---

different rates (Table 3-13). No N was applied to the N Leach plots for seven days following the start of the treatment. Standard N applications were maintained for the control. At the end of the N Leach treatment, N was gradually returned to the plots in low doses ( $15 \text{ kg ha}^{-1} \text{ NO}_3\text{-N}$ ).

**Table 3-13:** Time of treatment application and sampling for each variety (DAE = days after emergence). Emergence was calculated as the time when 90% of plants in each variety had emerged

Variety	Bintje	Russet Burbank	Markies
Planting Date	27/11/07	27/11/07	27/11/07
Emergence	6/01/08	23/12/07	20/12/07
Planting to Emergence (days)	41	27	24
Leaching (DAE)	10	17	25
1 <sup>st</sup> Sample (DAE)	24	31	39
2 <sup>nd</sup> Sample (DAE)	80	94	97

### *Assessments*

#### *Pre-treatment Assessments for Tuberization*

Random sampling across the three cultivars was commenced 14 days after plant emergence to determine time of tuberization (Plate 3-2). Five plants were selected from each cultivar and when four of the five plants were found to have tubers present treatment applications commenced.



**Plate 3-2:** Presence tubers during one of the many tuberization assessments.

### *Plant Sampling*

Plants were sampled at 2 dates after application of treatments (Table 3-13). One hundred plants from each cultivar were sampled at both assessments. At the first assessment, total tuber number was recorded and individual tuber mass was measured. At the second assessment tuber number was recorded and tubers were sorted into industry standard size categories, and weighed. Fresh and dried stem mass and stem number were recorded at both sampling times.

### *Soil Nitrogen and Organic Carbon*

Soil profile samples were taken at the centre of the row mound to a depth of 100 cm in 20 cm intervals in the three varieties five days after the start of the N Leach treatment. In the Russet Burbank cultivar plots, additional samples were taken 30 cm from the mound centre at the same depth intervals to 80 cm. From these field samples, a 10.0 g subsample was taken and N was extracted with 2 M KCl. These solution extracts were sent to CSBP laboratories in Perth Western Australia for colorimetric analysis of  $\text{NO}_3^-$  and  $\text{NH}_4^+$  (mineral nitrogen). Concentrations in the KCl extract were converted to  $\text{NO}_3^-$  and  $\text{NH}_4^+$  per unit volume of soil,  $T$  ( $\mu\text{mol}_\text{c} \text{ N cm}^{-3}$  soil) using equation 2-1:



---

*Rooting Depth*

Two potato root distribution assessments were made during the field trial to estimate the rooting depth and general root distribution in the soil profile. The presence of roots were assessed in auger samples taken in 20 cm increments to a depth of 100 cm directly below the row centre five days after the N Leach treatment was applied. In the Russet Burbank cultivar, root samples were also taken in the mound inter-row, 30 cm from the mound centre.

At plant maturity, three pits were excavated in the buffer zone around the outside of the trial area to a depth of 1.2 m to observe plant rooting depth (Plate 3-3). Root observations were also made in an area where no plants were grown to help distinguish between potato roots and those that were already present from previous pasture species.



**Plate 3-3: Soil pit excavated for root observations and bulk density measurement.**



*Statistical Analysis*

Statistical analysis of trial results was carried out using analysis of variance for tuber and stem mass and number (Fischer LSD). Tuber size distribution was assessed by dividing tubers into size classes and Chi squared analysis was used to compare the size distribution between treatments. All analysis was conducted in the statistical program SAS version 9.1 (2003).

## RESULTS

### *Plant Emergence*

Plant emergence was first noted 15 days after planting (DAP), and by 23 DAP plants from each cultivar had emerged. The date of first emergence varied between cultivars, with Russet Burbank emerging earlier than Markies and Bintje (Table 3-13). In addition to delayed first emergence, Bintje displayed a longer duration of emergence which was measured as the time from first emergence to 90% plant emergence. In all three cultivars, emergence was relatively uniform and even growth of plants was noted within seven weeks of planting.

**Table 3-14:** Details of plant emergence in the field compared to a glasshouse experiment.

Cultivar	Planting to 1 <sup>st</sup> emergence (days)	1 <sup>st</sup> emergence to completion of emergence (days)
Bintje	23	17
Russet Burbank	15	15
Markies	19	11
Bintje – Glasshouse trial	16	6

In comparison to the previous glasshouse trials, emergence in the field was slower and less uniform. Under glasshouse conditions, plant emergence in Bintje was first observed 16 DAP, compared to 23 DAP in the field, and only 6 days elapsed between the first plant emerging and 100% of plants emerging. While higher temperature in the glasshouse was likely to have promoted the more rapid growth, the presence of remnant clods of pasture turf in the field soil also contributed to delayed and more variable emergence in the field trial.

### *Soil Nitrogen Measurements*

Significantly lower NO<sub>3</sub><sup>-</sup> concentrations (P<0.005) were measured in the surface 20 cm of the soil profile directly under the mounds in the N Leach plots compared to the control after treatment application (Figure 3-2 and Figure 3-3). This treatment effect

---

was measured in all three varieties. There was no significant difference ( $P < 0.05$ ) in  $\text{NO}_3^-$  concentration between the N Leach and control treatments below this depth. Analysis of the  $\text{NO}_3^-$  in the inter-row space in the Russet Burbank variety showed that there was no difference in  $\text{NO}_3^-$  concentration between treatments at any depths (Figure 3-3B).  $\text{NO}_3^-$  contents in the inter-row space were much lower than in the centre of the mound indicating that the applied  $\text{NO}_3^-$  was spreading less than 30 cm laterally. Differences in  $\text{NO}_3^-$  concentrations in the 0–20 cm depths between varieties were a result of the different sampling times and potentially different uptake rates of the different cultivars.

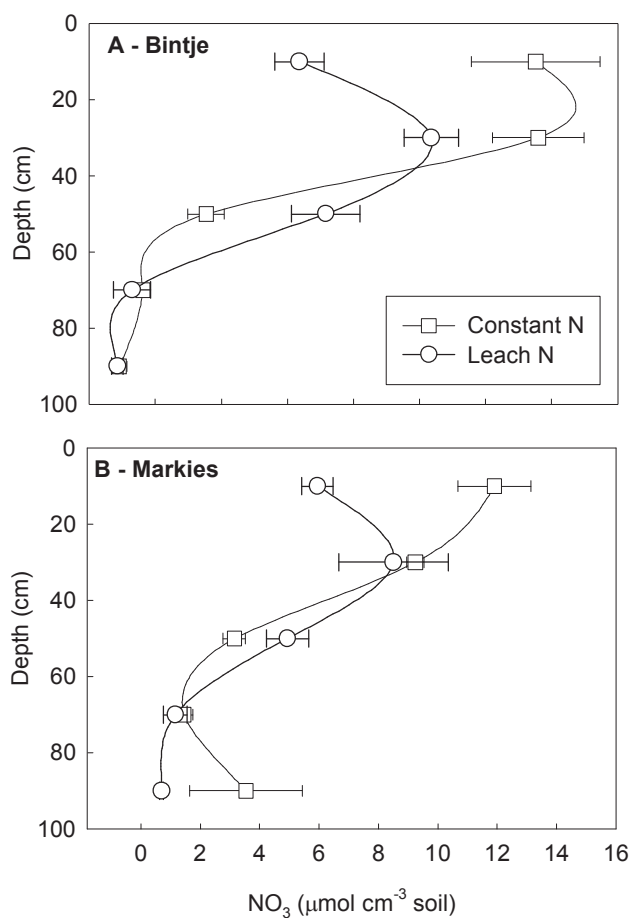


**Figure 3-2:** Soil  $\text{NO}_3^-$  ( $\mu\text{mol cm}^{-3}$  oven dry soil) under the centre of the mound in the Bintje (Chart A) and Markies (Chart B) potato cultivars in the Constant N and N Leach treatments. Error bars represent the standard error of the mean.

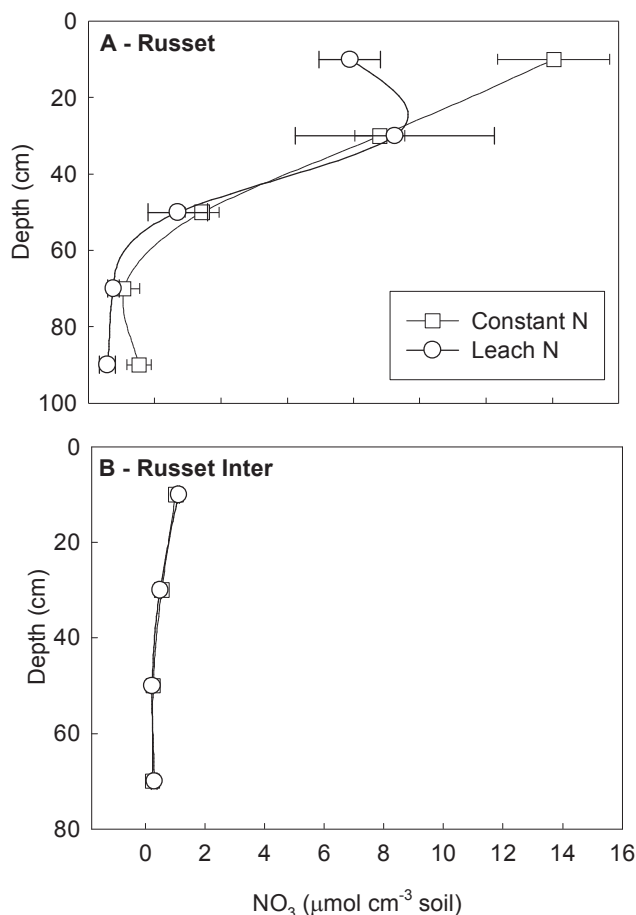


**Figure 3-3:** Soil  $\text{NO}_3^-$  ( $\mu\text{mol cm}^{-3}$  oven dry soil) in the Russet Burbank variety under the centre of the mound (Chart A) and in the inter-row space (Chart B) in the constant N and N Leach treatments. Error bars represent the standard error of the mean.

Assessment  $\text{NH}_4^+$  throughout the soil profile showed significant levels were present in the upper 40 cm of the profile directly under the soil mound (Figure 3-4 and Figure 3-5). The N Leach treatment did not influence concentrations of  $\text{NH}_4^+$ . Significantly lower levels were observed in the inter-row space compared to assessments directly under the plants. The presence of significant concentrations of  $\text{NH}_4^+$  in the soil was unexpected because it was not applied as fertiliser to the crop. Its accumulation must therefore be a product of organic matter mineralisation. Higher concentrations in the mound than the inter-row space suggests that soil moisture and perhaps  $\text{NO}_3^-$  concentrations played a role in its accumulation.

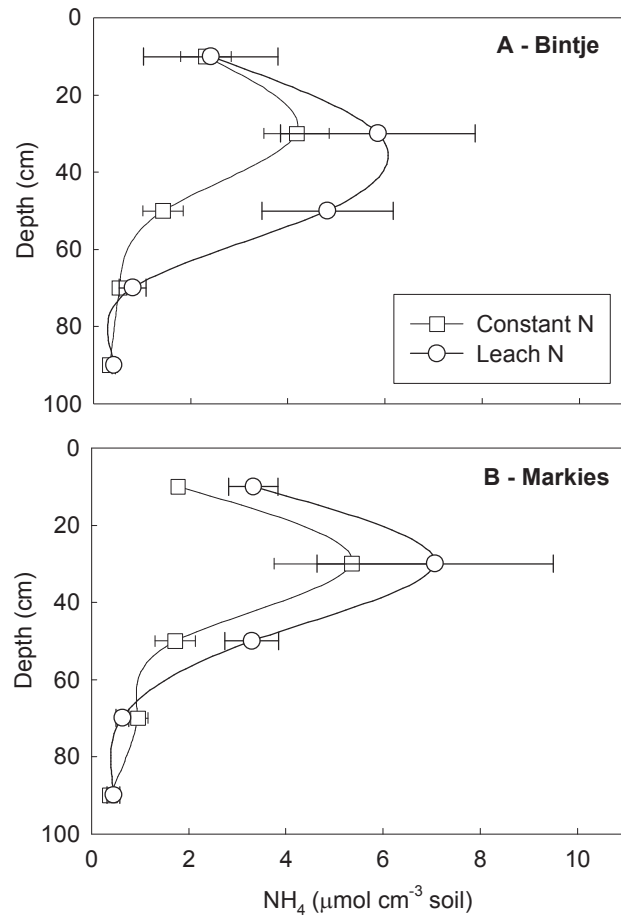


**Figure 3-4:** Soil  $\text{NH}_4^+$  ( $\mu\text{mol cm}^{-3}$  oven dry soil) under the centre of the mound in the Bintje (Chart A) and Markies (Chart B) potato cultivars in the Constant N and N Leach treatments. Error bars represent the standard error of the mean.

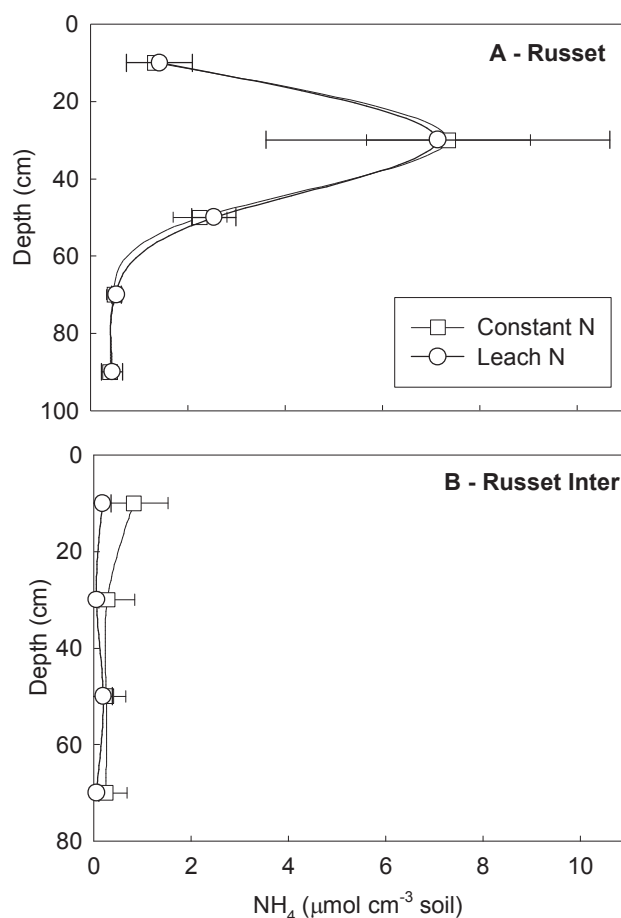


**Figure 3-5:** Soil  $\text{NH}_4^+$  ( $\mu\text{mol cm}^{-3}$  oven dry soil) in the Russet Burbank variety under the centre of the mound (Chart A) and in the inter-row space (Chart B) in the constant N and N Leach treatments. Error bars represent the standard error of the mean.

### ***Plant Rooting Depth***

Detailed root density assessments were not conducted during the experiment however observations of root distribution were made at the two plant assessment times. These assessments indicated that the vast majority of potato roots were concentrated in the upper 40 cm of the soil profile under the centre of the mound. An example of root density at three depths directly under the drip tape is shown in (Plate 3-4). Very few roots were present between 40–60 cm and no roots were observed below 60 cm in the soil. Assessments at the first sample time in the inter-row space of Russet Burbank indicated no roots were present at any depth. These observations confirmed that the vast majority of roots were concentrated in the upper 40 cm and did not spread into the inter-row space.

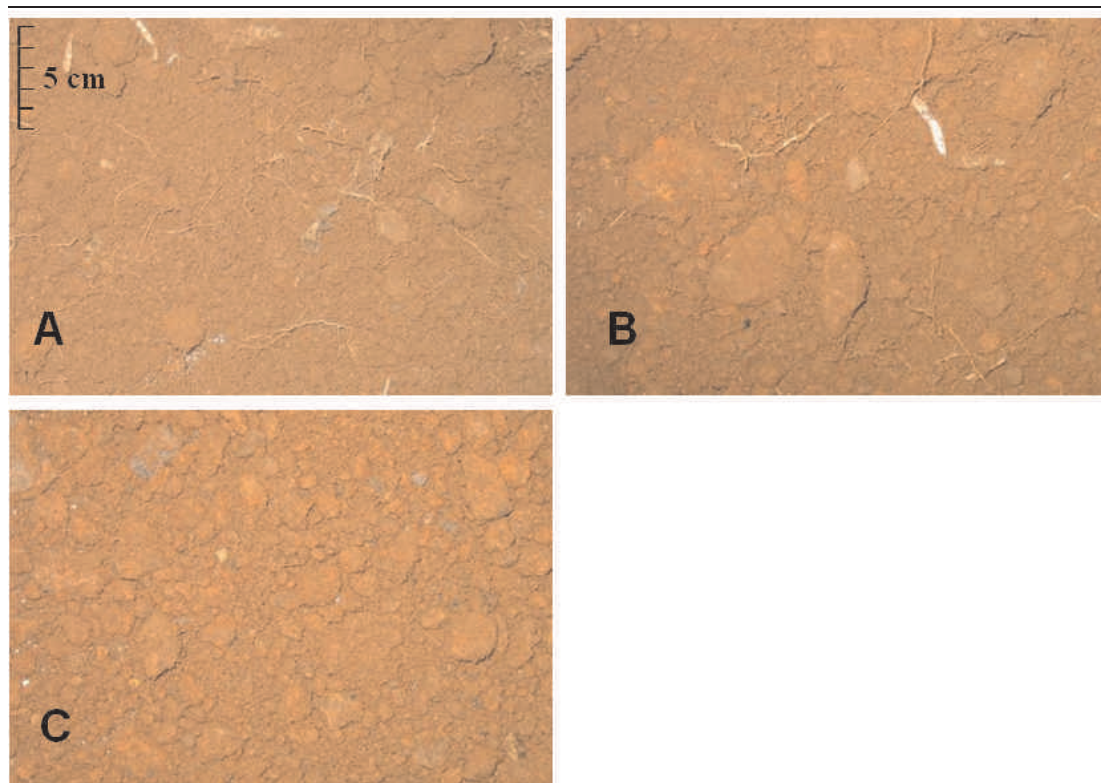


**Plate 3-4:** Root density in the centre of the mound from augured samples at 0–20 cm depth (A), 20–40 cm depth (B) and 40–60 cm depth (C).

### *Plant Assessments*

Analysis of tubers and stems from plants at both harvest times revealed no significant treatment effect ( $P < 0.05$ ) on tuber or stem number or mass in the three cultivars (Table 3-15 and Table 1-13). A higher tuber mass was expected in the N Leach treatment based on the finding in the glasshouse experiment. However  $\text{NO}_3^-$  was only reduced in the top 20 cm of the profile while roots extended to 40 cm and therefore it is likely that plants still had enough access to significant levels of soil  $\text{NO}_3^-$  in the N Leach treatment.

The trial was not designed to compare differences between the cultivars however some trends were observed. Higher tuber numbers were measured in Bintje in comparison to the Russet Burbank and Markies cultivars at both sample times and as a result the average mass of tubers was lower in the Bintje plants. Despite similar tuber numbers in the Russet Burbank and Markies cultivars the average and total tuber mass was much higher in the Markies cultivar (Table 3-15 and Table 1-13).



The green mass at the first harvest and dry mass measurements at the final harvest were higher in the Markies cultivar indicating that these plants may have been capable of producing larger amounts of assimilates due to greater light interception. Differences in growth and tuber number and size are likely to be a result of differences in the cultivars since plants were given the same nutrient and water applications. Different varieties were also produced at different times in the glasshouse and therefore the physiological age between the varieties may have also influenced some of the differences in plant growth.

In each cultivar, a significant decrease in tuber numbers per stem ( $P < 0.05$ ) was recorded between the initial sampling date and final sampling at crop maturity. Since no N Leach treatment effect was measured the two treatments were combined to determine changes in mean tuber number. Analysis indicated the level of resorption was 53% for the Bintje cultivar and 28% for both the Russet Burbank and Markies cultivars. This indicated that tuber resorption had a significant influence on final tuber number in the field experiment. There was therefore potential to have increased tuber retention if the N Leach treatment was applied effectively.

**Table 3-15:** Tuber and stem measurements 14 days post treatment application. No statistical significance was measured between treatments within potato varieties. Values in parentheses indicate the standard deviation of the mean.

	Bintje		Russet Burbank		Markies	
	Const N	N Leach	Const N	N Leach	Const N	N Leach
Tuber number per stem	13.9 (6.0)	13.9 (5.8)	5.0 (2.1)	4.8 (1.7)	3.9 (2.3)	4.2 (2.1)
Total Mass per stem (g)	113 (59)	106 (63)	123 (60)	117 (56)	204 (118)	220 (109)
Mean Tuber Mass (g)	8.3 (6.5)	8.4 (6.7)	13.0 (8.2)	11.5 (7.4)	62.5 (45.2)	62.9 (40.6)
Mean Stem Number	1.4 (0.6)	1.5 (0.7)	2.4 (1.0)	2.5 (0.8)	1.4 (0.6)	1.4 (0.5)
Mean Stem Mass (g)	298 (147)	287 (113)	159 (101)	154 (77)	342 (181)	383 (189)

**Table 3-16:** Tuber and stem measurements at plant maturity. No statistical significance was measured between treatments within potato varieties. Values in parentheses indicate the standard deviation of the mean.

	Bintje		Russet Burbank		Markies	
	Const N	N Leach	Const N	N Leach	Const N	N Leach
Tuber number per stem	5.96 (0.84)	7.1 (2.5)	3.5 (0.7)	3.6 (0.1)	2.8 (0.4)	3.0 (0.4)
Total Mass per stem (g)	669 (98)	783 (233)	458 (56)	481 (31)	779 (54)	744 (141)
Mean Tuber Mass (g)	112 (4)	111 (3)	133 (9)	134 (6)	282 (37)	245 (25)
Mean Stem Number	1.44 (0.25)	1.3 (0.3)	2.6 (0.5)	2.5 (0.2)	1.7 (0.2)	1.8 (0.2)
Mean dry mass/stem (g)	42.6 (12.9)	45.3 (16.4)	27.7 (7.8)	27.1 (15.5)	51.3 (4.8)	50.8 (6.8)

### *Tuber Size Distribution*

The N leach treatments had no significant effect ( $P < 0.05$ ) on the size distribution of Bintje and Russet Burbank tubers 14 days after treatment application (Figure 3-6). Significant differences in the size ranges 4–6, 16–32, 64–128 and >128g were measured in Markies (Figure 3-6). The differences however did not show a clear trend towards either increased or decreased tuber number in the higher size classes, suggesting the differences may have been due to natural variation. Assessments of tuber size distribution at maturity again showed no effect of the N leach treatment (Figure 3-7).

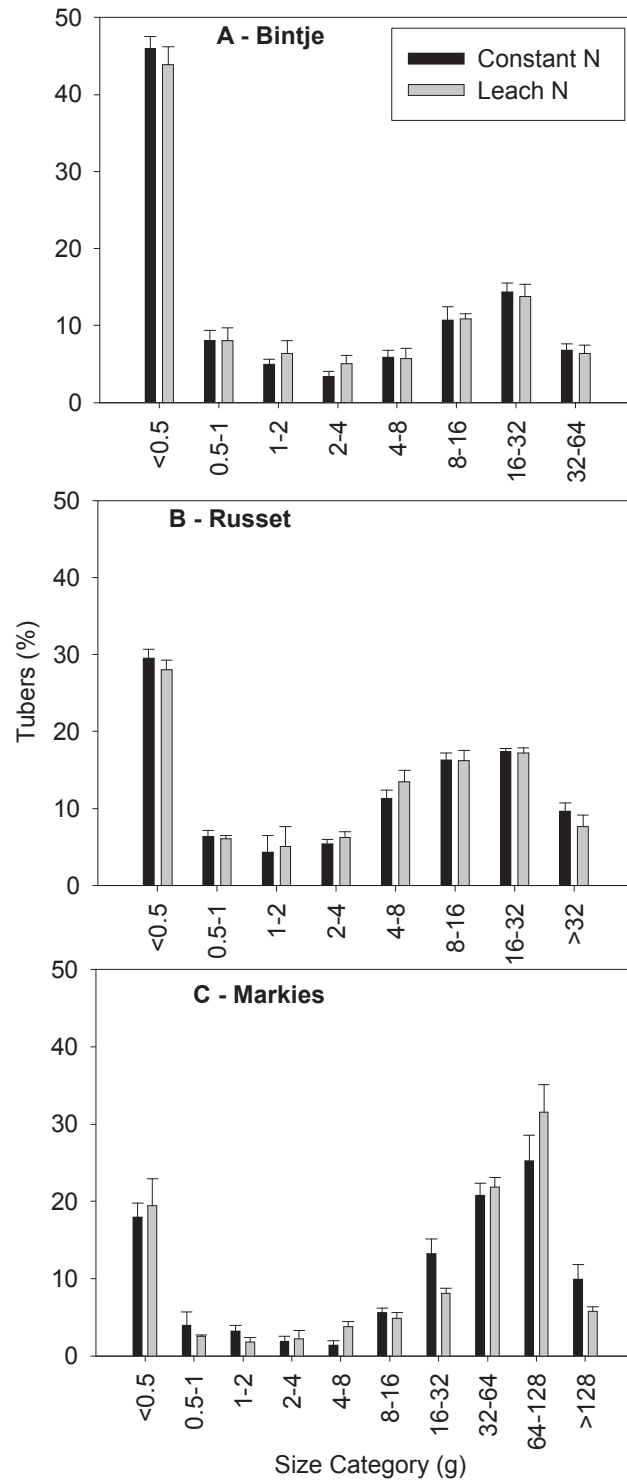


**Figure 3-6:** Percentage of tubers in selected size ranges in the variety Bintje at the first sample time. Error bars represent the standard error of the mean.

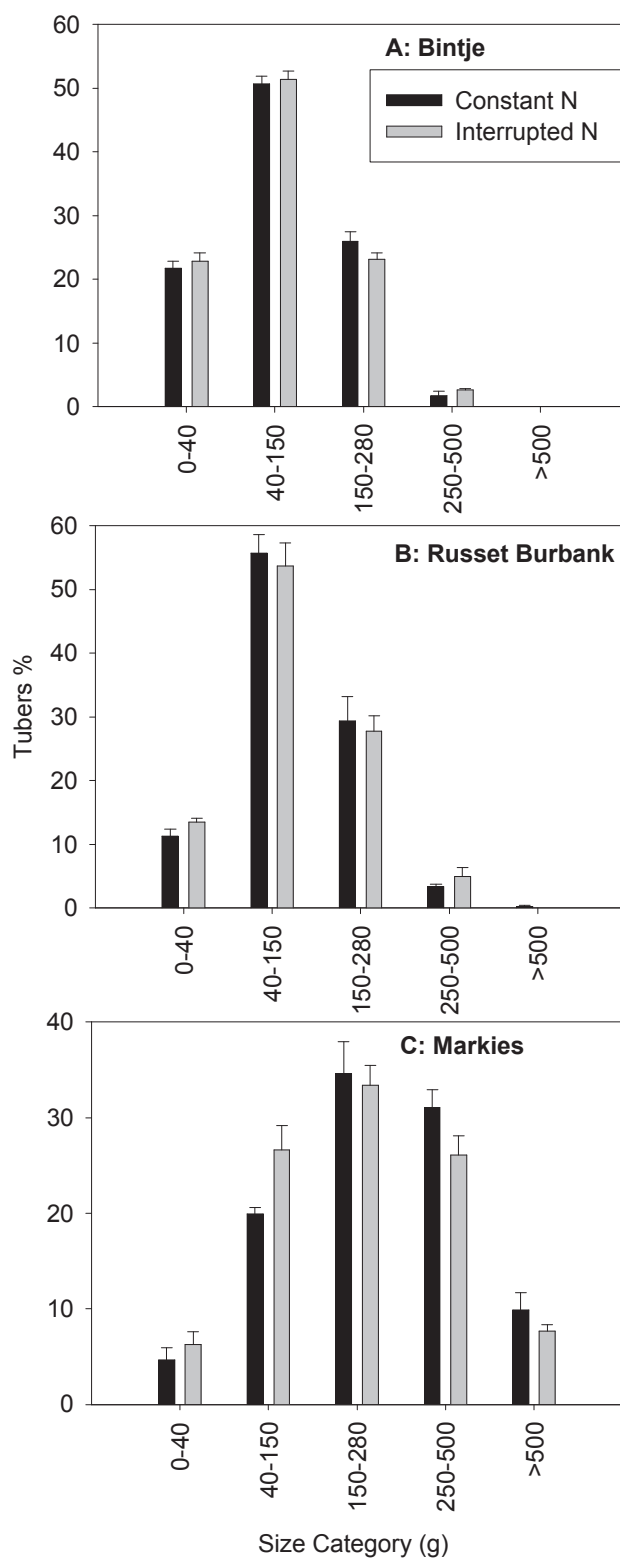


**Figure 3-7:** Percentage of tubers in selected size ranges in the variety Bintje at the second sample time. Error bars represent the standard error of the mean.

---

## DISCUSSION

In contrast to the glasshouse trial, no significant differences were measured in tuber number, mass or size distribution due to the N Leach treatment in the field experiment. While the volume of water added through the drip irrigation system was sufficient to significantly decrease the  $\text{NO}_3^-$  concentration in the upper 20 cm of the soil profile directly under the mound,  $\text{NO}_3^-$  concentration below 20 cm in the profile were not significantly different from the controls. The failure of the treatment to reduce the  $\text{NO}_3^-$  concentration in the lower root zone and the higher than anticipated concentrations of  $\text{NH}_4^+$  in the entire root zone, may have prevented a plant response to the treatment.

Analysis of  $\text{NO}_3^-$  below the mound centre after treatment application showed that concentrations of  $\text{NO}_3^-$  in the field soil were reduced from 13.15 to 6.23  $\mu\text{mol}_\text{c} \text{ N cm}^{-3}$  soil in the 0-20 cm depth on average in the three cultivars (Figure 3-2 and Figure 3-3). In comparison concentrations in the Red Ferrosol topsoil from the glasshouse trial were reduced from 12.67 to 4.19  $\mu\text{mol}_\text{c} \text{ N cm}^{-3}$  soil. Although concentrations were significantly reduced in the soil the amount of  $\text{NO}_3^-$  remaining was still higher than that in the N leach treatment in the glasshouse. The reduction in  $\text{NO}_3^-$  may still have been sufficient to cause the same plant response however this cannot be confirmed since root observations show much of the potato root system still had access to significant concentrations of  $\text{NO}_3^-$  in the 20–40 cm depth (Figure 3-2 and Figure 3-3). It is therefore unlikely that N availability was adequately restricted to the plants to induce a similar response to that observed in the glasshouse. Furthermore the higher concentrations of  $\text{NH}_4^+$  measured in the field may also make reduction in N concentrations difficult (Figure 3-4 and Figure 3-5). Factors that may have effected the leaching of  $\text{NO}_3^-$  are: i) the volume of water applied during the leaching treatment; ii) the use of the drip tape irrigation system to apply the leaching treatment; iii) the timing of the treatment application; iv) the presence of anion adsorption in the soil and; v) the build up of  $\text{NH}_4^+$  in the profile.

The leaching volume was equivalent to an overhead application of 26 mm across the trial area. However the drip tape supplied water directly into the soil mound rather than uniformly across the entire area and therefore the quantity of water applied to the root zone would have higher than this average value indicates. It was difficult to

---

---

predict the volume necessary to leach  $\text{NO}_3^-$  out of the root zone in the field because the rate of horizontal water movement under the drip tape system was not known.

The dripper system offered a number of advantages for trial design over other irrigation systems however it may have also created difficulties in leaching  $\text{NO}_3^-$ . The drip fertigation system enabled small and frequent applications of water and nutrients to be applied directly to the roots allowing maintenance of consistent levels throughout the experiment.

Root observations indicated a typical vertical distribution pattern however horizontal spread was lower than previously reported. Studies have shown 60 to 85% of roots are found in the upper 30 cm of the profile (Lesczynski and Tanner 1976; Smith 1968; Stalham and Allen 2001), with concentrations rapidly decreasing below this depth. In this trial, the majority of the roots were in the upper 40 cm of the soil which is in agreement with these finding however samples taken in the inter-row space showed no potato roots were present at any depth. Stalham and Allen (2001) and Smith (1968) found roots overlapped in the inter row space under overhead irrigation to create a homogenous root distribution. The absence of roots in the inter row may therefore be a result of the water distribution pattern of the dripper system resulting in roots concentrating in the wetted area and not expanding into the inter-row space. This has previously been observed by Hodgson *et al.* (1990) and Zhang *et al.* (1996).

Water and  $\text{NO}_3^-$  movement in soils irrigated with a dripper system will be different to those irrigated with an overhead system. If an overhead irrigation system was used, disregarding plant water uptake and variation in soil homogeneity, water will vertically infiltrate through the soil in one dimension carrying with it the  $\text{NO}_3^-$  in the soil solution. However water from a buried drip line will move vertically, laterally and even upwards carrying solute in the soil solution with it (Li *et al.* 2003). Soil samples were only taken directly under the drip tape and 30 cm laterally from the mound. Analysis of the inter-row measurements indicated that  $\text{NO}_3^-$  was not displaced to this area (Figure 3-3) therefore the amount of lateral spread described by was less than 30 cm even after extended irrigation during the N leach treatment. Prolonged irrigation using the dripper system may be sufficient to push the solute out of the plant root zone both vertically and horizontally however  $\text{NO}_3^-$  may accumulate at the edge of the mound where it may still accessible to the plant roots. The pattern of water movement and solute distribution will depend on soil type, dripper spacing

---

---

and dripper output (Cote *et al.* 2003) so estimation of the pattern of water movement in a particular situation is difficult without detailed knowledge of soil hydraulic parameters. The use of a buried dripper system was therefore beneficial in terms of restricting the root distribution in the soil however a better understanding of water distribution in the Red Ferrosol under this type of irrigation system is required to determine if sufficient leaching can be achieved with this method.

Variability in the time of emergence in the field compared to the glasshouse (Table 3-14) creates an additional hurdle to application of the N Leach treatment in the field as correct timing of treatment applications is difficult. Because tubers were planted mechanically in the field, planting depth and orientation of the tuber eyes could not be accurately controlled. Furthermore the soil contained some large clods of degrading clover based pasture turf (Plate 3-1) and during plant assessments it was observed that they impeded the emergence of some plants in the experiment. O'Brien *et al.* (1998) states that the time between emergence and tuberization is generally very similar between plants under the same conditions. Consequently, a greater variation in the time between planting and emergence results in higher variability in the timing of tuberization. Hand planting may have improved the evenness of emergence however this would not be practical on any significant scale. Earlier cultivation and increased tillage would improve the seedbed and increase mound evenness which may improve the emergence and increase the uniformity of crop growth.

There is potential that the level of  $\text{NO}_3^-$  leaching was influenced by anion adsorption in the soil which is known to occur in Red Ferrosol's (Moody 1994). A number of previous studies have shown that the rate of  $\text{NO}_3^-$  movement through the soil can be reduced by anion adsorption (Black and Waring 1976a; Duwig *et al.* 2003; Katou *et al.* 1996). Therefore if anion adsorption is significant in this soil then this may have reduced the rate of  $\text{NO}_3^-$  movement during the N leach application in the field. The influence of this potential factor was not investigated prior to the field experiment and its influence cannot be estimated without some direct measurement in the soil.

The amount of  $\text{NH}_4^+$  in the field soil was much higher than levels measured in the glasshouse experiment. Mean concentrations were highest in the 20–40 cm depth with mean concentrations of  $5.63 (\pm 3.44) \mu\text{mol}_\text{c} \text{ N cm}^{-3}$  soil in comparison to  $0.65 (\pm 0.12) \mu\text{mol}_\text{c} \text{ N cm}^{-3}$  soil in the glasshouse. Unlike  $\text{NO}_3^-$  levels, the N leach treatment did not appear to move  $\text{NH}_4^+$  through the soil profile since levels between

---

the N leach and control treatments were not significantly different (Figure 3-4 and Figure 3-5). This is probably a result of adsorption of  $\text{NH}_4^+$  by the soils cation exchange capacity (Table 3-4). The higher  $\text{NH}_4^+$  concentration in the field may therefore increase the difficulty of reducing N concentrations in this environment.

No  $\text{NH}_4^+$  was applied as fertiliser and therefore it must have been a product of soil organic matter mineralization which was probably accelerated by cultivation and irrigation in the field (Powlson 1980). The experiment site had been under clover based pasture for 20 years prior to the seed crop, and organic carbon levels were over 4.5% in the upper 40 cm of the soil profile. The soil at planting still contained large amounts of decomposing turf clumps throughout the cultivated layer. The frequent irrigation and warm temperatures over the growing season would have provided ideal conditions for soil microbes to break down some of the organic N pool converting it to  $\text{NH}_4^+$  (Jansson and Persson 1982). Lower  $\text{NH}_4^+$  concentrations were measured in the inter-row samples compared to directly under the drip line. This observation indicates that the higher soil moisture within the soil mound as a result of drip line irrigation was a significant factor in encouraging mineralisation. The season was dry and therefore breakdown in the inter-row space not wet by the drip irrigation did not progress at the rate observed directly under the mound centre.

Schmidt (1982) states that in most circumstances nitrifying bacteria convert  $\text{NH}_4^+$  to  $\text{NO}_3^-$  as rapidly as it is formed however this does not appear to have been the case during this experiment. The main factors affecting the rate of nitrification are temperature, moisture, pH and availability of oxygen (Schmidt 1982). Regular irrigation provided moist conditions, and the soil pH was 5.8 which was within the range at which nitrification takes place (Schmidt 1982) however Alexander (1965) states that activity of nitrifying microbes is markedly reduced even in slightly acid conditions. The  $\text{NH}_4^+$  accumulation may therefore be a result of rapid mineralization occurring at a rate at which nitrifying bacteria were not immediately converting all the  $\text{NH}_4^+$  to  $\text{NO}_3^-$  since their activity was limited by the mildly acidic soil conditions.

There are previous reports in the literature of significant  $\text{NH}_4^+$  accumulation in the field soils. Concentrations of  $\text{NH}_4^+$  in a Red Ferrosol from Queensland was found to be  $5.5 \mu\text{mol}_c \text{ N cm}^{-3}$  in the soil solution which was equivalent to  $1.87 \mu\text{mol}_c \text{ N g}^{-1}$  soil based on the 37% water capacity (Gillman and Bell 1978). This concentration, although still lower than the level measured in the field experiment ( $6.16 \mu\text{mol}_c \text{ N cm}^{-3}$ ),



---

<sup>3</sup> soil = 7.73  $\mu\text{mol}_c \text{ N g}^{-1}$  soil), is in the same order of magnitude. Furthermore this concentration does not take into account adsorbed  $\text{NH}_4^+$  which was not reported in the study and therefore the total amount of plant available  $\text{NH}_4^+$  would have been higher than 1.87  $\mu\text{mol}_c \text{ N g}^{-1}$ .

## CONCLUSION

The N Leach treatment was applied in the field to assess its impact on tuber formation and growth rate based in the results from the glasshouse experiment described in Chapter 2. Plant assessments showed no effect of the N Leach treatment however, leaching of  $\text{NO}_3^-$  was less than expected based on the preliminary trials in the glasshouse. Furthermore significant concentrations of  $\text{NH}_4^+$  accumulated in the soil which may have precluded a measurable tuber development response.

The N Leach treatment reduced  $\text{NO}_3^-$  concentration in the upper 20 cm of the profile in comparison to the control, but not below this depth. Therefore a significant proportion of the root zone still had access to high N concentrations. The insufficient leaching may have been the result of a number of factors. The drip irrigation method used in the trial may have resulted in horizontal displacement of  $\text{NO}_3^-$  that was still accessible to the roots. It was also possible that there was a significant amount of anion exchange in the soil which may have slowed the rate of  $\text{NO}_3^-$  movement. Finally the amount of water applied may have simply been insufficient to leach the  $\text{NO}_3^-$  sufficiently from the root zone despite the use of an efficient in mound dripper system.

To successfully apply the N Leach treatment in the field, a better understanding of water and solute movement in these soil types is required. Consideration of alternative irrigation techniques may also be warranted since a dripper system may not be as an effective leaching tool as broad scale sprinkler irrigation. The build-up of  $\text{NH}_4^+$  was another barrier to treatment application and must be considered and managed in soils containing significant levels of decomposing N-rich vegetative material. From the perspective of the N Leach application, focussing on reducing  $\text{NO}_3^-$  rather than  $\text{NH}_4^+$  concentrations will be simpler because the negatively charged ion was present in higher concentrations and was more mobile in the soil. As a result achieving the required change in soil N concentrations is more likely if manipulating  $\text{NO}_3^-$  is the focus of the study.

## CHAPTER 4

# NITRATE ADSORPTION AND ITS CONSEQUENCES IN A RED FERROSOL

### INTRODUCTION

The leaching treatment described in Chapter 3 was unsuccessful in moving  $\text{NO}_3^-$  below the plant root zone. Nitrate is mobile in most soils because it exists solely in the soil solution however the rate of movement may not be as rapid in soils where it is adsorbed. Previous field studies by Black and Waring (1976a) reported  $\text{NO}_3^-$  movement through a Red Ferrosol soil was significantly retarded relative to the soil water due to anion adsorption. Adsorption of  $\text{NO}_3^-$  may therefore have also contributed to the reduced rate of solute movement in comparison to soil water in the field experiment described in Chapter 3 since it was conducted on the same soil type. To test this hypothesis, a better understanding of water and  $\text{NO}_3^-$  movement was required.

This chapter describes a set of unsaturated horizontal absorption and batch experiments in which the movements of water and  $\text{NO}_3^-$  were measured during unsaturated flow. The adsorption isotherm for  $\text{NO}_3^-$  in the soil was also investigated to determine the level of adsorption across the range of solution concentrations in the column experiments.

### LITERATURE REVIEW

#### Adsorption of Anions by Soils

Adsorption is an important chemical processes in soils since it determines the quantity of plant nutrients, metals and organic chemicals such as pesticides that are retained on soil surfaces and influences the rate at which these substances move through the soil (Sparks 1995). In soils that have an anion exchange capacity, positively charged sites on the surface of clay minerals adsorb anions from the soil solution. *Adsorption* is defined as the condensation of liquids or dissolved substances

---

onto the surfaces of solids, and differs from *absorption* which is defined as the uptake of a substance by the body of another (Weast 1971).

Anion adsorption capacity of soils is affected by the type and amount of clay minerals in the soil, pH and organic carbon (OC) content. The minerals that contribute to anion absorption in soils are the kaolins (halloysite and kaolinite) and various iron and aluminium oxides and hydroxides, such as goethite, haematite and gibbsite (Yu 1997). Soil pH affects the proportion of positive and negative charge on the hydroxyl groups of the oxides and therefore influences the level of anion adsorption (Evangelou 1998). A decrease in pH results in protonation of hydroxyl groups and the development of positively charged surfaces, which adsorb anions. Organic carbon is negatively correlated with anion adsorption (Strahm and Harrison 2007). Marcos *et al.* (1998) observed an increase in anion adsorption in soils when the OC fraction was removed and an increase in anion adsorption with soil depth was linked to decreasing OC levels down the soil profile by Black and Waring (1976b).

The majority of studies investigating anion adsorption in variable charge soils have focussed on subsoils where anion adsorption typically increases with depth due to decreasing OC and increasing proportions of variable charge minerals (Bellini *et al.* 1996; Katou *et al.* 1996; Katou *et al.* 2001; Kinjo *et al.* 1971; Qafoku and Sumner 2001). This has also been the case in the few studies of adsorption in Red Ferrosol's from Australia (Black and Waring 1976b; 1979; Donn and Menzies 2005; Moody 1994). Despite anion adsorption generally being greater at depth an understanding of its significance in surface soils is important for nutrient management of shallow rooted vegetable crops such as potatoes (Stalham and Allen 2001). Black and Waring (1976c) measured absorption throughout the profile of an Australian Red Ferrosol. They confirmed that  $\text{NO}_3^-$  was adsorbed in the subsoil below 0.4 m, but found no adsorption in the surface soil (0-0.15 m). The lack of adsorption in the surface was attributed to higher OC levels and the lower soil pH and proportion of variable charge minerals. In contrast, retardation of  $\text{NO}_3^-$  movement relative to the rate of water movement in surface soil was observed by Duwig *et al.* (2003) in a variable charge Ferralsol (FAO classification) from New Caledonia.

Because the anion adsorption capacity of a soil is influenced by a number of soil properties, direct measurement is the most appropriate way to determine a soils capacity to adsorb anions. There is a lack of data on  $\text{NO}_3^-$  adsorption in surface soils

---

in general however investigation Tasmanian Red Ferrosol soils is further justified because it is the primary cropping soil in Tasmania (Loveday and Farquhar 1958a). Identifying the presence and significance of anion adsorption on  $\text{NO}_3^-$  retention may offer benefits for management of  $\text{NO}_3^-$  concentrations in vegetable crop root zones in these soils since rates of  $\text{NO}_3^-$  movement through this zone can be determined.

### **Adsorption Isotherms**

Adsorption of a compound in a soil is generally characterised by an adsorption isotherm, that is, an equation that relates the solution concentration to the amount adsorbed on the soil surface (Sparks 1995). Adsorption isotherms have been developed for a large number of solutes in a variety of soils. The list of solutes includes nutrients such as  $\text{K}^+$  (Bond and Phillips 1990b),  $\text{HPO}_4^{2-}$  (Olsen and Watanabe 1957) and  $\text{NO}_3^-$  (Kinjo and Pratt 1971). Adsorption isotherms are, however, unique to each specific solute and soil combination.

In soil chemistry the relationship between the solution and adsorbed concentrations is generally non-linear (Sposito 1989). The Freundlich and Langmuir equations have been used to describe adsorption of anions in previous studies (Duwig *et al.* 2000; Katou *et al.* 1996; Kinjo and Pratt 1971; Qafoku *et al.* 2000).

### ***Isotherm Equations and Examples***

The Freundlich and Langmuir isotherm equations were both originally developed to describe gas adsorption to planar surfaces (Sparks 1995), but have since been frequently used to describe adsorption of anions in soils. They were originally developed assuming: i) only monolayer coverage of surfaces occurs and; ii) there is no interaction between the adsorbed molecules. Neither of these are valid for adsorption on soils, so these equations should only be regarded as curve fitting models when they are used to describe adsorption in soils (Sposito 1989).

#### ***Freundlich Equation***

The Freundlich equation is the oldest non-linear adsorption equation. It has been used to describe adsorption of cations and anions (Black and Waring 1976c), and is

also the most commonly used equation to describe pesticide adsorption in soils (Buchter *et al.* 1989; Hassett and Banwart 1989). The Freundlich equation has the form (Sposito 1989):

$$C_a = \alpha C_w^n, \quad 4-1$$

where  $C_a$  is the concentration of adsorbed solute ( $\mu\text{mol}_c \text{ g}^{-1}$ ),  $C_w$  is the concentration of solute in the soil solution ( $\mu\text{mol}_c \text{ cm}^{-3}$ ),  $\alpha$  is a constant known as the distribution coefficient ( $\text{cm}^3 \text{ g}^{-1}$ ), and  $n$  is a dimensionless constant. The Freundlich equation will describe linear isotherms (when  $n = 1$ ) such as those described by Duwig *et al.* (2003). It will also describe the square root relationships for anion adsorption reported by Gillman (1981) where  $n = 0.5$ . The Freundlich distribution coefficient ( $\alpha$ ) may vary from 0.01 for weakly adsorbed compounds to over 5000 for strongly adsorbed compounds (Hassett and Banwart 1989).

If the plot of  $\log C_a$  versus  $\log C_w$  yields a straight line then  $\alpha$  and  $n$  can be determined using equation 4-2 (Sposito 1989):

$$\log C_a = \log \alpha + n \log C_w, \quad 4-2$$

If the log plot is non linear then the Freundlich equation is not appropriate for describing the adsorption data (Sposito 1989). One criticism of the Freundlich equation is that an upper limit to adsorption is not defined (Sparks 1995) however, as long as values are not extrapolated beyond the measured data, then the equation is useful.

### *The Langmuir Equation*

The Langmuir equation is also used to describe adsorption of both anions and cations in soils and is the most frequently used equation to describe adsorption of  $\text{NO}_3^-$  (Katou *et al.* 1996; Kinjo and Pratt 1971; Olsen and Watanabe 1957; Phillips 2006; Qafoku *et al.* 2000). The Langmuir equation provides an upper limit to adsorption; however this value must still only be considered an estimate because it generally lies outside the range of adsorption measurements. The Langmuir equation is written (Sposito 1989):

$$C_a = \frac{C_{\max} \phi C_w}{1 + \phi C_w}, \quad 4-3$$

where  $C_a$  is the concentration of adsorbed solute ( $\mu\text{mol}_c \text{ g}^{-1}$ ),  $C_w$  is the concentration of solute in the soil solution ( $\mu\text{mol}_c \text{ cm}^{-3}$ ),  $C_{\max}$  is the maximum amount of solute that can be adsorbed by the soil ( $\text{g cm}^{-3}$ ) and  $\phi$  determines the magnitude of the initial slope of the isotherm.

The Langmuir equation can be rearranged into the linear form (Sposito 1989):

$$\frac{C_a}{C_w} = \phi C_{\max} - \phi C_a, \quad 4-4$$

and if  $C_a/C_w$  is plotted against  $C_a$ ,  $-\phi$  will equal the slope of the linear curve and  $\phi C_{\max}$  will equal the y intercept (Sposito 1984).

Fitting measured adsorption data to the Freundlich or Langmuir equation enables adsorption to be calculated at any solution concentration within the range of measured values. Solution and adsorbed concentrations can also be calculated from measured total  $\text{NO}_3^-$  values in soils using the isotherm equations the bulk density and water content are known (Katou *et al.* 1996).

With modern computing software such as SAS (2003) however, functions such as the Freundlich and Langmuir equations can be fitted directly to measured data rather than using linear regression techniques on transformed equations (equation 4-2 and 4-4). The direct fit simplifies the parameter determination process since the transformations and linear curve analysis is not required. Furthermore confidence intervals for the equations parameters and the equation curve can be calculated during the direct fitting procedure. Despite the availability statistical software capable of directly fitting these Freundlich or Langmuir equations, recent studies have still used the linear form of these isotherms to determine the equation parameters (Katou 2004; Qafoku *et al.* 2000).

The data used to determine isotherms has also been limited in some studies. Katou (1996) described  $\text{NO}_3^-$  adsorption in a variable charge Andisol with the Langmuir isotherm based on a adsorption measurement at a single solution concentration of  $50 \mu\text{mol}_c \text{ NO}_3^- \text{ cm}^{-3}$ . The use of the Langmuir equation was justified because  $\text{Cl}^-$  and mixed  $\text{Cl}^-/\text{NO}_3^-$  solutions measured at three concentrations were described by this equation. The isotherm fitted to the single value was then used to derive adsorbed  $\text{NO}_3^-$  at a range of concentrations equal to and less than  $50 \mu\text{mol}_c \text{ NO}_3^- \text{ cm}^{-3}$ . The accuracy of adsorbed values derived from this isotherm at solution concentrations less

than the measured value may therefore be poor in this study. A single data point was also used by Clothier *et al.* (1988) to estimate the adsorption of  $\text{NH}_4^+$  assuming a linear isotherm. Again the accuracy of the isotherms derived in this study was questionable however limitations of the linear fit were acknowledged and Clothier *et al.* (1988) concluded this approach was acceptable for estimating  $\text{NH}_4^+$  retardation in horizontal columns in the study.

Most other studies have used at least four adsorption measurements to derive the isotherm curve (Black and Waring 1976c; Duwig *et al.* 2003; Qafoku *et al.* 2000). Increasing the number of measurement points provides a better indication of the shape of the isotherm, improving its accuracy.

### **Methods for Measuring the Adsorption Isotherm**

Various methods have been used to measure adsorption of anions and cations in reactive soils and some conflict exists in the literature over the suitability of particular methods to represent adsorption under field conditions.

#### ***Batch Method***

The batch method is the simplest technique. It involves equilibrating a solute with a soil and determining its distribution between the solution and adsorbed phases (Sparks 1995). This method has been used in a number of studies to determine anion adsorption in soils (Black and Waring 1976c; Kinjo and Pratt 1971).

Adsorption in batch experiments is often calculated by subtracting the amount of solute added to the soil from the amount in the equilibrated solution. In most cases the calculation is corrected for solute initially present in the soil by adding the initial amount present to the amount of solute added for equilibration (Black and Waring 1976b). Including this correction contributes to errors in adsorption measurements since concentrations must be determined on a separate sample (Green *et al.* 1980). If the initial concentration is very low in comparison to the equilibrating solutions then this correction will have little effect on the adsorption calculations and may be ignored (Green *et al.* 1980). Kinjo and Pratt (1971) reported adsorption isotherms for  $\text{NO}_3^-$  in which no correction was made for initial concentrations. However initial



---

concentrations were not reported and therefore the accuracy of adsorption measurements in their study is questionable.

Some batch studies have included an initial step that involves washing the soil with a concentrated ionic solution prior to equilibration with a second solution of lower concentration (Uehara and Gillman 1980; Wong *et al.* 1990). This method is appropriate if comparisons between different soils is required because indigenous ions are removed from the exchange (Katou *et al.* 2001). If a measurement of adsorption is required that provides an indication of ion adsorption under “natural” conditions where various ions of different adsorption affinity are present however, the initial concentrated wash is inappropriate.

### ***Continuous Saturated Flow Experiments***

An alternative to batch experiments is the saturated continuous flow method. This was used to measure anion adsorption by Clothier *et al.* (1988), Katou *et al.* (1996) and Qafoku and Sumner (2001). In this method a solution of known concentration is passed through a soil column until the in-flowing concentration equals that of the out-flowing solution. This indicates equilibrium has been reached between the solution and the soil (Green *et al.* 1980). The water content and total solute concentration in the soil sample are measured and adsorbed solute is calculated by the difference between the total solute (the amount of solute in the solution and adsorbed phase) and original solution concentration applied to the columns.

This method avoids the need for correction of initial  $\text{NO}_3^-$  concentrations required in the batch method. Technique is more involved however and care must be taken to ensure equilibrium between the solution and adsorbed phase is reached to avoid underestimation of adsorption (Sparks 1995). Despite the potential improvement in measurement accuracy since corrections are not required for concentration originally in the soil, errors of up to 50% for adsorption at low solution concentrations were documented in a study of  $\text{NH}_4^+$  adsorption by Clothier *et al.* (1988).

---

***Unsaturated Flow Method***

Katou *et al.* (2001) described an unsaturated horizontal flow method using horizontal columns for determining solute adsorption in variable charge subsoil. This method has since been used by Duwig *et al.* (2003) and Katou (2004) to measure anion adsorption isotherms. In this technique water is absorbed by a column packed with a soil that has been equilibrated with a solute. By measuring the total solute concentration and water content ahead of the piston front, the adsorbed and solution concentration in the soil can be derived (Katou *et al.* 2001). By conducting a number of experiments in which different concentrations of solute were initially incorporated in the soil, an adsorption isotherm can be produced. Katou *et al.* (2001) states this method is advantageous because adsorption of weakly reactive ions can be determined without desorption of indigenous ions which they identified as a potential issue in the saturated flow method which has the potential to lead to overestimation of adsorption in unsaturated flow conditions.

This technique is more involved than batch and saturated column methods and only yields one adsorption point per column. As a result, production of an isotherm involves conducting a number of column experiments to obtain an acceptable number of isotherm points.

***TFE Displacement***

The TFE displacement method (Phillips and Bond 1989) has been used to determine adsorption isotherms for cations (Bond and Phillips 1990b; c) but has not been used in anion adsorption studies. This method enables solution and adsorbed concentrations to be determined in unsaturated soil. The soil solution is displaced by centrifuging the soil with a dense water-immiscible liquid (1,1,2-Trichloro-1,2,2-Trifluoroethane or TFE) and small solution volumes can be extracted without the need for dilution of the sample. The remaining soluble ions can then be extracted and measured.

The displacement of soil solution using this method is within the limits imposed by the soil moisture characteristic and the acceleration of the centrifuge. Preliminary

---

studies by Dr D.E. Smiles (personal communication 2009) show that solution can be extracted up to suctions of approximately two thirds wilting point of the soil.

This technique is advantageous in comparison to the unsaturated flow method of Katou *et al.* (2001) because a range of points on the adsorption isotherm are measured from a single column. However, the extraction is time consuming, yields a small volume of soil solution (0.15 to 2.5 cm<sup>3</sup>), and the TFE liquid used to displace the soil solution must be handled carefully because it is an environmental pollutant.

### ***Comparisons of Methods***

Some reports have indicated that the batch method can over-estimate adsorption due to breakdown of soil aggregates in weakly structured soil (Barrow and Shaw 1979) or abrasion of soil surfaces (Sparks 1995) however findings in different studies are conflicting. Katou *et al.* (2001) and Wong *et al.* (1990) previously claimed that the batch experiments overestimated adsorption in comparison to column techniques. The pre-treatment of batch samples with a concentrated solution wash, however, meant these findings were misleading since this wash was not applied prior to equilibration in the column experiments. More appropriate comparisons were made by Hodges and Johnson (1987), Bond and Phillips (1990b) and Burgisser *et al.* (1993) because both column and batch samples were treated with the same solution wash prior to adsorption experiments. Hodges and Johnson (1987) found batch experiments overestimated adsorption of SO<sub>4</sub><sup>2-</sup> in comparison to saturated column flow studies while Burgisser *et al.* (1993) found no difference when they compared Cd<sup>2+</sup> adsorption using similar methods. Bond and Phillips (1990b) also found no difference between batch methods and unsaturated column studies using TFE displacement in unsaturated horizontal columns. These studies show that there is still some question as to whether batch methods are appropriate for describing adsorption. There is also a lack of studies that have compared isotherm methods on soils that have not been pre-treated with a solute wash to remove indigenous ions.

In well structured soils such as Red Ferrosol's (Isbell 1994) aggregate breakdown, which is considered the main factor in overestimation of adsorption (Barrow and Shaw 1979; Schweich *et al.* 1983) may not be an issue and therefore the batch method is likely to be suitable. Findings from these previous studies indicate care

---

---

should be taken to ensure soils are mixed gently during equilibration to reduce the risk of aggregate breakdown when the batch method is used to measure adsorption.

### **Column Studies to Measure Water and Solute Transport**

Laboratory experiments on disturbed samples have been frequently used to study water and solute movement in soils and the effects of solute adsorption. Black and Waring (1976c) and Kinjo *et al.* (1971) measured the pore volumes required to leach a solute through vertical columns under both saturated and unsaturated flow conditions to determine the rate of solute movement relative to the soil water.

Horizontal columns have also been used to study water and solute movement under unsaturated flow. This method is advantageous because the flow is not influenced by gravity (Smiles *et al.* 1978). As a result, when water is applied at zero suction to soil columns containing relatively low initial water contents, flow equations describing water movement resulting from the matric potential gradient along the column are simplified. This method has been used to measure anion and cation movement in relation to the invading water in reactive and non-reactive soil materials in a number of studies (Bond and Phillips 1990c; Clothier *et al.* 1988; Duwig *et al.* 2003; Katou *et al.* 1996; Smiles and Philip 1978; Smiles and Smith 2004). Solute adsorption can be measured in these studies by observing the movement of inflowing solute relative to the soil water with a delay of the solute indicating adsorption (Katou *et al.* 1996). The frequent use of the horizontal column method in the literature and the way in which the location of water and solute can be accurately determined means that this method is a good way of measuring water and solute flow in soils to investigate solute adsorption.

By conducting horizontal column experiments to measure the movement of water and  $\text{NO}_3^-$  through the profile and the simple and rapid batch experiments to determine the distribution of  $\text{NO}_3^-$  in the solution and adsorbed phases a detailed understanding of  $\text{NO}_3^-$  movement and distribution should be achieved for the soil. Although there has been some question as to the suitability of batch methods for describing adsorption, their accuracy can be assessed in the horizontal columns by comparing the inflowing solution concentration with the derived solution concentration near the inlet of the column. These concentrations should be very similar since continual displacement of the soil solution in this zone results in equilibrium at the inflowing solution

---

concentration (Smiles *et al.* 1978). Confirmation that these concentrations are the same will provide confidence in the suitability of the batch method to describe adsorption for unsaturated flow conditions.

## THEORY OF WATER AND SOLUTE FLOW

The movement of water and solute in a horizontal one dimensional column can be described by a series of equations that help predict the location of inflowing water and solute in a soil column to study solute adsorption.

Table 4-1 lists symbols used in equations and throughout this chapter.

**Table 4-1:** Symbols used in equations.

Symbol	Unit	Meaning
$v$	$\text{cm}^3 \text{cm}^{-2} \text{s}^{-1}$	Water flux
$K$	$\text{cm s}^{-1}$	Unsaturated hydraulic conductivity
$\psi$	cm	negative head or suction
$x$	cm	Distance
$D$	$\text{cm}^2 \text{s}^{-1}$	Hydraulic diffusivity
$\theta$	$\text{cm}^3 \text{cm}^{-3}$	Volumetric water content
$c$	$\text{cm}^3 \text{cm}^{-3} \text{cm}^{-1}$	specific water capacity
$v_s$	$\mu\text{mol}_c \text{cm}^{-2} \text{s}^{-1}$	Solute flux
$D_s$	$\text{cm}^2 \text{s}^{-1}$	Diffusion-dispersion solute coefficient
$\rho$	$\text{g cm}^{-3}$	Bulk density
$t$	s	Time
$X$	$\text{cm s}^{-1/2}$	Boltzmann transformation ( $x t^{-1/2}$ )
$S(\theta_i, \theta_0)$	$\text{cm}^3 \text{cm}^{-2} \text{s}^{-1/2}$	Sorptivity
$\beta$	$\text{g cm}^{-3}$	Adsorption isotherm slope
$\Gamma$	$\mu\text{mol}_c \text{cm}^{-3}$	Concentration of solute per volume of soil in $\mu\text{moles}$ of charge
$C_0$	$\mu\text{mol}_c \text{cm}^{-3}$	Concentration of solute in the inflowing solution
$C_w$	$\mu\text{mol}_c \text{cm}^{-3}$	Concentration of solute in soil solution
$C_d$	$\mu\text{mol}_c \text{cm}^{-3}$	Concentration of solute in soil solution after column dilution
$C_K$	$\mu\text{mol}_c \text{cm}^{-3}$	Concentration in the KCl extract
$C_a$	$\mu\text{mol}_c \text{g}^{-1}$	Concentration of adsorbed solute per unit mass of soil
$C_{ad}$	$\mu\text{mol}_c \text{g}^{-1}$	Concentration of adsorbed solute after column dilution
$V_d$	$\text{cm}^3$	Volume of decanted or displaced soil solution
$V_{Kr}$	$\text{cm}^3$	Volume of KCl remaining in samples after the extract is decanted
$V_r$	$\text{cm}^3$	Volume of solution remaining after decantation of the soil solution
$V_{KT}$	$\text{cm}^3$	Total volume of solution present during the KCl extract
$V_s$	$\text{cm}^3$	Volume of the decanted or displaced soil solution
$V_d$	$\text{cm}^3$	Volume of undiluted solution displaced from soil during the TFE extract
$f_{OD}$	g	Oven dry soil mass

**Water Flow**

Pathways for water flow through soil are highly irregular, containing constrictions and dead ends. Equations for water flow neglect the detailed flow pattern and treat the conducting body as uniform (Hillel 1980).

Non hysteretic water flow in a horizontal column is described by Darcy's law in the form described by the equation (Hillel 1980):

$$v = -D(\theta) \frac{\partial \theta}{\partial x}. \quad 4-5$$

where  $v$  is the water flux ( $\text{cm}^3 \text{ cm}^{-2} \text{ s}^{-1}$ ),  $\theta$  is the volumetric water content ( $\text{cm}^3 \text{ cm}^{-3}$ ),  $D(\theta)$  is the hydraulic diffusivity ( $\text{cm}^2 \text{ s}^{-1}$ ) and  $x$  is the horizontal distance (cm).  $D(\theta)$  is defined by the equation:

$$D(\theta) = K(\theta) \frac{\partial \psi}{\partial \theta}. \quad 4-6$$

where  $K$  is the hydraulic conductivity ( $\text{cm s}^{-1}$ ) and  $\partial \psi / \partial \theta$  describes the soil moisture characteristic slope.

The water continuity equation is written (Hillel 1980):

$$\frac{\partial \theta}{\partial t} = - \frac{\partial v}{\partial x}, \quad 4-7$$

where  $t$  is time (s),  $x$  is horizontal distance (cm). The left hand side (LHS) describes the rate of change of the water content at a given position. The right hand side (RHS) describes the way the water flux changes at any time with location,  $x$ .

Combining equation 4-7 and 4-5 we get the equation for horizontal unsteady flow (Hillel 1980):

$$\frac{\partial \theta}{\partial t} = \frac{\partial}{\partial x} \left( D(\theta) \frac{\partial \theta}{\partial x} \right) \quad 4-8$$

---

**Solute Flow**

To describe solute flow during unsaturated horizontal water flow not influenced by gravity, a solute flux equation is combined with a solute continuity equation (Jury *et al.* 1991). Non-volatile reactive solutes exist in soils in the dissolved phase ( $C_w$ ) and the adsorbed phase ( $C_a$ ).  $C_a$  is assumed to be stationary and therefore solute flux is described only for  $C_w$  (Jury *et al.* 1991). The solute flux equation is written (Jury *et al.* 1991):

$$v_s = -D_s \frac{\partial C_w}{\partial x} + vC_w, \quad 4-9$$

where the solute flux,  $v_s$ , has the units  $\mu\text{mol}_c \text{ cm}^2 \text{ s}^{-1}$ ,  $C_w$  has the units  $\mu\text{mol}_c \text{ cm}^{-3}$  and  $D_s$  has the units  $\text{cm}^2 \text{ s}^{-1}$ . In this equation the first term on the RHS ( $-D_s(\partial C_w / \partial x)$ ) describes diffuse movement of solution solute relative to the soil water and the second term ( $vC_w$ ) describes movement of solute with the soil water.

The solute continuity equation describes the addition and movement of a solute through a soil in one dimension (Jury *et al.* 1991):

$$\frac{\partial \Gamma}{\partial t} + \frac{\partial v_s}{\partial x} + r_s = 0, \quad 4-10$$

where  $\Gamma$  is the total solute concentration ( $\mu\text{mol}_c \text{ cm}^{-3}$  soil) and  $r_s$  represents loss of solute due to plant uptake or biological reactions ( $\mu\text{mol}_c$ ). It is assumed  $r_s = 0$  in these experiments.

The total concentration of a non-volatile solute can be described in terms of  $C_w$  and  $C_a$  (Jury *et al.* 1991):

$$\Gamma = \theta C_w + \rho C_a, \quad 4-11$$

where  $\rho$  is the bulk density ( $\text{g cm}^{-3}$ ) and  $C_a$  has the units  $\mu\text{mol}_c \text{ g}^{-1}$  soil. Ignoring  $r_s$ , the continuity equation can now be written:

$$\frac{\partial \theta C_w}{\partial t} + \frac{\partial \rho C_a}{\partial t} = -\frac{\partial v_s}{\partial x}. \quad 4-12$$

The first and second terms on the left hand side describe the rate of change of soil solution solute and adsorbed solute respectively in the column at any fixed value of  $x$ . The right hand side describes the way the solute flux changes at any time with

---

location,  $x$ . Combining the flux equation with the continuity equation gives the convection dispersion equation for solute (Jury *et al.* 1991):

$$\frac{\partial \theta C_w}{\partial t} + \frac{\partial \rho C_a}{\partial t} = \frac{\partial}{\partial x} \left( D_s \frac{\partial C_w}{\partial x} \right) - \frac{\partial v C_w}{\partial x}, \quad 4-13$$

The first term on the RHS describes the movement of solution solute relative to the soil water and the second term describes movement of solution solute with the soil water.

If equation 4-14 is differentiated by parts and two terms eliminated using equation 4-7 equation for solute flow becomes:

$$\theta \frac{\partial C_w}{\partial t} + \rho \frac{\partial C_a}{\partial t} = \frac{\partial}{\partial x} \left( D_s \frac{\partial C_w}{\partial x} \right) - v \frac{\partial C_w}{\partial x}. \quad 4-14$$

This is equivalent to equation 10 from Katou *et al.* (1996) without the terms for a second solute.

To account for the influence of solute adsorption on its movement through the column the variable,  $\beta$ , is introduced which represents the slope of the adsorption isotherm. Equation 4-14 is now written (Smiles, D.E. personal communication, 2009):

$$(\theta + \rho \beta) \frac{\partial C_w}{\partial t} + v \frac{\partial C_w}{\partial x} = \frac{\partial}{\partial x} \left( D_s \frac{\partial C_w}{\partial x} \right). \quad 4-15$$

If the slope of the adsorption isotherm ( $dC_a/dC_w$ ) is linear then  $\beta$  will be a constant otherwise its value will change with the solution concentration.

### Initial and Boundary Conditions for Absorption Experiments

Soil was well mixed to ensure uniform initial water and solute content. Columns were packed to achieve uniform bulk density. To start the experiment a solution of known concentration was applied at zero suction to the inlet end of the column and absorption of solution by the column was measured.

These experiments are designed to realise the following conditions:



---


$$\begin{aligned}\theta &= \theta_i; C_w = C_i; x > 0; t = 0 \\ \theta &= \theta_0; C_w = C_0; x = 0; t > 0\end{aligned}\tag{4-16}$$

where values of  $\theta_i$  and  $C_i$  represent the initial water content ( $\text{cm}^3 \text{ cm}^{-3}$ ) and solution concentration ( $\mu\text{mol}_c \text{ cm}^{-3}$ ) throughout the column prior to the absorption of any solution into the column,  $\theta_0$  and  $C_0$  are the water content ( $\text{cm}^3 \text{ cm}^{-3}$ ) and solution concentrations ( $\mu\text{mol}_c \text{ cm}^{-3}$ ) at the inlet of the column where horizontal distance ( $x$ ) equals zero. The values of  $\theta_0$  and  $C_0$  remain constant during the period of the absorption experiment.

### Boltzmann Substitution

The Boltzmann substitution ( $X=xt^{1/2}$ ) eliminates both  $x$  and  $t$  from the flow equations 4-8 and 4-15 and the boundary conditions 4-16 (Smiles *et al.* 1978). If these equations are appropriate descriptions for water and solute flow, and the initial and boundary conditions are realised, then  $\theta$  and  $C_w$  will be unique functions of  $X$ . This is shown graphically when water and solute profiles measured over different times converge. If this is not the case, then the flow equations are incorrect and/or the experimental conditions are not realised.

The Boltzmann substitution into Equations 4-16, 4-8 and 4-15, produces equations 4-17, 4-18 and 4-19 (Smiles *et al.* 1978):

$$\begin{aligned}\theta &= \theta_i; C_w = C_i; X \rightarrow \infty \\ \theta &= \theta_0; C_w = C_0; X = 0\end{aligned}\tag{4-17}$$

$$\frac{d}{dX} \left( D(\theta) \frac{d\theta}{dX} \right) + \frac{X}{2} \frac{d\theta}{dX} = 0, \text{ and}\tag{4-18}$$

$$\frac{d}{dX} \left( D_s \frac{dC_w}{dX} \right) + \frac{g}{2} \frac{dC_w}{dX} = 0,\tag{4-19}$$


---

where:

$$g(X) = (\theta + \rho\beta)X - \int_{\theta_i}^{\theta} X d\theta. \quad 4-20$$

### The Piston Front and Solute Front

Figure 4-1 shows the water content profile during water absorption in a horizontal column. The area  $a+b$  in Figure 4-1 represents the amount of new water added to the column ( $\text{cm}^3 \text{ cm}^{-2} \text{ s}^{-1/2}$ ) in the  $X$  coordinate. This is equal to the sorptivity,  $S$  ( $\theta_i, \theta_0$ ; Philip 1957):

$$S = \int_{\theta_i}^{\theta_0} X d\theta. \quad 4-21$$

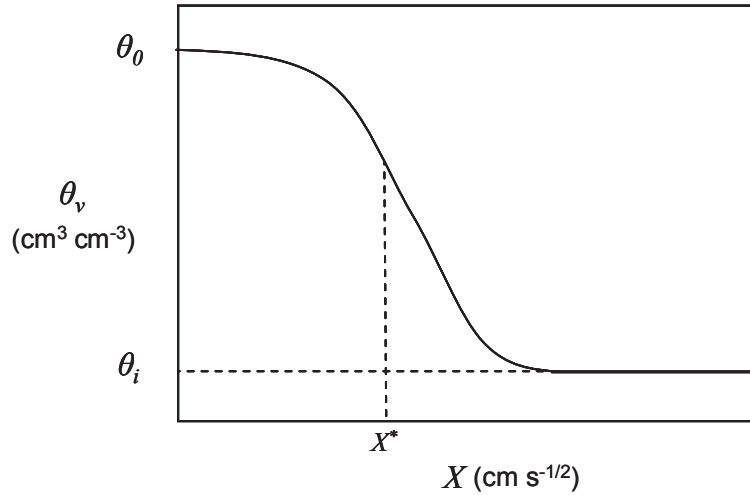


**Figure 4-1:** Water profile indicating the sorptivity ( $a+b$ ) and the piston front  $X^*$  where  $c=b$ .

Water entering a relatively dry horizontal column appears to displace the antecedent water, which accumulates beyond a plane of separation of between the two (Smiles *et al.* 1978). This feature of unsaturated flow is described as piston displacement and the position of the plane of separation is described as the piston front. In Figure 4-1 the new column water is located behind  $X^*$  (the piston front) where the areas  $b$  and  $c$  are equal. The piston front is described by the equation:

$$\int_{\theta_i}^{\theta_0} X d\theta = \int_0^{X^*} \theta dX, \quad 4-22$$

---

where the LHS is the area  $a+b$  and the RHS is the area  $a+c$  in Figure 4-1.

The position of the solute front relative to the piston front will depend on the solute reaction with the soil. A non-reactive solute will travel with the invading water and the solute front will be distributed about the piston front. Smiles *et al* (1978) reported that the solute front in a non-reactive soil was located where:

$$\theta X^* = \int_{\theta_i}^{\theta} X d\theta. \quad 4-23$$

A reactive solute will interact with the soil during absorption and the solute front will be delayed in relation to the inflowing water. Equation 4-15, 4-19 and 4-20 contain the reaction term  $\beta$  which represents an average slope of the adsorption isotherm and describes the retardation of the solute front due to solute adsorption by the soil.

The location of the solute front for a reactive solute is located where (Bond and Phillips 1990a):

$$(\theta + \rho\beta)X^* = \int_{\theta_i}^{\theta} X d\theta. \quad 4-24$$

Equation 4-24 shows how changes in adsorption, indicated by changes in the value of  $\beta$  ( $\text{cm}^3 \text{g}^{-1}$ ), influence the position of the solute front in relations to  $X^*$ .

### Location and Shape of the Solute Front

If piston displacement occurred without any diffusion between the inflowing and antecedent solution the solute front,  $X_s$  ( $\text{cm s}^{-1/2}$ ), would exist as a vertical step in concentration (Hillel 1980). There is, however, dispersion between the inflowing solution containing high solute concentrations and the original solution. As a result the solute front is described as the mean position of the solute curve shown as the vertical line in Figure 4-2 (Hillel 1980). This position can be estimated where the areas  $a$  and  $b$  are equal.

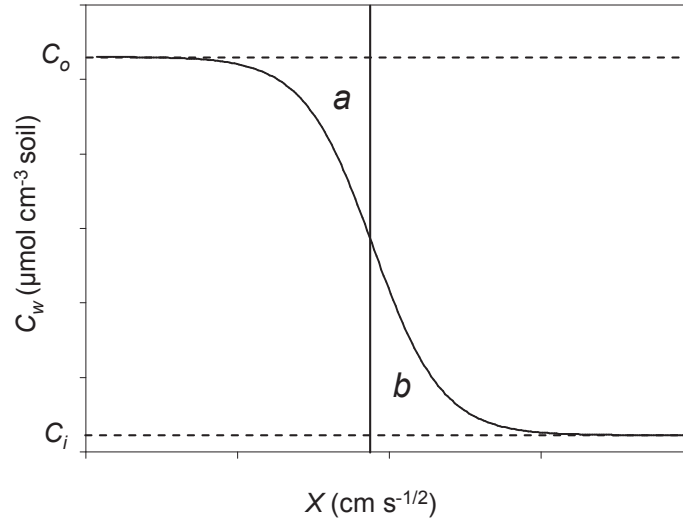


**Figure 4-2:** Diagram showing how the position of the solute front,  $X_s$  ( $\text{cm s}^{-1/2}$ ), is estimated where areas  $a$  and  $b$  are equal.

If no solute entering the column is lost the total amount of solute that has entered the column ( $\mu\text{mol}_c \text{ cm}^{-2} \text{ s}^{-1/2}$ ) should be equal to the product of concentration,  $C_o$  ( $\mu\text{mol}_c \text{ cm}^{-3}$ ), and the sorptivity,  $S$  ( $\text{cm}^3 \text{ cm}^{-2} \text{ s}^{-1/2}$ ). This should be equal to the integral of the total solute profile described in equation 4-25 (Smiles and Gardiner 1982):

$$SC_o = \int_{\Gamma_i}^{\Gamma_0} X d\Gamma, \quad 4-25$$

where  $\Gamma_0$  is the total concentration of solute in the solution and adsorbed phases at the leading edge of the column ( $X = 0 \text{ cm s}^{-1/2}$ ) per unit volume of soil ( $\mu\text{mol}_c \text{ cm}^{-3} \text{ soil}$ ) and  $\Gamma_i$  is the initial total concentration of solute in the solution ( $C_w$ ) and adsorbed ( $C_a$ ) phases prior to absorption of the solute ( $\mu\text{mol}_c \text{ cm}^{-3} \text{ soil}$ ). Values of  $\Gamma$  are calculated from  $C_w$  ( $\mu\text{mol}_c \text{ cm}^{-3} \text{ solution}$ ) and  $C_a$  ( $\mu\text{mol}_c \text{ g}^{-1} \text{ soil}$ ) using equation 4-11.

The equations 4-8, 4-15, 4-18 and 4-19 describe the water and solute movement under unsaturated unsteady flow in one dimension according to the prescribed boundary conditions (equation 4-16 and 4-17) and should describe the horizontal column experiments presented in this chapter.

**EXPERIMENTAL OVERVIEW**

To investigate and quantify anion adsorption in the Red Ferrosol horizontal column experiments were used to determine  $\text{NO}_3^-$  adsorption and retardation in the soil. Batch experiments were also conducted to determine the distribution of  $\text{NO}_3^-$  between the solution and adsorbed phase in the columns. To confirm the suitability of batch experiments to describe  $\text{NO}_3^-$  adsorption a second series of column experiments were then performed and adsorption was measured using the TFE displacement method. The significance of adsorption and the suitability of the batch and TFE methods were discussed.

## PART A – HORIZONTAL COLUMN AND BATCH EXPERIMENTS

### Materials and Methods

Soil from the 0-15 cm depth of the Red Ferrosol field soil described in Chapter 3 was oven dried at 40° C, and the sample that passed a 2.0 mm sieve stored for further use. Soil properties are presented in Table 4-2.

#### *Soil Column Description*

Soil columns were similar to those described by Smiles *et al.* (1978) to measure water and solute adsorption by the soil. Columns were constructed of acrylic sections attached to a Mariotte bottle (Plate 4-1). Section lengths varied from 0.9-2.6 cm. Sections were clamped together to create a 25 cm long column. The internal diameter was 2 cm. The acrylic material enabled the advance of the wetting front to be observed and the section orientation allowed rapid partitioning of the column at the end of the experiment by pushing down on column sections.



**Plate 4-1:** Soil column attached to the Mariotte bottle.

**Table 4-2:** Soil chemical and physical properties for the surface soil (0-15 cm depth)<sup>2</sup>.

pH	5.8					
EC mS cm <sup>-1</sup>	0.10					
Soil Solution Cations	Ca	K	Mg	Na	NH <sub>4</sub> -N	
(μmol <sub>e</sub> cm <sup>-3</sup> soil solution)	46.5	19.96	11.04	18.32	13.33	
Soil Solution Anions	NO3-N	Cl	PO4-P	SO4-S		
(μmol <sub>e</sub> cm <sup>-3</sup> soil solution)	45.84	15.07	0.52	2.90		
Exchangeable Cations	Ca	K	Mg	Na		
(μmol <sub>e</sub> g <sup>-1</sup> soil)	827.46	114.17	83.34	0		
Organic Carbon (%)	4.73					
Particle Size Distribution (%)	Sand	Silt	Clay			
OC removed	80	12	8			
OC and iron oxides removed	45	22	33			
Clay Mineralogy (%)	Quartz	Amorphous <sup>3</sup>	Kaolinite, Organic	Garnet, Gibbsite	Epidote	Smectite, Rutile, Amphibole
	25-35	15-25	10-15	5-10	2-5	<5

<sup>2</sup> pH and EC were measured on a 1:5 water extract (Rayment and Higginson 1992). Solution concentrations were measured from samples at a water content of  $0.55 \text{ cm}^3 \text{ cm}^{-3}$  and exchangeable cations were extracted with a 1 M NH<sub>4</sub>Cl extract following the water soluble extraction. Organic carbon was analysed with the Walkley and Black (1934) method. Particle size (USDA) was measured using a pipette method with organic carbon removed by mixing with hydrogen peroxide and iron oxides removed by mixing with sodium dithionate (McKenzie *et al.* 2002). Clay mineralogy was measured using x-ray diffraction on sample treated with hydrogen peroxide and sodium dithionate.

### *Column Packing and Flow Experiment*

A 200 g sample of air dried, sieved soil was wet to  $\theta_g = 0.15 \text{ g g}^{-1}$ , mixed thoroughly and equilibrated overnight. The soil (approximately 90 g) was added to the acrylic column in 4 cm increments and packed to a bulk density of approximately  $1.0 \text{ g cm}^{-3}$  with a drop hammer (Smiles and Smith 2004). The column was mounted horizontally (Plate 4-1).

A  $110 \text{ } \mu\text{mol}_\text{c} \text{ cm}^{-3} \text{ NO}_3^-$  solution was produced by dissolving 13.49 g of  $\text{Ca}(\text{NO}_3)_2 \cdot 4\text{H}_2\text{O}$  in a  $1000 \text{ cm}^3$  volumetric flask. This solution was supplied to the inlet of the column at zero suction using a Mariotte bottle.

Table 4-3 shows the period of solution absorption, bulk density and initial and boundary water contents in the columns.

**Table 4-3:** Details for individual column experiments.  $\rho$  is the bulk density ( $\text{g cm}^{-3}$ ),  $\theta_i$  is the initial column water content,  $\theta_0$  is the water content at  $x=0$ ,  $t>0$ . Values in parentheses represent the standard deviation of the mean.

Time	$\rho^1$ ( $\text{g cm}^{-3}$ )	$\theta_i$ ( $\text{cm cm}^{-3}$ )	$\theta_o$ ( $\text{cm cm}^{-3}$ )
<i>Experiment set 1</i>			
26	1.03 (0.02)	0.15 (0.00)	0.56
47	1.03 (0.02)	0.15 (0.00)	0.55
96	1.04 (0.02)	0.15 (0.00)	0.55
Mean	1.03 (0.01)	0.15 (0.00)	0.55 (0.01)
<i>Experiment set 2</i>			
30	1.04 (0.02)	0.16 (0.00)	0.58
43	1.04 (0.06)	0.16 (0.00)	0.58
70	1.02 (0.03)	0.16 (0.00)	0.62
Mean	1.03 (0.01)	0.16 (0.00)	0.59 (0.02)

The advance of the wetting front was measured over time to confirm absorption was progressing at a linear rate when plotted against the square root of time (Plate 4-2; Smiles and Gardiner 1982). When the wetting front reached a predetermined distance the column was rapidly divided by releasing the clamps holding the column together and pushing down on the sections to isolate each section from its neighbours (Plate



4-2). The soil from each column section (3-9 g oven dry soil) was quickly transferred into pre-weighed 50 cm<sup>3</sup> falcon centrifuge tubes, sealed and weighed.

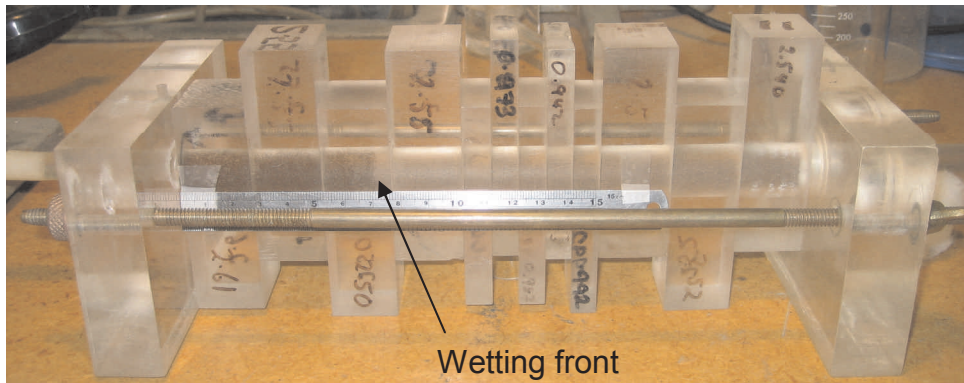


**Plate 4-2:** A soil column showing the position of the wetting front in the column. By releasing the clamp pressure and pushing down on the sections the column was rapidly divided.

### *Nitrate Extraction and Analysis*

#### *Water Soluble Nitrate Extraction*

Deionised water was added to the soil samples in an approximate soil to water ratio of 1:5.5 ( $\pm 0.4$ ). The soil plus water was weighed. Samples were shaken for 4 hours in an end-over-end shaker and then centrifuged at  $9\,800\text{ m s}^{-2}$  for 10 minutes. The supernatant was decanted into clean pre-weighed falcon tubes, weighed and the electrical conductivity and pH of the solutions was measured using pH and EC meters (Rayment and Higginson 1992). The soil and solution remaining in the centrifuge tube was weighed.

#### *Adsorbed Nitrate Extraction*

Between 15 and 40 cm<sup>3</sup> of 2M KCL was added to the soil (plus residual water extract) to form a 1:5.5 (SD $\pm 0.5$ ) soil solution ratio (Rayment and Higginson 1992). The tubes were reweighed and shaken for one hour to extract adsorbed NO<sub>3</sub><sup>-</sup>. The soil plus 2M KCl samples were centrifuged at  $9\,800\text{ m s}^{-2}$  for 10 minutes and the supernatant was decanted in pre-weighed falcon tubes and weighed. Soil remaining in the tubes was washed by shaking for 30 min in 20 cm<sup>3</sup> of deionised water to remove remaining KCl salts. The tubes were centrifuged at  $9\,800\text{ m s}^{-2}$  for 10 minutes and the wash solution was discarded. The washing procedure was repeated once more. The washed soil that remained in the base of the centrifuge tubes was transferred to a 105 °C oven

to determine its oven dry mass (Rayment and Higginson 1992). Water and KCl extracts were analysed for  $\text{NO}_3\text{-N}$  on an Alpkem autoanalyser (Alpkem 1992).

All dilutions and solution volumes were measured gravimetrically throughout the experiments. Since solutions are presented volumetrically the 2M KCl extracts weights were adjusted according to a density of  $1.09 \text{ g cm}^{-3}$  (Weast 1971). Other solution volumes were assumed to have a density of  $1.0 \text{ g cm}^{-3}$ .

### *Calculations*

#### *Water Soluble Nitrate*

The soil solution concentration in the diluted solution,  $C_d$  ( $\mu\text{mol}_\text{c} \text{ NO}_3^- \text{ cm}^{-3}$ ), is given directly by measurement of the diluted extract.

#### *Total Nitrate*

Total  $\text{NO}_3^-$ ,  $\Gamma$  ( $\mu\text{mol}_\text{c} \text{ NO}_3^- \text{ cm}^{-3}$  soil), was determined by calculating the total amount of  $\text{NO}_3^-$  ( $\mu\text{mol}_\text{c}$ ) in the water and KCl extracts. The first product in the brackets in equation 4-26 describes the amount in the decanted soil solution, the second is the amount in the decanted KCl extract and the third is the amount remaining in the soil after the KCl extract was decanted. This total amount of  $\text{NO}_3^-$  is then expressed per unit volume of soil by multiplying the amount of  $\text{NO}_3^-$  by the bulk density and dividing it by the oven dry soil mass of the sample. This calculation assumes that the concentration remaining in the soil after the KCl extract was decanted was equal to the KCl extract concentration,  $C_K$  ( $\mu\text{mol}_\text{c} \text{ NO}_3^- \text{ cm}^{-3}$ ). Thus:

$$\Gamma = (C_d V_d + C_K V_K + C_K V_{Kr}) \rho / f_{od}, \quad 4-26$$

where,  $V_d$  is the volume of the decanted soil solution extract ( $\text{cm}^3$ ),  $V_K$  is the volume of the decanted KCl extract ( $\text{cm}^3$ ),  $V_{Kr}$  is the volume of extract remaining in the soil sample after the KCl extract was decanted ( $\text{cm}^3$ ),  $f_{od}$  is the mass of oven dry soil (g) and  $\rho$  is the bulk density ( $\text{g cm}^{-3}$ ).

#### *Adsorbed Nitrate*

Adsorbed  $\text{NO}_3^-$  in the diluted samples,  $C_{ad}$  ( $\mu\text{mol}_\text{c} \text{ NO}_3^- \text{ g}^{-1}$  oven dry soil), was calculated by rearranging equation 4-11 and substituting the undiluted concentrations  $C_w$  and  $C_a$  with the diluted concentrations  $C_d$  and  $C_{ad}$  (Table 4-1):

---


$$C_{ad} = (\Gamma - \theta C_d) / \rho$$

4-27

$C_{ad}$ ,  $\Gamma$ ,  $C_d$  and  $\rho$  are described above.  $\theta$  is the volumetric water content of the soil after dilution of the column ( $\text{cm}^3 \text{ cm}^{-3}$ ).

### ***Batch Experiment***

Dilution of the soil solution changed the equilibrium between the soil solution and adsorbed phase. As a result values measured in the horizontal columns described adsorption at solution concentrations further down the isotherm than at the concentrations prior to dilution. Batch experiments were therefore conducted to describe adsorption of  $\text{NO}_3^-$  across the full range of soil solution concentrations in the columns prior to dilution.

Batch experiments were conducted using a method similar to that described by Kinjo and Pratt (1971) and Black and Waring (1976c).

Soil was prepared as for the column experiments. Three replicates were conducted and adsorption measurements were duplicated for each solution concentration. Seven solutions containing 1.79, 3.57, 7.14, 14.23, 28.57, 57.14 and 114.29  $\mu\text{mol}_\text{c} \text{ NO}_3^- \text{ cm}^{-3}$  were prepared from a stock solution of  $\text{Ca}(\text{NO}_3)_2 \cdot 4\text{H}_2\text{O}$ . Air dry soil (10 g) was weighed into a pre-weighed 50  $\text{cm}^3$  falcon centrifuge tubes and 20  $\text{cm}^3$  of the  $\text{NO}_3^-$  solutions were added to each and weighed. The tubes were mixed overnight in an end-over-end shaker to obtain equilibrium between the soil and solution, centrifuged at 9 800  $\text{m s}^{-2}$  for 10 minutes and the supernatant decanted into clean tubes and weighed. The soil sample, including solution remaining in the tubes after decanting, was weighed. Adsorbed  $\text{NO}_3^-$  was extracted using the procedure used in the diluted column method. Analysis of the water soluble and KCl solutions were also conducted as described above.

By measuring the amount of  $\text{NO}_3^-$  adsorbed directly with the KCl extract, a correction was not required for  $\text{NO}_3^-$  initially present in the soil in contrast to the method previously used by Black and Waring (1976b) and Green *et al.* (1980).

---

### Calculations

#### *Water Soluble Nitrate*

The concentration of the equilibrated soil solution,  $C_w$  ( $\mu\text{mol}_c \text{NO}_3^- \text{cm}^{-3}$ ) was measured directly.

#### *Adsorbed Nitrate*

Adsorbed  $\text{NO}_3^-$  was also calculated from the KCl extract using equation 4-28:

$$C_a = (C_K V_K - C_w V_r) / f_{od}, \quad 4-28$$

where  $C_K$  is the concentration of  $\text{NO}_3^-$  in the KCl extract ( $\mu\text{mol}_c \text{NO}_3^- \text{cm}^{-3}$ ),  $V_K$  is the total volume of solution in the soil after addition of the KCl extract (including water already present in the soil),  $C_w$  is the concentration of  $\text{NO}_3^-$  in the equilibrated solution extract ( $\mu\text{mol}_c \text{NO}_3^- \text{cm}^{-3}$ ) and  $V_r$  is volume of the equilibrated solution remaining after decantation in the soil prior to addition of KCl ( $\text{cm}^3 \text{cm}^{-3}$ ). The first product in the brackets of equation 4-28 indicates the amount of  $\text{NO}_3^-$  ( $\mu\text{mol}_c$ ) in solution after the KCl extract which includes both the KCl solution and solution carried over from the initial solution equilibration. The second product in the brackets describes the amount of  $\text{NO}_3^-$  in the solution that was carried over into the KCl extraction. Subtracting these products gives the amount of adsorbed  $\text{NO}_3^-$  ( $\mu\text{mol}_c$ ). The concentration ( $\mu\text{mol}_c \text{NO}_3^- \text{g}^{-1}$  soil) is expressed per gram of oven dry soil.

Once the solution and adsorbed concentrations were calculated, the data was graphed and the Langmuir equation was fitted to the data.

### Statistical Analysis

Arbitrary curves were fitted to the water and solute profiles and the contrasts of the fitted curve parameters were tested using the *nlmixed* procedure in the statistical program SAS (version 9.1 2003). To take into account measurement error in the  $X$  coordinate ( $\text{cm s}^{-1/2}$ ), a random effect was introduced into the model analysis to represent a maximum horizontal distance error of one centimetre in the soil column measurements. This analysis indicated whether or not the water and solute profiles normalised by the Boltzmann ( $\text{cm s}^{-1/2}$ ) were significantly different.

---

Parameters for the isotherm equations were calculated from the adsorption data using the non-linear curve model in the statistical program SAS (version 9.1). To test for differences between replicates and methods, separate curves were fitted to each data set. The F-distribution from the separate curve fits was then compared to the F-distribution of the individual curves to assess if they were significantly different. If there was no difference, a single curve was used to describe all the data.

## Results

### *Horizontal Column Water and Total Nitrate Profiles*

#### *Profile Convergence*

The water and total  $\text{NO}_3^-$  profiles in horizontal columns varied with time after absorption by the relatively dry soil as shown in Figure 4-3A and Figure 4-4A. When the profiles were plotted against the Boltzmann variable,  $X$  ( $\text{cm s}^{-1/2}$ ; Figure 4-3B and Figure 4-4B), statistical analysis indicated that, within acceptable errors, all the water and  $\text{NO}_3^-$  profiles were described by a single curve ( $P < 0.05$ ). That is, profiles scaled with the square root of time, indicating that the water flow and solute equations 4-8, 4-15, 4-19 and 4-18 were valid for the column experiments under the prescribed boundary conditions of equations 4-16 and 4-17.

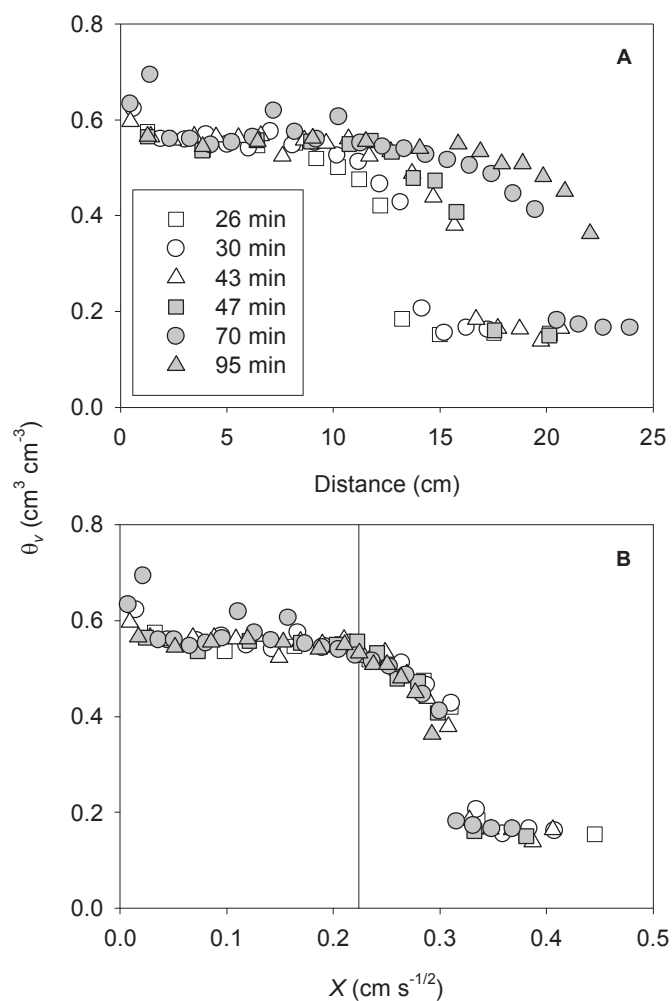


**Figure 4-3:** Volumetric water content profiles  $\theta_v$  ( $\text{cm}^3 \text{cm}^{-3}$ ) for the horizontal columns. Chart A shows the profiles plotted against horizontal distance,  $x$  (cm) and Chart B shows the profiles plotted against the Boltzmann variable,  $X$  ( $\text{cm s}^{-1/2}$ ). The solid vertical line in Chart B indicates the location of the piston front calculated with equation 4-23 ( $X=0.22 \text{ cm s}^{-1/2}$ ).

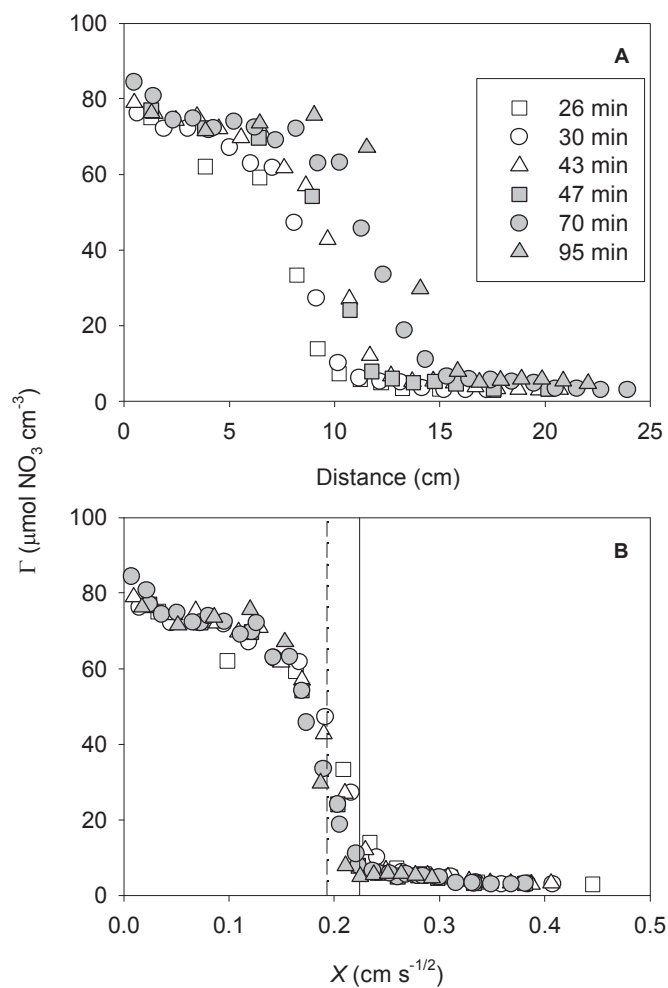


**Figure 4-4:** Total  $\text{NO}_3^-$  profiles in the horizontal columns ( $\mu\text{mol}_e \text{NO}_3^- \text{cm}^{-3}$  oven dry soil). Chart A shows the profiles plotted against horizontal distance,  $x(\text{cm})$  and Chart B shows the profiles plotted against the Boltzmann variable,  $X(\text{cm s}^{-1/2})$ . The solid vertical line in Chart B indicates the location of the piston front ( $X=0.22 \text{ cm s}^{-1/2}$ ) and the dashed line indicates the location of the solute front ( $X=0.19 \text{ cm s}^{-1/2}$ ).



*Nitrate Recovery*

To confirm all the  $\text{NO}_3^-$  added to the column was recovered, the integrals of the solute profiles were compared to the product of the sorptivity and inflowing solution concentration which should be equal according to equation 4-25. The average integral of the total solute profile according to the right hand side of equation 4-25 was  $13.06 \pm 0.29 \mu\text{mol}_c \text{ cm}^{-2} \text{ s}^{-1/2}$  and inflowing solution concentration ( $SC_0$ ) was  $13.28 \pm 0.20 \mu\text{mol}_c \text{ cm}^{-2} \text{ s}^{-1/2}$ . The differences between amounts were within the standard deviations of the measurements indicating that, accounting for experimental error, all the added  $\text{NO}_3^-$  was recovered in the columns.

*Piston and Solute Fronts*

The piston front, indicating the theoretical boundary between the inflowing and antecedent water based on the assumption that the latter was completely displaced during unsaturated absorption (equation 4-22), occurred at  $X^*=0.22 \text{ cm s}^{-1/2}$  (Figure 4-3B). The piston front was not calculated for the 95 minute column because the leading edge of the invading solution was not measured. By comparing the position of the piston front with the solute front, effects of  $\text{NO}_3^-$  adsorption by the soil may be identified.

The solute front was estimated by calculating  $X$  where the areas  $a$  and  $b$  are equal in Figure 4-2. The average position of the solute front,  $X_T$ , in the total  $\text{NO}_3^-$  profiles was  $0.19 \text{ cm s}^{-1/2}$  (Figure 4-4B). The solute front was located behind the piston front which showed  $\text{NO}_3^-$  movement was retarded relative to the inflowing water by approximately 14% in the columns. This delay indicated that  $\text{NO}_3^-$  was adsorbed by the soil.

---

### *Limitations of the Column Experiments*

Dilution of the columns resulted in a new equilibrium forming between the soil solution and adsorbed phases and therefore the concentrations in the soil columns at the original water contents could not be calculated without further measurements. As a result the only definitive measurement of  $\text{NO}_3^-$  in the columns was the total  $\text{NO}_3^-$  ( $\mu\text{mol}_\text{c} \text{ cm}^{-3}$  soil).

To calculate the correct solution and adsorbed concentrations an adsorption isotherm was required to describe adsorption over the range of concentrations in the column prior to dilution.

### ***Adsorption Isotherm***

Figure 4-5 shows the batch experiment data and a Langmuir equation fit to the values. The isotherm was only derived from the batch measurements because it was used to calculate solution and adsorbed concentrations in the horizontal columns. If the column data was included in the isotherm derivation the isotherm would not represent an independent data set. As a result calculation of the solution and adsorbed concentrations would have been inappropriate. Although the column data was not included in the isotherm fit Figure 4-5 indicates that the data sat within the 95% confidence intervals of the curve fitted to the batch data. The column data is presented in Figure 4-5 by plotting the concentrations of the diluted solution data and corresponding adsorbed values. Plotting the batch and column data on the same chart indicates that the batch isotherm produced the same results as those measured in the column at the lower concentration range.

The Langmuir equation was chosen in preference to the Freundlich equation because it provided the best fit to the data (Table 4-4). The estimated parameters were  $\phi = 0.0282$  (95% CI  $\pm 0.0032$ ) and  $C_{\text{max}} = 18.18$  (95% CI  $\pm 2.35$ ). Derivation of the Langmuir parameters by direct fitting the data in SAS (version 9.1 2003) produced a very similar fit to when the linear form of the equation was used (equation 4-4) however the direct fitting method was chosen because confidence interval for the parameters and fitted curve could be calculated. The fit of the four parameters sets to the measured data are shown in Appendix 4.

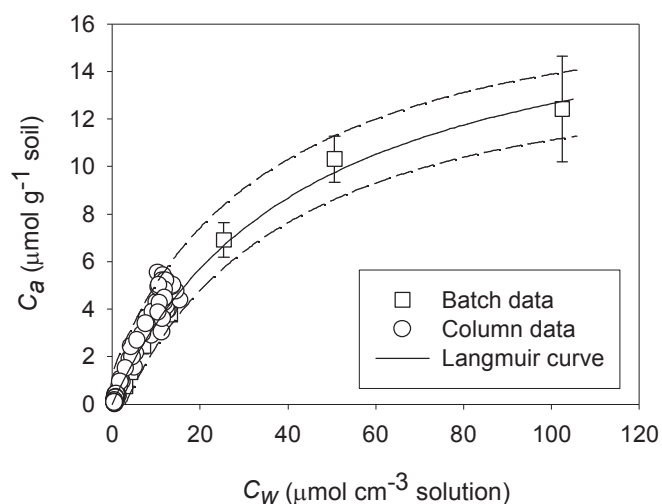


**Figure 4-5:** The Langmuir equation fitted to the batch adsorption isotherm data. The dotted line indicated the 95% confidence intervals of the curve fit. The diluted column indicates that the batch measurements follow the same trend at the lower solution concentrations measured in the horizontal column experiments.

**Table 4-4:** Root mean square error (RMSE) and  $R^2$  values for the different isotherm equations fitted to the batch data using direct or linear fitting models. The Langmuir and Freundlich isotherms were fitted either directly using SAS (version 9.1, 2003) or by derivation using the linear form of the isotherm equations (4-2 and 4-4).

Batch Isotherm Fit	RMSE	$R^2$
Langmuir – SAS	2.35	0.99
Langmuir – Linear	2.34	0.98
Freundlich – SAS	2.36	0.96
Freundlich – Linear	2.36	0.92

### ***Soil Solution and Adsorbed Nitrate***

Soil solution  $\text{NO}_3^-$  was calculated using the batch isotherm and total  $\text{NO}_3^-$  measurements from the column experiment by manipulating the Langmuir equation 4-3 and the total  $\text{NO}_3^-$  equation 4-11.

If  $\Gamma$ , the total amount of  $\text{NO}_3^-$  ( $\mu\text{mol}_\text{c} \text{NO}_3^- \text{cm}^{-3}$  soil) is given by equation 4-11, substitution for  $C_a$  from equation 4-11 into the Langmuir equation 4-3 and rearrangement yields:

$$C_w^2 \theta \phi + C_w (\theta - \Gamma \phi + \rho C_{\max} \phi) - \Gamma = 0 \quad 4-29$$

Equation 4-29 is quadratic so  $C_w$  is given by (Smiles D.E. personal communication 2009):

$$C_w = \frac{\Gamma \phi - \theta - \rho C_{\max} \phi \pm \sqrt{(\theta - \Gamma \phi + \rho C_{\max} \phi)^2 + 4 \theta \phi \Gamma}}{2 \theta \phi} \quad 4-30$$

Due the  $\pm$  term in equation 4-30, two possible answers exist for the solution concentration. Both were calculated to determine which answer was appropriate.

Once the concentration in the soil solution was been calculated the adsorbed concentration was determined by rearranging equation 4-11:

$$C_a = (\Gamma - \theta C_w) / \rho \quad 4-31$$

Equation 4-31 differs from equation 4-27 because the solution and adsorbed concentrations  $C_w$  and  $C_a$  indicate concentrations in the undiluted solution as opposed to the diluted concentrations,  $C_d$  and  $C_{ad}$ .

Figure 4-6 shows the solution and adsorbed profiles calculated using equations 4-30 and 4-31.

### Testing the Isotherm

To test the suitability of the batch isotherm the inflowing solution concentration ( $109.64 \pm 2.37 \mu\text{mol}_\text{c} \text{NO}_3^- \text{cm}^{-3}$ ) was compared to the average solution concentration near the inlet of the columns ( $107.49 \pm 4.53 \mu\text{mol}_\text{c} \text{NO}_3^- \text{cm}^{-3}$ ). The concentrations near the inlet of the columns should be similar to the concentration of the inflowing solution because continual displacement of the soil solution at the column inlet results in equilibrium at the inflowing solution concentration. These two values were within the standard deviation of the measurements indicating that the batch isotherm appeared suitable for describing the distribution between soil solution and adsorbed  $\text{NO}_3^-$  in the soil.

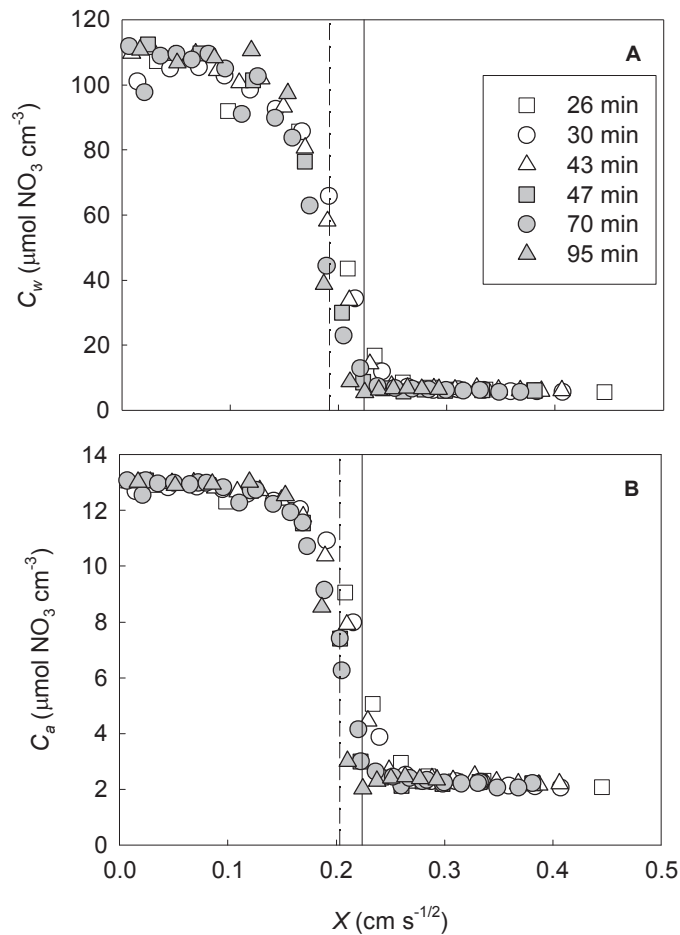


**Figure 4-6:** Solution  $\text{NO}_3^-$  profiles calculated from batch adsorption isotherms plotted against the  $X$  coordinate ( $\text{cm sec}^{-1/2}$ ) for solution (Chart A) and adsorbed (Chart B)  $\text{NO}_3^-$ . The solid vertical line indicates the position of the piston front ( $0.22 \text{ cm sec}^{-1/2}$ ) and the dashed line indicates the location of the solute front ( $0.19 \text{ cm sec}^{-1/2}$  for  $C_w$  and  $0.21 \text{ cm sec}^{-1/2}$  for  $C_a$ ) for the  $\text{NO}_3^-$  profiles.

### **Preliminary Discussion and Conclusions**

By measuring the absorption of water and  $\text{NO}_3^-$  by repacked soil columns and conducting batch experiments to identify the amount of  $\text{NO}_3^-$  adsorbed by the soil some preliminary findings/conclusions regarding solute distribution in the Red Ferrosol surface soil could be made:

1. The water and solute profiles converged when plotted against the Boltzmann variable confirming that the water and solute flow equations for the horizontal columns (equation 1-6, 1-16, 1-13 and 1-17) appeared valid for the prescribed boundary conditions (equation 1-14 and 1-15).
2. Integration of the total solute profiles (Figure 4-4) indicated that all the  $\text{NO}_3^-$  applied was recovered during analysis.
3. The solute front was retarded relative to the piston front in the horizontal columns confirming the presence of anion adsorption in the soil (Figure 4-4B and Figure 4-6).
4. Development of an adsorption isotherm using the batch experiments enabled soil solution and adsorbed concentrations to be calculated and tested by matching the inflowing solution concentration with the concentrations near the inlet of the column (Figure 4-5).

The batch isotherm appeared to adequately describe the distribution of  $\text{NO}_3^-$  between the solution and adsorbed phases. However previous studies have questioned the suitability of the batch method to describe adsorption of solute suggesting that it may overestimate adsorption (Hodges and Johnson 1987; Katou *et al.* 2001; Sparks 1995; Wong *et al.* 1990). A second series of column studies were therefore conducted and an alternative method (water immiscible displacement; Phillips and Bond 1989) was investigated to see if it produced the same isotherm as the batch method and consequently the same solution and adsorbed  $\text{NO}_3^-$  profiles for the diluted columns.

## PART B – HORIZONTAL COLUMN EXPERIMENTS INVESTIGATING TFE DISPLACEMENT

### Materials and Methods

In Part B four column experiments were conducted. Nitrate was extracted from two columns using a modified dilution method involving an ethanol wash between the water soluble and KCl extracts for comparison with the columns from Part A. In the other two columns  $\text{NO}_3^-$  was extracted using TFE displacement (Phillips and Bond 1989). Using this method soil solution could be extracted without dilution and these columns were therefore used to determine the adsorption isotherm for comparison with the batch experiments from Part A. Basic details of the columns are shown in Table 4-5.

**Table 4-5:** Details for individual column experiments in Part B. Symbols are described in Table 4-1.

Time (min)	$\text{NO}_3^-$ extraction method	$\rho^1$ ( $\text{g cm}^{-3}$ )	$\theta_i$ ( $\text{cm}^3 \text{ cm}^{-3}$ )	$\theta_0$ ( $\text{cm}^3 \text{ cm}^{-3}$ )
80	Dilution	1.05 (0.02)	0.16	0.55
320	Dilution	1.03 (0.03)	0.16	0.56
80	TFE	1.03 (0.07)	0.16	0.57
320	TFE	1.03 (0.03)	0.16	0.55
Mean		1.04 (0.04)	0.16 (0.00)	0.56 (0.01)

### Nitrate Extraction Methods

#### *Modified Dilution Method*

Following extraction of the water soluble extract described in the materials and methods from Part A,  $20 \text{ cm}^3$  of 70% ethanol was added to the remaining soil sample and solution and mixed in an end over end shaker for 30 minutes to remove the remaining water soluble  $\text{NO}_3^-$  (Phillips and Bond 1989). Samples were then centrifuged for 10 minutes at  $9\,800 \text{ m s}^{-2}$  and the supernatant discarded. The ethanol wash was repeated and after the second supernatant was decanted the remaining solution and soil sample was weighed.

KCl extraction was then carried out as described in part A.

---

### *TFE Method*

The TFE extraction method followed that of Phillips and Bond (1989). Water soluble  $\text{NO}_3^-$  was extracted from the column samples through centrifugation with 10  $\text{cm}^3$  of dense ( $\rho \sim 1.5 \text{ g cm}^{-3}$ ), water-immiscible TFE to displace the soil solution. Samples were centrifuged at  $78,500 \text{ m s}^{-2}$  for 1 hour at  $5^\circ\text{C}$  and the displaced soil solution was removed using a pipette withdrawing as little TFE as possible. If TFE was drawn into the pipette the sharp boundary between the TFE and soil water enabled separation of the two. The solution was transferred into a pre-weighed 10  $\text{cm}^3$  volumetric flask and weighed. The volumetric flask was then made to volume with high purity water and its mass was recorded. The TFE was decanted from the soil sample and the ethanol wash, KCl extract, oven dry determination and  $\text{NO}_3^-$  measurements were conducted as described in the dilution column procedure in Part A. In samples where the water content of the soil was less than  $0.30 \text{ cm}^3 \text{ cm}^{-3}$ , no soil water could be displaced by centrifugation with TFE. In these samples the dilution procedure method was used to extract water soluble  $\text{NO}_3^-$ .

The adsorbed  $\text{NO}_3^-$  was then extracted using the procedure described in part A.

### ***Calculations***

#### *Dilution Columns*

##### *Water Soluble Nitrate*

The soil solution concentration in the diluted solution,  $C_d$  ( $\mu\text{mol}_\text{c} \text{ NO}_3^- \text{ cm}^{-3}$ ), is determined by direct measurement of the diluted extract.

##### *Total Nitrate*

The total  $\text{NO}_3^-$ ,  $\Gamma$  ( $\mu\text{mol}_\text{c} \text{ NO}_3^- \text{ cm}^{-3}$  oven dry soil), calculation in equation 4-32 differs from 4-26 in Part A because of the inclusion of the ethanol wash in the columns. It is calculated using:

$$\Gamma = (C_d V_s + C_K V_{KT}) / \rho f_{od}, \quad 4-32$$

where  $C_d$  is the concentration of the diluted soil solution ( $\mu\text{mol}_\text{c} \text{ NO}_3^- \text{ cm}^{-3}$ ),  $V_s$  is the decanted volume of the diluted soil solution ( $\text{cm}^3$ ),  $C_K$  is the concentration of the KCl

---



extract ( $\mu\text{mol}_c \text{NO}_3^- \text{cm}^{-3}$ ),  $V_{KT}$  is the total volume of solution present in the soil during the KCl wash ( $\text{cm}^3$ ),  $\rho$  is the bulk density ( $\text{g cm}^{-3}$ ) and  $f_{od}$  is the oven dry soil mass (g). The first product in the brackets describes the amount of  $\text{NO}_3^-$  ( $\mu\text{mol}_c$ ) in the decanted volume of the equilibrated soil solution. The second product describes the amount of  $\text{NO}_3^-$  in the KCl extract and equilibrated solution remaining after decantation. The total amount of  $\text{NO}_3^-$  was converted to  $\mu\text{mol}_c \text{NO}_3^- \text{cm}^{-3}$  of oven dry soil by dividing by bulk density multiplied by the oven dry soil mass.

#### *Adsorbed Nitrate*

Adsorbed  $\text{NO}_3^-$  in the diluted samples,  $C_{ad}$  ( $\mu\text{mol}_c \text{NO}_3^- \text{g}^{-1}$ ), was calculated using equation 4-27.

#### *TFE Columns*

##### *Soil Solution Nitrate*

Solution  $\text{NO}_3^-$ ,  $C_w$  ( $\mu\text{mol}_c \text{NO}_3^- \text{cm}^{-3}$ ), was calculated by adjusting for the dilution of the solution after TFE extraction from the soil sample:

$$C_w = \frac{C_d V_s}{V_d}, \quad 4-33$$

where  $C_d$  and  $V_s$  are described above and  $V_d$  is the volume of soil solution displaced from the soil by the TFE ( $\text{cm}^3$ ). The total amount of  $\text{NO}_3^-$  ( $\mu\text{mol}_c$ ) in the diluted soil extract was calculated by multiplying the diluted concentration ( $C_d$ ) by the volume of the diluted solution ( $V_s$ ). The concentration in the undiluted extract ( $C_w$ ) was then calculated by dividing the total amount of  $\text{NO}_3^-$  extracted by the volume of the undiluted extract ( $V_d$ ).

##### *Total Nitrate*

Total  $\text{NO}_3^-$  ( $\mu\text{mol}_c \text{NO}_3^- \text{cm}^{-3}$  soil) in the TFE columns was calculated using equation 4-34:

$$\Gamma = (C_w V_d + C_K V_{KT}) / \rho f_{od}, \quad 4-34$$

where  $C_w$  represents the concentration displaced from the soil with TFE ( $\mu\text{mol}_c \text{NO}_3^- \text{cm}^{-3}$ ) and  $V_d$  represents the volume of this displaced solution ( $\text{cm}^3$ ). The first product

---

in the brackets describes the amount of  $\text{NO}_3^-$  ( $\mu\text{mol}_c$ ) in the soil solution displaced by the TFE. The second product describes the amount of  $\text{NO}_3^-$  in the KCl extract and ethanol remaining after the ethanol washes. The total amount of  $\text{NO}_3^-$  is converted to  $\mu\text{mol}_c \text{NO}_3^- \text{cm}^{-3}$  of oven dry soil by dividing by bulk density multiplied by the oven dry soil mass.

Equation 4-34 differs from the diluted column equations 4-26 and 4-32 because the undiluted solution concentration,  $C_w$ , was measured in the column in contrast to the diluted value content,  $C_d$ . Equation 4-34 also differed to 4-26 because of the inclusion of the ethanol wash.

#### *Adsorbed Nitrate*

Adsorbed  $\text{NO}_3^-$ ,  $C_a$  ( $\mu\text{mol}_c \text{NO}_3^- \text{g}^{-1}$  oven dry soil), in the KCl extract was calculated using equation 4-31.

## Results

Results from the diluted and TFE columns measured in Part B are presented separately in this chapter because of the different purposes of the column sets. The TFE columns were used to derive the adsorption isotherm for comparison with the batch isotherm. The diluted columns were conducted to compare the differences in solution and adsorbed profiles derived from the batch and TFE isotherms and to test the repeatability of the method by comparison with the diluted columns from Part A.

### *Horizontal Column Water and Total Nitrate Profiles in Diluted Columns*

The water and total  $\text{NO}_3^-$  profiles from the columns extracted using the dilution method converged when plotted against the Boltzmann variable,  $X$  ( $\text{cm s}^{-1/2}$ ) as observed in the columns from Part A.

To confirm all the  $\text{NO}_3^-$  added to the columns was recovered in the experiment, the average integral of the two solute profiles were compared to the product of the sorptivity and initial solution concentration (equation 4-25). The average integral of the total solute profile according to equation 4-25 was  $12.74 \pm 0.21 \mu\text{mol}_c \text{ cm}^{-2} \text{ s}^{-1/2}$  and the product of the sorptivity and inflowing solution concentrations was  $13.04 \pm 0.24 \mu\text{mol}_c \text{ cm}^{-2} \text{ s}^{-1/2}$ . The difference between these values was within the standard deviation of the measurements indicating that, as for the columns described in Part A, all the  $\text{NO}_3^-$  added was recovered in the analysis.

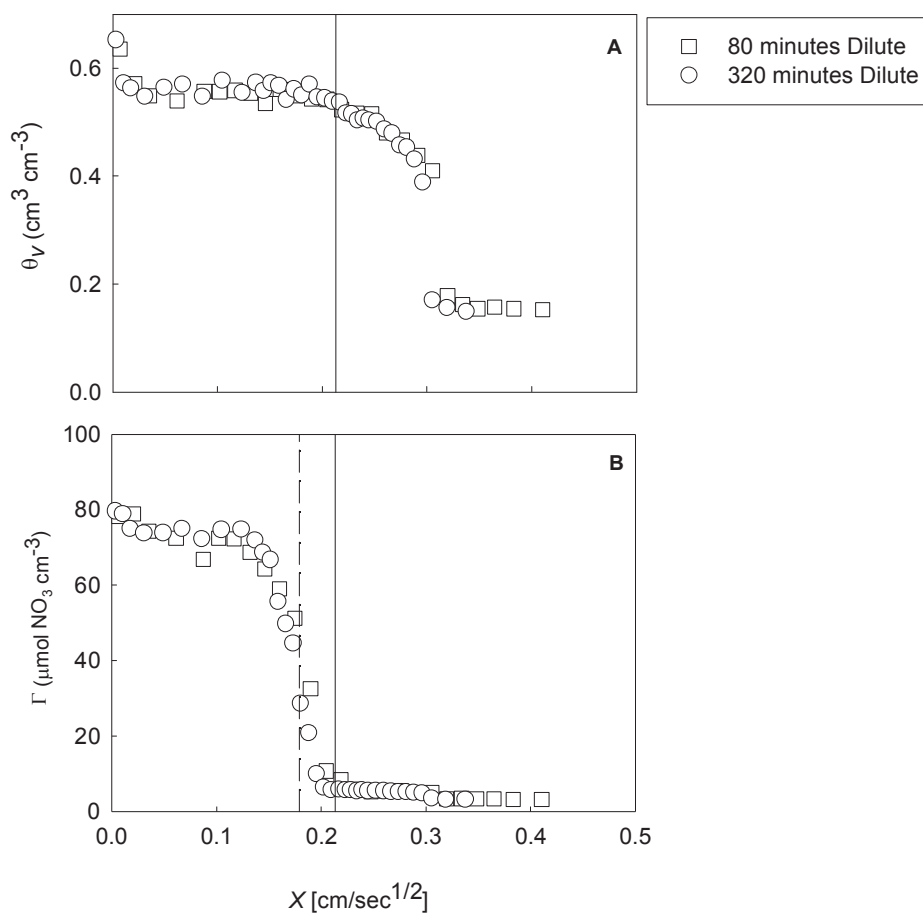


**Figure 4-7:** Diluted column volumetric water content ( $\text{cm}^3 \text{cm}^{-3}$ ) and total  $\text{NO}_3^-$  ( $\mu\text{mol}_c \text{NO}_3^- \text{cm}^{-3}$  soil) profiles plotted against the Boltzmann variable ( $\text{cm sec}^{-1/2}$ ). The solid vertical line indicates the position of the piston front ( $0.21 \text{ cm sec}^{-1/2}$ ) and the dashed line indicates the location of the solute front ( $0.18 \text{ cm sec}^{-1/2}$ ) for the total  $\text{NO}_3^-$  profile.

*Comparisons between Diluted Columns from Part A and B*

Analysis of curves fitted to the water and total  $\text{NO}_3^-$  profiles from the diluted columns in Part A and B indicated that there was no significant difference ( $P < 0.05$ ) between the two data sets when plotted against  $X$  ( $\text{cm s}^{-1/2}$ ). Furthermore, comparisons of the total  $\text{NO}_3^-$  profile integrals from Part A and B were within the standard error of the measurements ( $13.06 \pm 0.29$  versus  $12.74 \pm 0.21 \mu\text{mol}_c \text{ cm}^{-2} \text{ s}^{-1/2}$ ). This indicated that the ethanol wash did not have a significant effect on the estimated recovery of  $\text{NO}_3^-$  from the soil columns.

The column experiments from Part A and Part B were conducted 10 months apart. The fact that no significant difference was measured between the columns demonstrated the repeatability and reliability of the method for measuring water and solute movement through soil.

*TFE Columns and Isotherm Comparison**Water and Total Nitrate Profiles*

As for the diluted columns the water and total  $\text{NO}_3^-$  profiles from the two TFE columns converged when plotted against  $X$  ( $\text{cm s}^{-1/2}$ ; Figure 4-8). Retardation of the solute front in the total  $\text{NO}_3^-$  profiles ( $X^*_T = 0.18 \text{ cm s}^{-1/2}$ ) in relation to the piston front ( $X^* = 0.22 \text{ cm s}^{-1/2}$ ) was also observed.

Using equation 4-25 the total  $\text{NO}_3^-$  integral was within the standard deviation of the product of the sorptivity and inflowing concentration ( $11.95 \pm 0.62$  versus  $12.80 \pm 0.82 \mu\text{mol}_c \text{ cm}^{-2} \text{ s}^{-1/2}$ ). All  $\text{NO}_3^-$  added to the columns was therefore recovered using TFE extraction within measurement error. Thus the TFE extraction method was suitable for measuring  $\text{NO}_3^-$  concentrations in the columns and had the significant advantage that the soil solution could be extracted from the sample without dilution.

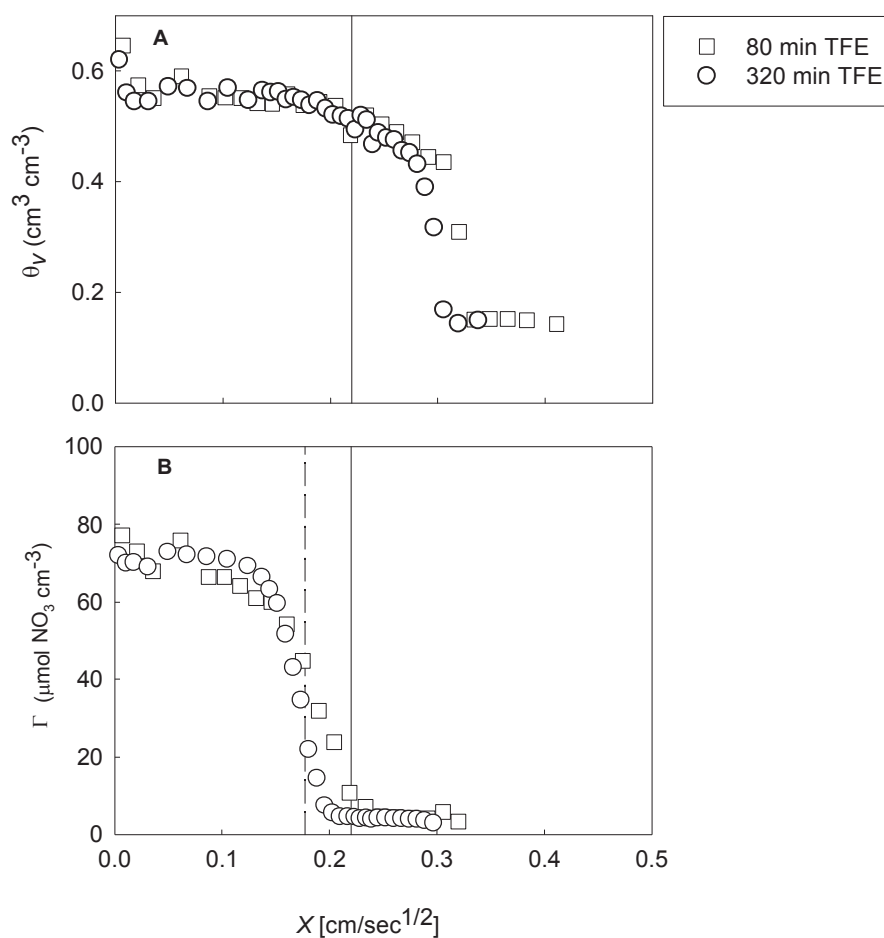


**Figure 4-8:** TFE column volumetric water content ( $\text{cm}^3 \text{cm}^{-3}$ ) and total  $\text{NO}_3^-$  ( $\mu\text{mol}_e \text{NO}_3^- \text{cm}^{-3}$  soil) profiles plotted against the Boltzmann variable ( $\text{cm sec}^{-1/2}$ ). The solid vertical line indicates the position of the piston front ( $0.21 \text{ cm sec}^{-1/2}$ ) and the dashed line indicates the location of the solute front ( $0.18 \text{ cm sec}^{-1/2}$ ) for the total  $\text{NO}_3^-$  profile.

*Adsorption Isotherm*

Because the TFE method enabled extraction of solution  $\text{NO}_3^-$  without dilution of the column sections an adsorption isotherm could be produced by plotting the adsorbed versus solution concentrations over a range of concentrations between the inflowing solution ( $C_0$ ) and initial ( $C_i$ ) soil concentrations (Figure 4-9A).

As for the batch isotherm, the suitability of the Freundlich and Langmuir equations was investigated to determine which function fitted the adsorption data best. Small differences in the RMSE and  $R^2$  values were observed between the equations using both the direct fitting method with SAS (version 9.1, 2003) and the linear forms of the equations (4-2 and 4-4; Table 4-6). The fit the Langmuir equation was used because the calculation of solution and adsorbed concentrations was simpler (Appendix 3). The equation was fitted directly in SAS (version 9.1, 2003) to obtain confidence intervals for the parameters and the fitted curve. The parameters estimated for Langmuir equation were  $\phi = 0.00766$  (95% CI  $\pm 0.00194$ ) and  $C_{max} = 23.17$  (95% CI  $\pm 3.43$ ). Graphs for the four isotherm fits are shown in Appendix 4. The TFE isotherm was determined without inclusion of the diluted column data so the solution and adsorbed profiles in these columns could be derived from an independent data set, as for the batch isotherm.

Statistical analysis of the isotherms produced using the TFE and batch methods indicated that they were significantly different ( $P < 0.05$ ; Figure 4-9). The diluted column data measured in Part B appeared to follow the batch isotherm curve (Figure 4-9B) as observed for the diluted column data in Part A (Figure 4-5B and Figure 4-5) rather than the TFE isotherm. This indicated that differences between the TFE and batch/diluted column methods may have influenced adsorption measurements.

The batch and diluted column equilibration/extraction procedures are similar. They both involve extended shaking of the soil samples in a high solution to soil ratio 1:5.5 ( $\pm 0.4$ ) prior to the decantation and measurement of the soil solution and extraction of exchangeable  $\text{NO}_3^-$  with KCl. In contrast, soil solution was extracted with minimal disturbance of the soil sample after horizontal absorption using the TFE procedure at solution to soil ratios less than one. These differences may have influenced the amount of  $\text{NO}_3^-$  adsorbed by the soil.

---

Although a significant difference was measured between the TFE and batch isotherms the difference in the amount of adsorbed  $\text{NO}_3^-$  at the higher end of the isotherm curve was only approximately  $2 \mu\text{mol}_\text{c} \text{NO}_3^- \text{g}^{-1} \text{soil}$  (Figure 4-9). The concentrations of solution and adsorbed  $\text{NO}_3^-$  in the horizontal columns may therefore not be significantly different when calculated from the two isotherms. To test this hypothesis both TFE and batch isotherms were used to derive solution and adsorbed  $\text{NO}_3^-$  profiles from the total  $\text{NO}_3^-$  measurements in the diluted columns from Part A and B.

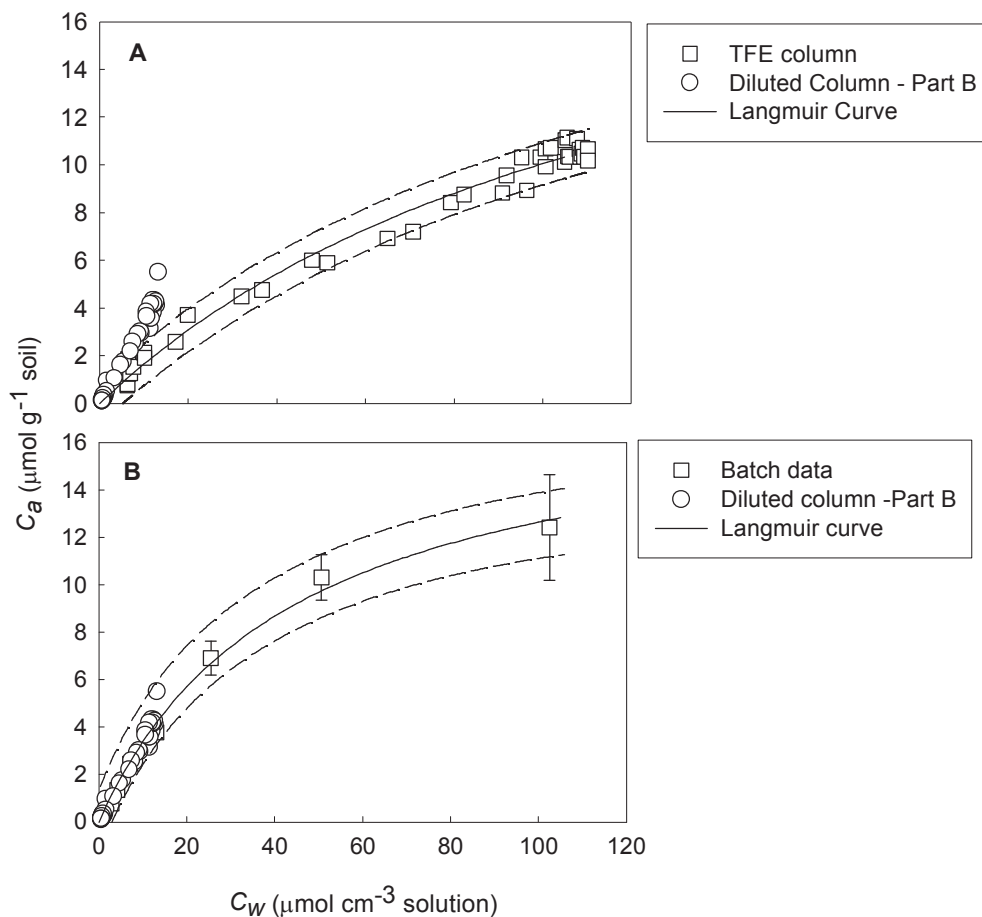


**Figure 4-9:** Isotherms from the TFE columns (Chart A) and the Batch experiments (Chart B) plotted against the diluted column data from part B. The solid line represent the Langmuir equation fitted to the TFE or batch data using SAS (version 9.1, 2003) and the dashed lines indicate the 95% confidence intervals of the fitted equation. The round symbols represent the diluted column data from Part B. These values were not included in the isotherm fit.



**Table 4-6:** Root mean square error (RMSE) and  $R^2$  values for the different isotherm fitting methods fitted to the TFE isotherm. The Langmuir and Freundlich isotherms were fitted either directly using SAS (version 9.1, 2003) or by derivation with the linear form of the isotherm equations (4-2 and 4-4).

TFE Isotherm Fit	RMSE	$R^2$
Langmuir – SAS	2.37	0.99
Langmuir – Linear	2.40	0.99
Freundlich – SAS	2.38	0.99
Freundlich – Linear	2.38	0.99

### *Testing the Isotherms*

#### *Soil Solution Nitrate*

Figure 4-10 shows the solution  $\text{NO}_3^-$  profiles of the diluted columns in Part A and B plotted against  $X \text{ cm s}^{-1/2}$ . Values were calculated from the total  $\text{NO}_3^-$  data (Figure 4-4B and Figure 4-7B) using the parameters from both the TFE and batch isotherms using equation 4-30. They are compared in Figure 4-10 to show a comparison of the profiles. The concentrations of the soil solution  $\text{NO}_3^-$  were slightly higher calculated from the TFE isotherm however statistical analysis of curves fitted to the soil solution  $\text{NO}_3^-$  profiles indicated that they were not significantly different ( $P < 0.05$ ).

To confirm both isotherms produced suitable soil solution profiles the solution concentrations near the inlet of the columns were compared with the inflowing solution concentration. Table 4-7 shows the inflowing concentrations as well as the concentration of the soil solution at  $X < 0.05 \text{ cm s}^{-1/2}$  for the diluted columns from Part A and B calculated from both the two isotherms. It was established in Part A that the solution concentrations calculated from the batch isotherm matched the inflowing concentrations. The same result was observed when the batch isotherm was used to calculate solution concentration for the diluted columns in Part B (Table 4-7).

Very similar results were also observed when the TFE isotherm was used to calculate the solution concentrations near the inlet of the column. The concentration near the column inlet was outside the standard deviations of the inflowing solution concentrations in Part B however the difference was less than 5% (Table 4-7). Both

the batch and TFE isotherms therefore appeared suitable for describing the solution concentrations in the columns.

**Table 4-7:** Mean inflowing solution concentration and soil solution  $\text{NO}_3^-$  concentrations near the inlet of the column ( $X < 0.01 \text{ cm s}^{-1/2}$ ) for the batch and TFE isotherms.

Diluted column set/Isotherm	Mean $C_w$ $X < 0.05$ ( $\mu\text{mol}_e \text{ NO}_3^- \text{ cm}^{-3}$ )	Standard deviation
Inflowing solution concentration	109.64	2.37
Part A – Batch Isotherm	107.49	4.53
Part B – Batch Isotherm	110.69	0.90
Part A – TFE Isotherm	111.46	4.55
Part B – TFE Isotherm	114.65	0.80

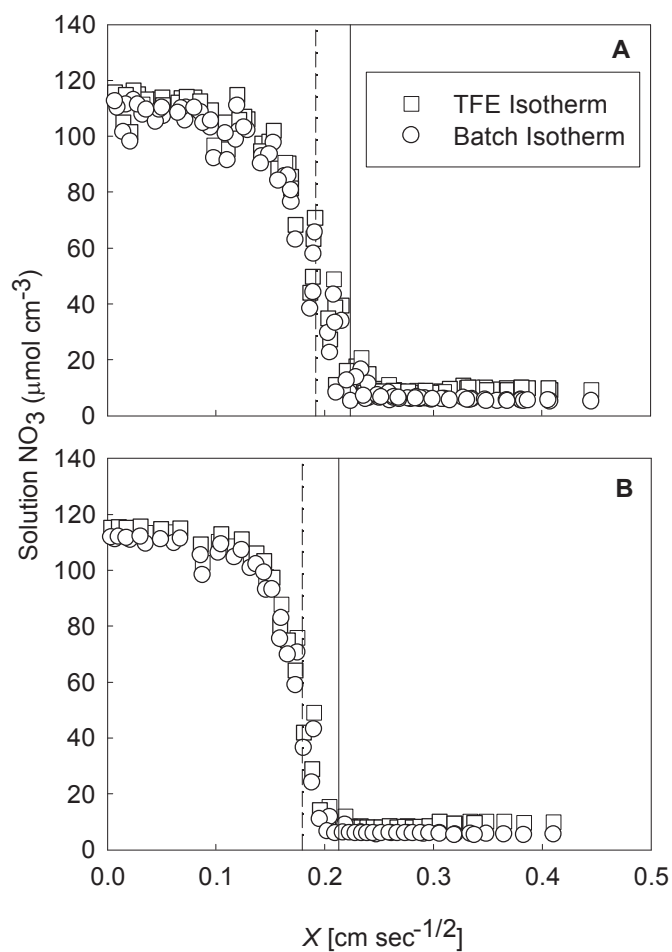


**Figure 4-10:** Solution  $\text{NO}_3^-$  profiles calculated from the TFE and batch adsorption isotherms plotted against the  $X$  coordinate ( $\text{cm sec}^{-1/2}$ ) for columns from Part A (Figure A), and Part B (Figure B). The solid vertical line indicates the position of the piston front ( $0.21 \text{ cm sec}^{-1/2}$ ) and the dashed line indicates the location of the solute front ( $0.18 \text{ cm sec}^{-1/2}$ ) for the solution  $\text{NO}_3^-$  profile.

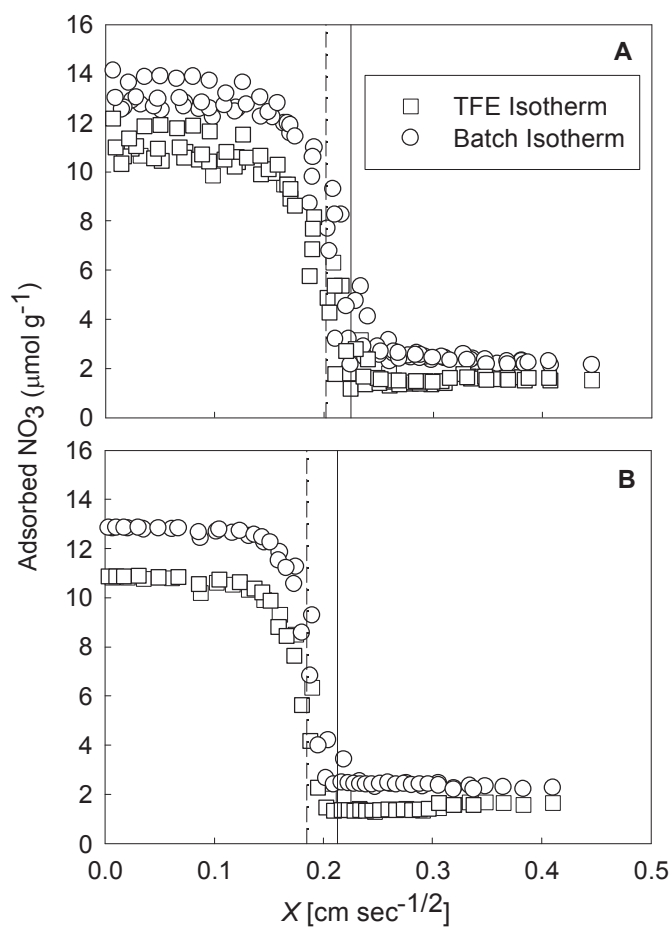
*Adsorbed Nitrate*

Figure 4-11 shows the adsorbed  $\text{NO}_3^-$  profiles calculated for the diluted horizontal columns in Part A and B using both the TFE and batch isotherms. In contrast to the soil solution data, the adsorbed  $\text{NO}_3^-$  profiles calculated from the two isotherms were easily distinguishable with the profiles calculated using the batch isotherm showing higher levels of adsorbed  $\text{NO}_3^-$ . Statistical analysis of curves fitted to the profiles calculated from the two isotherms confirmed that they were significantly different ( $P < 0.05$ ; Figure 4-11).

The effect of the isotherms was only clear when the adsorbed profiles were calculated because of the high proportion of  $\text{NO}_3^-$  in the solution versus the adsorbed phase. The sum of solution and adsorbed  $\text{NO}_3^-$  must be identical since they were derived from the same total  $\text{NO}_3^-$  values (Figure 4-4 and Figure 4-7B) using equation 4-30 and 4-31. Therefore the significantly higher  $\text{NO}_3^-$  level in the adsorbed profiles calculated from the batch isotherm must correspond to a lower amount in the solution values. This is shown in the average concentrations near the inlet of the column (Table 4-7). However, as a result of the higher proportion of total  $\text{NO}_3^-$  in the soil solution phase, the concentration difference in the solution profiles was not significant ( $P < 0.05$ ).

The difference measured between the isotherms and their influence on the partitioning between the solution and adsorbed  $\text{NO}_3^-$  phases raised the question of which is most suitable for describing adsorption. It was discussed above that the difference between the isotherms was probably a result of the treatment of the soil samples during equilibration/extraction. The purpose of the isotherm was to describe adsorption during unsaturated flow and therefore the TFE method is considered the most appropriate method for measuring adsorption for this purpose because soil solution was extracted with minimal disturbance of the soil sample after saturated flow using this procedure.

Because the TFE isotherm is considered the most suitable measure of adsorption the solution and adsorbed  $\text{NO}_3^-$  profiles calculated from TFE isotherm were used to estimate the solute fronts (Figure 4-10 and Figure 4-11)



**Figure 4-11:** Adsorbed  $\text{NO}_3^-$  profiles calculated from the TFE and batch adsorption isotherms plotted against the  $X$  coordinate ( $\text{cm sec}^{-1/2}$ ) for the column data from Part A (Figure A), and Part B (Figure B). The solid vertical line indicates the position of the piston front ( $0.21 \text{ cm sec}^{-1/2}$ ) and the dashed line indicates the location of the solute front ( $0.19 \text{ cm sec}^{-1/2}$ ) for the adsorbed  $\text{NO}_3^-$  profile.

### **Comparisons of Adsorption in the Red Ferrosol with Other Studies**

Figure 4-12 shows  $\text{NO}_3^-$  adsorption isotherms from three variable charge soils plotted against the TFE isotherm measured for the Red Ferrosol in this study. The basic soil properties for the three soils are presented in Table 4-8. The isotherm plots are approximations since the isotherm for the soil reported from Black and Waring (1976c) was estimated from graphed data, Duwig *et al.* (2003) only measured adsorption up to  $70 \mu\text{mol}_\text{c} \text{NO}_3^- \text{cm}^{-3}$  and Katou *et al.* (1996) only measured adsorption from a single point at  $50 \mu\text{mol}_\text{c} \text{cm}^{-3}$ . Furthermore adsorption was measured using different methods in all four studies. Despite these limitations some simple comparisons can be made between the different isotherms which can be related to differences in the soil properties.

The subsoil studied by Katou *et al.* (1996) had the highest adsorption capacity of the three examples (Figure 4-12B). This can be linked to the very low organic carbon content in the soil compared to the other soils and its significant proportion of variable charge minerals (Table 4-8). Even though the Red Ferrosol measured by Black and Waring (1976c) was a subsoil and therefore had lower levels of organic carbon and a higher the Red Ferrosol surface soil from this thesis, the adsorption isotherms were similar. The proportion of variable charge minerals were similar (14.4 versus 9-12%) and therefore the lower pH (5.8) in the soil from this thesis in comparison to the levels reported by Black and Waring (1976c) may explain why adsorption levels were similar. The lower pH would have resulted in more positively charged sites would be present on the clay minerals at this lower value which may have counteracted the neutralising effect of the high OC levels. The high percentage of variable charge minerals in the soil investigated by Duwig *et al.* (2003) in comparison to the other examples (Table 4-8) is probably the main reason why adsorption was observed in this soil since the high pH and OC contents in comparison to the other studies would indicate that adsorption is unlikely.

These comparisons demonstrate adsorption was similar to some reports of adsorption in topsoils and subsoils. These comparisons indicate that pH and amounts of OC and variable charge minerals must all be assessed when comparing the soils since they all play a role in the levels of positive charge development in the soil.

---

**Table 4-8:** Summarised soil properties for three example isotherms shown in Figure 4-12.

Study	Sample depth (cm)	Measurement method	pH	OC (%)	Variable charge minerals (%)
Black and Waring (1976c)	40-90	Batch	6.1-6.5	0.77-0.23	14.4
Duwig <i>et al.</i> (2003)	0-10	Unsaturated column	6.9	5.47	53.7
Katou (1996)	30-150	Saturated column	6.0	0.02	26.4

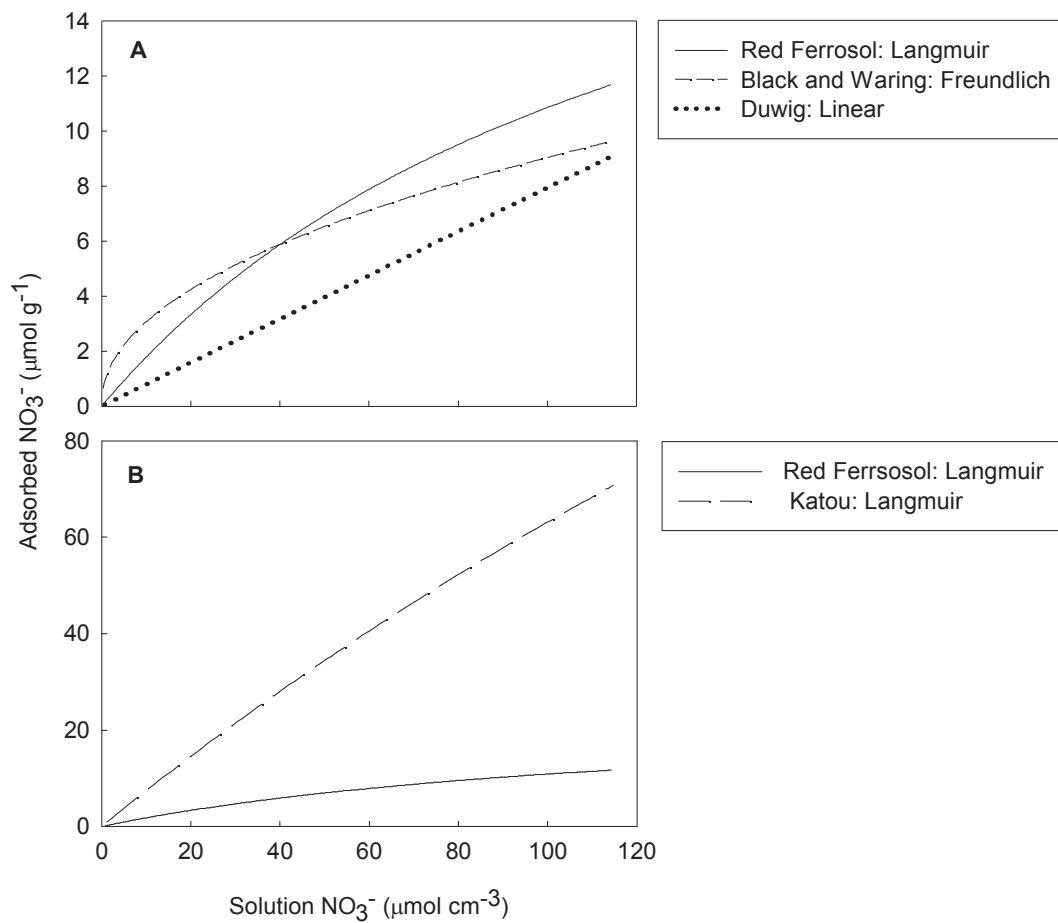


**Figure 4-12:** Comparisons of adsorption isotherms. Chart A: The Red Ferrosol from this study and isotherms described by Black and Waring (1976c) and Duwig *et al.* (2003). Chart B: The Red Ferrosol from this study and the isotherm reported by Katou *et al.* (1996).

## GENERAL DISCUSSION

The rate of  $\text{NO}_3^-$  movement through horizontal columns packed with a Red Ferrosol surface soil was retarded in relation to the inflowing water which indicated  $\text{NO}_3^-$  was adsorbed by the soil. Adsorption in surface soils has rarely been described and is more common in subsoils because proportions of variable charge minerals are lower near the soil surface while organic carbon levels are higher (Black and Waring 1976c; Strahm and Harrison 2007). Retardation of  $\text{NO}_3^-$  has been reported in a variable charge surface soil from New Caledonia (Duwig *et al.* 2003), but there have previously been no detailed studies of surface-soil adsorption in Australia. The measurement of retarded  $\text{NO}_3^-$  transport and development of an adsorption isotherm contributes to the small number of studies that have shown anion adsorption in surface soils. Furthermore these findings provide information on the  $\text{NO}_3^-$  absorption capacity of a soil that plays an important role in Tasmania's agricultural industry and may therefore be used to improve understanding of  $\text{NO}_3^-$  transport in these soils.

### Isotherm Measurement

Comparisons between the two adsorption isotherm measurement methods indicated that significantly higher  $\text{NO}_3^-$  adsorption was measured in the batch experiments (Figure 4-9) and diluted columns. The difference in the isotherms did not have a significant effect on the derived soil solution  $\text{NO}_3^-$  profiles from the horizontal column experiments, however they did result in significantly different adsorbed profiles (Figure 4-11).

The increased adsorption measured in the batch experiments was considered to be a result of mixing during equilibration and the higher solution to soil ratio used in comparison to the TFE method. Previous studies suggested batch experiments may overestimate adsorption due to aggregate breakdown or abrasion of soil surfaces both of which may expose more exchange sites (Barrow and Shaw 1979; Schweich *et al.* 1983; Sparks 1995). Green *et al.* (1980) suggested that the soil to solution ratio was only likely to have an effect on adsorption if differences in ratios have an effect on the dispersion and suspension of soil particles. This comment by Green *et al.* (1980) highlights the differences between the two methods used. In the batch experiments the soil existed in a water suspension where it was mixed for 16 hours end-over-end.

---



Over this time it was likely that there was some disaggregation of the soil which potentially exposed further exchange sites. In contrast, the incorporation of the  $\text{NO}_3^-$  solution with the soil in the TFE procedure relied upon the capillary forces in the soil absorbing the solution under unsaturated conditions with no physical mixing. The subsequent sectioning of the column and centrifugation of the samples with the TFE liquid in this method would still have resulted in much less soil disturbance in comparison to the batch experiments. The mixing of the samples in the saturated solution is therefore considered the reason for the higher adsorption measured in the batch experiments. If an accurate measurement of adsorption under natural flow conditions is required then the unsaturated horizontal absorption method employing TFE displacement is a more appropriate method than batch experiments which may overestimate adsorption under these conditions.

The literature review indicated that there were few valid comparisons between flow and batch methods for determining ion adsorption in soils and that these studies showed conflicting results (Bond and Phillips 1990b; Burgisser *et al.* 1993; Hodges and Johnson 1987). This studies from this thesis differed to these three reports because no solute wash was undertaken prior to the adsorption experiments and, as a result, provides a more realistic measure of adsorption under field conditions since indigenous ions were not displaced. Avoiding pre-treatment of the soil is particularly relevant for measurement of monovalent ion adsorption because these ions are unlikely to displace polyvalent ions already present in the soil unless concentrations are very high (Bohn *et al.* 1979; Katou *et al.* 2001). With the difference between the treatment of samples in this study in comparison to previous reports in mind and the finding that batch experiments did overestimate adsorption then it is concluded that the unsaturated column method employing TFE displacement is the most appropriate way of determining solute adsorption under field-type flow scenarios.

If information on the rate of water and solute movement is also required the unsaturated horizontal column method using TFE displacement has further advantages because water and solute profiles are determined in the same study (Figure 4-10).

---

### Fitting the Adsorption Isotherm

Directly fitting the parameters for the Langmuir and Freundlich equations using modern statistical software capable of fitting non linear functions to data had a number of advantages: i) the fit to the adsorption data was improved (Table 4-6; Appendix 4); ii) confidence intervals for the equation parameters and fitted curve could be calculated (Figure 4-9) and; iii) the process of determining parameters was simplified because the curve was fitted directly to the measured data without the need for any transformation. Despite these benefits most soil chemistry texts, including those published relatively recently, recommend using the linear plot of the isotherms to determine their parameters (Sparks 1995; Sposito 1984; Sumner 1999). Consequently this method had been used in most studies to identify parameters for the isotherm equations (Black and Waring 1976c; Katou *et al.* 1996; Katou *et al.* 2001; Kinjo and Pratt 1971; Qafoku *et al.* 2000).

The linearisation of the Langmuir isotherm to determine equation parameters can result in high uncertainty during parameter determination particularly if adsorption measurements are made at low solution concentrations where measurement error is higher. The y-axis of the linear plot represents the ratio of adsorbed to soil solution solute,  $C_a/C_w$  (equation 4-4), and therefore at low concentrations this ratio can be highly variable when based on the quotient of two small number which are both prone to significant measurement errors. Figure 4-13A shows the linear plot of the Langmuir isotherm and the scatter of data at low concentrations represented by the adsorption values from the diluted columns. Figure 4-13B shows the linear plot of the values in the TFE isotherm. The higher concentration values reduced the variation in the  $C_a/C_w$  and as a result the parameters estimated for the Langmuir equation produced a good fit to the data (Table 4-6 and Appendix 4). However Figure 4-13B still indicates the increased variability in  $C_a/C_w$  at lower solution concentrations.

Although the linear method did produce acceptable parameters for the Langmuir equation using the TFE isotherm data the advantages discussed above make the direct fitting method more appropriate. Previous studies that have used the linear form of the equation and very few isotherm points such as Katou *et al.* (1996) cannot expect to produce parameters that accurately describe adsorption for the soil.

---

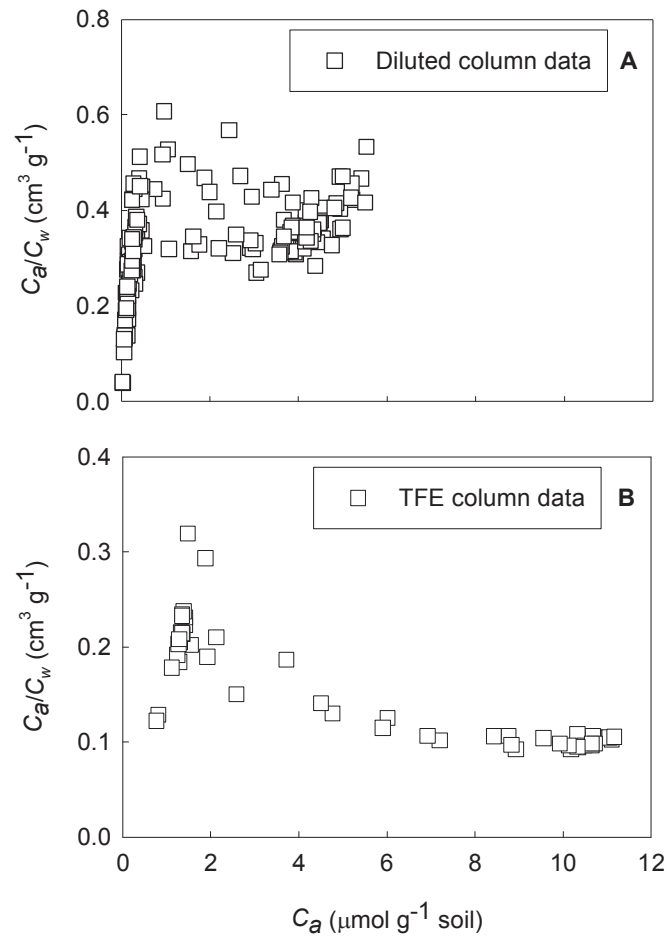


**Figure 4-13:** The linear plot of the Langmuir isotherm (equation 4-4) for the diluted column data from Part A and B (Figure A) and the TFE column data (Figure B).

**Significance of Nitrate Retardation**

Nitrate was retarded by 14% in relation to the inflowing soil water when a  $109.64 \mu\text{mol}_e \text{NO}_3^- \text{cm}^{-3}$  solution was absorbed by the Red Ferrosol. Equation 4-24 shows that the isotherm slope ( $\beta$ ) describes the amount of  $\text{NO}_3^-$  retardation under one dimensional flow. For a linear isotherm, where  $\beta$  is constant, the level of retardation will not change with changes in solution concentration however the isotherm for the Red Ferrosol is non linear (Figure 4-9A). As a result,  $\beta$  increases with decreasing solution concentration and retardation of  $\text{NO}_3^-$  movement will thus be higher as the soil solution concentration decreases.

The retardation of  $\text{NO}_3^-$  in relation to the soil water may be reduced under different flow scenarios. Clothier and Elrick (1985) studied non-reactive solute dispersion from a point source in three dimensions and showed that the distance between the solute front and the wetting front was smaller in comparison to one dimensional flow in the same soil. This was due to the expanding flow field in three dimensions. The significance of  $\text{NO}_3^-$  retardation will therefore be influenced by both the flow scenario and solution concentration in the soil.

It is impractical to conduct experiments describing  $\text{NO}_3^-$  distribution under all the possible flow scenarios and solution concentrations however, a soil model validated against measured data would allow some investigations of  $\text{NO}_3^-$  transport and adsorption under different flow conditions and at different concentrations in the soil. The convergence of water and solute profiles plotted against  $X (\text{cm}^{-1/2})$  indicated that the flow equations (1-6, 1-16, 1-13 and 1-17) appeared valid for the prescribed boundary conditions (equations 4-15 and 4-16). Thus the data from these experiments should be suitable for validation of a soil model that implements the same water and solute flow equations. Furthermore the parameters for the Langmuir isotherm describing  $\text{NO}_3^-$  adsorption in the soil can be directly included in some soil models to describe adsorption in the soil (Simunek and Senja 2007). Validation of a model for the Red Ferrosol soil may allow some conclusions to be made about the significance of  $\text{NO}_3^-$  adsorption in the soil and the distribution of water and  $\text{NO}_3^-$  under different flow scenarios.

---

### Experiment Assumptions

Some assumptions must be made in regard to the movement of ions other than  $\text{NO}_3^-$  during absorption of the  $\text{NO}_3^-$  solution by the soil because they were not measured in these experiments. It was assumed that as  $\text{NO}_3^-$  moved through the column during absorption all monovalent anions initially present were displaced and accumulated ahead of the solute front. Katou *et al.* (1996) assumed  $\text{NO}_3^-$  did not cause  $\text{SO}_4^{2-}$  desorption during horizontal absorption of a  $47 \mu\text{mol}_\text{c} \text{ cm}^{-3}$   $\text{NO}_3^-$  solution but did observe some desorption in saturated column experiments when concentrations of over  $114 \mu\text{mol}_\text{c} \text{ NO}_3^- \text{ cm}^{-3}$  were used. Therefore some divalent and trivalent anions may have also been displaced during absorption the  $\text{NO}_3^-$  solution in this study.

Nitrate was applied in the form of  $\text{Ca}(\text{NO}_3)_2$  and as a result a significant amount of  $\text{Ca}^{2+}$  was also applied to the soil during the absorption experiments. Calcium has a strong affinity for cation for exchange sites (Bohn *et al.* 1979), so it was assumed that it displaced all monovalent and divalent cations during absorption because no other cations were present in the invading solution. Although the distribution of other anions and the cations was not measured, the horizontal columns experiments in combination with the adsorption isotherm provide a detailed description of  $\text{NO}_3^-$  distribution during unsteady adsorption into Red Ferrosol surface soil.

Adsorption in variable charge soils is influenced by pH (Evangelou 1998). Katou *et al.* (1996) assumed the net proton surface charge density (Sposito 1984) was unlikely to change during absorption of a neutral salt solution and therefore considered adsorption to only be influenced by changes in solution concentration because no  $\text{H}^+$  or  $\text{OH}^-$  was added to the soil to influence pH. However in this thesis changes in pH of approximately one unit were observed in the equilibrated soil solutions from blank samples to the highest solution concentrations added ( $109.64 \mu\text{mol}_\text{c} \text{ cm}^{-3}$ ). As a result it was concluded that the increased adsorption measured at higher solution concentration in the soil was a result of compression of the diffuse double layer around soil particles which increased the surface charge density (Ji 1997) and the subsequent reduction in pH that resulted from the addition of the  $\text{Ca}(\text{NO}_3)_2$  solution.

## CONCLUSION

Movement of  $\text{NO}_3^-$  through a Red Ferrosol surface soil was retarded in relation to the inflowing soil water indicating the presence of anion adsorption in the soil. Although anion adsorption is commonly observed in variable charge soils at depth, surface adsorption is less common and has not been documented in detail in an Australian soil.

Investigations into the  $\text{NO}_3^-$  adsorption isotherm for the soil indicated that batch experiments overestimated adsorption when they were used to determine adsorption under unsaturated flow conditions. This was probably due to the extended mixing of the soil in batch experiments in a high solution to soil ratio causing aggregate breakdown. Previous studies showed conflicting results in terms of the suitability of the batch experiments but no comparisons had previously been conducted on soils that were not initially washed with solute to remove indigenous ions. The findings from this study indicated that the unsaturated flow column method using TFE displacement provided a more accurate measurement of adsorption than batch experiments under unsaturated flow conditions. Furthermore the column method used in this study provides details of water and  $\text{NO}_3^-$  transport as well as producing isotherm data from the single experimental procedure.

Adsorption retarded  $\text{NO}_3^-$  transport relative to the soil water in the one dimensional horizontal columns however this may have little significance on  $\text{NO}_3^-$  distribution in multidimensional flow scenarios such as infiltration from drip irrigation. Development of water and solute flow parameters in a soil model will provide a way of investigating the significance of  $\text{NO}_3^-$  adsorption under different flow scenarios and at different solute concentrations to estimate  $\text{NO}_3^-$  distribution in the field. The data from the horizontal columns can be used to validate water and solute flow in a soil water model.

---

## CHAPTER 5

### MODELLING WATER AND NITRATE MOVEMENT

#### INTRODUCTION

Simulation models can be useful tools to examine water and solute movement in soil profiles for a variety of practical purposes including improving water and nutrient use efficiency (Cote *et al.* 2003; Siyal and Skaggs 2009; Skaggs *et al.* 2004) and assessing environmental hazards due to nutrient and pesticide applications (Boivin *et al.* 2006; de Vos *et al.* 2000; Phillips 2006; Sarmah *et al.* 2006). However, validation of models against measured data is required to have confidence in their predictions. In this chapter, water and  $\text{NO}_3^-$  movement data generated from laboratory experiments using a Red Ferrosol surface soil were used to validate Hydrus 2D/3D model. Hydrus was then used to simulate movement of  $\text{NO}_3^-$  in the field trial described in Chapter 3 to determine if  $\text{NO}_3^-$  could be leached from the root zone using extended periods of irrigation and different irrigation methods.

#### LITERATURE REVIEW

##### Modelling Water and Solute Transport

There are a number soil water models which have been developed to describe solute and/or water movement in one dimension and from point or line sources that represent drip irrigation applications. LeachM (Wagenet and Hutson 1989) and Hydrus 1D (Simunek *et al.* 2002) are examples of one dimensional models capable of predicting water and solute transport. Wet-Up was designed by Cook *et al.* (2003) to predict wetting front distributions from dripper systems in three dimensions while Hydrus 2D/3D (Simunek *et al.* 2006a) and numerical procedures described by Wu and Chieng (1995a; 1995b) are capable of describing water and solute movement in two and three dimensions.

In this study, the Hydrus 1D and 2D/3D models (Simunek *et al.* 2002; 2006a) were used because of their ability to simulate solute flow under various water flow scenarios. The governing flow equations for water and solute used in Hydrus 1D and

2/3D are solved using Galerkin-type linear finite elements (Simunek *et al.* 2006b). Details of the flow equations are provided in Appendix 5.

Hydrus 1D has been used to accurately simulate water movement in horizontal columns, similar to those described in Chapter 4 (Simunek *et al.* (2000). Phillips (2006) also referred to unpublished data in which Hydrus was used to successfully predict transport of  $\text{Cl}^-$  and  $\text{K}^+$  in unsaturated repacked horizontal columns.

Several studies have also demonstrated the capability of Hydrus 2D/3D to describe water and non-reactive solute distribution under drip irrigation in laboratory and field experiments (Ajdary *et al.* 2007; Gardenas *et al.* 2005; Li *et al.* 2005; Siyal and Skaggs 2009; Skaggs *et al.* 2004). Reactive solute transport has also been modelled under these irrigation scenarios using Hydrus (Hanson *et al.* 2006) but model validation examples are absent from the literature.

Modelling of water and solute movement in heavier textured soils such as the clay loam Red Ferrosol from the field experiment described in Chapter 3, has received relatively little attention in comparison to lighter textured sand and loam soils (Li *et al.* 2005; Skaggs *et al.* 2004). Exceptions are the studies by Khalil *et al.* (2007) and Arbat *et al.* (2008), who used Hydrus 2D to model water and nitrogen distribution in sandy clay loams. Gardenas *et al.* (2005) also included two clays soils in their  $\text{NO}_3^-$  leaching simulation using Hydrus 2D, however they did not report the validation of the model predictions.

Water and solute movement in heavier textured soils, and validation of reactive solute transport under drip irrigation, are two areas that must be addressed in this study if suitable parameters are to be determined for the Red Ferrosol soil.

### ***Parameter determination using Inverse Optimisation***

If measured data is available soil hydraulic parameters can be determined using inverse optimisation. Using this procedure both soil hydraulic and solute reaction parameters can be estimated from measured data such soil profile pressure heads, soil water contents, and soil moisture retention or unsaturated hydraulic conductivity data (Simunek and Senja 2007). The inverse procedure is based on the minimization of a



---

suitable objective function, which calculates the discrepancy between the observed values and the model predictions (Simunek and Senja 2007).

The inverse method has been used in a number of studies to determine soil hydraulic parameters in both laboratory and field environments using water content and matric potential data (Arbat *et al.* 2008; Simunek *et al.* 2000; Simunek *et al.* 1998). Although inverse modelling provides a relatively efficient way of determining soil hydraulic parameters, care must be taken to ensure parameters are physically realistic. Hopmans *et al.* (2002) suggest that inverse optimisations should be conducted with different initial parameters to ensure parameter sets are unique. Non-uniqueness occurs when objective function is minimised for a range of parameters making it unclear as to which parameter combinations are physically realistic (Hopmans *et al.* 2002). This problem is overcome by decreasing the number of parameters to be estimated by the optimisation procedure or by including alternative measurements in the optimisation procedure.

Simunek *et al.* (2000) demonstrated the ability for soil hydraulic parameters to be estimated from horizontal columns similar to those described in Chapter 4. The water profiles from the horizontal columns may therefore be used to determine soil hydraulic properties for the Red Ferrosol using inverse optimisation. However horizontal columns do not take into account the effect of gravity on water flow (Philip 1969). Parameters estimated from the horizontal columns should be tested under flow conditions such as infiltration from a point source that are affected by gravity after prolonged water application. Identification of parameters suitable for describing water flow in alternate flow scenarios will also provide greater confidence that they are physically realistic (Sonnleitner *et al.* 2003).

## EXPERIMENTAL OVERVIEW

Inverse optimisation was undertaken with the aim of identifying soil hydraulic parameters for the Red Ferrosol which could be used in combination with the  $\text{NO}_3^-$  reaction parameters identified in Chapter 4 to validate water and solute flow in Hydrus. Based on identification of suitable parameters, the second aim of the chapter was to use these validated parameters to explore some management options for the Red Ferrosol in the field to improve the N Leach treatment described in Chapter 3.

---

## MATERIALS AND METHODS

### Measuring Soil Hydraulic Properties

Soil samples used to determine hydraulic conductivity and water retention were prepared as described in Chapter 4.

#### *Saturated Hydraulic Conductivity*

Hydraulic conductivity of the Red Ferrosol surface soil was measured using the falling head method described by Reynolds *et al.* (2002). A column of water (4.2 cm in diameter and 12 cm high) was applied to wet repacked soil core packed to a bulk density of 1.0 with air dry soil sieved to <2 mm. The soil cores were 2 cm high and had an internal diameter the same as the water column sitting above it. Triplicate measurements of conductivity were recorded on four separate cores.

#### *Water Retention*

Water retention of the soil was measured in the soil using three methods. Retention at -100 and -300 cm was measured using ceramic suction plates based on the method described by Cresswell (2002) for measuring water retention in undisturbed cores. Triplicate soil samples were packed into rings 5 cm in diameter and 1 cm high to a bulk density of 1.0 g cm<sup>-3</sup>. The soil was equilibrated on the suction plates in two ways: i) soil was wet to saturation from the bottom up by placing samples on saturated suction plates prior to equilibration at -100 or -300 cm and; ii) air dry samples were placed on the suction plates under suction heads of -100 and -300 cm and allowed to equilibrate. After 14 days samples were removed from the suction plates, weighed and their oven dry water content was determined (Rayment and Higginson 1992). Water retention of samples drained from saturation were measured at -15 bars in triplicate using the pressure plate method (Cresswell 2002). The third method used to determine water retention in the Red Ferrosol was the filter paper method between suctions of -30 and  $-3.8 \times 10^4$  cm of water (Greacen *et al.* 1989).

---

### Estimating Hydraulic Parameters for Hydrus

Various inverse optimisations using the horizontal column data described in Chapter 4 were conducted to determine soil hydraulic parameters for the van Genuchten equations (van Genuchten 1980; Appendix 5). The horizontal column data from the first column series in Chapter 4 provided water profiles from 25 cm horizontal columns after six different time periods of water absorption. Spurious or outliers in the data set were removed from the data set used in the inverse solution (Hopmans *et al.* (2002)). Hydrus 1D was used in preference to the Hydrus 2D for inverse modelling because a greater number of water content values could be included in the inverse procedure.

Inverse optimisations were also conducted with and without the soil moisture retention data. The accuracy of parameters obtained with and without this second set of measurements were then compared. When the retention data was included in the optimisations, the *ret* descriptor was included in the optimisation description. For examples the *Fit All* inverse scenario described in Table 5-1 will be described as *Fit All (ret)* if the moisture retention data is also included in the optimisation.

Table 5-1 shows the various optimisation scenarios conducted in Hydrus. During all the optimisations the initial water content was set to  $0.155 \text{ (cm}^3 \text{ cm}^{-3}\text{)}$ . To simulate free water absorption using a pressure head value a time variable boundary condition was applied to the surface of the column at a water tension ( $\psi$ ) of  $-0.01 \text{ cm}$ . Initial estimates for  $\theta_r$  and  $\theta_s$  were  $0.05$  and  $0.58 \text{ (cm}^3 \text{ cm}^{-3}\text{)}$  and  $K_{sat}$  was set to  $0.10 \text{ cm min}^{-1}$ . The  $\theta_s$  and  $K_{sat}$  values were taken from independent measurements in the falling head  $K_{sat}$  experiments.  $\theta_r$  and  $\theta_s$  and  $K_{sat}$  were set or optimised depending on the particular optimisation scenario. The remaining parameters  $\alpha$ ,  $n$ , and  $l$  were fitted in all inverse procedures with the initial values taken from the 12 default soils in the Hydrus soil catalogue.

All parameter sets that showed a good fit to the column data were tested against the third horizontal column data set described in Chapter 4. This data was not included in the optimisation and provided a set to test of the optimised parameters on a separate data set. The parameters were then used to simulate water distribution in the 3D wedge experiments which provided an independent test for the parameters.

**Table 5-1:** Inverse optimizations conducted in Hydrus 1D. Each optimisation scenario was conducted with and without soil moisture retention values included in the inverse data set. Ticks indicate optimised parameters while X indicates the parameters were set for each scenario. In all procedures  $\alpha$ ,  $n$ , and  $l$  were set to values from the 12 default soils in the Hydrus soil catalogue.

Inverse scenarios	$\theta_r$	$\theta_s$	$K_{sat}$	$A$	$n$	$l$
<i>Fit all</i>	✓	✓	✓	✓	✓	✓
<i>Set <math>\theta_r</math></i>	X	✓	✓	✓	✓	✓
<i>Set <math>\theta_r \theta_s</math></i>	X	✓	✓	✓	✓	✓
<i>Set <math>\theta_s</math></i>	✓	X	✓	✓	✓	✓
<i>Set <math>\theta_r \theta_s</math></i>	X	X	✓	✓	✓	✓
<i>Set <math>\theta_r K_{sat}</math></i>	X	✓	X	✓	✓	✓
<i>Set <math>K_{sat}</math></i>	✓	✓	X	✓	✓	✓
<i>Set <math>\theta_s K_{sat}</math></i>	✓	X	X	✓	✓	✓
<i>Set all</i>	X	X	X	✓	✓	✓

### Simulating Horizontal Absorption of Water and Nitrate

Hydrus 2D/3D was used to model water distribution in the horizontal column experiments using the same initial and boundary conditions used in the Hydrus 1D model during inverse optimisation. To simulate horizontal flow in Hydrus 2D/3D the geometry was set to a 2D horizontal plane. The domain geometry of the flow domain was set to a 2 cm diameter by 50 cm long column. Simulations were conducted for the two absorption periods in from Chapter 4 Part A (Table 4-5).

To simulate absorption of the  $\text{NO}_3^-$  solution a third type solute boundary was applied to the inlet of the column ( $x=0$  cm) and a constant concentration of  $110 \mu\text{mol NO}_3 \text{ cm}^{-3}$  was applied to the boundary over the period of absorption. Nitrate reaction parameters were included in the form of the Langmuir equation (4-3) where  $k_d = 0.177 (\text{cm}^3 \text{ g}^{-1})$  and  $\phi = 0.00775$  (Appendix 5). Bulk density was set to  $1.03 \text{ g cm}^{-3}$ . The longitudinal and transverse dispersivities were set to 0.3 and 0.03 cm based on values used by Ajdary *et al.* (2007) and the diffusion coefficient was neglected as it was considered negligible relative to the dispersion (Ajdary *et al.* 2007; Hanson *et al.* 2006). Solute transport was simulated for all ten columns from the two column series described in Chapter 4.

### Simulating Point Source Infiltration of Water and Nitrate

To test the suitability of the soil hydraulic properties to describe water and  $\text{NO}_3^-$  distribution under a different flow scenario, a three dimensional wedge experiment was designed to measure  $\text{NO}_3^-$  distribution from a point source to represent a drip type irrigation system. Experimental design, measurement and model simulations are described below.

#### *Water and Nitrate Distribution from a Point Source: Data Collection*

Figure 5-1 shows the wedge used to measure three dimensional water and solute distribution from a point source. The angle of the wedge at the application point was  $15^\circ$  which represents  $1/24^{\text{th}}$  of a cylinder. This soil wedge was based on the design by Li *et al.* (2003) who indicated there was no difference between using a wedge with  $15^\circ$  or  $90^\circ$  angle to measure water distribution from a point source. A wedge design was selected because it required less soil.

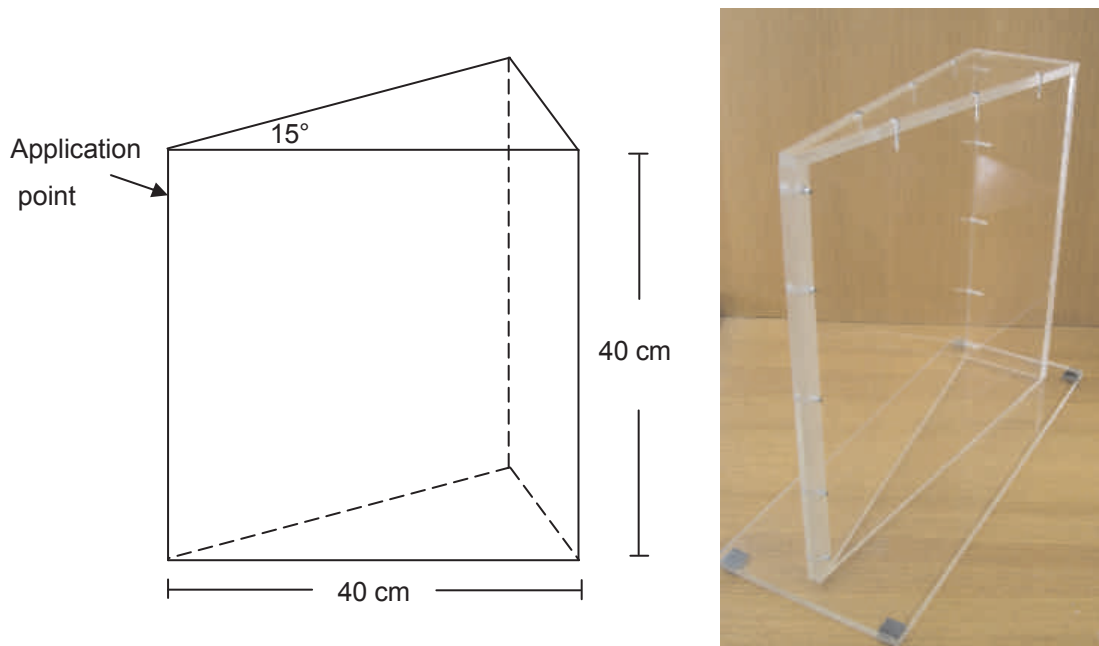


**Figure 5-1:** Diagram and photograph of the wedge.

### Packing and Treatment Application

The soil was mixed thoroughly with water to reach a water content of approximately  $0.2 \text{ (g g}^{-1}\text{)}$  and left to equilibrate overnight. Soil was added to the wedge in 5 cm increments and packed with a drop hammer to a bulk density as close to unity as possible without causing significant layering ( $\rho=0.95 \text{ g cm}^{-3}$ ). Solution was applied in the  $15^\circ$  corner of the wedge at a depth of 5 cm (Figure 5-1) with a peristaltic pump at a rate of  $50 \text{ cm}^3 \text{ hr}^{-1}$ ; equivalent to a dripper output of  $1200 \text{ cm}^3 \text{ hr}^{-1}$  in a  $360^\circ$  flow environment.

Figure 5-2 shows the two irrigation scenarios applied in the experiments. Both treatments received an 0.5 hour ( $25 \text{ cm}^3$ ) application of  $110 \mu\text{mol}_\text{c} \text{ NO}_3^- \text{ cm}^3$  in the form of a  $\text{Ca}(\text{NO}_3)_2 \cdot 4\text{H}_2\text{O}$  solution. This application was equivalent to an application of 60 kg N/ha assuming a dripper spacing of 20 cm and a row width of 85 cm. The initial  $\text{NO}_3^-$  application was followed immediately by a 1.5 hour application of water in both irrigation scenarios. Scenario A was sampled immediately after the completion of the water application. In scenario B, the soil was allowed to ‘rest’ for 16 hours after the initial solute and water applications, and water was applied for a further 6 hours before sampling (Figure 5-2).

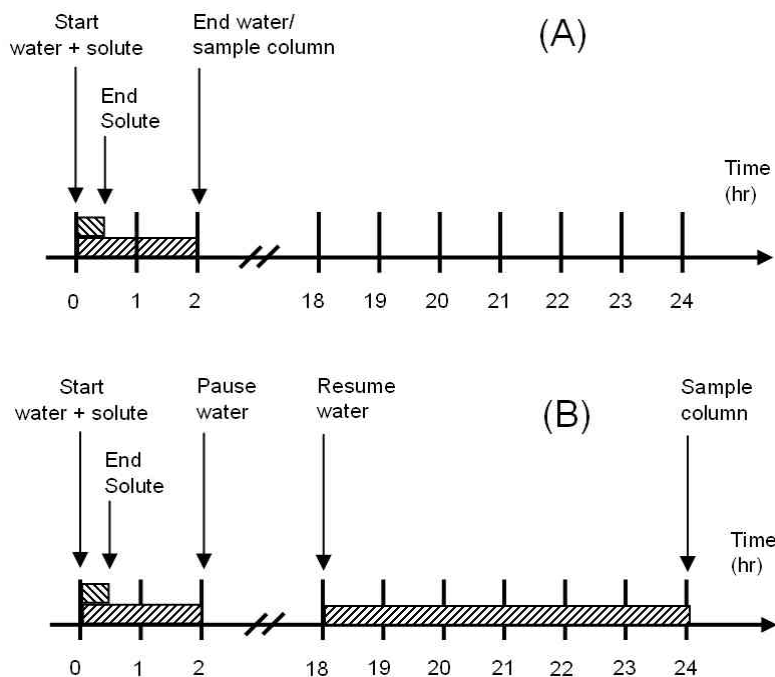


**Figure 5-2:** Schematic showing the two irrigation scenarios applied to the wedge columns.

### Sampling

Figure 5-3 shows the sampling strategy used in the wedge experiments. At the completion of each irrigation scenario the wedge was laid horizontally and the side panel removed to permit cross sectional sampling of the soil. A 5 cm grid was placed over the column and a soil core (2 cm internal diameter) samples taken from the centre of each 5 x 5 cm section. Care was taken to ensure the core was pushed all the way through the column at each sampling position to ensure a representative sample was made. Additional soil samples were taken at the edge of the wetting front. Each core sample was transferred into pre-weighed soil moisture tin and thoroughly mixed. A sub-sample was transferred into a pre-weighed falcon centrifuge tube, weighed and retained for  $\text{NO}_3^-$  analysis. The remainder was weighed and oven dried to calculate the moisture content of the soil (Rayment and Higginson 1992).

Two molar KCl was added to the soil samples in a 1:5 soil to solution ratio, weighed and mixed for 60 minutes in an end-over-end shaker (Rayment and Higginson 1992). The samples were then centrifuged for 10 minutes at  $9800 \text{ m s}^{-2}$ , and the supernatant was decanted into a pre-weighed tube and weighed. The supernatant was weighed and analysed for  $\text{NO}_3^-$  calorimetrically on an AlpKem auto analyser (AlpKem 1992).

All dilutions and solution volumes were measured gravimetrically throughout the experiments. Since solutions are presented on a volumetric basis, the 2M KCl extract weights were converted to a volumetric basis using a density of  $1.09 \text{ g cm}^{-3}$  (Weast 1971). Other solution volumes were assumed to have a density of  $1.0 \text{ g cm}^{-3}$ .

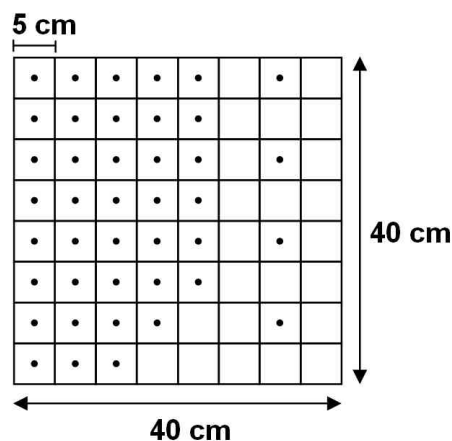


**Figure 5-3:** A typical sampling pattern for the wedge column. The dots indicate the centre of the sample (2 cm diameter).

---

### *Calculations*

Concentrations of  $\text{NO}_3^-$  in the KCl extract represented the total amount of  $\text{NO}_3^-$  in solution and on the soil exchange sites. This was converted to total  $\text{NO}_3^-$  per unit volume of soil,  $T$  ( $\mu\text{mol}_\text{c} \text{NO}_3^- \text{cm}^{-3}$  soil) using equation 2-1

The concentration of  $\text{NO}_3^-$  in the soil solution,  $C_w$  ( $\mu\text{mol}_\text{c} \text{NO}_3^- \text{cm}^{-3}$ ), was calculated from the Langmuir adsorption isotherm calculated using the water immiscible displacement method described in Chapter 4 using equation 4-30. Solution concentrations were used to compare concentrations in the wedge column with those predicted in Hydrus.

### ***Water and Nitrate Distribution from a Point Source: Modelling***

To simulate water and  $\text{NO}_3^-$  distribution in the wedge columns a 40 x 40 cm flow domain was created in 2-D axi-symmetrical vertical flow geometry (Figure 5-4). The infiltration point at 5 cm depth was represented by a semi circle with a radius of 3 cm. Initial attempts to use an application point with a lower radius led to model instability with many of the parameter sets. The smallest radius that could be used was 3 cm. The flux from the source, represented by a sphere with a radius of 3 cm, was  $10.61 \text{ cm hr}^{-1}$  which is equivalent to a dripper output of  $1200 \text{ cm}^3 \text{ hr}^{-1}$ . This was calculated using the equation 5-1:

$$\sigma = \frac{Q}{4\pi r^2}, \quad 5-1$$

where  $\sigma$  is the flux from the surface of the source ( $\text{cm hr}^{-1}$ ),  $Q$  is the total volumetric flux ( $\text{cm}^3 \text{ hr}^{-1}$ ) and  $r$  is the radius of the spherical source (cm).

The FE mesh of the flow domain was set to 0.5 cm. No flux was allowed through the boundaries around the column. The infiltration source was set as a variable flux boundary so that water and solute applications could be controlled according to the two irrigation scenarios described for the wedge columns (Figure 5-4).

Solute flux was applied as described for horizontal absorption however the time variable boundary condition was used to apply the solute only for the first 0.5 hours of water application to the column experiments.



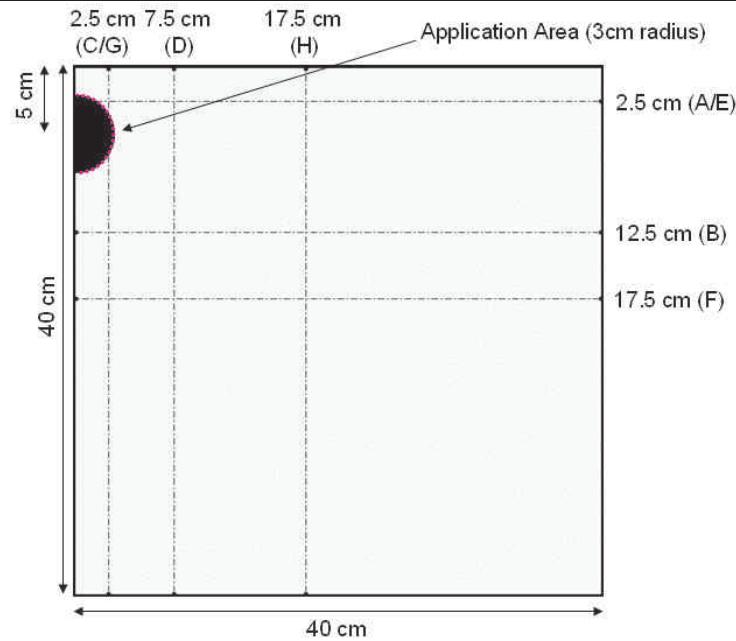


**Figure 5-4:** Geometry of the 2D axis-symmetrical vertical flow domain in Hydrus 2D. Horizontal and vertical transects and their symbols correspond to the water and solute profile plots in Figure 5-8 and Figure 5-9.

### Simulating Line Source Infiltration of Water and Nitrate

To simulate  $\text{NO}_3^-$  distribution in the field experiment, a flow domain representing a cross section of half a soil mound was produced in a 2D vertical plane flow geometry (Figure 5-5A). The FE mesh of the flow domain was set to 3 cm with FE mesh refinement to 0.5 cm around the flux area. No flux was allowed through the boundaries on either side of the flow domain since any contact with the edge was considered to be mirrored by the other mound half or the adjacent mound. The infiltration source was set as a variable flux so water applications could be controlled according to the leaching applications applied in the field. To simulate water distribution, a deeper 200 cm profile was used with the same boundary and flux conditions.

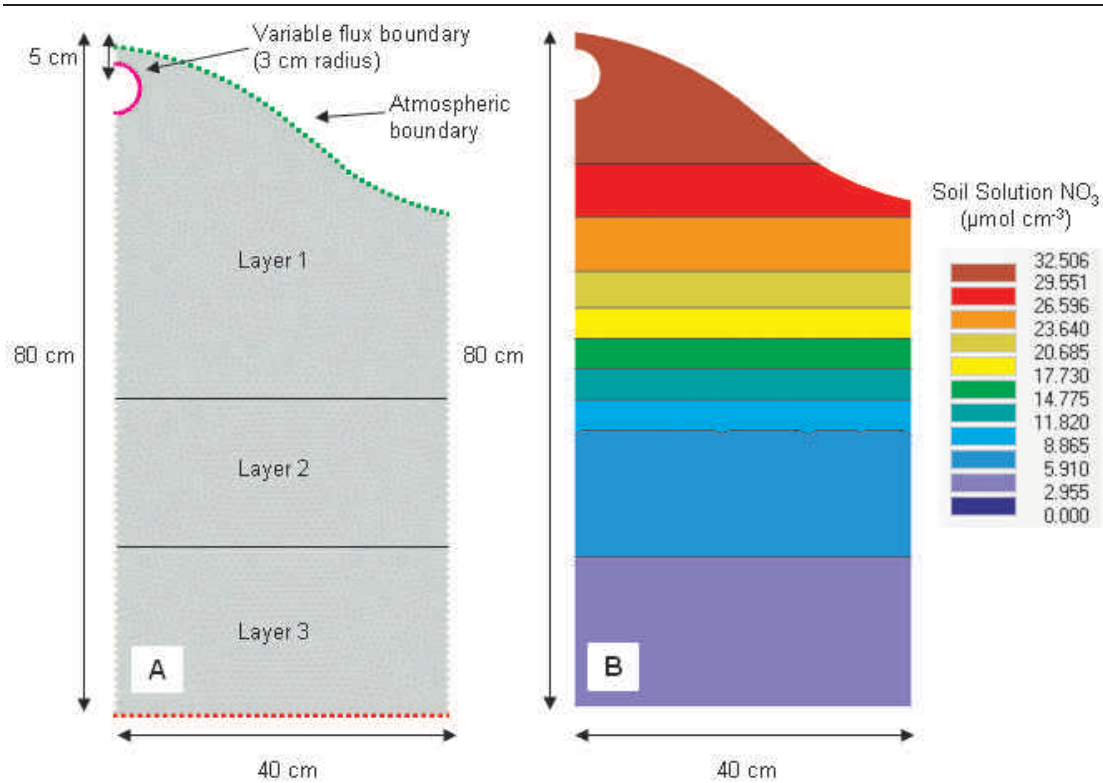


**Figure 5-5:** Boundary and initial concentrations in the soil. Chart A shows the variable flux boundary (purple area) applied to simulate the dripper application and the atmospheric boundary (green area) for simulation of overhead irrigation. Chart B shows the initial soil solution concentration prior to any leaching. The initial soil solution  $\text{NO}_3^-$  concentrations ( $\mu\text{mol cm}^{-3}$ ) were based on the untreated control from the field experiment measured directly below the drip tape.

The initial soil water content was set to  $0.35 \text{ cm}^3 \text{ cm}^{-3}$  and the initial soil solution  $\text{NO}_3^-$  concentrations ( $\mu\text{mol cm}^{-3}$ ) based on the untreated control from the field experiment measured directly below the drip tape (Figure 5-5B). Total  $\text{NO}_3^-$  concentrations measured in the KCl extract (Figure 3-2) were converted to solution concentrations using equation (4-30) from Chapter 4.

Water redistribution from individual drippers was assumed to overlap 60 minutes after the commencement of irrigation based on measurements in the wedge experiments. The assumption of a line source has also been used by other authors (Gardenas *et al.* 2005; Skaggs *et al.* 2004). Application from the drip tape in the field can therefore be approximated by a line source with a radius of 3 cm and a flux of  $3.18 \text{ cm hr}^{-1}$  calculated using equation 5-1:

$$\sigma = \frac{Q}{2\pi rx}, \quad 5-2$$

where  $\sigma$  is the flux from the surface of the source ( $\text{cm hr}^{-1}$ ),  $Q$  is the total volumetric flux ( $\text{cm}^3 \text{ hr}^{-1}$ )  $r$  is the radius of the spherical source (cm) and  $x$  is the distance between each dripper (cm). Overhead sprinkler irrigation applications were simulated by applying an atmospheric boundary condition to the mound surface. A precipitation event was then simulated over the surface at an application rate of  $2.5 \text{ cm hr}^{-1}$  (equivalent to  $25 \text{ mm hr}^{-1}$ ).

Applications of water to compare with field measurement involved a 3.5 hour initial application followed two one hour applications two and four days after the initial leach application and then three days redistribution. For all other simulations water application scenarios were run as continuous applications for 48 hours with print times every 30 minutes to monitor the distribution of  $\text{NO}_3^-$  over time.

No solute boundary conditions were applied to the flow domain since no solute was applied in the field simulations. To observe the effect adsorption on the distribution of  $\text{NO}_3^-$  already present in the soil, the reaction parameters determined in Chapter 4 were included in the model.

### *Accounting for Bulk Density Changes in the Profile with Rosetta*

The parameters obtained using inverse optimisation described flow in the Red Ferrosol at a soil bulk density near unity. However the field soil density varied from  $0.84 \text{ g cm}^{-3}$  in the surface to  $1.20 \text{ g cm}^{-3}$  at 100 cm (Table 5-2).

**Table 5-2:** Bulk density of the Red Ferrosol soil profile measure in the field.

Depth (cm)	$\rho \text{ (g cm}^{-3}\text{)}$	Standard Deviation
0-20	0.81	0.14
20-40	1.00	0.04
40-60	1.11	0.18
60-80	1.13	0.26
80-100	1.22	0.31

The surface (0-20 cm) bulk density of  $0.85 \text{ g cm}^{-3}$  was expected to settle to approximately  $1.0 \text{ g cm}^{-3}$  over the season which matches previously measured bulk densities under cultivated Red Ferrosol's (Sparrow *et al.* 1999). Bulk density in the

20-40 cm depth was  $1.00 \text{ g cm}^{-3}$  and therefore the parameters fitted by inverse modelling, at a bulk density of  $1.03 \text{ g cm}^{-3}$ , were used in the upper 40 cm of the profile.

To estimate soil hydraulic properties at the higher bulk densities, the Rosetta pedo transfer function model (Schaap *et al.* 2001) was used. The soil particle size measurements after the dithionate leach (Table 3-7) and moisture retention at -33 and -1500 kPa, were used along with the bulk densities to estimate soil hydraulic parameters below 40 cm in the profile.

The solute flow domain shown in Figure 5-5A was then divided into three soil layers and the parameters for the corresponding bulk densities were applied to each section. To simulate the water flow deeper in the profile a fourth section was added to the flow domain and parameters were estimated from 80-200 cm at a bulk density of  $1.22 \text{ g cm}^{-3}$  and measured particle size analysis from the 40-80 cm depth. No measurements were made below this depth.

### ***Simulations in a Sandy Soil***

Simulations were also conducted on a sand soil. The only variation in the model for these simulations were changes to the soil hydraulic properties to those for a typical sand described by Carsel and Parrish (1988;  $\theta_r = 0.05 \text{ cm}^3 \text{ cm}^{-3}$ ,  $\theta_s = 0.43 \text{ cm}^3 \text{ cm}^{-3}$ ,  $\alpha = 0.145 \text{ cm}^{-1}$ ,  $n = 2.68$ ,  $K_{sat} = 29.7 \text{ cm hr}^{-1}$  and  $l = 0.5$ ) and changing the initial water content to  $0.15 \text{ cm}^3 \text{ cm}^{-3}$  due to the lower water holding capacity of the soil. The mean bulk density was  $1.49 \text{ g cm}^{-3}$  (Rawls *et al.* 1982).

### **Statistical Analysis**

The root mean square error (RMSE) was calculated to determine the error between the measured and simulated water content and  $\text{NO}_3^-$  concentrations. Comparisons of the RMSE values with predictions from different parameter sets allow parameters sets that produced the lowest errors to be identified. Comparisons of simulated RMSE values with those calculated from measured data allow the significance of the model error to be assessed in relation to measurement error. This method has been commonly used to measure the quality of model predictions in previous studies (Ajadary *et al.* 2007; Arbat *et al.* 2008; Patel and Rajput 2008; Skaggs *et al.* 2004).

## RESULTS

### Model Validation: Horizontal Absorption

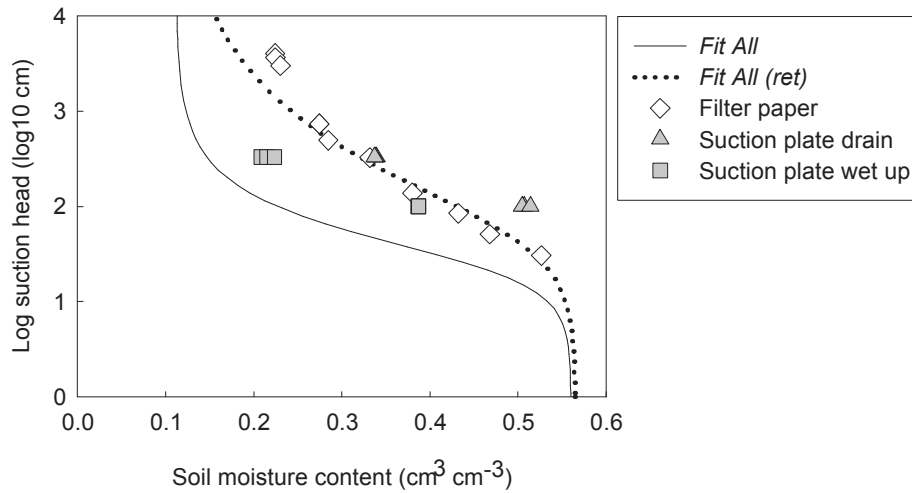
Table 5-3 shows the *Fit All* and *Fit All (ret)* soil hydraulic parameters which were fitted to the horizontal absorption data using inverse optimisation (Table 5-1). These particular parameter sets were selected because of their low objective function values and their fit to the measured horizontal and wedge column data. Confidence intervals of the *Fit All (ret)* parameters, which also included the soil moisture retention parameters in the inverse optimisation, were lower for most parameters in comparison to the *Fit All* scenario. The value of the sum of squares of the objective function, describing the goodness of fit to the measured data, was also lower in the *Fit All (ret)* parameter set (0.008 versus 0.014). However previous objective values of 0.152 and 0.073 were reported for by Simunek *et al.* (2000) for two soils using data from very similar absorption columns and therefore both the parameter sets in this study are considered to fit the measured data well.

Figure 5-6 shows the moisture retention curves for the two parameters sets plotted against the measured soil moisture retention data. The *Fit All (ret)* parameters matched the measured values more closely than the *Fit All* parameters. A better fit by the *Fit All (ret)* was expected because they were directly fitted to the retention data during inverse optimisation. The better fit to these parameters suggests that the *Fit All (ret)* parameters may be more physically realistic.

To determine which parameter set was most appropriate for describing water and  $\text{NO}_3^-$  flow both parameter sets were compared with horizontal column data not included in the inverse optimisation and independently measured data from the point source wedge experiments.

**Table 5-3:** Parameter estimation results for the best inverse parameters. Values in parentheses indicate the 95 % confidence intervals of the fitted parameters

Inverse scenarios	$\theta_r$ ( $\text{cm}^3 \text{ cm}^{-3}$ )	$\theta_s$ ( $\text{cm}^3 \text{ cm}^{-3}$ )	$\alpha$ ( $\text{cm}^{-1}$ )	$n$	$K_{sat}$ ( $\text{cm min}^{-1}$ )	$l$
<i>Fit All</i>	0.112 (0.247)	0.560 (0.007)	0.036 (0.006)	2.030 (0.684)	0.115 (0.061)	3.847 (5.442)
<i>Fit All (ret)</i>	0.100 (0.027)	0.565 (0.011)	0.018 (0.003)	1.408 (0.072)	0.127 (0.052)	2.956 (2.967)



**Figure 5-6:** The moisture retention curves of the *Fit All* and *Fit All (ret)* parameters sets plotted against the measured soil moisture retention data.

Predictions of water distribution after absorption of solute into the horizontal columns using the two parameter sets are shown in Figure 5-7A. To simplify the charts, the profiles were plotted against the Boltzmann variable  $X$  ( $\text{cm s}^{-1/2}$ ) because the data converges using this transformation (see Chapter 4). Water profile simulations are compared with the water content profiles from Part B of Chapter 4 which were not included in the optimisation. The *Fit All* parameter showed slightly lower RMSE values than the *Fit All (ret)* parameters set when tested against data that was not used for the inverse parametisation (Table 5-4) however differences between the simulations were very small (Figure 5-7A). A good fit to the water profile data was expected because the analysis between the fitted data (Part A columns) and independent data (Part B columns) in Chapter 4 showed that they were not statistically different ( $P < 0.05$ ).

Predictions of  $\text{NO}_3^-$  distribution after solute absorption by the columns are shown in Figure 5-7B. The chart was simplified by presenting the predicted solute distribution for a single infiltration time of 70 minutes. Although the profiles converge when plotted against the Boltzmann variable, and the solute fronts converge for all infiltration times, the shape of the solute front steepens with time. The fit of the predicted and measured data is therefore better than what Figure 5-7A indicates for some of the data points. This is demonstrated by the low RMSE values in Table 5-4.

As for the water profile data the *Fit All* parameters again provided a slightly better description of the  $\text{NO}_3^-$  profiles according to the RMSE calculations when the  $\text{NO}_3^-$

---

reaction parameters included in all simulations (Table 5-4) however the fit of the two parameter sets is indistinguishable in Figure 5-7B. The RMSE values indicated that the simulated error was slightly higher than the measured error using both parameters sets, however they still show a good fit to the data when the Langmuir isotherm parameters were included in the simulations ( $R^2=0.97$ ; Table 5-4). These results indicated that inverse optimisation produced parameters that described horizontal absorption of water and  $\text{NO}_3^-$  well in the soil and also indicated that inclusion of the soil moisture retention data in the inverse optimisation did not improve the fit to horizontal column data.

Because both the *Fit All* and *Fit All (ret)* parameters sets offered very good predictions of water and solute distribution under horizontal absorption they were both used to predict water and solute distribution in the three dimensional soil wedge experiments which offered an independent test of the parameters in an alternative flow scenario to what was used for the inverse parametisation.

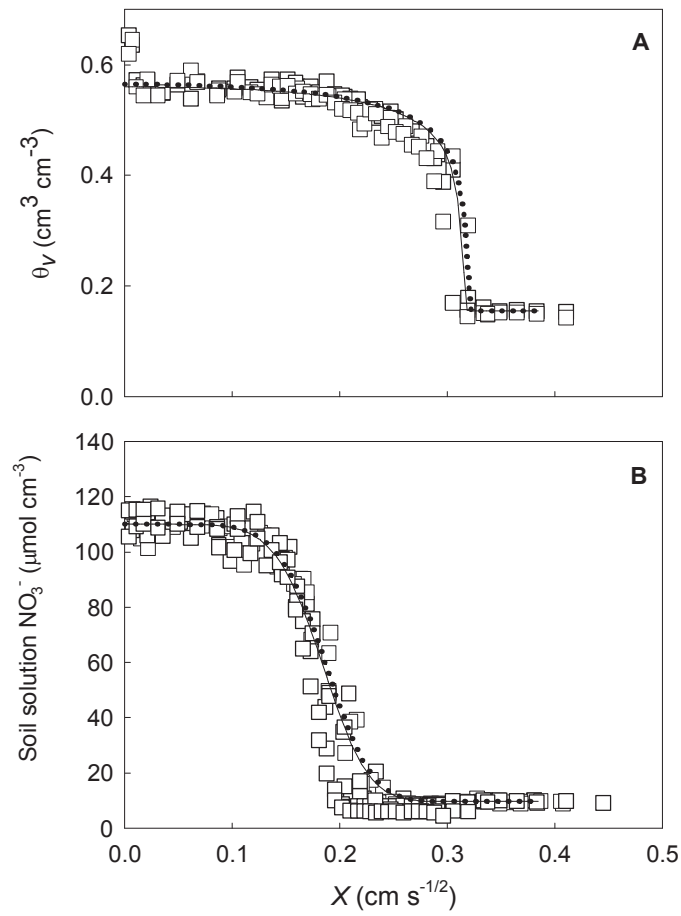


**Figure 5-7:** Fit of *Fit All* (solid line) and *Fit All (ret)* (dotted line) parameters to the measured water profile data (square symbols) from columns in Part B of Chapter 4 not included in the inverse parametisation (Figure A) and soil solution  $\text{NO}_3^-$  data from all horizontal columns from Chapter 4 (square symbols; Figure B). The soil hydraulic properties were fitted to the water contents of column from Part A in Chapter 4 and were therefore not included in the figures. The predicted lines are from a single infiltration time (70 minutes).



**Table 5-4:** Root mean square error (RMSE) of the fit of the predicted water and  $\text{NO}_3^-$  profiles in comparison to the measured data in the horizontal column experiments presented in Figure 5-7 using the *Fit All* and *Fit All (ret)* parameter sets. The “measured” RMSE values in the table indicate the variation in the measured data calculated from the columns from Part B of Chapter 4 where two  $\text{NO}_3^-$  and water measurements were made at identical points in the columns.

Parameters	$\theta_v$ ( $\text{cm}^3 \text{ cm}^{-3}$ )		$\text{NO}_3^-$ ( $\mu\text{mol}_c \text{ cm}^{-3} \text{ soln}$ )	
	RMSE	$R^2$	RMSE	$R^2$
<i>Fit All</i>	0.02	0.89	7.02	0.97
<i>Fit All (ret)</i>	0.03	0.90	7.60	0.97
Measured	0.04		6.19	

### Model Validation: 3D Wedge Infiltration

Figure 5-8 and Figure 5-9 show the measured and predicted water and  $\text{NO}_3^-$  profiles for the wedge experiments at a number of horizontal and vertical transects (Figure 5-4) after the two irrigation scenarios (Figure 5-2) using the *Fit All* and *Fit All (ret)* parameters. Comparisons of the fits indicated that the *Fit All* parameters produced the best predictions of water distribution in the wedge data. This is most evident in Figure 5-8G and H which shows better prediction of vertical infiltration with the *Fit All* parameters. This result is confirmed by the lower RMSE and  $R^2$  values which describe the accuracy of the predictions from the two parameter sets in comparison to the measured data (Table 5-5).

The inverse procedure was optimised using the horizontal column data and therefore the fitted parameters were not fitted to flow conditions influenced by gravity. This may explain why vertical displacement was underestimated by the *Fit All (ret)* parameters in the wedge columns but does not explain why the *Fit All* parameters were more appropriate.

The poorer fit using the *Fit All (ret)* parameters was unexpected because increasing the range of measurement types in the inverse optimisation should increase the reliability of the parameters (Hopmans *et al.* 2002). However this is only valid if the data included is appropriate for the flow conditions under which the parameters are being optimised. The majority of the measured retention points shown in Figure 5-6

describe water retention under drainage from higher water content. However the horizontal column and wedge experiments represent water flow under wetting up conditions (hysteresis). Including the water retention data in the optimisations may have therefore adjusted parameters for a retention curve biased towards retention under drainage and as a result may have decreased their suitability. Figure 5-6 provides some evidence for this with the *Fit All* parameter curve being closer to the wet up water content values at the 330 kPa tension measurement ( $\log=2.5$ ) in comparison the *Fit All (ret)* curve. Furthermore comparisons between the suction plate data that was equilibrated by wetting up or drainage showed the water contents were different and therefore this provides further evidence that the moisture retention curve may not have been appropriate for the wetting up conditions.

As shown above, the *Fit All* data indicated greater vertical infiltration than the *Fit All (ret)* parameters (Figure 5-8G and H). Comparisons of the retention curves in Figure 5-6 indicate water will drain from the soil at a lower tension if the *Fit All* parameters are used. Therefore, due to the influence of gravity, water flow based on the *Fit All* parameters will lead to greater vertical movement in comparison to the *Fit All (ret)* parameters. This suggests that the measured moisture retention curve does not provide the most appropriate data for prediction of soil hydraulic parameters under these soil wedge flow scenarios.

Mean bulk density in the horizontal absorption columns was  $1.03 \text{ g cm}^{-3}$  and soil used in the retention curve measurements was also packed to a bulk density of  $1.0 \text{ g cm}^{-3}$ . However the mean wedge bulk density of the wedge columns was  $0.95 \text{ g cm}^{-3}$ . As a result the pore size distribution may have been different in these experiments and this may have influenced the moisture retention of the soil. By including the soil moisture retention data, measured at a bulk density of  $1.0 \text{ g cm}^{-3}$ , in the optimisation the parameters may have been optimised for a retention curve that was not ideal for describing conditions for the lower bulk density wedge experiments. This may also explain the better fit using the *Fit All* parameters that did not include the soil moisture retention data.

For the purpose of describing water flow in the Red Ferrosol soil the *Fit All* parameters were most appropriate because they showed a better fit to both the column and independently measured wedge data (Figure 5-7A and Figure 5-8). Because the majority of the moisture retention measurements were determined under drainage

rather than wetting up conditions these measurements may not provide a suitable description of water retention for the experimental conditions of the laboratory column and wedge studies. The *Fit All* parameters were therefore used in combination with the  $\text{NO}_3^-$  reaction parameters, to predict water and  $\text{NO}_3^-$  distribution in a simulated field environment.

**Table 5-5:** Root mean square error (RMSE) of the fit of the two parameter sets used to predict water and  $\text{NO}_3^-$  distribution in the wedge experiments. The “measured” RMSE values in the table indicate the variation in the measured data calculated from the wedge experiments from Irrigation Scenario B columns where two  $\text{NO}_3^-$  and water measurements were made at identical points in the wedges.

Parameters	Irrigation treatment	$\theta_v$ ( $\text{cm}^3 \text{ cm}^{-3}$ )		$\text{NO}_3^-$ ( $\mu\text{mol}_c \text{ cm}^{-3} \text{ soln}$ )	
		RMSE	$R^2$	RMSE	$R^2$
<i>Fit All</i>	Scenario A	0.04	0.94	2.40	0.95
	Scenario B	0.03	0.93	3.85	0.81
<i>Fit All (ret)</i>	Scenario A	0.07	0.80	4.20	0.77
	Scenario B	0.07	0.75	4.41	0.61
Measured		0.03		2.64	

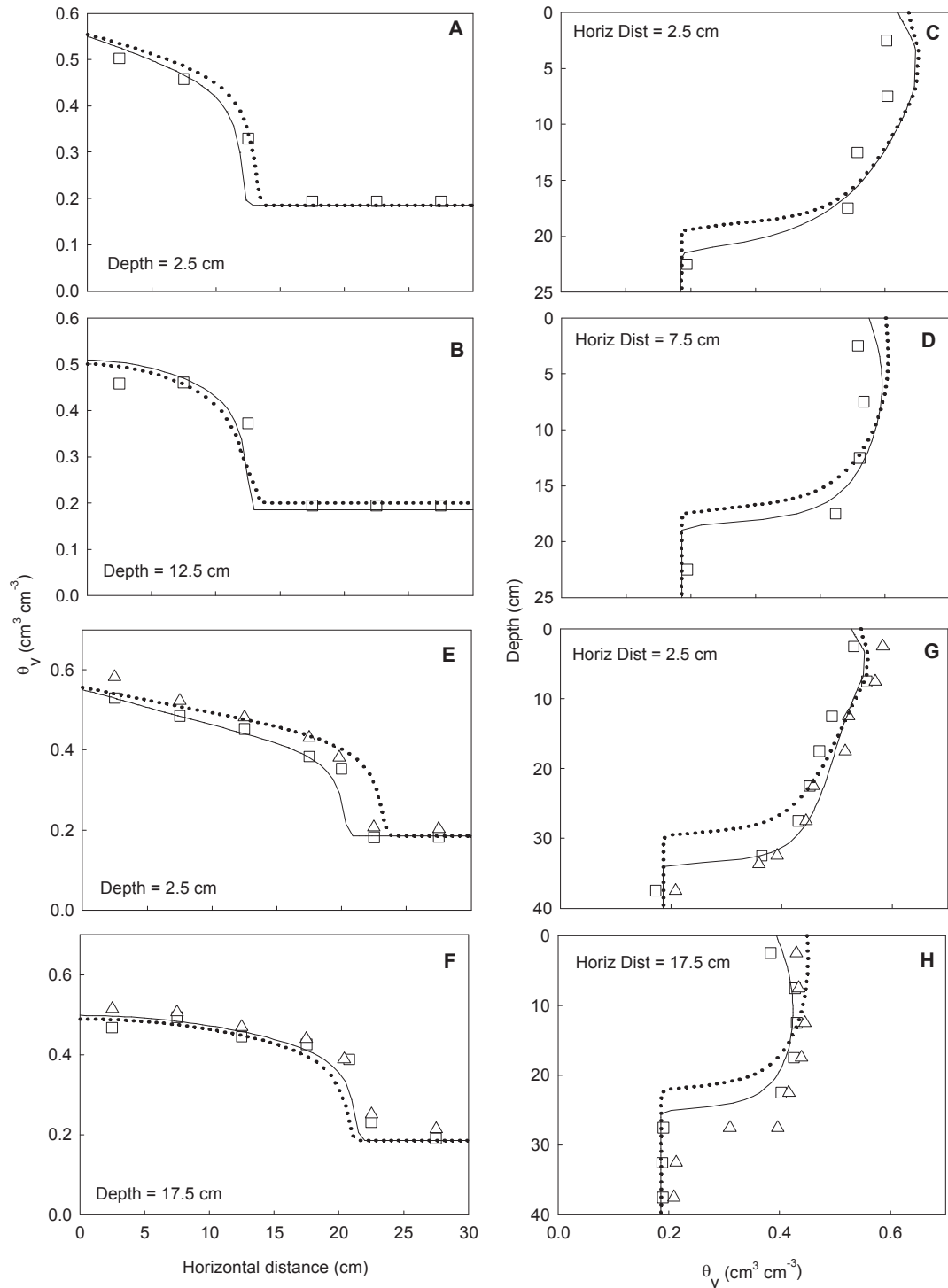


**Figure 5-8:** Horizontal and vertical transects of water content ( $\text{cm}^3 \text{cm}^{-3}$ ) in the wedge columns. The symbols indicate measured points, the solid line represents simulations using the *Fit All* inverse parameters and the dotted line represents simulations using the *Fit All (ret)* parameters. Figures A to D show transects from irrigation scenario A (2hr experiment; Figure 5-2) and figures E to G; transects from irrigation scenario B (24hr experiment; Figure 5-2). The location of these transects is shown in Figure 5-4.

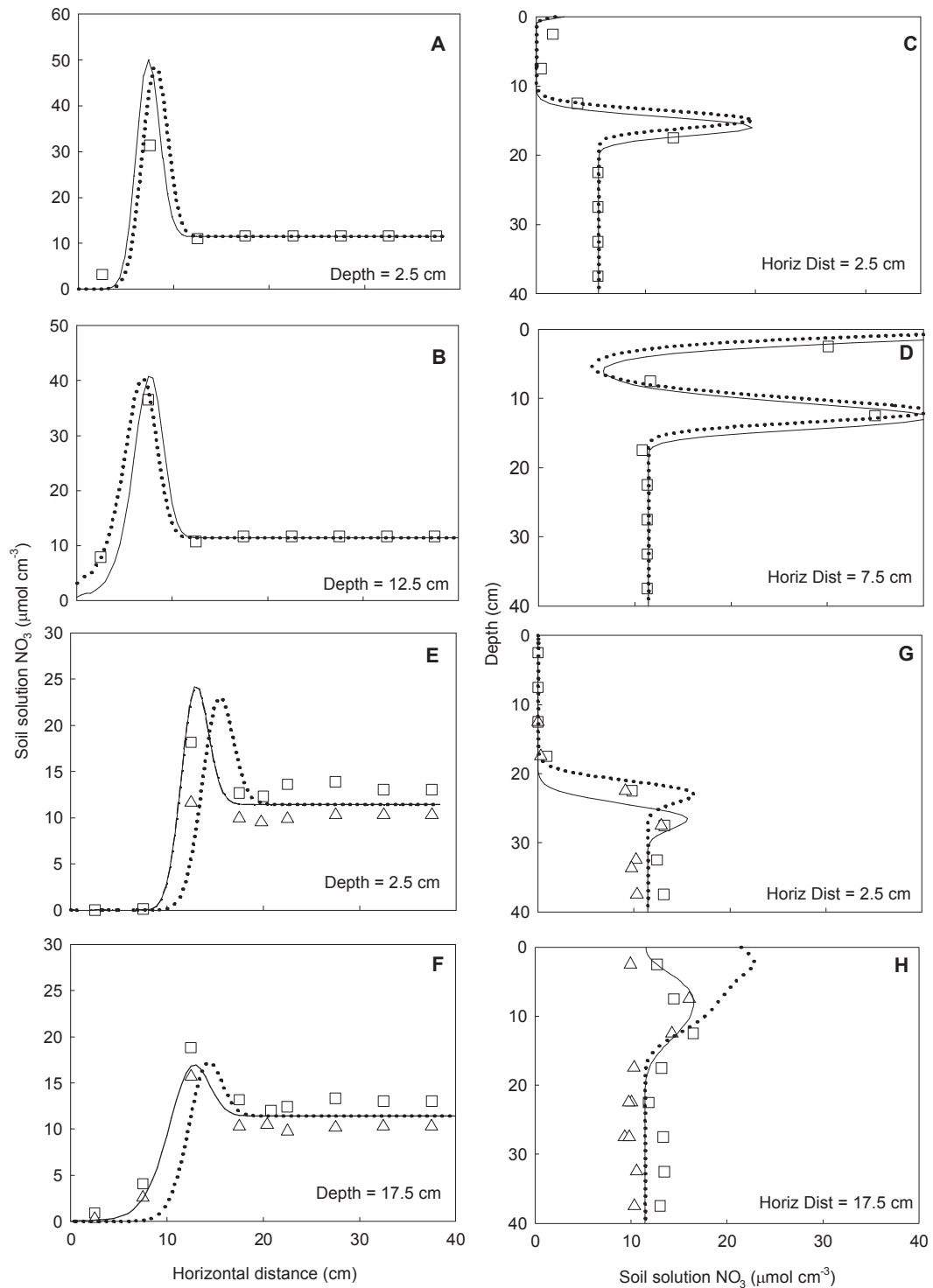


**Figure 5-9:** Horizontal and vertical transects of soil solution  $\text{NO}_3^-$  concentration ( $\mu\text{mol}_e \text{cm}^{-3}$ ) in the wedge columns. The symbols indicate measured points, the solid line represents simulations using the *Fit All* parameters and the dotted line represents simulations with the *Fit All (ret)* parameters. The  $\text{NO}_3^-$  reaction parameters were included in all the simulations. Figures A to D show transects from irrigation scenario A (2hr experiment; Figure 5-2) and figures E to G; transects from irrigation scenario B (24hr experiment; Figure 5-2). The location of these transects is shown in Figure 5-4.

### Simulating Nitrate Distribution in the Field

Figure 5-10 shows the measured and predicted vertical  $\text{NO}_3^-$  distribution under the mound centre in the N Leach and Control treatments. This figure indicates that concentration of  $\text{NO}_3^-$  in the 0-20 cm zone was reduced to close to zero in the simulation while field samples indicated that, although concentrations were significantly reduced in comparison to the Control in the 0-20 cm depth, concentrations of  $16.7 \mu\text{mol}_\text{c} \text{NO}_3^- \text{cm}^{-3}$  soil solution still remained in the soil. This result indicates that some caution is required when interpreting predictions under field conditions.

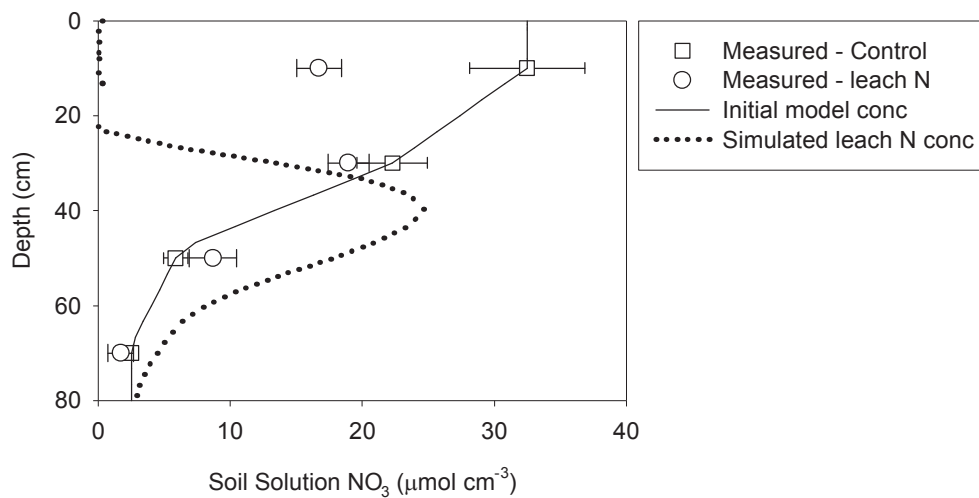


**Figure 5-10:** Vertical  $\text{NO}_3^-$  distribution both measured in the field trial and simulated in Hydrus. The leached data represents concentrations after the initial 26 mm application and two subsequent 7.5 mm applications over the following 7 days prior to assessment of  $\text{NO}_3^-$  concentrations (Table 5-3).

Nitrate concentrations were measured seven days after the leaching application, just before N supply was returned, and mineralisation and nitrification may have therefore produced some  $\text{NO}_3^-$  in the 0-20 cm depth during this time (Jansson and Persson 1982). Previously reported rates cannot account however for the majority of the  $\text{NO}_3^-$  present in the leached zone of the soil in the field measurement. *In situ* production of N from mineralisation from a site nearby the field trial was  $5.1 \mu\text{mol}_\text{c} \text{N g}^{-1} \text{soil}$  in the upper 10 cm of the profile over 140 days during a time of year very similar to that of the potato growing season (Wang *et al.* 1996). This amount of N produced was

---

equivalent to a mean production rate of  $0.04 \mu\text{mol}_c \text{ N g}^{-1} \text{ soil day}^{-1}$ . Although the mineralisation rates of Wang *et al.* (1996) were measured in soils of establishing forests rather than in an irrigated crop, studies on different soil types under pasture and cropping systems have also reported mineralization levels in the same order of magnitude (Angus *et al.* 2006; Powlson 1980). As a result, the rate of production reported by Wang *et al.* (1996) is considered an acceptable approximation of mineralisation in the field soil. Based on these previous findings, even if  $\text{NO}_3^-$  production was an order of magnitude higher than previously reported, production due to mineralisation is unlikely to account for the  $16.7 \mu\text{mol}_c \text{ NO}_3^- \text{ cm}^{-3}$  soil solution (equivalent to  $8.8 \mu\text{mol}_c \text{ N g}^{-1}$ ) remaining in the 0-20 cm depth.

Accumulation of  $\text{NO}_3^-$  near the soil surface may explain the discrepancy between the modelled and measure values in the 0-20 cm depth. Accumulation of solutes at the soil surface has been reported in other studies (Fritton *et al.* 1967; Hassan and Ghaibeh 1977; Nakayama *et al.* 1973). Subsurface drip irrigation can further increase this accumulation because of the upward movement of water from the drip system pushes solute towards the surface (Roberts *et al.* 2009; Roberts *et al.* 2008). The intensity of soil sampling to confirm  $\text{NO}_3^-$  distribution in the soil mound was not sufficient to quantify whether significant accumulation had occurred in the surface in the filed study. Furthermore, frequent fertiliser applications were made through the drip system over the weeks between planting and the N Leach application. Consequently, there may have been accumulation of  $\text{NO}_3^-$  at the surface prior to soil sampling. If surface accumulation did occur then the high concentrations at the soil surface would masked the lower concentrations in the remainder of the soil around the drip line in the 0-20 cm soil sample after the application of the N Leach irrigation treatment.

Simulations of water and solute flow were made using a line source. This was done under the assumption that drip wetting fronts would overlap after approximately 60 minutes (based from the wetting pattern measured in the wedge experiments) and therefore after this time water flow would behave as if it was from a single line source. However Figure 5-9 shows that  $\text{NO}_3^-$  is displaced by the expanding water front and therefore some  $\text{NO}_3^-$  in the soil would also be displaced into the space between each drip as well as laterally into the inter-row space and as a result some  $\text{NO}_3^-$  will accumulate in the centre of the mound. Displacement from the centre of the

---

---

mound may therefore not be as efficient as indicated by the model and this may also explain the discrepancy between the predicted and measured  $\text{NO}_3^-$  concentrations.

The presence of preferential or bypass flow may have also accounted for some of the differences between the modelled and measured data. The presence of this flow scenario is a result of moving through larger pores and root channels, bypassing water and solute stored in smaller soil pores (Simunek and Genuchten 2008). This type of flow has been investigated in a number of previous modelling studies using Hydrus (Dousset *et al.* 2007; Haws *et al.* 2005; Kohne *et al.* 2005; Kohne *et al.* 2004; Simunek and Genuchten 2008; Ventrella *et al.* 2000). However with the very limited field data collected and good predictions of water flow in the laboratory studies, the mobile/immobile water flow scenarios were not investigated in this study.

Comparisons between the simulations and measured field data are limited due to the coarse sampling technique used in the field trial. However the model offered a useful tool to explore potential strategies for improving the N Leach treatment such as increasing water applications and investigating alternative water application methods.

Figure 5-11A and C show the distribution of water and  $\text{NO}_3^-$  after 120 mm of water was applied to the soil through a dripper system simulating conditions in the field. The effect of the increasing bulk density is shown in the water profile at the 40 cm depth where lateral movement of water is increased at the boundary where bulk density increased. The 120 mm water application is presented because, according to the simulations, it is the amount of water required to reduce  $\text{NO}_3^-$  to the desired concentration directly under the soil mound using the drip irrigation system.

Although leaching was adequate directly below the mound after 120 mm application the simulations indicated that  $\text{NO}_3^-$  was only displaced about 22 cm from the centre of the mound. Field observations indicated that roots extended up to 30 cm laterally (Figure 5-11B). Based on this observation, plant roots would most likely have access to significant amounts of  $\text{NO}_3^-$ . Simulations of water movement by Cote *et al.* (2003) indicated that reducing the application rate through the dripper system increased the horizontal infiltration of water. Reducing the application rate by a factor of four in the Red Ferrosol, however, only had a minor influence on the horizontal distribution of  $\text{NO}_3^-$  in the soil after the 120 mm of water application (data not shown) and as a

---

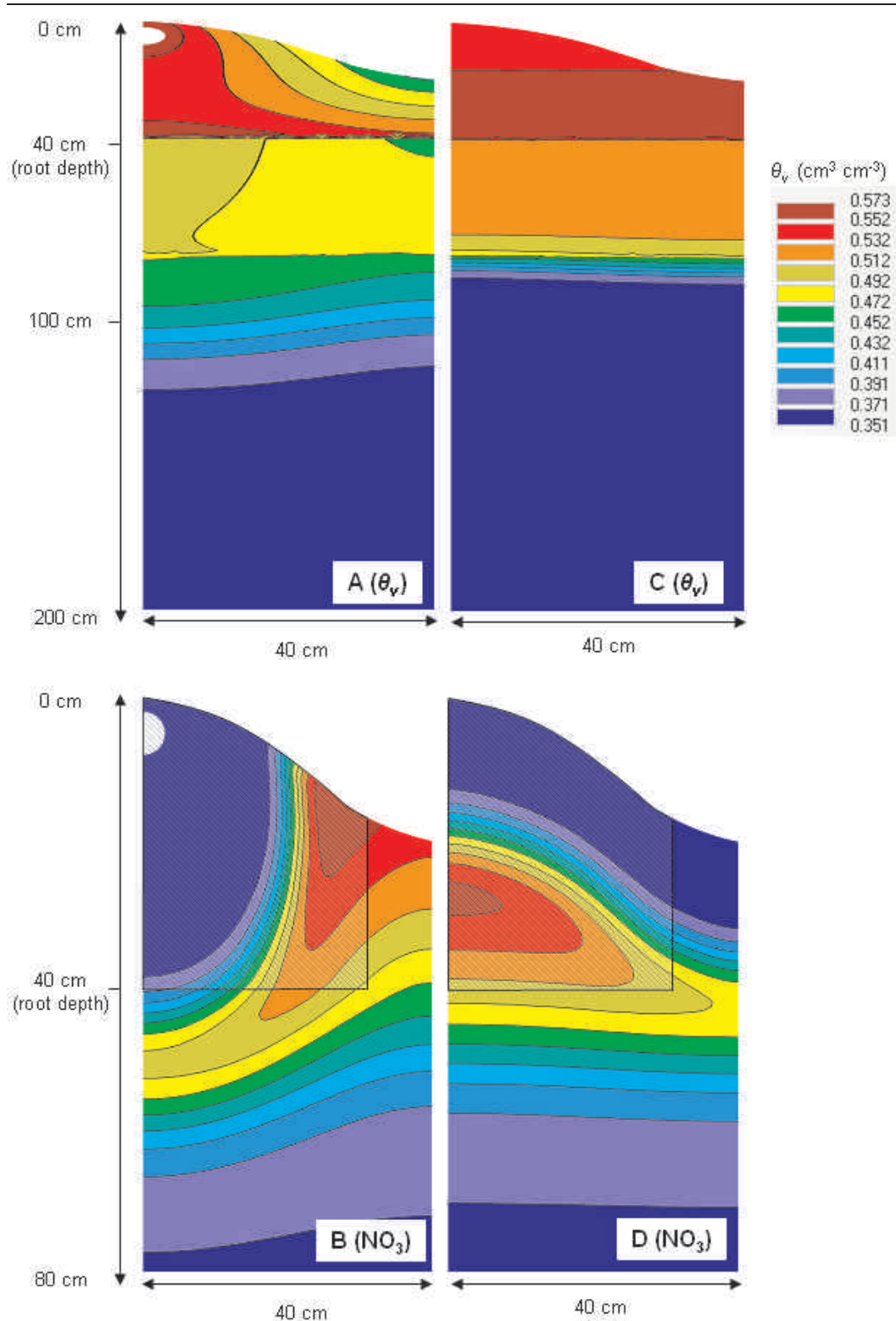


---

result was not considered an effective strategy for increasing horizontal displacement of  $\text{NO}_3^-$  in this soil. The predicted distribution pattern resulting from the drip irrigation system indicates that this irrigation method may not offer an effective strategy for reducing  $\text{NO}_3^-$  concentration in the root zone given the lateral distribution of plant roots in the soil.

Field experiment measurements indicated that lateral root distribution did not appear to extend greater than 30 cm into the inter-row space, however other studies on potatoes showed roots from opposite mounds overlapped (Stalham and Allen 2001). An alternative irrigation method that avoids horizontal displacement may therefore offer a more effective leaching strategy.

Figure 5-11D shows the effect of applying the equivalent 125 mm application through an overhead irrigation system. This indicates that an even water application across the surface results in one dimensional downward flow which avoids horizontal displacement of  $\text{NO}_3^-$ . Because water is applied over the whole soil surface rather than through a single point in the centre of the mound the depth of  $\text{NO}_3^-$  penetration is only 13 cm rather than the required 40cm (Figure 5-11B and C). Therefore if overhead irrigation is used to leach  $\text{NO}_3^-$  below 40 cm in the Red Ferrosol higher is required.



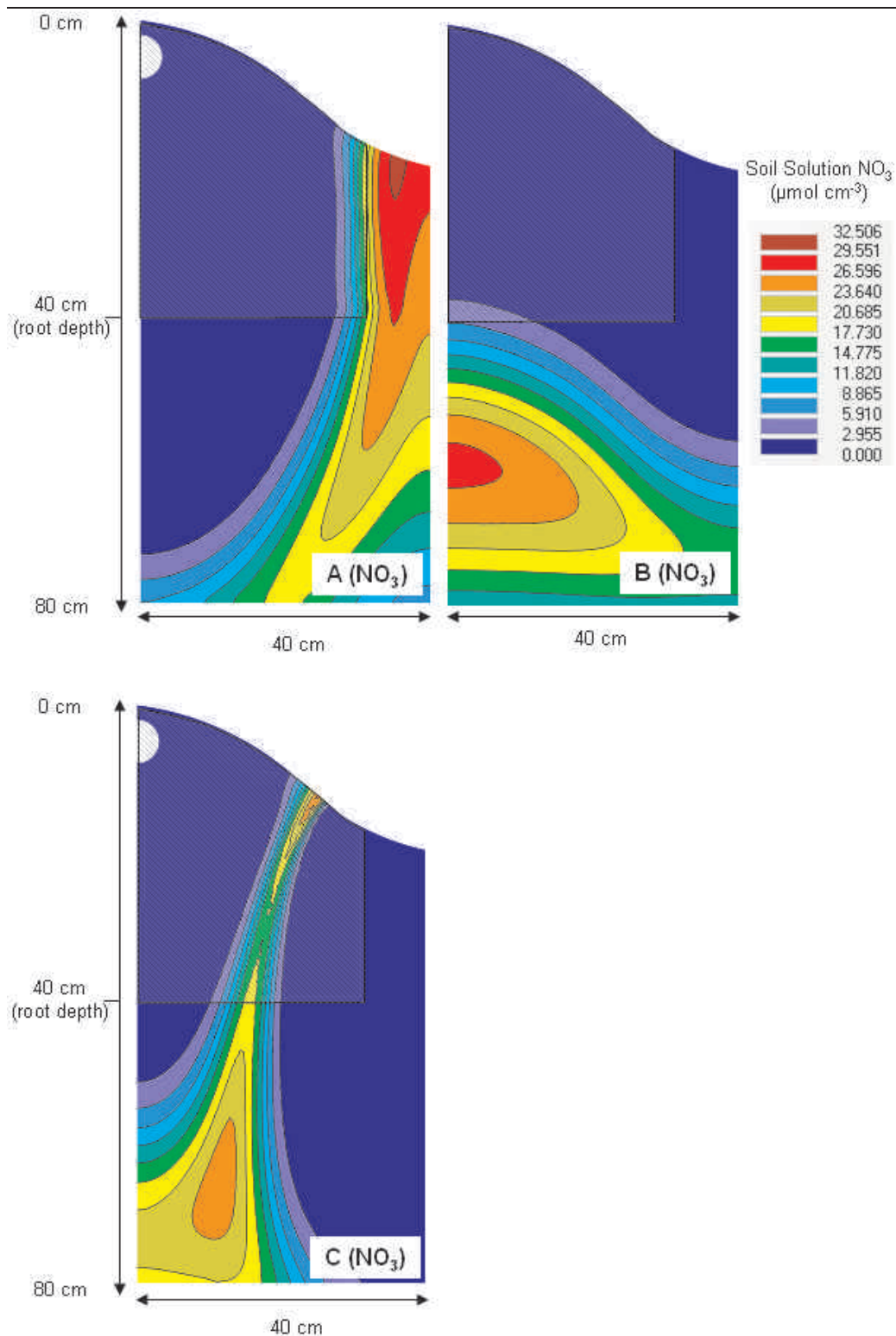
**Figure 5-11:** Simulated water and  $\text{NO}_3^-$  distribution in the Red Ferrosol from the field experiment after 120 mm of irrigation. Figure A and B show the simulated water and  $\text{NO}_3^-$  distribution through the drip system and Figure C and D show the simulated water and  $\text{NO}_3^-$  distribution through an overhead irrigation system after the equivalent water applications. The shaded area of the profile indicates the root zone estimated from field observations.

Figure 5-12B indicates that an application of 325 mm would be required to reduce soil solution  $\text{NO}_3^-$  concentrations to below  $8 \mu\text{mol}_\text{c} \text{ cm}^{-3}$  in the root zone of the field experiment using overhead irrigation according to model simulations. Overhead irrigation may therefore be an effective leaching strategy if this volume of water is applied since the downward leach pattern removes  $\text{NO}_3^-$  below 40 cm in the whole soil profile.

The equivalent volume applied through the drip system also reduced  $\text{NO}_3^-$  concentrations sufficiently based on the root zone measurements from the field experiment since lateral displacement reduced concentrations to less than  $8 \mu\text{mol}_\text{c} \text{ cm}^{-3}$  in the root zone (Figure 5-12A). Despite the greater lateral displacement after this extended irrigation,  $\text{NO}_3^-$  still accumulated in the upper soil layers at the edge of the wetting pattern in the inter-row space. Although roots were not observed in this area in the field experiment, they have been found to occupy this zone in previous studies (Stalham and Allen 2001). Furthermore, using the drip system from the field experiment, it would take over two days to apply this volume of water to the soil.

A third leaching strategy was also investigated in which a second drip line was placed in the inter-row space to see whether increasing drip line frequency across the soil would result in increased downward displacement of  $\text{NO}_3^-$ . Figure 5-12C shows the distribution pattern after the equivalent 325 mm application was made using this irrigation method. These simulations indicate that increasing dripper frequency did decrease the amount of  $\text{NO}_3^-$  in the soil surface however a result of the lateral displacement from the dripper in the inter-row space concentrated band of  $\text{NO}_3^-$  was actually pushed towards the centre of the mound. Therefore the placement of a second dripper in the mound centre still did not result in complete removal of  $\text{NO}_3^-$  from the root zone which was achieved using the overhead irrigation method using equivalent water volume applications.

Comparisons of equivalent water volume applications through these three irrigation scenarios indicated that overhead irrigation was the best method for leaching  $\text{NO}_3^-$  from the upper 40 cm of the soil horizon and out of reach of the plant roots.



**Figure 5-12:** Simulated  $\text{NO}_3^-$  distribution in the Red Ferrosol from the field experiment after 325 mm of irrigation through contrasting irrigation systems. Figure A shows the simulated  $\text{NO}_3^-$  distribution through the drip system, Figure B shows distribution using an overhead irrigation system and Figure C shows the distribution when a second drip line is placed on the soil surface in the inter-row space. The shaded area of the profile indicates the root zone estimated from field observations.

Seasonal water requirements for potatoes have been reported to be between 316 and 610 mm by Wolfe *et al.* (1983) and between 240 and 319 mm by Panigrahi *et al.* (2001). The 325 mm of water required to leach  $\text{NO}_3^-$  from the root in the Red Ferrosol according to the model is therefore equivalent to the total seasonal water requirements reported in these previous studies. As a result, this leaching treatment may be impractical on a commercial scale due to the volume of water required. One potential way to reduce the amount of water necessary to leach  $\text{NO}_3^-$  is to choose a site that does not contain an anion exchange capacity since adsorption of  $\text{NO}_3^-$  resulted in a 20% increase in the volume of water required in comparison to simulations without adsorption (data not shown). Also choosing a coarser textured soil with a lower water holding capacity may increase the rate of water movement and subsequent displacement of  $\text{NO}_3^-$  if the overhead irrigation system is used.

Using parameters for a typical sand described by Carsel and Parrish (1988), Figure 5-13B demonstrates that in a coarse textured sand with no  $\text{NO}_3^-$  adsorption the volume of water required to leach  $\text{NO}_3^-$  below the root zone using overhead irrigation was less than half that in the Red Ferrosol (125 mm versus 325 mm). This indicates that the choice of a coarser textured soil has the potential to significantly reduce the volume of water required to achieve the displacement of  $\text{NO}_3^-$  necessary.

Figure 5-13A shows the equivalent volume of water applied to the sand through the dripper system. This simulation indicated that in the coarser textured highly permeable sand, gravity had a greater influence on the pattern of water flow than in the light clay Red Ferrosol and as a result horizontal displacement was reduced in this soil. To attempt to increase horizontal displacement in the sand under drip irrigation the dripper output rate was decreased from 1200 to 400  $\text{cm}^3 \text{ hr}^{-1}$  in accordance to the recommendations of Cote *et al.* (2003; Figure 5-13C). Lowering the dripper rate did increase the horizontal displacement of  $\text{NO}_3^-$  in the sand, however high concentrations still remained in the root zone and inter-row space indicating that the dripper system was still inappropriate.

Figure 5-13D shows the effect of applying the same 125 mm water volume through a drip system with a second drip line placed in the inter-row space. As observed in the Red Ferrosol simulations, this method again resulted in a concentrated band being pushed into the root zone area by lateral water flow from the dripper in the inter-row space. Due to the reduced lateral displacement of  $\text{NO}_3^-$  in the sand the model

indicated that this leaching method was less appropriate in this soil in comparison to the Red Ferrosol an even larger concentrated band was pushed towards the soil mound in this soil. Comparisons between Figure 5-13D and Figure 5-12C are limited however since the volumes of water applied were based on the amount required to leach  $\text{NO}_3^-$  below 40 cm in the two soils based on overhead irrigation in the particular soil and the volumes applied were therefore different (125 versus 325 mm).

The accumulation of  $\text{NO}_3^-$  in a narrow band as a result of the interaction between the two drip lines shown in Figure 5-12C and Figure 5-13D for the two soils also indicates the potential pattern of  $\text{NO}_3^-$  distribution between drippers along the drip line as discussed above. If these narrow concentrated bands accumulate between each dripper along the row then the drip system will be even more ineffective than indicated by the simulations. This also further justifies the hypothesis that  $\text{NO}_3^-$  accumulation in the mound resulted in the higher  $\text{NO}_3^-$  measurements in the field in comparison to the model simulations in Figure 5-7.

Comparisons of three alternative leaching systems in two different soils clearly indicated that an overhead irrigation method for leaching  $\text{NO}_3^-$  from the root zone is the most suitable method because horizontal displacement of  $\text{NO}_3^-$  resulting in accumulation at the edge of the root zone and in the inter-row space is avoided. In contrast  $\text{NO}_3^-$  movement from an overhead irrigation system, assuming a uniform distribution across the soil surface, occurs dominantly downwards. Further, simulations using the alternative coarse textured sand indicated that the N Leach treatment may be achieved with a significantly lower water volume if soil type is considered during experimental design.



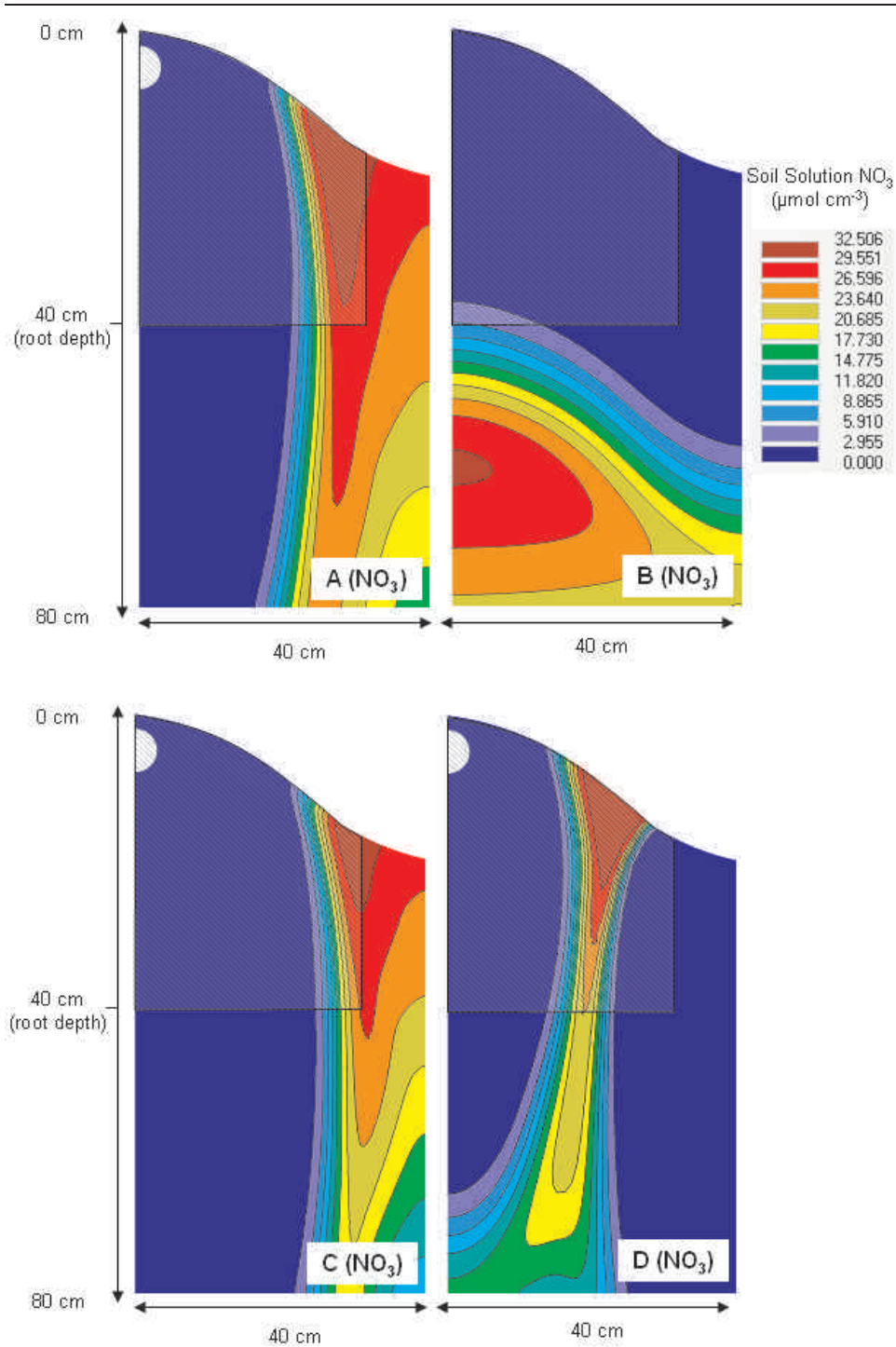


**Figure 5-13:** Simulated  $\text{NO}_3^-$  distribution in a contrasting sandy soil under conditions of the field experiment after 135 mm of irrigation. Figure A shows the simulated  $\text{NO}_3^-$  distribution through the drip system. Figure B shows the distribution after irrigation through an overhead irrigation system. Figure C shows the  $\text{NO}_3^-$  distribution after water application through the drip system at a rate of  $400 \text{ cm}^3 \text{ hr}^{-1}$  in comparison to  $1200 \text{ cm}^3 \text{ hr}^{-1}$  in Figure A. Figure D shows the  $\text{NO}_3^-$  distribution after water was applied through the buried drip line and a second drip line sitting on the soil surface in the inter-row space. The shaded area of the profile indicates the root zone estimated from field observations.

---

## DISCUSSION

### Model Validation

Inverse parametisation in Hydrus 1D produced soil hydraulic parameters that adequately described horizontal absorption and point source infiltration of water in the Red Ferrosol surface soil when used in Hydrus 2D/3D.

Inclusion of soil retention data in the inverse optimisation procedure along with the horizontal column data reduced the suitability of parameters for describing water infiltration from a point source. Twarakavi *et al.* (2008) showed that fitting soil hydraulic parameters to moisture retention data in the RETC model, which uses the same objective function as Hydrus (van Genuchten *et al.* 2005), without unsaturated hydraulic conductivity data can lead to an estimation of parameters that do not always describe hydraulic conductivity satisfactorily. However it was more likely that in this study the soil moisture retention curve measured under drainage type conditions may not have been appropriate for describing the wetting up conditions of the flow experiment due to hysteresis effects. Because there was some question of the suitability of the retention data, and the fact that the optimisations without this data described flow better in the wedge experiments, the parameters obtained from the inverse optimisations using only the horizontal column data were used to predict water flow in the field simulations.

Inverse optimisation had been previously used to estimate soil hydraulic parameters in Hydrus 1D by improving the N Leach treatment (2000) however parameters that adequately described adsorption of the fitted data were not tested against independently measured values or in a contrasting flow scenario. Sonnleitner *et al.* (2003) suggests that inverse parameterization can often produce parameters that will only be suitable for the flow scenario to which they were fitted. In some circumstances where parameters are estimated for a single purpose (Abbasi *et al.* 2003; Arbat *et al.* 2008; Simunek *et al.* 2000) it may be argued that the ability of the parameters to describe water movement in alternative flow scenarios is not important. However this study showed that parameters generated by inverse modelling in horizontal columns were able to simulate water movement from drip irrigation in a two dimensional field environment. This showed the potential of the model to estimate water and solute flow in the field under different irrigation scenarios.



---

Although flow of solutes that are adsorbed to soil exchange sites have been simulated under point source infiltration in previous studies using Hydrus 2D/3D (Hanson *et al.* 2006) validation under these flow scenarios has received little attention. Ben-Gal and Dudley (2003) stated that predictions of reactive P transport from a drip irrigation system showed a similar distribution to measured data but did not make any statistical comparisons between the predicted and measured concentrations. Reactive solute transport has been previously validated under other flow scenarios (Moradi *et al.* 2005; Persicani 1995) and non-reactive solute transport has been validated under drip irrigation (Ajdary *et al.* 2007; Li *et al.* 2005). The wedge experiments in this study showed reactive solute distribution from a point source in the Red Ferrosol soil. By including the  $\text{NO}_3^-$  reaction parameters with the soil hydraulic parameters the model accurately predicted solute distribution in the model. This finding confirms Hydrus is capable of describing reactive solute transport from a point source.

The infiltration area representing a drip emitter in the model had to be expanded to account for instability from the water flux exceeding the hydraulic conductivity of the soil. This was raised as a potential issue by Skaggs *et al.* (2004) however the soil used in his study did not cause difficulties in the model. Cote *et al.* (2003) also found the model became unstable when higher dripper output rates were used to model point source applications in a loam soil but did not investigate methods for overcoming this issue. Increasing the radius of the application point from 1 cm, used in previous studies (Cote *et al.* 2003; Skaggs *et al.* 2004), to 3 cm overcame the instability in the model and accurate predictions of water flow were achieved. This issue of infiltration exceeding the adsorption capacity of the soil needs to be considered carefully in situations such as subsurface water application where there is potential for flux to exceed the hydraulic conductivity of the soil.

When different initial estimates were used for parameters in some cases different parameters values were produced that still fitted the inverse data (data not shown). This indicated that soil hydraulic properties were non-identifiable using the inverse procedure (Hopmans *et al.* 2002). However the *Fit All* parameter set (Table 5-1 and Table 5-3) was considered appropriate for describing water flow in the Red Ferrosol because they were validated in both the horizontal columns and wedge experiments. Furthermore saturated water content and saturated hydraulic conductivity were determined in separate vertical laboratory columns for the Red Ferrosol so initial

---

---

estimates of these parameters were based on measured data. In some optimisations these parameters were set to their measured values (Table 5-1 ) however enabling their optimisation reduced the value of the objective function and improved the fit of simulations in both the horizontal column and wedge experiments without changing the initial values by more than 5%. Previous studies have often relied on initial guesses of parameter values rather than using measured values to improve the confidence optimised parameters (Abbasi *et al.* 2003; Arbat *et al.* 2008; Simunek *et al.* 2000) however knowledge of the correct values for saturated water content and saturated hydraulic conductivity increased confidence in the parameter estimates.

### Field Simulations

Validation of the model in column studies provided some confidence in its ability to predict water and solute flow in the Red Ferrosol under field conditions. However the model does not consider all factors that may have influenced  $\text{NO}_3^-$  distribution in this environment over extended periods of time.

For example, modelling in this study did not include  $\text{NO}_3^-$  production by mineralisation and nitrification or uptake by roots. As discussed above, production of N in the seven day period over which  $\text{NO}_3^-$  concentrations are to be reduced in the root zone likely to be in the order of  $0.04 \mu\text{mol}_e \text{ N g}^{-1} \text{ soil day}^{-1}$  and therefore unlikely to have a significant effect on nitrogen concentrations in the soil over this time. Maximum plant uptake by potatoes was estimated to be  $4.5 \text{ kg ha}^{-1} \text{ day}^{-1}$  by Li *et al.* (2006). Uptake over the entire growing season was reported to be up to 153 and  $250 \text{ kg N ha}^{-1}$  by Gayler *et al.* (2002) and Van Delden *et al.* (2003) respectively which is equivalent to a mean uptake of between  $0.9$  and  $2.3 \text{ kg ha}^{-1} \text{ day}^{-1}$ . These rates are likely to be higher during the rapid stages of plant growth because the uptake rate of potatoes is not uniform throughout the life of the crop (Li *et al.* 2006). An uptake rate of  $4.5 \text{ kg ha}^{-1} \text{ day}^{-1}$  is therefore considered a reasonable approximation during rapid growth stages such as at tuberization (when the N Leach treatment was applied). Assuming a uniform root distribution to a depth of 40 cm and lateral distribution of 30 cm, this uptake rate is equivalent to  $0.1 \mu\text{mol}_e \text{ g}^{-1}$  of soil  $\text{day}^{-1}$  in the root zone. The aim of the N Leach treatment was to reduce  $\text{NO}_3^-$  concentrations from up to  $16.9 \mu\text{mol}_e \text{ g}^{-1}$  soil ( $32.5 \mu\text{mol}_e \text{ cm}^{-3}$  soil solution) to levels less than  $5.6 \mu\text{mol}_e \text{ g}^{-1}$  soil using the extended irrigation treatment. Production of N due to mineralisation and

---

uptake by plants are therefore considered minor in terms of these large changes in  $\text{NO}_3^-$  concentrations that are only maintained for the short of 7 day period. The model can therefore be considered a reasonable approximation of  $\text{NO}_3^-$  dynamics in the field soil over a short period of time.

As mentioned previously preferential flow was not investigated in these studies and may explain why some  $\text{NO}_3^-$  remained in the top 20 cm of the soil. However with the very limited number of measurements it was not possible to calibrate the model to determine parameters for preferential flow. Furthermore the presence of immobile water was not the only factor likely to have lead to  $\text{NO}_3^-$  remaining in the upper 20 cm of the soil since mineralisation, accumulation at the soil surface and in between drippers within the mounds were also likely to have effected the efficiency of the leaching applications.

The model did not simulate movement of  $\text{NH}_4^+$  in the soil. Although there was no  $\text{NH}_4^+$  fertiliser applied, some accumulation did occur in the field soil presumably as a result of mineralisation (see Chapter 3). Measurements of  $\text{NH}_4^+$  in the field indicated that the N Leach treatment had no effect on its distribution as a result of strong adsorption to the soil in comparison to  $\text{NO}_3^-$ . This is in agreement with other studies that investigated movement of  $\text{NH}_4^+$  and  $\text{NO}_3^-$  through soils that did not contain anion adsorption (Clothier *et al.* 1988; Li *et al.* 2003). In simulations of N transport by Li *et al.* (2005),  $\text{NH}_4^+$  was not modelled because adsorption by the measurement used for validation indicated that cation exchange capacity limited any significant displacement. In this study  $\text{NO}_3^-$  was also adsorbed by the soil however the field measurements indicated that it was still much more mobile than the  $\text{NH}_4^+$ . Concentrations of  $\text{NO}_3^-$  were also significantly since it was the form of N applied to the experiment and therefore leaching of  $\text{NO}_3^-$  was the primary focus of the study. Due to its low mobility and the short simulation periods in this study  $\text{NH}_4^+$  was considered immobile and was not included in model simulations.

Anion adsorption was assumed to be uniform down the profile and including the adsorption parameters in the model increased the leaching volume required by 20%. However levels of organic carbon decreased in samples below 40 cm (Table 3-5) and the proportion of variable charge oxides increased with depth (Table 3-6). The level of  $\text{NO}_3^-$  adsorption is likely to increase with depth in the field as observed in previous studies (Black and Waring 1976c; Duwig *et al.* 2003). If this is the case the model

---

therefore may underestimate the volumes of water required to leach  $\text{NO}_3^-$  below the root zone in the Red Ferrosol. To determine if adsorption did increase down the profile measurements further adsorption isotherms using the method identified in Chapter 4 would need to be conducted in samples below 20 cm.

Because no validation was made with field measurements simulations under field conditions were only considered an estimate of water and  $\text{NO}_3^-$  distribution. However model predictions still provided a useful way for comparing  $\text{NO}_3^-$  distribution after different periods of irrigation and under different irrigations systems in contrasting soil types.

The predicted water and  $\text{NO}_3^-$  distribution patterns under the drip system were similar to observations from previous studies (Cote *et al.* 2003; Gardenas *et al.* 2005). Comparisons of drip and overhead irrigation methods have generally concluded that drip irrigation is more favourable because: i) applications are targeted directly to the root zone which reduces water volumes and nutrient applications required and; ii) leaching below the root zone is reduced due to the lower water volumes required and lateral and even upward distribution of water (Bernstein and Francois 1973; Cooley *et al.* 2007; Hanson 2003). Although the multi dimensional distribution patterns are favourable under a standard production system, they increased the difficulty of the N Leach treatment application in this study. The lateral displacement of  $\text{NO}_3^-$  in the soil which resulted in accumulation of  $\text{NO}_3^-$  in the inter-row space led to investigations of increased drip line frequency by placing a second line in the inter-row space, and simulation of the N leach application through an overhead irrigation system. The overhead application method was identified as the most appropriate system for leaching  $\text{NO}_3^-$  from the root zone due to the one dimensional vertical flow pattern from the even water distribution across the soil surface.

The greater vertical water and  $\text{NO}_3^-$  distribution predicted in the coarser textured sand under drip irrigation applications in comparison a finer textured soil such as the Red Ferrosol has also been previously observed (Cote *et al.* 2003; Gardenas *et al.* 2005). This has led to changes in recommended management practices such reducing drip application rates to increase the horizontal distribution of water in the soil and reduce its movement below the root zone (Cote *et al.* 2003). This approach was investigated for both soils in the simulations from thi study however lateral displacement was still

---

not increased sufficiently. Using a coarser textured soil did however decrease the volume required to leach  $\text{NO}_3^-$  below 40 cm using the overhead irrigation system.

Some of the difference between the leaching volume required between the Red Ferrosol and the sand was a result of the  $\text{NO}_3^-$  adsorption in the Red Ferrosol however the difference in moisture retention properties between the soils also played a significant role. The effect of anion adsorption on the movement of  $\text{NO}_3^-$  was discussed in detail in Chapter 4 and has also been shown by Black and Waring (1976c) and Katou *et al.* (1996). However even when the  $\text{NO}_3^-$  reaction parameters were not included in the simulation the leaching volume from overhead irrigation required in the Red Ferrosol was 260 mm (Figure not shown) in comparison to 135 mm in the coarse sand. The difference between the soils is related to their different moisture retentions and bulk densities. Hillel (1980) states that coarser textured sandy soils have macro-pores that only hold water near saturation or low tensions while soils with higher clay contents have many more meso-pores and micro-pores that hold water under higher tensions. The average clay content for the typical sand used in the Hydrus simulations was not reported by Carsel and Parrish (1988) or Rawls *et al.* (1982) however according to the USDA soil classification used to categorise soils in these studies, sands contain less than 10% clay (Sumner 1999). In comparison, the Red Ferrosol contained 33% clay. Thus, the water content at -33 kPa of tension, which is the notional field capacity of the soil after 2-3 days of drainage from saturation (McKenzie *et al.* 2002), was 9.1 % in the sand and 22.5% in Red Ferrosol. Furthermore the bulk density of the sand was  $1.49 \text{ g cm}^{-3}$  throughout the profile while the bulk density in the Red Ferrosol ranged from  $1.03\text{-}1.20 \text{ g cm}^{-3}$  and as a result the pore volume was lower in the sand. As a result the volume of water required to displace the antecedent water (and consequently the  $\text{NO}_3^-$  present in the solution) was less in the sand than the Red Ferrosol.

The potential risks of  $\text{NO}_3^-$  to leaching into waterways should be considered due to the nature of the N Leach treatment. Calculations of the total amount of  $\text{NO}_3^-$  based on the average concentrations between the mound centre and inter-row space measurements indicate that there was roughly  $370 \text{ kg NO}_3^- \text{ ha}^{-1}$  in the top 40 cm of the soil profile in the field experiment. The loss of  $\text{NO}_3^-$  below the root zone due to the leaching treatment would therefore be 370 kg based on the one hectare growing area. Previous estimates of  $\text{NO}_3^-$  leaching in standard ware potato crops were between 20

---

---

and  $190 \text{ kg ha}^{-1}$  over the growing season (Neeteson *et al.* 1989) which is significantly less than what would result from application of the N Leach treatment to the seed crop. However the area of land used for ware potato production is far higher than for first generation potato seed. In 2006/2007 approximately 35,000 hectares of potatoes were planted in Australia (AUSVEG 2008). One quarter of this production occurred in Tasmania (IRIS 2009) which is equivalent to 8,700 ha of potatoes crops in the state. As a result, even if leaching levels from these potato crops are as low as  $20 \text{ kg ha}^{-1}$  the total loss of  $\text{NO}_3^-$  under these crops would be  $1.74 \times 10^3 \text{ kg}$ . Therefore the 370 kg leached under the one hectare used for first generation seed production is considered insignificant in comparison to commercial crops.

## CONCLUSION

Good predictions of water distribution from a point source in wedge experiments were obtained from soil hydraulic parameters derived from water content profiles measured in horizontal absorption columns using inverse optimisation. By including reaction parameters for  $\text{NO}_3^-$  obtained from adsorption isotherm studies from Chapter 4,  $\text{NO}_3^-$  distribution was also described well by the model. These findings were interesting because parameters obtained from inverse optimisation are often not tested under alternative flow scenarios to which they are validated and suggest that simple column experiments have the potential to be used to determine parameters for modelling flow in more complicated scenarios.

The parameters obtained from the laboratory columns were used to predict water and  $\text{NO}_3^-$  distribution under conditions simulating the conditions of the field experiment. These simulations were not validated with measured data and therefore the model only offers an approximation of water and solute distribution in the field. However the field modelling demonstrated that Hydrus is a useful tool for exploring potential alternative scenarios to improve the N Leach treatment such as extended water applications and the use of different irrigation methods and alternative soil types.

To confirm the potential improvements in strategies for applying the N Leach treatment field validation of the model is required. Detailed field measurement of both water and  $\text{NO}_3^-$  distribution in the soil mound and inter-row space is necessary. Further measurements of adsorption in the Red Ferrosol below 20 cm are also required to confirm whether retardation of  $\text{NO}_3^-$  flow increases with depth because this would increase the volume of water required. The reduced water volumes necessary to apply the treatment in a coarser textured soil that does not contain an anion exchange capacity indicated by the model is also worth giving serious consideration if a treatment such as the one suggested in this study is to be used. Confirmation of the water volumes required in alternative soils would also however require some field measurements.



---

## CHAPTER 6

### DISCUSSION

First generation seed potato crops grown from minitubers are high value crops that generally occupy small field areas and thus provide a unique opportunity to intensively manage plant growth to improve production. Minitubers typically produce few tubers when they are planted in the field (Struik 2007a), which poses problems for growers as it limits yield in the first generation. Low tuber yield in the first field generation may also extend the number of field generations required to produce commercially viable numbers of seed tubers. Management of the problem has previously relied on manipulation of the physiological status, or physiological age, of minitubers prior to planting (Struik and Wiersema 1999), but this approach has limitations because the seed crop grower may not have control over timing of production of the minitubers. The ability to manipulate tuber number and size distribution in seed potato crops grown from minitubers through controlling nutrient availability during crop growth would add to and complement strategies based on manipulation of physiological age prior to planting.

Previous studies have shown there is potential to increase potato plant growth and yield through strategic control of nitrogen availability. The majority of these studies were conducted in hydroponics where maintaining high concentrations of  $\text{NO}_3^-$  was shown to delay and inhibit tuberization (Krauss 1978; 1980; 1985; Krauss and Marschner 1982). The applicability of these findings under field scenarios has been questioned by some authors (Ewing 1990; O'Brien *et al.* 1998) however few studies have investigated strategic manipulation of soil nitrogen concentration on potato plant development in soils.

Glasshouse pot experiments indicated that limiting  $\text{NO}_3^-$  supply from planting to tuberization restricted vegetative growth which reduced tuber set and lowered tuber yield. This response was consistent with previous conclusions that plants require sufficient nitrogen to produce optimum vegetative growth necessary to maximise tuber formation (O'Brien *et al.* 1998). However, maintaining nitrogen supply at a rate that promotes vegetative growth after tuber initiation may restrict tuber set and growth since high nitrogen supply has been previously linked to reduced assimilate partitioning to tubers in potatoes as well as storage organs in other plant species

---



(Kursanov 1984; Oparka *et al.* 1987). Previous work on the effects of nitrogen supply on tuber growth is limited. Oparka *et al.* (1987) did show larger proportions of assimilates were transported to tubers under low nitrogen conditions, however there have been no reports on the effects of strategically manipulating nitrogen supply to plants at key growth stages apart from in soil free hydroponics studies. In this study, a treatment capable of increasing tuber growth rate in a soil based system was developed. The treatment was based upon a balance between two key aspects: i) the importance of sufficient nitrogen supply in early growth to maximise light interception by the crop (O'Brien *et al.* 1998) and; ii) the risks of high nitrogen supply on reduced assimilate partitioning to tubers (Oparka *et al.* 1987). By maintaining adequate  $\text{NO}_3^-$  supply following planting, then leaching  $\text{NO}_3^-$  from the soil for a short period at the time of tuber initiation to reduce N availability, tuber growth rate was increased. It was concluded that the increased tuber growth rate achieved using this method had practical applications since this treatment could increase tuber yield, and potentially tuber number by reducing the likelihood of tuber resorption.

Further study on the effects of reducing  $\text{NO}_3^-$  supply to the plant on tuber growth rate is required to test the hypothesis proposed from this study that increased tuber growth rate will reduce the rates of resorption, particularly in a field environment. There is evidence that increasing tuber size may avoid resorption (Burstall *et al.* 1987) and therefore the leach N treatment applied in the glasshouse may provide a method for increasing the number of tubers retained on the plant. Furthermore, comparisons of tuber number shortly after tuberization with numbers at the final harvest in the field experiment indicated significant tuber resorption of 27-54% occurred in the three cultivars studied. This was similar to levels of 23-40% and 30-40% reported by Cho and Iritani (1983), and demonstrates there is scope for increasing the retention of tubers on plants in early generation seed crops.

The development of a field based treatment to reduce soil  $\text{NO}_3^-$  concentrations is significantly more complicated in comparison to the pot based glasshouse system due to differences in water flow from the irrigation system, larger plant root zones, and biological production of N. Nitrate concentrations were reduced in pots in the glasshouse experiment (12.67 to 4.19  $\mu\text{mol NO}_3^- \text{ cm}^{-3}$  soil) through prolonged irrigation which was sufficient to cause a significant tuber development response. Water movement in the pots was one dimensional and the root zone was restricted by

---

the boundaries of the 10 L pot. In contrast the root zone in the field experiment was distributed further both vertically and laterally with observations indicating that roots were concentrated in the upper 40 cm and lateral expansion was no greater than 30 cm. The field based leaching application failed to move  $\text{NO}_3^-$  below the root zone depth of 40 cm, only significantly reducing  $\text{NO}_3^-$  concentrations in the upper 20 cm of the soil profile in the zone directly under the soil mound. The inadequate displacements of  $\text{NO}_3^-$  in the field experiment highlighted the need to better understand water and  $\text{NO}_3^-$  movement in Red Ferrosol soil in order to develop appropriate crop management treatments.

The project identified three main processes that needed to be understood in order to develop an N manipulation treatment for improving potato production in a field environment. These processes were: i) water movement in the soil and its pattern of distribution under different irrigation systems; ii) reactions between  $\text{NO}_3^-$  and the soil if variable charge minerals are present; and iii) production of N due to biological activity.

Experiments in horizontal soil columns provided key data for understanding water and  $\text{NO}_3^-$  movement in the Red Ferrosol. A delay in the movement of  $\text{NO}_3^-$  through the column was identified by observing its distribution relative to the water. These experiments indicated the presence anion adsorption since the inflowing solute was found to be delayed in relation to the inflowing water (Katou *et al.* 1996). By using a water immiscible displacement method (Phillips and Bond 1989) to extract soil solution and adsorbed  $\text{NO}_3^-$  from the columns, and fitting the Langmuir equation to the data, a  $\text{NO}_3^-$  adsorption isotherm was determined for the soil.

Red Ferrosol's are known for their moderate anion exchange capacities (Isbell 1994) however the observation of adsorption in surface soils is uncommon. Black and Waring (1976c) investigated adsorption of  $\text{NO}_3^-$  in a different Red Ferrosol using column and batch experiments but only observed adsorption below 40 cm and no other detailed investigations of adsorption in Red Ferrosol surface soils have been reported. The presence of anion adsorption in the surface soil from this study was unexpected since organic carbon levels, which are negatively correlated with anion adsorption (Strahm and Harrison 2007), were high (4.7%). Furthermore the soil was only mildly acidic (pH=5.8) so many of the sites capable of developing adsorbing anions would not have developed a positive charge under these conditions. There

---

were however significant levels of iron and aluminium oxides in the surface soil (20-30%) which develop positive charge near pH 9 and 8 respectively (Parks 1964) and therefore this may explain the measurement of anion adsorption. The study by Black and Waring (1976c) showed their soil had similar oxide levels and less organic carbon but still did not measure anion adsorption in the surface soil. The lower pH in the Red Ferrosol from this study (5.8 versus 6.1-6.5) is therefore likely to be the reason why adsorption was observed. Because of the various factors that influence adsorption direct measurement is considered the only practical way of determining the presence and significance of anion adsorption.

Significant variation in the accuracy of different methods used to assess  $\text{NO}_3^-$  adsorption was demonstrated in the study. The frequently used batch methods (Black and Waring 1976b; Kinjo and Pratt 1971) overestimated adsorption in the unsaturated flow conditions of the horizontal columns in comparison to the water immiscible displacement method described by Phillips and Bond (1989). Previous studies had shown contrasting findings when flow and batch methods were compared (Bond and Phillips 1990b; Burgisser *et al.* 1993; Hodges and Johnson 1987) however no studies had previously compared the methods in soils that had not been pre-treated with a solute wash to remove indigenous ions. This pre-treatment of a soil may remove ions that would otherwise have not been adsorbed by the equilibrating solution particular if the ion being investigated has a weak adsorption affinity (Katou *et al.* 2001) and may therefore result in overestimation of adsorption. When comparisons between methods were made in untreated soil samples in this study, it was concluded that the water-immiscible displacement method was more suitable because it caused minimal soil disturbance during equilibration of the solution and soil. This method was therefore considered to represent conditions that were more realistic under unsaturated water flow. Given the potential impact of  $\text{NO}_3^-$  adsorption on rates of leaching, accurate determination of adsorption is important in the development of modelling tools to assist in soil nitrogen management decision making and therefore careful thought should be made regarding pre-treatment of soils and the equilibration method used to determine adsorption.

Mineralisation must also be considered when describing nitrogen dynamics in soils. It was concluded that the rate of mineralisation was unlikely to influence the N Leach treatment in the field since the aim of this treatment was only to reduce soil N levels

---

over a period of seven days. However mineralisation was likely to have contributed to the amount of N in the soil over the growing season of the crop, and in particular may affect the N amount needing to be displaced at the time of application of the N Leach treatment, and may also play a significant role in the levels of N available to the plants over the growing season. Evidence for mineralisation is provided by the higher than anticipated concentration of ammonium measured in the soil. Since no  $\text{NH}_4^+$  was applied as fertiliser then this form of N must have been produced by biological activity.

The build up of  $\text{NH}_4^+$  in soils is uncommon since it is generally converted to  $\text{NO}_3^-$  by heterotrophic organisms as rapidly as it is formed (Schmidt 1982). Ammonium only accumulates when supply exceeds the needs of these organisms (Leeper and Uren 1993) however conversion of  $\text{NH}_4^+$  to  $\text{NO}_3^-$  by nitrifying bacteria is also sensitive to pH with optimal activity between a values of 7-9 (Alexander 1965). The potentially rapid mineralisation rates and mildly acidic soil conditions (pH=5.8) may have suppressed microbial ammonium breakdown. Field results indicated that the leaching treatment had no effect on the movement of  $\text{NH}_4^+$ . Previous studies have also shown the movement of  $\text{NH}_4^+$  over short periods to be minor in comparison to  $\text{NO}_3^-$  due to adsorption by the cation exchange capacity (Li *et al.* 2003). From the perspective of the N Leach treatment in the field in the  $\text{NH}_4^+$  present in the soil was therefore considered immobile and simply part of the baseline N level in the soil. In most situations where no  $\text{NH}_4^+$  is applied this concentration is unlikely to be a factor influencing the N Leach treatment due to its rapid conversion to  $\text{NO}_3^-$ . However the accumulation of rates in the 20-40 cm depth of  $5.63 \mu\text{mol cm}^{-3}$  soil observed in the field experiment indicated that management strategies may be required to avoid build up of concentrations to these levels. Ammonium concentrations could potentially be managed by selecting a site that has a more favourable pH for nitrification or earlier site preparation so potential breakdown of turf does not result in a rapid flush of  $\text{NH}_4^+$  production during crop growth.

Although build up of  $\text{NH}_4^+$  may create issues with application of the N Leach treatment, slow conversion of  $\text{NH}_4^+$  in the soil may be favourable for general production because mobility of N is reduced and is therefore less susceptible to leaching. Further studies in to the accumulation of  $\text{NH}_4^+$  in the Red Ferrosol may

---

---

therefore be beneficial for improving the N Leach treatment and further understanding properties that effect nitrification rates in soils.

As well as identifying  $\text{NO}_3^-$  reaction parameters in the Red Ferrosol, the water and  $\text{NO}_3^-$  profiles measured for the horizontal columns, along with some further point source infiltration experiments, provided the basis for development and validation of soil hydraulic and solute reaction parameters for the Hydrus soil model. Validation of parameters in contrasting flow scenarios provided some confidence of the ability for the parameters to describe water and solute flow in the field however without validation in this environment the model only offered a guide for the distribution of water and  $\text{NO}_3^-$  in the soil. Field simulations indicated that an overhead irrigation method was most suitable for applying the N Leach treatment suitable because of the uniform vertical displacement of solute. Anion adsorption was estimated to increase water applications to achieve the required change in  $\text{NO}_3^-$  concentrations by 20 % and was therefore considered to be a significant factor influencing the potential reduction in  $\text{NO}_3^-$  concentrations. Further measurements of adsorption below the surface layer are still necessary to gauge its significance in the lower horizons. According to other studies, anion adsorption generally increases with depth (Black and Waring 1976c; Duwig *et al.* 2003) and may therefore have an even greater influence on  $\text{NO}_3^-$  dynamics in the Red Ferrosol than shown in this study.

Although the presence of adsorption increased the difficulty of the leach N treatment application in this study, it is a beneficial soil characteristic for general crop production. As indicated in the model simulations, the presence of adsorption slowed the movement of  $\text{NO}_3^-$  through the profile. This will therefore reduce the leaching rate of  $\text{NO}_3^-$  and other negatively charged ions through the soil. As a result these nutrients will remain in the root zone for longer and will be more likely to be absorbed by plants. The increased plant uptake will reduce the quantity of nutrients lost below the root zone would have the potential to pollute groundwater and base flow to streams.

Model simulations indicated that the irrigation volume required to leach  $\text{NO}_3^-$  from the potato root zones in the Red Ferrosol was equivalent to the total seasonal water requirements of potato crops (Panigrahi *et al.* 2001; Wolfe *et al.* 1983) suggesting that this treatment may not to be commercially feasible on this soil type. Red Ferrosol's are the main potato production soil type in Tasmania, so development of management

---

---

strategies based on manipulation of soil  $\text{NO}_3^-$  concentrations would require a shift in industry focus for first generation seed production to alternate soils. Simulations of  $\text{NO}_3^-$  movement in a coarser textured sandy soil demonstrated that the leaching volumes required were less than half that required for Red Ferrosol. Production of the first field generation crop in a coarse textured soil may therefore improve the viability of such a treatment. Because of the small size of first generation potato crops, transferring production from the northwest of Tasmania dominated by the Red Ferrosol soils to an area such as the northeast where coarser textured Podzols are more common (Cotching *et al.* 2009) would not lead to significantly greater costs of production. If this treatment can be proven viable then uptake by the industry may therefore be relatively straightforward.

If the method of manipulating N was shown to offer significant increases in tuber numbers and was considered for use in second or third generation seed crops alternative methods of treatment application may be required due to the volumes of water required and the risk of environmental pollution due to the larger sizes of these crops. It may be possible to carefully manage N supply so adequate levels are maintained during early vegetative growth but allow plant uptake to reduce N supply sufficiently to encourage tuber growth after tuberization. This approach would require detailed knowledge of plant requirements and an understanding of nitrogen dynamics in the particular soil since maintenance of  $\text{NO}_3^-$  in the root zone would be very important to ensure deficiencies of N did not occur early during growth. Due to natural variation in the field the correct rates may change over relatively short distances and this may make correct applications difficult. The Red Ferrosol used in this study may also be unsuitable for this method if rapid mineralisation over the tuber growth period maintains  $\text{NO}_3^-$  concentrations in the soil at levels that stimulate above ground growth. A lighter textured soil with low organic carbon levels may therefore also make control of  $\text{NO}_3^-$  concentrations simpler using this approach.

Nitrate leaching below the root zone is undesirable in agricultural situations because it results in potential losses in productivity and profitability, and can result in groundwater and water way pollution (Simunek *et al.* 2008). Despite these issues, the investigation of the leaching treatment was justified in this study because minituber crops are only grown once at a particular site due to risks of pathogen carry-over and

---

---

the crop area is small. In addition, the first seed potato generation is a high value crop and thus loss of  $\text{NO}_3^-$  due to leaching is unlikely to be of economic significance.

Reducing N availability to potato plants at the tuber initiation growth stage was identified as a potential method for increasing tuber yield and reducing resorption in high value first generation seed potato crops. This treatment increased tuber growth rate in the glasshouse however application of this treatment in a field environment was complicated due to the irrigation system used and the greater area of the potato root distribution. The identification of anion adsorption and significant mineralisation further complicated the ability to apply the treatment in the field soil. Detailed water and  $\text{NO}_3^-$  column experiments helped determine patterns of water and  $\text{NO}_3^-$  movement and enabled validation of the Hydrus model to predict their movement under different scenarios. Simulations demonstrated the benefit of overhead irrigation for application of the leaching treatment and identified the potential reductions in water volumes that could be achieved on a coarser textured sandy soil with no anion exchange capacity. Knowledge gained from the detailed measurements in the Red Ferrosol and model simulations have improved the understanding of N dynamics in this difficult soil and therefore improved the likelihood of successful N manipulation. This trial work suggests the industry focus minituber production on lighter textured soils with lower levels of both variable charge minerals and organic matter levels. However, further trial work is required to confirm whether the proposed control of N supply can offer real benefits to the seed potato production industry in Tasmania.



## CONCLUSIONS AND RECOMENDATIONS

The availability of N influences tuber number and tuber growth in potatoes. Sufficient N is required to maximise tuber set, however maintaining a high N supply during early growth may delay tuber initiation and after tuber initiation may limit the growth of tubers. By limiting N supply at tuber initiation, the tuber growth rate can be increased. Increased tuber growth rate, linked to greater partitioning to below ground rather than above ground plant organs, was considered likely to lead to higher tuber yield as well as higher tuber numbers through reduced tuber resorption. Given the importance of maximising tuber numbers per plant in early generation seed potato production, further work investigating the effects of nitrogen supply on resource partitioning and tuber resorption processes is recommended.

This project confirmed that, if N supply is to be manipulated in the field detailed knowledge of soil physical, chemical and biological properties is required for the soil type in which N manipulation treatments are to be imposed. Quantitative assessment of key properties also facilitates the development of models that may assist in the formulation of crop management treatments. In particular, water movement is a key driver in the transport of N through the soil and therefore measurement of properties such as bulk density, water retention and hydraulic conductivity will aid in the predictions of N distribution.

The form of N in the soil will also influence its rate of movement since the cationic  $\text{NH}_4^+$  or anionic  $\text{NO}_3^-$  form will interact with cation and anion exchange capacities depending on the soil type. Nitrate is generally considered to move with the soil water in most soils and therefore application of N in this form should make reductions in root zone availability simpler in most soils. In Tasmania however, the primary cropping soils are Red Ferrosols which contain variable charge minerals. Anion adsorption was demonstrated to be a barrier to rapid movement of  $\text{NO}_3^-$  through these soils. Anion adsorption can be assessed using relatively simple laboratory measurements however care must be taken in choosing a method that matches conditions under which adsorption is occurring otherwise its significance may be under or overestimated.



---

Production of N due to the breakdown of organic materials by soil microbes is a factor that must be considered in all soils. The rate of N production is influenced by various environmental factors and may be significant under warm and moist conditions which are likely to occur over the growing season of an irrigated crop. If N supply is going to be strategically controlled over extended periods then understanding of production due to biological activity is also required.

The interactions between processes affected by different soil physical and chemical properties make predictions of solute movement difficult in soils, and it was concluded that soil water models may be a valuable tool to assist in this task. Models such as Hydrus 2D/3D (Simunek *et al.* 2006a) are capable of predicting water and solute transport under various flow scenarios as well as production of N due to mineralisation, and can therefore greatly assist in the design of treatments to manipulate N supply. The quality of model predictions relies on the quality of data available for determining model parameters and validating the predictions. Increasing the accuracy of predictions with careful parameter identification and validation may enable accurate modelling of N transport in soils to precisely control N availability, which may offer the potential to improve seed potato production in early generation seed crops.

This study identified a potential treatment for increasing tuber number in high value, small production area seed crops grown from minitubers. Successful development of a commercial treatment would contribute to improved production efficiency for the Tasmanian potato industry. Nitrate adsorption and mineralisation were identified as potential barriers to successful treatment application and it is recommended that consideration be given to production on alternative soil types if the method is to be developed and used commercially in Tasmania..

---

## REFERENCES

- Abbasi F, Simunek J, Feyen J, Genuchten MTv, Shouse PJ (2003) Simultaneous inverse estimation of soil hydraulic and solute transport parameters from transient field experiments: homogeneous soil. *Transactions of the Asae* 46, 1085-1095.
- Ajdary K, Singh DK, Singh AK, Manoj K (2007) Modelling of nitrogen leaching from experimental onion field under drip fertigation. *Agricultural Water Management* 89, 15-28.
- Alexander M (1965) Nitrification. In 'Soil Nitrogen'. (Eds WE Bartholomnew, FE Clark). (American Society of Agronomy: Madison).
- Allison MF, Fowler JH, Allen EJ (2001) Responses of potato (*Solanum tuberosum*) to potassium fertilizers. *Journal of Agricultural Science* 136.
- Alpkem (1992) 'The flow solution.' (Alpkem Corportation: Wilsonville, OR.).
- Angus JF, Bolger TP, Kirkegaard JA, Peoples MB (2006) Nitrogen mineralisation in relation to previous crops and pastures. *Australian Journal of Soil Research* 44, 355-365.
- Arbat G, Puig-Bargues J, Barragan J, Bonany J, Ramirez de Cartagena F (2008) Monitoring soil water status for micro-irrigation management versus modelling approach. *Biosystems Engineering* 100, 286-296.
- AUSVEG (2008) Vegetable Spotlight - Potatoes. AUSVEG, Clayton North, Victoria.
- Balamani V, Veluthambi K, Poovaiah BW (1986) Effect of calcium on tuberization in potato (*Solanum tuberosum* L.). *Plant Physiology* 80.
- Barrow NJ, Shaw TC (1979) Effects of solution:soil ratio and vigour of shaking on the rate of phosphate adsorption by soil. *Journal of Soil Science* 30, 67-76.
- Belanger G, Walsh JR, Richards JE, Milburn PH, Ziadi N (2000) Yield response of two potato cultivars to supplemental irrigation and N fertilization in New Brunswick. *American Journal of Potato Research* 77, 11-21.

---

Belanger G, Walsh JR, Richards JE, Milburn PH, Ziadi N (2001) Tuber growth and biomass partitioning of two potato cultivars grown under different N fertilization rates with and without irrigation. *American Journal of Potato Research* 78.

Belanger G, Walsh JR, Richards JE, Milburn PH, Ziadi N (2002) Nitrogen fertilization and irrigation affects tuber characteristics of two potato cultivars. *American Journal of Potato Research* 79.

Bellini G, Sumner ME, Radcliffe DE, Qafoku NP (1996) Anion transport through columns of highly weathered acid soil: Adsorption and retardation. *Soil Science Society of America Journal* 60, 132-137.

Ben-Gal A, Dudley LM (2003) Phosphorus availability under continuous point source irrigation. *Soil Science Society of America Journal* 67, 1449-1456.

Bernstein L, Francois LE (1973) Comparisons of drip, furrow, and sprinkler irrigation. *Soil Science* 115, 73-86.

Black AS, Waring SA (1976a) Nitrate Leaching and Adsorption in a Krasnozem from Redland Bay, Old .1. Leaching of Banded Ammonium-Nitrate in a Horticultural Rotation. *Australian Journal of Soil Research* 14, 171-180.

Black AS, Waring SA (1976b) Nitrate Leaching and Adsorption in a Krasnozem from Redland Bay, Qld .2. Soil Factors Influencing Adsorption. *Australian Journal of Soil Research* 14, 181-188.

Black AS, Waring SA (1976c) Nitrate Leaching and Adsorption in a Krasnozem from Redland Bay, Qld .3. Effect of Nitrate Concentration on Adsorption and Movement in Soil Columns. *Australian Journal of Soil Research* 14, 189-195.

Black AS, Waring SA (1979) Adsorption of Nitrate, Chloride and Sulfate by Some Highly Weathered Soils from Southeast Queensland. *Australian Journal of Soil Research* 17, 271-282.

Boersig MR, Wagner SA (1988) Hydroponic systems for production of seed tubers. In 'American Potato Journal' pp. 470-471.

Bohn HL, McNeal BL, O'Connor GA (1979) 'Soil chemistry.' (John Wiley and Sons: New York).

- 
- Boivin A, Simunek J, Schiavon M, Genuchten MTv (2006) Comparison of pesticide transport processes in three tile-drained field soils using HYDRUS-2D. *Vadose Zone Journal* 5, 838-849.
- Bond WJ, Phillips IR (1990a) Approximate solutions for cation transport during unsteady, unsaturated soil water flow. *Water Resources Research* 26, 2195-2205.
- Bond WJ, Phillips IR (1990b) Cation exchange isotherms obtained with batch and miscible-displacement techniques. *Soil Science Society of America Journal* 54, 722-728.
- Bond WJ, Phillips IR (1990c) Ion transport during unsteady water flow in an unsaturated clay soil. *Soil Science Society of America Journal* 54, 636-645.
- Broadbent FE, Clark FE (1965) Denitrification. In 'Soil Nitrogen'. (Eds WV Batholomew, FE Clark). (American Society of Agronomy: Wisconsin).
- Buchter B, Davidoff B, Amacher MC, Hinz C, Iskandar IK, Selim HM (1989) Correlation of Freundlich Kd and n retention parameters with soils and elements. *Soil Science* 148, 370-379.
- Burgisser CS, Cernik M, Borkovec M, Sticher H (1993) Determination of Nonlinear Adsorption Isotherms from Column Experiments: An Alternative to Batch Studies. *Environmental Science and Technology* 27, 943-948.
- Burstall L, Thomas MN, Allen EJ (1987) The relationship between total yield, number of tubers and yield of large tubers in potato crops. *Journal of Agricultural Science, UK* 108.
- Bus CB, Wustman R (2007) The canon of potato science: 28. Seed tubers. *Potato Research* 50, 319-322.
- Carsel RF, Parrish RS (1988) Developing joint probability distributions of soil water retention characteristics. *Water Resources Research* 24, 755-769.
- Castro CA (1988) Effect of nitrogen and potassium fertilizers on yield and quality of two potato cultivars. *Anais da UTAD* 1.
- Cho JL, Iritani WM (1983) Comparison of growth and yield parameters of russet Burbank for a two year period. *American Potato Journal* 60, 569-576.
-

- 
- Choudhury AK, Saikia M, Suhrawardy J, Dutta KC (1996) Effect of irrigation and nitrogen levels on growth and tuber yield of potato. *Indian Journal of Soil Conservation* 24.
- Clothier BE, Elrick DE (1985) Solute dispersion during axisymmetric three-dimensional unsaturated water flow. *Soil Science Society of America Journal* 49, 552-556.
- Clothier BE, Sauer TJ, Green SR (1988) The movement of ammonium nitrate into unsaturated soil during unsteady absorption. *Soil Science Society of America Journal* 52, 340-345.
- Cook FJ, Thorburn PJ, Fitch P, Bristow KL (2003) WetUp: a software tool to display approximate wetting patterns from drippers. *Irrigation Science* 22, 129-134.
- Cooley ET, Lowery B, Kelling KA, Wilner S (2007) Water dynamics in drip and overhead sprinkler irrigated potato hills and development of dry zones. *Hydrological Processes* 21, 2390-2399.
- Cotching WE, Lynch S, Kidd DB (2009) Dominant soil orders in Tasmania: distribution and selected properties. *Australian Journal of Soil Research* 47, 537-548.
- Cotching WE, Wright DN (1994) A Review of the Major Challenges for Long Term Management of Krasnozems in Australia. In 'Soils Ain't Soils - Whats Special about Krasnozems'. Ulverstone, Tasmania. (Eds A Fulton, L Sparrow).
- Cote CM, Bristow KL, Charlesworth PB, Cook FJ, Thorburn PJ (2003) Analysis of soil wetting and solute transport in subsurface trickle irrigation. *Irrigation Science* 22, 143-156.
- Cresswell H (2002) The soil water characteristic. In 'Soil physical measurement and interpretation for land evaluation'. (Eds N McKenzie, K Coughlan, H Cresswell). (CSIRO: Melbourne ).
- Davison AC, Hinkley DV (1997) 'Bootstrap methods and their application ' (Cambridge University Press: New York).
- de Vos JA, Hesterberg D, Raats PAC (2000) Nitrate leaching in a tile-drained silt loam soil. *Soil Science Society of America Journal* 64, 517-527.
-

---

Donn MJ, Menzies NW (2005) Simulated rainwater effects on anion exchange capacity and nitrate retention in Ferrosols. *Australian Journal of Soil Research* 43, 33-42.

Dousset S, Thevenot M, Pot V, et al. (2007) Evaluating equilibrium and non-equilibrium transport of bromide and isoproturon in disturbed and undisturbed soil columns. *Journal of Contaminant Hydrology* 94, 261-276.

Dubetz S, Bole JB (1975) Effect of nitrogen, phosphorus, and potassium fertilizers on yield components and specific gravity of potatoes. *American Potato Journal* 52.

Duwig C, Becquer T, Charlet L, Clothier BE (2003) Estimation of nitrate retention in a Ferralsol by a transient-flow method. *European Journal of Soil Science* 54, 505-515.

Duwig C, Becquer T, Vogeler I, Vauclin M, Clothier BE (2000) Water dynamics and nutrient leaching through a cropped Ferralsol in the Loyalty Islands (New Caledonia). *Journal of Environmental Quality* 29, 1010-1019.

Evangelou VP (1998) 'Environmental Soil and Water Chemistry: Principles and Applications.' (John Wiley and Sons, Inc: New York).

Ewing EE (1985) Cuttings as simplified models of the potato plant. In 'Potato physiology' pp. 153-207. (Academic Press, Inc.: Orlando, Florida USA).

Ewing EE (1990) Induction of tuberization in potato. In 'The molecular and cellular biology of the potato.' (CAB International: Wallingford UK).

Ewing EE, Struik PC (1992) Tuber formation in potato: induction, initiation and growth. *Horticultural Reviews* 14, 89-197.

Firestone MK (1982) Biological denitrification. In 'Nitrogen in agricultural soils' pp. 289-326. (American Society of Agronomy: Madison, Wisconsin USA).

Fritton DD, Kirkham D, Shaw RH (1967) Soil Water and Chloride Redistribution Under Various Evaporation Potentials. *Soil Science Society of America Journal* 31, 599-603.

Gardenas AI, Hopmans JW, Hanson BR, Simunek J (2005) Two-dimensional modeling of nitrate leaching for various fertigation scenarios under micro-irrigation. *Agricultural Water Management* 74, 219-242.

---

---

Gayler S, Wang E, Priesack E, Schaaf T, Maidl FX (2002) Modeling biomass growth, N-uptake and phenological development of potato crop. *Geoderma* 105, 367-383.

Gillman GP (1981) Effects of pH and ionic strength on the cation exchange capacity of soils with variable charge. *Australian Journal of Soil Research* 19, 93-96.

Gillman GP, Bell LC (1978) Soil solution studies on weathered soils from tropical north Queensland. *Australian Journal of Soil Research* 16, 67-77.

Greacen EL, Walker GR, Cook PG (1989) Procedure for the filter paper method of measuring soil water suction. CSIRO Division of Soils108, Canberra, Australia.

Green RE, Davidson M, Biggar JW (1980) An Assessment of Method for Determining Adsorption-Desorption of Organic Chemicals. In 'Agrochemicals in Soils'. (Eds A Banin, U Kafkafi) pp. 73-89. (Pergamon Press: Oxford).

Hanson B (2003) Can irrigated agriculture in California meet ground water quality standards through improved irrigation? *International Water & Irrigation* 23, 26-28, 30.

Hanson BR, Simunek J, Hopmans JW (2006) Evaluation of urea-ammonium-nitrate fertigation with drip irrigation using numerical modeling. *Agricultural Water Management* 86, 102-113.

Hassan FA, Ghaibeh AS (1977) Evaporation and Salt Movement in Soils in the Presence of Water Table. *Soil Science Society of America Journal* 41, 470-478.

Hassett JJ, Banwart WL (1989) The sorption of nonpolar organics by soils and sediments. In 'Reactions and Movement of Organic Chemicals in Soils'. (Eds BL Sawhney, K Brown) pp. 31-44. (SSSA Special Publication, Soil Science Society of America, Madison).

Haws NW, Rao PSC, Simunek J, Poyer IC (2005) Single-porosity and dual-porosity modeling of water flow and solute transport in subsurface-drained fields using effective field-scale parameters. *Journal of Hydrology (Amsterdam)* 313, 257-273.

Hillel D (1980) 'Fundamentals of soil physics.' (Academic Press: New York).

Hodges SC, Johnson GC (1987) Kinetics of sulfate adsorption and desorption by Cecil soil using miscible displacement. *Soil Science Society of America Journal* 51, 323-331.

---



---

Hodgson AS, Constable GA, Duddy GR, Daniells IG (1990) A comparison of drip and furrow irrigated cotton on a cracking clay soil. 2. Water use efficiency, waterlogging, root distribution and soil structure. *Irrigation Science* 11, 143-148.

Hopmans JW, Šimůnek J, Romano N, Durner W (2002) Inverse Methods, Chapter 3.6.2. In 'Methods of Soil Analysis, Part 4, Physical Methods'. (Eds JH Dane, GC Topp). (SSSA, Madison: Wisconsin).

IRIS (2009) Infrastructure Resource Information Service - Agricultural Supply - Vegetables. (Department of Infrastructure, Energy and Resources).

Isbell RF (1994) Krasnozems - a profile. *Australian Journal of Soil Research* 32, 915-929.

Isbell RF (1996a) 'The Australian soil classification.' (CSIRO Publishing: Collingwood Australia).

Isbell RF (1996b) 'The Australian Soil Classification.' (CSIRO: Victoria).

Jackson SD (1999) Multiple signaling pathways control tuber induction in potato. *Plant Physiology* 119.

Jansson SL, Persson J (1982) Mineralization and immobilization of soil nitrogen. In 'Nitrogen in agricultural soils' pp. 229-252. (American Society of Agronomy: Madison, Wisconsin USA).

Ji GL (1997) 'Chemistry of variable charge soils.' (Oxford University Press: New York).

Jury WA, Gardner WR, Gardner WH (1991) 'Soil Physics.' (John Wiley and Sons, Inc.: New York).

Kamara L, Zartman R, Ramsey RH (1991) Cotton-root distribution as a function of trickle irrigation emitter depth. *Irrigation Science* 12, 141-144.

Katou H (2004) Determining competitive nitrate and chloride adsorption in an Andisol by the unsaturated transient flow method. *Soil Science and Plant Nutrition* 50, 119-127.



---

Katou H, Clothier BE, Green SR (1996) Anion transport involving competitive adsorption during transient water flow in an Andisol. *Soil Science Society of America Journal* 60, 1368-1375.

Katou H, Uchimura K, Clothier BE (2001) An unsaturated transient flow method for determining solute adsorption by variable-charge soils. *Soil Science Society of America Journal* 65, 283-290.

Keeney DR (1982) Nitrogen management for maximum efficiency and minimum pollution. In 'Nitrogen in agricultural soils' pp. 605-649. (American Society of Agronomy: Madison, Wisconsin USA).

Khalil A, Singh DK, Singh AK, Manoj K (2007) Modelling of nitrogen leaching from experimental onion field under drip fertigation. *Agricultural Water Management* 89, 15-28.

Kinjo T, Pratt PF (1971) Nitrate Adsorption: I. In some acid soils of Mexico and South America. *Soil Science Society of America Journal* 35, 722-725.

Kinjo T, Pratt PF, Page AL (1971) Nitrate Adsorption: III. Desorption Movement and Distribution in Andepts. *Soil Science Society of America Journal* 35, 728-732.

Koda Y, Okazawa Y (1983) Influences of environmental, hormonal and nutritional factors on potato tuberization in vitro. *Japanese Journal of Crop Science* 52.

Kohne JM, Mohanty BP, Simunek J (2005) Inverse dual-permeability modeling of preferential water flow in a soil column and implications for field-scale solute transport. *Vadose Zone Journal* 5, 59-76.

Kohne JM, Mohanty BP, Simunek J, Gerke HH (2004) Numerical evaluation of a second-order water transfer term for variably saturated dual-permeability models. *Water Resources Research* 40, W07409.

Krauss A (1978) Tuberization and abscisic acid content in *Solanum tuberosum* as affected by nitrogen nutrition. *Potato Research* 21.

Krauss A (1980) Influence of nitrogen nutrition on tuber initiation of potatoes. In 'Physiological aspects of crop productivity. Proceedings of the 15th Colloquium of the International Potash Institute'. (International Potash Institute: Bern Switzerland).

- 
- Krauss A (1985) Interaction of nitrogen nutrition, phytohormones, and tuberization. In 'Potato physiology'. (Academic Press Inc.: Orlando, Florida USA).
- Krauss A, Marschner H (1982) Influence of nitrogen nutrition, daylength and temperature on contents of gibberellic and abscisic acid and on tuberization in potato plants. *Potato Research* 25.
- Kursanov AL (1984) 'Assimilate Transport in Plants.' (Elsevier: Amsterdam).
- Leeper GW, Uren NC (1993) 'Soil science: an introduction.' (University Press: Melbourne).
- Lesczynski DB, Tanner CB (1976) Seasonal variation of root distribution of irrigated, fieldgrown Russet Burbank potato. *American Potato Journal* 53, 69-78.
- Li H, Parent LE, Karam A (2006) Simulation modeling of soil and plant nitrogen use in a potato cropping system in the humid and cool environment. *Agriculture, Ecosystems & Environment* 115, 248-260.
- Li J, Zhang J, Rao M (2005) Modeling of waterflow and nitrate transport under surface drip fertigation. *Transactions of the Asae* 48, 627-637.
- Li J, Zhang J, Ren L (2003) Water and nitrogen distribution as affected by fertigation of ammonium nitrate from a point source. *Irrigation Science* 22, 19-30.
- Lommen WJM (2007) The canon of potato science: 27. Hydroponics. *Potato Research* 50, 315-318.
- Loveday J (1974) 'Methods for analysis of irrigated soils.' (Commonwealth Agricultural Bureaux: Farnham Royal).
- Loveday J, Farquhar RN (1958a) 'The Soil and Some Aspects of Land Use in the Burnie, Table Cape and Surrounding Districts, Northwest Tasmania.' (CSIRO: Melbourne).
- Loveday J, Farquhar RN (1958b) 'The Soils and Some Aspects of Land Use in the Burnie, Table Cape, and Surrounding Districts, Northwest Tasmania.' (CSIRO: Melbourne).
-

---

Marcos MLF, Buurman P, Meijer EL (1998) Role of organic matter and sesquioxides on variable charge of three soils from Galicia, Spain. *Communications in Soil Science and Plant Analysis* 29, 2441-2457.

McBride MB (1994) 'Environmental Chemistry of Soils.' (Oxford University Press: New York).

McKenzie N, Coughlan K, Cresswell H (2002) 'Soil physical measurement and interpretation for land evaluation.' (CSIRO: Melbourne ).

Mmolawa K, Or D (2000) Root zone solute dynamics under drip irrigation: a review. *Plant and Soil* 222.

Moody PW (1994) Chemical Fertility of Krasnozems - A Review. *Australian Journal of Soil Research* 32, 1015-1041.

Moradi A, Abbaspour KC, Afyuni M (2005) Modelling field-scale cadmium transport below the root zone of a sewage sludge amended soil in an arid region in Central Iran. *Journal of Contaminant Hydrology* 79, 187-206.

Nakayama FS, Jackson RD, Kimball BA, Reginato RJ (1973) Diurnal Soil-Water Evaporation: Chloride Movement and Accumulation Near the Soil Surface. *Soil Science Society of America Journal* 37, 509-513.

Neeteson JJ, Greenwood DJ, Draycott A (1989) Model calculations of nitrate leaching during the growth period of potatoes. *Netherlands Journal of Agricultural Science* 37, 237-256.

O'Brien PJ, Allen EJ (1986) Effects of nitrogen fertilizer applied to seed crops on seed yields and regrowth of progeny tubers in potatoes. *Journal of Agricultural Science, UK* 107.

O'Brien PJ, Allen EJ, Firman DM (1998) A review of some studies into tuber initiation in potato (*Solanum tuberosum*) crops. *Journal of Agricultural Science* 130, 251-270.

Olsen SR, Watanabe FS (1957) A Method to Determine a Phosphorus Adsorption Maximum of Soils as Measured by the Langmuir Isotherm. *Soil Science Society American Proceedings* 21, 144-149.

---

- 
- Oparka KJ, Davies HV, Prior DAM (1987) The Influence of Applied Nitrogen on Export and Partitioning of Current Assimilate by Field-Grown Potato Plants. *Annals of Botany* 59, 311-323.
- Oparka KJ, Marshall B, MacKerron DKL (1986) Carbon partitioning in a potato crop in response to applied nitrogen. In 'Phloem Transport'. (Eds J Cronshaw, WJ Lucas, RT Giaquinta, RL Alan) pp. 577-587.
- Ozgen S, Palta JP (2004) Supplemental calcium application influences potato tuber number and size. *HortScience* 40.
- Painter CG, Augustin J (1976) The effect of soil moisture and nitrogen on yield and quality of the Russet Burbank potato. *American Potato Journal* 53.
- Panigrahi B, Panda SN, Raghuwanshi NS (2001) Potato water use and yield under furrow irrigation. *Irrigation Science* 20, 155-163.
- Parks GA (1964) The isoelectric points of solid oxides, solid hydroxides, and aqueous hydroxo complex systems. *Chemical Reviews* 65, 177-198.
- Patel N, Rajput TBS (2008) Dynamics and modeling of soil water under subsurface drip irrigated onion. *Agricultural Water Management* 95, 1335-1349.
- Peech M, Cowan RL, Baker JH (1962) A critical study of the Barium chloride-Triethanolamine and ammonium acetate methods for determining exchangeable Hydrogen of soils. *Soil Science Society of America Proceedings*.
- Persicani D (1995) Analysis of leaching behaviour of sludge-applied metals in two field soils. *Water, Air, and Soil Pollution* 83, 1-20.
- Peterson RL, Barker WG (1979) Early tuber development from expanded stolon nodes of *Solanum tuberosum* var. Kennebec. *Botanical Gazette* 140, 398-406.
- Philip JR (1957) The theory of infiltration: 4. Sorptivity and algebraic infiltration equations. *Soil Science* 84, 257-264.
- Philip JR (1969) Theory of Infiltration. *Advances in Hydroscience* 5, 215-296.
- Phillips IR (2006) Modelling water and chemical transport in large undisturbed soil cores using HYDRUS-2D. *Australian Journal of Soil Research* 44, 27-34.
-

- 
- Phillips IR, Bond WJ (1989) Extraction procedure for determining solution and exchangeable ions on the same soil sample. *Soil Science Society of America Journal* 53, 1294-1297.
- Powlson DS (1980) Effect of cultivation on the mineralization of nitrogen in soil. *Plant and Soil* 57, 151-153.
- Qafoku NP, Sumner ME (2001) Retention and transport of calcium nitrate in variable charge subsoils. *Soil Science* 166, 297-307.
- Qafoku NP, Sumner ME, Radcliffe DE (2000) Anion transport in columns of variable charge subsoils: nitrate and chloride. *Journal of Environmental Quality* 29, 484-493.
- Radley RW (1963) The effect of season on the growth and development of the potato. In 'The Growth of the Potato'. (Eds JD Ivins, FL Milthorp) pp. 211-220. (Butterworths: London).
- Rawls WJ, Brakensiek DL, Saxton KE (1982) Estimation of soil water properties. *Transactions of the ASAE (American Society of Agricultural Engineers)* 25, 1316-1320, 1328.
- Rayment GE, Higginson FR (1992) 'Australian laboratory handbook of soil and water chemical methods.' (Inkata Press: Melbourne).
- Reynolds WD, Elrick DE, Youngs EG, Amoozegar A, Booltink HWG, Bouma J (2002) Saturated and Field-Saturated Water Flow Parameters. In 'Methods of Soil Analysis, Part 4, Physical Methods'. (Eds JH Dane, GC Topp). (SSSA, Madison: Wisconsin).
- Roberts S, Weaver WH, Phelps JP (1982) Effect of rate and time of fertilization on nitrogen and yield of Russet Burbank potatoes under center pivot irrigation. *American Potato Journal* 59, 77-86.
- Roberts T, Lazarovitch N, Warrick AW, Thompson TL (2009) Modeling salt accumulation with subsurface drip irrigation using HYDRUS-2D. *Soil Science Society of America Journal* 73, 233-240.
- Roberts TL, White SA, Warrick AW, Thompson TL (2008) Tape depth and germination method influence patterns of salt accumulation with subsurface drip irrigation. *Agricultural Water Management* 95, 669-677.
-

- 
- Rolot JL, Seutin H (1999) Soilless production of potato minitubers using a hydroponic technique. In 'Potato Research' pp. 457-469. (European Association for Potato Research: Wageningen Netherlands).
- Sarmah AK, Close ME, Dann R, Pang L, Green SR (2006) Parameter estimation through inverse modelling and comparison of four leaching models using experimental data from two contrasting pesticide field trials in New Zealand. *Australian Journal of Soil Research* 44, 581-597.
- SAS (2003) SAS 9.1. (SAS Institute Inc.: Cary, USA).
- Sattelmacher B, Marschner H (1979) Tuberization in potato plants as affected by applications of nitrogen to the roots and leaves. *Potato Research* 22.
- Schaap MG, Leij FJ, Genuchten MTv (2001) ROSETTA: a computer program for estimating soil hydraulic parameters with hierarchical pedotransfer functions. *Journal of Hydrology (Amsterdam)* 251, 163-176.
- Schmidt EL (1982) Nitrification in soil. In 'Nitrogen in agricultural soils' pp. 253-288. (American Society of Agronomy: Madison, Wisconsin USA).
- Schweich D, Sardin M, Gaudet JP (1983) Measurement of a cation exchange isotherm from elution curves obtained in a soil column: preliminary results. *Soil Science Society of America Journal* 47, 32-37.
- Sharma RP, Ezekiel R (1993) Influence of time of nitrogen application on number and size of potato (*Solanum tuberosum*) tubers. *Indian Journal of Agronomy* 38, 154-156.
- Simmons KE, Kelling KA (1987) Potato Responses to Calcium Application on Several Soil Types. *American Potato Journal* 64, 119-136.
- Simunek J, Hopmans JW, Nielsen DR, Genuchten MTv (2000) Horizontal infiltration revisited using parameter estimation. *Soil Science* 165, 708-717.
- Simunek J, Senja M (2007) 'Hydrus 2D/3D -User Manual version 1.02.' (PC-Progress: Prague).
- Simunek J, Senja M, Genuchten Rv (2002) Hydrus 1D.
-

---

Simunek J, Senja M, Genuchten Rv (2006a) Hydrus 2D/3D. (PC-Progress s.r.o. Prague, Czech Republic.

Simunek J, van Genuchten MT, Senja M (2006b) 'The HYDRUS Software Package for Simulating the Two and Three Dimensional Movement of Water, Heat, and Multiple Solutes in Variably-Saturated Media. Technical Manual.' (PC-Progress: Prague).

Simunek J, Wendroth O, Genuchten MTv (1998) Parameter estimation analysis of the evaporation method for determining soil hydraulic properties. *Soil Science Society of America Journal* 62, 894-905.

Simunek J, Kohne M, Kodesova R, Sejna M (2008) Simulating nonequilibrium movement of water, solutes, and particles using HYDRUS: A review of recent applications. *Soil and Water Research* 3, 42-51.

Simunek J, Genuchten MTv (2008) Modeling nonequilibrium flow and transport processes using HYDRUS. *Vadose Zone Journal* 7, 782-797.

Siyal AA, Skaggs TH (2009) Measured and simulated soil wetting patterns under porous clay pipe sub-surface irrigation. *Agricultural Water Management* 96, 893-904.

Skaggs TH, Trout TJ, Simunek J, Shouse PJ (2004) Comparison of HYDRUS-2D simulations of drip irrigation with experimental observations. *Journal of Irrigation and Drainage Engineering* 130, 304-310.

Smiles DE, Gardiner BN (1982) Hydrodynamic dispersion during unsteady, unsaturated water flow in a clay soil. *Soil Science Society of America Journal* 46, 9-14.

Smiles DE, Philip JR (1978) Solute transport during absorption of water by soil: laboratory studies and their practical implications. *Soil Science Society of America Journal* 42, 537-544.

Smiles DE, Philip JR, Knight JH, Elrick DE (1978) Hydrodynamic dispersion during absorption of water by soil. *Soil Science Society of America Journal* 42, 229-234.

Smiles DE, Smith CJ (2004) Absorption of artificial piggery effluent by soil: a laboratory study. *Australian Journal of Soil Research* 42, 961-975.



- 
- Smith O (1968) 'Potatoes: Production, Storing, Processing.' (AVI Publishing Company: Connecticut).
- Sommerfeldt TG, Knutson KW (1968) Greenhouse study of early potato growth response to soil temperature, bulk density and nitrogen fertilizer. *American Potato Journal* 45, 231-237.
- Sonnleitner MA, Abbaspour KC, Schulin R (2003) Hydraulic and transport properties of the plant-soil system estimated by inverse modelling. *European Journal of Soil Science* 54, 127-138.
- Sparks DL (1995) Environmental soil chemistry. In 'Environmental soil chemistry.' p. xii + 267 pp. (Academic Press, Book Marketing Department: San Diego USA).
- Sparrow LA, Chapman KSR (2003) Effects of nitrogen fertiliser on potato (*Solanum tuberosum* L., cv. Russet Burbank) in Tasmania. 1. Yield and quality. *Australian Journal of Experimental Agriculture* 43, 631-641.
- Sparrow LA, Cotching WE, Cooper J, Rowley W (1999) Attributes of Tasmanian ferrosols under different agricultural management. *Australian Journal of Soil Research* 37, 603-622.
- Sposito G (1984) The surface chemistry of soils. In 'The surface chemistry of soils.' p. 234 pp. (Oxford University Press: New York USA).
- Sposito G (1989) The chemistry of soils. In 'The chemistry of soils.' (Oxford University Press: New York USA).
- Stalham MA, Allen EJ (2001) Effect of variety, irrigation regime and planting date on depth, rate, duration and density of root growth in the potato (*Solanum tuberosum*) crop. *Journal of Agricultural Science* 137.
- Stevenson FJ (1985) Cycles of soil: carbon, nitrogen, phosphorus, sulfur, micronutrients. In 'Cycles of soil: carbon, nitrogen, phosphorus, sulfur, micronutrients.' p. 380 pp. (John Wiley & Sons, Inc.: New York USA).
- Strahm BD, Harrison RB (2007) Mineral and organic matter controls on the sorption of macronutrient anions in variable-charge soils. *Soil Science Society of America Journal* 71, 1926-1933.
-



---

Struik PC (2007a) The canon of potato science: 25. Minitubers. *Potato Research* 50, 305-308.

Struik PC (2007b) The canon of potato science: 40. Physiological age of seed tubers. *Potato Research* 50, 375-377.

Struik PC, Wiersema SG (1999) 'Seed Potato Technology.' (Wageningen Pers: Wageningen).

Sumner ME (1999) 'Handbook of Soil Science.' (CRC Press: London).

Sweetlove LJ, Hill SA (2000) Source metabolism dominates the control of source to sink carbon flux in tuberizing potato plants throughout the diurnal cycle and under a range of environmental conditions. *Plant, Cell and Environment* 23, 523-529.

Sweetlove LJ, Kossmann J, Riesmeier JW, Trethewey RN, Hill SA (1998) The control of source to sink carbon flux during tuber development in potato. *Plant Journal* 15, 697-706.

Twarakavi NKC, Saito H, Simunek J, Genuchten MTv (2008) A new approach to estimate soil hydraulic parameters using only soil water retention data. *Soil Science Society of America Journal* 72, 471-479.

Uehara G, Gillman GP (1980) Charge characteristics of soils with variable and permanent charge minerals: I. Theory. *Soil Science Society of America Journal* 44, 250-252.

Van Delden A, Schroder JJ, Kropff MJ, Grashoff C, Booij R (2003) Simulated potato yield, and crop and soil nitrogen dynamics under different organic nitrogen management strategies in The Netherlands. *Agriculture, Ecosystems & Environment* 96, 77-95.

van Genuchten MTv (1980) A closed-form equation for predicting the hydraulic conductivity of unsaturated soils. *Soil Science Society of America Journal* 44, 892-898.

van Genuchten MTv, Simunek J, Leij FJ, Senja M (2005) RETC - code for quantifying the hydraulic functions of unsaturated soils Riverside, California).

---

Vecchio V, Ghiselli L, Andrenelli L, Benedettelli S (2004) Effect of nitrogen interruption on in vitro tuberization and potato microtuber storage. *Advances in Horticultural Science* 18, 63-67.

Ventrella D, Mohanty BP, Simunek J, Losavio N, Genuchten MTv (2000) Water and chloride transport in a fine-textured soil: field experiments and modeling. *Soil Science* 165, 624-631.

Waddell JT, Gupta SC, Moncrief JF, Rosen CJ, Steele DD (1999) Irrigation and nitrogen management effects on potato yield, tuber quality, and nitrogen uptake. *Agronomy Journal* 91.

Wagenet RJ, Hutson JL (1989) LEACHM: Leaching estimation and solute movement - A processed base model of water and solute movement, transformations, plant uptake and chemical reactions in the unsaturated zone. Continuum volume 2. (Water Resources Institute, Cornell University Ithica, New York).

Walkley A, Black IA (1934) An examination of the Degtjareff method for determining soil organic matter and a proposed modification of the chromic acid titration method. *Soil Science* 37, 39-28.

Wang XJ, Smethurst PJ, Holz GK (1996) Nitrogen mineralisation indices in ferrosols under eucalypt plantations of north-western Tasmania: association with previous land use. *Australian Journal of Soil Research* 34, 925-935.

Weast RC (1971) 'Handbook of chemistry and physics.' (The Chemical Rubber Company).

Werner HO (1934) The effect of a controlled nitrogen supply with different temperatures and photoperiods upon the development of the potato plant. *Nebraska Agricultural Experimental Station, Research Bulletin* 75, 1-132.

Wolfe DW, Fereres E, Voss RE (1983) Growth and yield response of two potato cultivars to various levels of applied water. *Irrigation Science* 3, 211-222.

Wong MTF, Hughes R, Rowell DL (1990) Retarded leaching of nitrate in acid soils from the tropics: measurement of the effective anion exchange capacity. *Journal of Soil Science* 41, 655-663.

- 
- Wu G, Chieng ST (1995a) Modeling multicomponent reactive chemical transport in nonisothermal unsaturated/saturated soils. Part 1. Mathematical model development. *Transactions of the Asae* 38, 817-826.
- Wu G, Chieng ST (1995b) Modeling multicomponent reactive chemical transport in nonisothermal unsaturated/saturated soils. Part 2. Numerical simulations. *Transactions of the Asae* 38, 827-838.
- Wurr DCE, Hole CC, Fellows JR, Milling J, Lynn JR, O'Brien PJ (1997) The effect of some environmental factors on potato tuber numbers. *Potato Research* 40, 297-306.
- Xu X, Lammeren AAMv, Vermeer E, Vreugdenhil D (1998) The role of gibberellin, abscisic acid, and sucrose in the regulation of potato tuber formation in vitro. *Plant Physiology* 117.
- Yu TR (1997) 'Chemistry of variable charge soils.' (Oxford University Press: New York).
- Zhang M, Alva AK, Li YC, Calvert DV (1996) Root distribution of grapefruit trees under dry granular broadcast vs. fertigation method. *Plant and Soil* 183, 79-84.
- Zhou J, Xi J, Chen Z, Li S (2006) Leaching and transformation of nitrogen fertilizers in soil after application of N with irrigation: a soil column method. *Pedosphere* 16, 245-252.
-

## **APPENDICES**

**APPENDIX 1 – ACID KURO SOL WATER AND NITRATE PROFILE**

**APPENDIX 2 – RED FERROSOL SOIL PROFILE**

**APPENDIX 3 – CALCULATION OF WATER SOLUBLE NITRATE FROM  
TOTAL NITRATE VALUES**

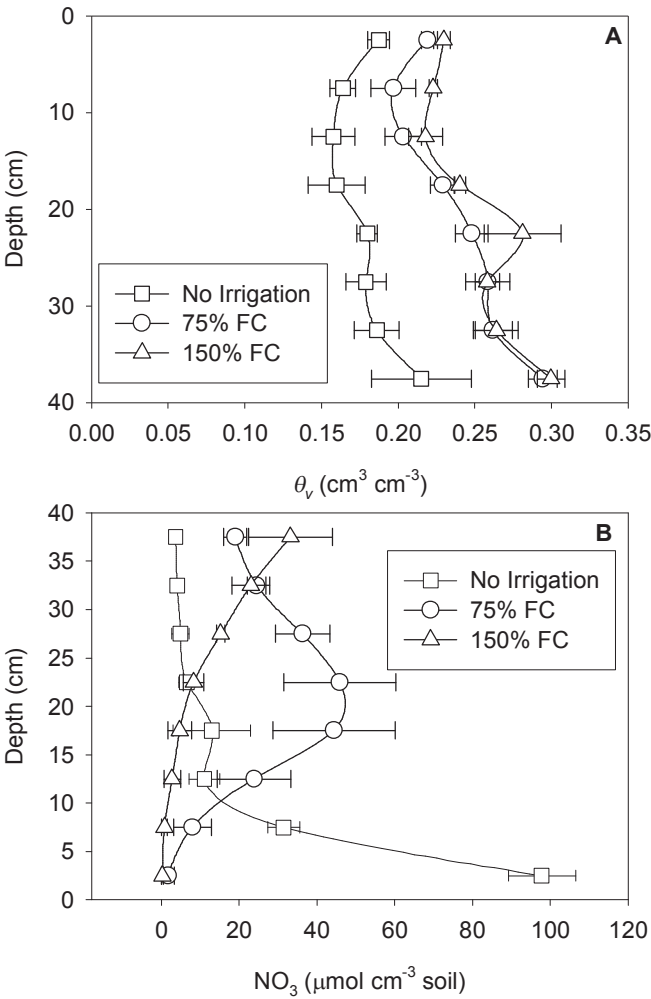
**APPENDIX 4 – LANGMUIR AND FREUNDLICH ISOTHERM FITS USING  
DIRECT AND LINEAR FITTING METHODS**

**APPENDIX 5 – GOVERNING WATER AND SOLUTE FLOW EQUATIONS  
FOR HYDRUS**

APPENDIX 1 – ACID KURO SOL WATER AND NITRATE PROFILE

Appendix Table 1: Field capacity and leaching application applied to the Acid Kurosol with a field capacity of 0.18 cm<sup>3</sup> cm<sup>-3</sup> and bulk density of 1.15 g cm<sup>-3</sup>.

Treatment	Leaching volume (cm <sup>3</sup> )
No Irrigation	0
75% FC	118
150% FC	236



Appendix Figure 14: Volumetric water content (Figure A) and total NO<sub>3</sub><sup>-</sup> content (Figure B) of the Acid Kurosol.

## APPENDIX 2 – RED FERROSOL SOIL PROFILE

### Site Information

Location	Moina, Tasmania (41°29'28.80" S 14°603'34.70" E)
Elevation	508 m
Date	2/07/09
Describer	Richard Doyle/James Kirkham
Exposure Type	Soil Pit
Soil Classification	FE, AA, AG, CK, 1
Australian soil classification	Red Mesotrophic Humus Ferrosol medium slightly gravelly clay loamy clayey deep

### Land form

Slope	Gentle waning lower slope
Erosion	None
Site Disturbance	Cultivation, Irrigated
Vegetation	Crop/Pasture
Surface coarse fragments	Very few 20-60 mm

### HORIZON

- A1 – 0-25 cm:** 5YR2.5/2 moist; Clay Loam; Strongly developed structure, 5-10mm, Polyhedral; Strongly developed structure, 2-5 mm; Polyhedral; Non Sticky; Non-plastic; Normal plasticity; Very weak (moist); Earthy fabric; Many macropores (0.075-1 mm); Few moderately weak, subangular, dispersed, coarse fragments (6-20 mm); Many very fine (<1mm) roots; Sharp wavy change to –
- B21 – 25-50 cm:** 2.5YR3/3 moist; Gritty, Light Clay; Strongly developed structure, 10-20 mm polyhedral; Strongly developed 2-5 mm polyhedral; Non Sticky; Non-plastic; Normal plasticity; Very weak (moist); Rough-ped fabric; Many macropores (0.075-1 mm); very few, Ferruginous nodules (2-6 mm); Common moderately weak, subangular, dispersed, coarse fragments (6-20 mm); Many very fine roots; Diffuse, smooth change to –
- B22 – 50-75 cm:** 2.5YR3/3 moist; Gravelly, Light Clay; Strongly developed structure, 5-10 mm polyhedral; Strongly developed 2-5 mm polyhedral; Non Sticky; Non-plastic; Normal plasticity; Very weak (moist); Rough-ped fabric; Many macropores (0.075-1 mm); very few, Ferruginous nodules (2-6 mm); Common moderately weak, subangular, dispersed, coarse fragments (6-20 mm); Common very fine roots; Abrupt, smooth change to –
- D – 75-105+ cm:** 10YR7/8 moist; Common distinct mottles (>15mm), 7.5YR6/8; Heavy, Silty Clay Loam; Strongly developed structure, 10-20mm Angular blocky; Strongly developed structure, 2-5mm polyhedral; Moderately sticky; Moderately plastic; Very weak (moist) Earthy fabric; Common macropores (1-2mm); Few, distinct, Mangan cutins; Few very fine roots.

### APPENDIX 3 – CALCULATION OF WATER SOLUBLE NITRATE FROM TOTAL NITRATE VALUES

When the Langmuir equation is used, the soil solution  $\text{NO}_3^-$  can be calculated by manipulating the Langmuir equation (4-3) and the total  $\text{NO}_3^-$  equation (4-31) To produce the quadratic equation (4-29).

In contrast when the Freundlich equation (4-1) is used the solution concentration is calculated by combining equation and equation 4-31 to give:

$$(\Gamma - \theta C_w) / \rho = \alpha C_w^n \quad \text{A-1}$$

where  $\Gamma$  is the total  $\text{NO}_3^-$  ( $\mu\text{mol}_\text{c} \text{ cm}^{-3}$  soil),  $\theta$  is the volumetric water content ( $\text{cm}^3 \text{ cm}^{-3}$ ),  $C_w$  is the solution  $\text{NO}_3^-$  concentration ( $\mu\text{mol}_\text{c} \text{ cm}^{-3}$ ),  $\rho$  is the bulk density ( $\text{g cm}^{-3}$ ) and  $\alpha$  and  $n$  are the constants from the Freundlich equation(4-1). Rearrangement of equation A-1 yields:

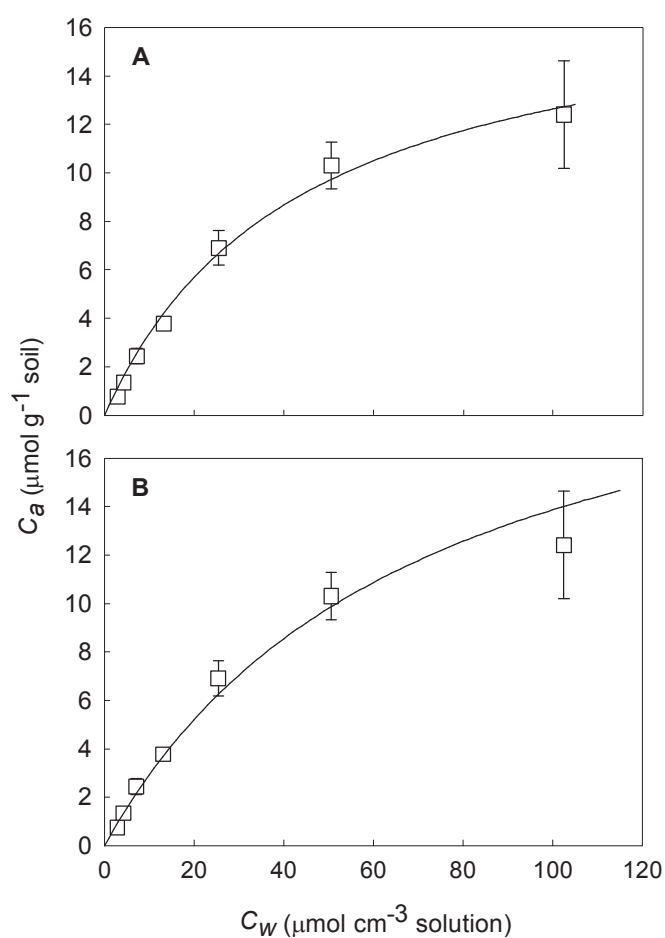
$$\Gamma = \rho \alpha C_w^n + \theta C_w \quad \text{A-2}$$

For values of  $n \neq 0.5$  or 1 this equation is difficult to solve for  $C_w$ , however numerical solutions can be calculated using the *Solver* function in Microsoft Excel which uses the generalised reduce gradient nonlinear optimisation code to solve non linear problems (Microsoft 2003).

If both equations give equally acceptable fits to the isotherm data then the Langmuir equation may be chosen since it is simpler to solve.

## APPENDIX 4 – LANGMUIR AND FREUNDLICH ISOTHERM FITS USING DIRECT AND LINEAR FITTING METHODS

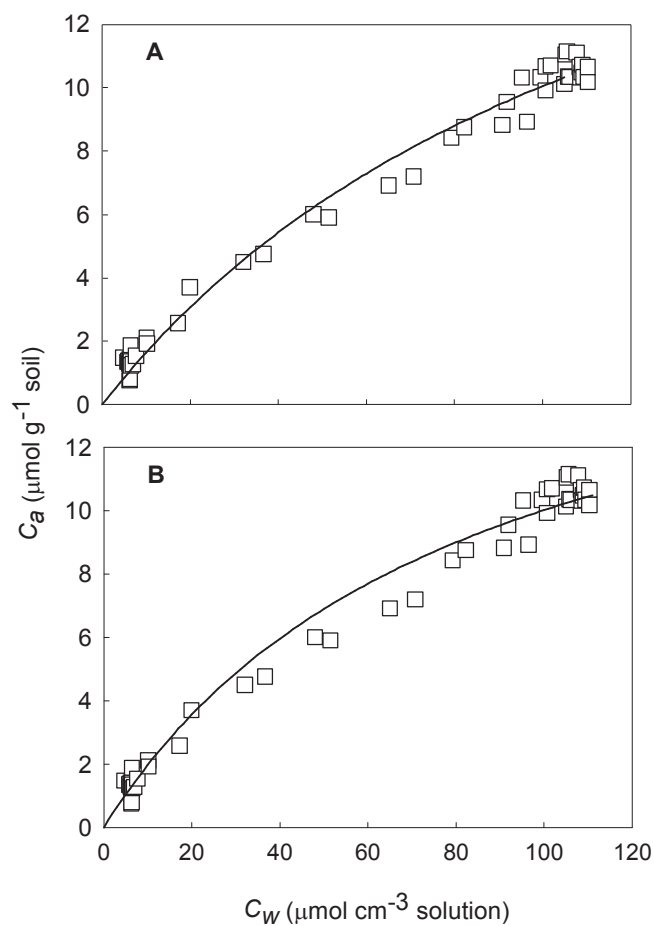
### BATCH DATA: LANGMUIR ISOTHERM



**Appendix Figure 15:** Comparison of the Langmuir equation fit to the batch isotherm data using direct fitting in SAS (Figure A) and the linear fit method using equation 4-4 (Figure B).

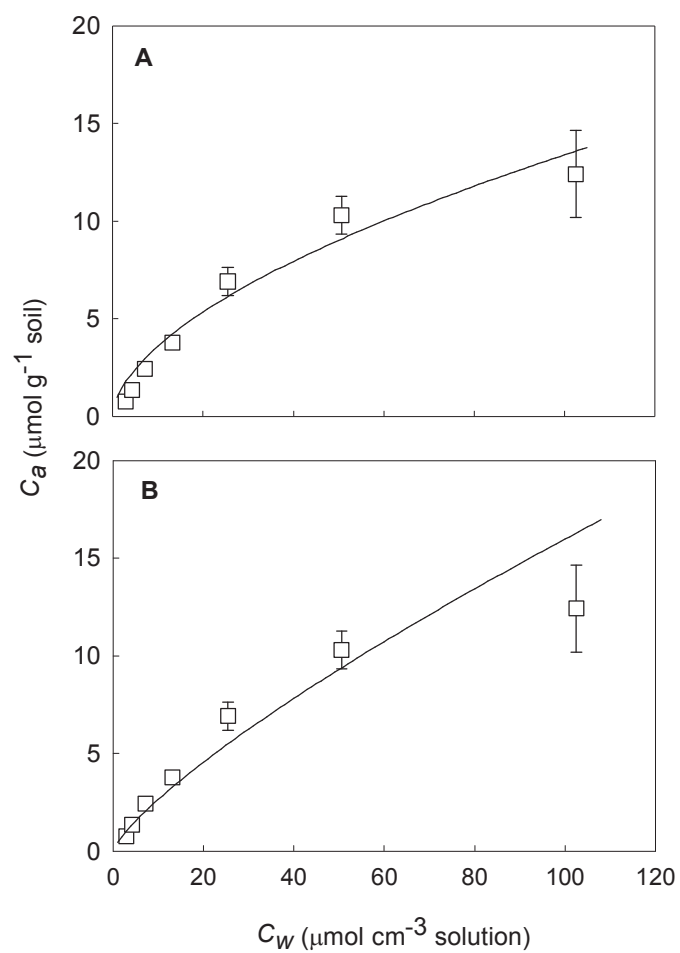


## TFE DATA: LANGMUIR ISOTHERM



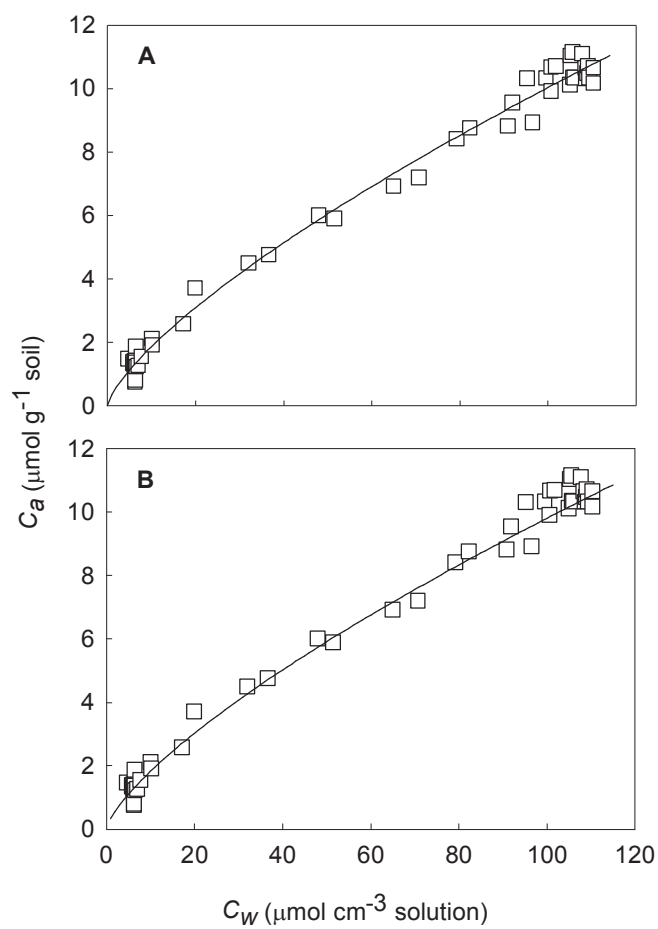
**Appendix Figure 16:** Comparison of the Langmuir equation fit to the TFE isotherm data using direct fitting in SAS (Figure A) and the linear fit method using equation 4-4 (Figure B).

## BATCH DATA: FREUNDLICH ISOTHERM



**Appendix Figure 17:** Comparison of the Freundlich equation fit to the batch isotherm data using direct fitting in SAS (Figure A) and the linear fit method using equation 4-2 (Figure B).

## TFE DATA: FREUNDLICH ISOTHERM



**Appendix Figure 18:** Comparison of the Freundlich equation fit to the batch isotherm data using direct fitting in SAS (Figure A) and the linear fit method using equation 4-2 (Figure B).

## APPENDIX 5 – GOVERNING WATER AND SOLUTE FLOW EQUATIONS FOR HYDRUS

### WATER FLOW

Water flow is described by the Richards Equation modified to describe horizontal flow in one dimension with no loss of water due to evaporation of root uptake (Simunek *et al.* 2008a):

$$\frac{\partial \theta}{\partial t} = \frac{\partial}{\partial x} \left( K \frac{\partial \psi}{\partial x} \right), \quad \text{A-3}$$

where  $\theta$  is the volumetric water content ( $\text{cm}^3 \text{ cm}^{-3}$ ),  $t$  is time (min),  $x$  is the horizontal distance (cm),  $\psi$  is the water tension (cm) and  $K$  is the hydraulic conductivity ( $\text{cm min}^{-1}$ ) given by:

$$K(\psi, x) = K_{sat}(x) K_r(h, x), \quad \text{A-4}$$

where  $K_r$  is the relative hydraulic conductivity (no unit) and  $K_{sat}$  is the saturated hydraulic conductivity ( $\text{cm min}^{-1}$ ; Simunek *et al.* 2008).

The modified form of the Richards equation that describes water movement in two dimensions assuming no loss of water through root uptake or evaporation can be written (Simunek *et al.* 2006):

$$\frac{\partial \theta}{\partial t} = \frac{\partial}{\partial x_i} \left[ K \left( K_{ij}^A \frac{\partial \psi}{\partial x_j} \right) + K_{iz}^A \right] \quad \text{A-5}$$

where  $x_i$  ( $i=1,2$ ) are the spatial coordinates (cm), and  $K_{ij}^A$  and  $K_{iz}^A$  are components of a dimensionless anisotropy tensor  $K^A$ . Assuming flow is isotropic (that is,  $K$  is equal in horizontal and vertical directions) the diagonal entries of  $K_{ij}^A$  equal one and the off-diagonal entries equal zero (Simunek *et al.* 2006).

In the two dimensional flow scenario  $K$  is given by:

$$K(\psi, x) = K_{sat}(x, z) K_r(h, x, z). \quad \text{A-6}$$

If equation A-5 is applied to planar flow in a vertical cross section,  $x_1=x$  is the horizontal coordinate and  $x_2=z$  is the vertical coordinate. Equation A-5 can also describe axi-symmetric flow when  $x_1=x$  represents a radial coordinate (Gardenas *et al.* 2005). The transcripts  $i$  and  $j$  in equation A-5 denote either the  $x$  or  $z$  coordinate.

To solve the Richards equation, Hydrus implements the soil hydraulic functions of the van Genuchten-Mualem to describe unsaturated hydraulic conductivity in terms of soil water retention parameters (Simunek *et al.* 2006). Water retention is described by equation A-7 (Simunek *et al.* 2006):

$$\theta(\psi) = \begin{cases} \theta_r \frac{\theta_s - \theta_r}{[1 + |\alpha\psi|^n]^m} & \psi < 0 \\ \theta_s & \psi \geq 0 \end{cases} \quad \text{A-7}$$

and unsaturated conductivity is written (Simunek *et al.* 2006):

$$K(\psi) = K_s S_e^l [1 - (1 - S_e^{1/m})^m]^2 \quad \psi < 0 \quad \text{A-8}$$

where:

$$m = 1 - 1/n, \quad n > 1 \quad \text{A-9}$$

and:

$$S_e = \frac{\theta - \theta_r}{\theta_s - \theta_r} \quad \text{A-10}$$

In the above equations  $\theta_r$  is the residual water content ( $\text{cm}^3 \text{ cm}^{-3}$ ),  $\theta_s$  is the saturated water content ( $\text{cm}^3 \text{ cm}^{-3}$ ),  $\alpha$  ( $\text{cm}^{-1}$ ),  $n$  (no unit) and  $l$  (no unit) are curve fitting parameters for the hydraulic conductivity function and  $S_e$  is the effective water content ( $\text{cm}^3 \text{ cm}^{-3}$ ).

When the van Genuchten-Mualem model is used to solve Richards equation in Hydrus there are six soil hydraulic parameters required ( $\theta_r$ ,  $\theta_s$ ,  $\alpha$ ,  $n$ ,  $l$  and  $K_{sat}$ ).

## SOLUTE FLOW

One dimensional transport of reactive solute flow assuming no transformation of solute is written (Simunek *et al.* 2008a):

$$\frac{\partial \theta C_w}{\partial t} + \frac{\partial \rho C_a}{\partial t} = \frac{\partial}{\partial x} \left( \theta D^w \frac{\partial C_w}{\partial x} \right) - \frac{\partial v C_w}{\partial x}, \quad \text{A-11}$$

where  $C_w$  is the solution concentration of the solute ( $\mu\text{mol}_c \text{ cm}^{-3}$ ),  $C_a$  is the amount of adsorbed solute ( $\mu\text{mol}_c \text{ g}^{-1}$ ),  $\rho$  is the bulk density ( $\text{g cm}^{-3}$ ) and  $D^w$  is the diffusion coefficient for the liquid phase ( $\text{cm}^2 \text{ min}^{-1}$ ).

---

For two dimensional flow of reactive solute flow assuming no transformation of solute is written (Simunek *et al.* 2006):

$$\frac{\partial \theta C_w}{\partial t} + \frac{\partial \rho C_a}{\partial t} = \frac{\partial}{\partial x_i} \left( \theta D_{ij}^w \frac{\partial C_w}{\partial x_j} \right) - \frac{\partial v_i C_w}{\partial x_i} \quad \text{A-12}$$

Adsorption of a non transforming solute is described by the generalised non linear equation which accounts for adsorption described by the Freundlich, Langmuir or linear equations (Simunek *et al.* 2006):

$$C_w = \frac{k_s C_a^\omega}{1 + \phi C_a^\omega}, \quad \text{A-13}$$

and:

$$\begin{aligned} \frac{\partial C_w}{\partial t} = & \frac{k_s \omega C_a^{\omega-1}}{(1 + \phi C_a^\omega)^2} \frac{\partial C_a}{\partial t} + \frac{C_a^\omega}{1 + \phi C_a^\omega} \frac{\partial k_s}{\partial t} - \frac{k_s C_a^{2\omega}}{(1 + \phi C_a^\omega)^2} \frac{\partial \phi}{\partial t} \\ & + \frac{k_s C_a^\omega \ln C_a}{(1 + \phi C_a^\omega)^2} \frac{\partial \omega}{\partial t}, \end{aligned} \quad \text{A-14}$$

where  $k_s$  ( $\text{cm}^3 \text{ g}^{-1}$ ),  $\omega$  (no unit) and  $\phi$  ( $\text{cm}^3 \text{ g}^{-1}$ ) are constants. In the case of the Langmuir equation  $k_s = C_{\max} \phi$  (where  $C_{\max}$  and  $\phi$  are the Langmuir equation constants) and  $\omega=1$ . When  $\phi=0$  equation A-13 and A-14 describe the Freundlich equation ( $k_s$  and  $\omega$  represent the Freundlich equation constants). When  $\omega=1$  and  $\phi=0$  equation A-13 and A-14 describe linear adsorption.